U.PORTO

FEUP FACULDADE DE ENGENHARIA
UNIVERSIDADE DO PORTO

Data-based engineering techniques for the management of concrete bridges

by

HELDER FILIPE MOREIRA DE SOUSA

Supervisor

Prof. Joaquim Figueiras

(Faculdade de Engenharia da Universidade do Porto – FEUP)

Co-supervisor

Prof. João Bento

(Instituto Superior Técnico da Universidade Técnica de Lisboa – IST-UTL)

A thesis submitted for the degree of Doctor of Philosophy in Civil Engineering
at the Faculty of Engineering of the University of Porto

March 2012

Members of the Jury*:

Manuel António de Matos Fernandes, Full Professor from *Faculdade de Engenharia da Universidade do Porto, Portugal* (President of the Jury, by subdelegation from the School Principal)

Hugo Corres Peiretti, Full Professor from *Universidad Politécnica de Madrid, Spain.*

António José Luis dos Reis, Full Professor from *Instituto Superior Técnico da Universidade Técnica de Lisboa, Portugal.*

Luis Miguel Pina de Oliveira Santos, Head Researcher from *Laboratório Nacional de Engenharia Civil, Portugal.*

António Abel Ribeiro Henriques, Full Professor from *Faculdade de Engenharia da Universidade do Porto, Portugal.*

Defence on July 16, 2012,

Faculdade de Engenharia da Universidade do Porto, Portugal,

Author information:

www.hfmsousa.com / mail@hfmsousa.com

University/Research Unit information:

LABEST – Laboratory for the Concrete Technology and Structural Behaviour

Department of Civil Engineering

FEUP – Faculty of Engineering of the University of Porto

Rua Dr. Roberto Frias, s/n

4200 – 465 Porto, Portugal

www.fe.up.pt / www.fe.up.pt/labest

* without including the supervisor and the co-supervisor.

DEDICATION

To my father,

Nelson

ACKNOWLEDGMENTS

Firstly, the author expresses his true gratefulness to Professor Joaquim Figueiras, founding member of the research group LABEST, of the Faculty of Engineering, University of Porto, for supervising his academic career from the end of the Civil Engineering graduation to the closure of this present work, as PhD candidate. The author's enlightenment relative to the structural behaviour of civil infrastructures was immensely enriched through the wise and insightful vision of Professor Figueiras, who had also introduced to him the subject of Structural Health Monitoring. The author also demonstrates his sincerely gratitude to Dr João Bento, an Executive Board Member of BRISA S.A. (at the time of the development of the Lezíria Bridge project) and co-supervisor of this work, who shared with the author his scientific rigour, broad vision and guidance. The completion of this thesis his profoundly based on their involvement, appreciation and contribution.

The author also expresses his sincere gratitude to Professor Abel Henriques, who had an important contribution in the discussion of some themes addressed in the present thesis, with his opinions and constructive suggestions.

The implementation of the monitoring system in Lezíria Bridge during construction was a *lifetime experience* for the author. As one would expect for in-situ works, there are many relevant if not decisive personal contributions. Whether with a direct or indirect participation, the author wishes to thank to all those who contributed to the success of the implementation of this system. Being almost impossible to name all of them (dozens if not hundreds!), some of them have crossed the author's experience not only at a professional level but also at social and human levels. Special thanks are addressed to Mr Monteiro, Mr Cláudio, Mrs Helena, Ms Paula Silva, Dr Mário Pimentel, Dr Sandra Nunes, Dr Lino Maia,

Mr Rui Pinheiro and Mr Rogério, from the LABEST team; Mr Amândio Pinto, Mr Remy Faria and Mr Miguel from the NewMENSUS team, people with whom the author had the pleasure to work as a founding member of the company; Mr Paulo Silva, Mr Rui Narciso, Mr Peixoto, Mr Cabrera, Mr Dias, Mr Neto, Mr João Marques, Mr Guimarães, Mr Diogo Valério, Ms Vanda Santos, from the contractor TACE; Mr Sabino and Mr Jorge from EFACEC and also Mrs Vera Perdigão and Mr Alfredo Raposo, from the bridge owner, BRISA.

For many times, the knowledge sharing with closest colleagues was very important in the resolution of some problems that the author felt along his journey. Sincere thanks are also addressed to all of them namely, Bruno Costa, Dimande, Carlos Sousa and Filipe Cavadas. The discussion sessions, many times lunch or dinner, had mixed science and friendship into enjoyable moments.

The author developed the main part of his work at Faculty of Engineering, University of Porto, more precisely at the LABEST research group, that offered the necessary conditions to accomplish his task. In addition, the financial support through the PhD grant SFRH/BD/25339/2005 awarded by the Fundação para a Ciência e a Tecnologia (The Portuguese Foundation for Science and Technology) was fundamental to carry on the author's work. The author is grateful to both institutions.

In a very particular way, the author is deeply grateful to Professor Piqueiro, who kindly accepted his request to take some aerial photographs of Lezíria Bridge. The unforgettable flight that turn this request into a reality was one of the most exciting and unique experiences in the author's life.

Even without a direct contribution to the work herein presented, the author expresses his profound recognition and appreciation to his closest friends, without whom this journey would not have the grateful colours of life namely, Emanuel, Romão, Sandra, Ricardo, Elisabete, Patricia, Clara and Joana. In a very special manner, the author expresses his truly

gratitude, and everlasting affection, to the Perdigão family for their hospitality and unconditional friendship whilst his stay at Lezíria Bridge.

This work represents a reward also to the author's closest family. From his father, mother and sister, the author received their love, education and unconditional support, which were, and are, the basis for the author's beliefs, wills and personality. To them, Nelson, Rosa Maria and Liliana, the author is eternally grateful. A very special thanks to his uncle Gil is also addressed, who since early ages fed the author's curiosity about science and world aspects, with his simplicity, vision, friendship and willingness.

At last, the author wishes to address his wife, Filipa, who has been his harbour, with her love, affection and dedication. For the last six years, the author recognizes her unconditional support in dealing with the natural hurdles along this journey. What sometimes seemed almost insurmountable to the author, her radiance found, or helped, in finding the route to the goal. For that, and for more than that, the author expresses his unconditional Love.

AGRADECIMENTOS

Em primeiro lugar, o autor expressa o seu sincero agradecimento ao Professor Joaquim Figueiras, fundador do grupo de investigação LABEST da Faculdade de Engenharia da Universidade do Porto, como supervisor da sua carreira académica desde o fim da sua licenciatura em Engenharia Civil até ao presente momento como doutorando. A sua sapiência e perspicácia na abordagem à problemática do comportamento estrutural de infra-estruturas civis foram contributos únicos na formação técnica do autor como especialista na área, que mais solidamente se concretizou através do contacto, desde cedo, com a área da monitorização da integridade estrutural. O autor demonstra igualmente o seu sincero apreço ao Dr. João Bento, membro da Comissão Executiva da empresa BRISA S.A. (aquando do desenvolvimento do projecto da Ponte da Lezíria) e co-supervisor da presente dissertação, pelo seu rigor científico, visão ampla e orientação. A conclusão deste trabalho está intimamente apoiada nas suas participações, valorizações e contribuições.

O autor expressa também o seu sincero agradecimento ao Professor Abel Henriques, pela sua importante contribuição na discussão de alguns temas abordados na presente tese, através das suas opiniões e sugestões sempre construtivas.

A implementação do sistema de monitorização da Ponte da Lezíria, durante a construção, foi uma *experiência de vida* para o autor. Como seria expectável em trabalhos de campo, houve contributos importantes de muitas pessoas, que em muitos casos se revelaram pessoalmente decisivos. Deste modo, o autor expressa o seu agradecimento a todos aqueles que directamente ou indirectamente tenham contribuído para o sucesso da implementação deste sistema. Ainda que sendo praticamente impossível referenciar o nome de todos (dezenas ou talvez até centenas!), algumas dessas pessoas cruzaram-se com o autor nesta experiência não só a um nível profissional, mas também a um nível social e humano. A

esses, são endereçados especiais agradecimentos, nomeadamente: Sr. Monteiro, Sr. Cláudio, Sra. Helena, Sra. Paula, Dr. Mário Pimentel, Dr. Sandra Nunes, Dr. Lino Maia, Sr. Rui Pinheiro e Sr. Rogério da equipa LABEST-FEUP; Sr. Amândio Pinto, Sr. Remy Faria e Sr. Miguel da equipa NewMENSUS, com os quais o autor teve o prazer de trabalhar como membro fundador desta empresa; Sr. Paulo Silva, Sr. Rui Narciso, Sr. Peixoto, Sr. Cabrera, Sr. Dias, Sr. Neto, Sr. João Marques, Sr. Guimarães, Sr. Diogo Valério, Sr. Vanda Santos da construtora TACE; Sr. Sabino e o Sr. Jorge da empresa EFACEC, bem como Sra. Vera Perdigão, Sr. Alfredo Raposo da empresa BRISA, concessionária da Ponte da Lezíria.

Por diversas ocasiões, a partilha do conhecimento com colegas próximos foi muito importante na resolução de alguns problemas que se depararam ao autor ao longo da sua caminhada. Francos agradecimentos são também endereçados a todos eles nomeadamente, Bruno Costa, Dimande, Carlos Sousa e Filipe Cavadas pelas várias sessões de discussão, muitas delas durante horas de almoço e jantar, que se revelaram sempre momentos agradáveis e em que a amizade e a ciência se misturaram de uma forma sinérgica.

O autor desenvolveu grande parte do seu trabalho na Faculdade de Engenharia da Universidade do Porto, mais precisamente no grupo de investigação LABEST, instituição a qual proporcionou as condições necessárias para que os objectivos propostos fossem atingidos. Além disso, o suporte financeiro conseguido através da bolsa de estudos SFRH/BD/25339/2005, obtida por mérito através da Fundação para a Ciência e a Tecnologia, foi fundamental. O autor está sinceramente agradecido a ambas as instituições.

De um modo muito particular, o autor está profundamente agradecido ao Professor Piqueiro, o qual acedeu encarecidamente ao seu pedido em obter algumas fotografias aéreas da Ponte da Lezíria. O voo inesquecível que permitiu a realização deste pedido foi uma das experiências mais excitantes e únicas na vida do autor.

Ainda que sem uma contribuição directa no presente trabalho, o autor expõe o seu profundo reconhecimento e apreço aos seus amigos mais próximos, sem os quais esta

longa jornada não conteria as belas cores da vida nomeadamente, Emanuel, Romão, Sandra, Ricardo, Elisabete, Patrícia, Clara e Joana. De uma forma muito especial, o autor expressa a sua verdadeira consideração, e afecto para sempre, à família Perdigão pela sua hospitalidade e amizade incondicional enquanto da sua estadia na Ponte da Lezíria.

Este trabalho apresenta-se, também, como uma recompensa para a sua família mais próxima. Do seu pai, mãe e irmã, o autor recebeu o seu amor, educação e apoio incondicional, valores que foram, e são, o suporte das convicções, querenças e personalidade do autor. A eles, Nelson, Rosa Maria e Liliana, o autor está eternamente grato. Um agradecimento muito especial ao seu tio Gil, o qual desde cedo o fez despertar para as curiosidades da ciência e do mundo, com a sua simplicidade, visão, amizade e boa disposição.

Finalmente, o autor deseja expressar-se à sua esposa, Filipa, a qual tem sido o seu porto de abrigo com o seu amor, afecto e dedicação. Durante os últimos seis anos, o autor reconhece o seu incondicional apoio perante os naturais obstáculos que foram aparecendo ao longo desta jornada. O que algumas vezes pareceu intransponível ao autor, o brilho do seu ser sempre encontrou, ou ajudou a encontrar, o caminho para o sucesso. Por isso, e por muito mais do que isso, o autor expressa o seu Amor incondicional.

ABSTRACT

This thesis addresses the development and implementation of engineering techniques based on data collected by monitoring systems focussing on the bridge management. During the last decades, the number of bridges has grown exponentially and due to their ageing, the malfunctions that naturally appear in their serviceable phase become a critical problem. Structural Health Monitoring (SHM) has become progressively a reliable tool, which in fact can act as an integrated part of the management system, as a complement to the visual inspections procedures. However, the application of monitoring data for bridge management is not performed in a straightforward manner yet. The main reasons appear to be: (1) the quantity and variety of the collected data that makes it difficult to establish standard procedures for knowledge extraction; (2) the uncertainties concerning the effective behaviour of the structure, material properties, environmental conditions and loading, render the task even more difficult; (3) the final target, being it operational, tactical or management-related, which dictates the level of complexity of the data processing.

In view of the above observations, the following priorities were established, which guide the present thesis: (1) to enumerate, describe and detail all the main phases of the implementation of an integrated monitoring system in a large-scale bridge regarding its life-cycle management; (2) to develop and integrate the required data-based engineering techniques in a software system able to illustrate the implementation of the suggested approach; (3) to build a detailed and rigorous FEM enabling the evaluation and discussion of the quality of the monitoring data extracted; (4) to analyse and discuss the monitoring data in order to generate confidence for its effective use in the bridge management, based on the developed and implemented engineering techniques.

Supported in a large-scale bridge recently built in Portugal – Lezíria Bridge – that is equipped with an integrated monitoring system devoted to long-term observation, the usefulness of the monitoring data collected by these systems concerning the bridge life-cycle management is herein confirmed by the results presented in this thesis.

Keywords: Concrete bridges; integrated monitoring systems, monitoring data processing, shrinkage, creep, temperature, numerical analysis, structure lifetime, management.

RESUMO

A presente dissertação centra-se no desenvolvimento e implementação de técnicas de engenharia baseadas em dados recolhidos por sistemas de monitorização estrutural, com o objectivo de ajudarem à tomada de decisões na gestão de pontes.

O aumento exponencial da construção de pontes nas últimas décadas, aliado ao facto destas envelhecerem progressivamente, torna actualmente a questão da detecção das anomalias, que naturalmente surgem ao longo da vida útil, num problema crítico. Os Sistemas de Monitorização da Integridade Estrutural têm-se revelado como uma ferramenta útil, e que de uma forma gradual podem de facto se tornar parte integrante dos sistemas de gestão de pontes, em complemento aos habituais procedimentos de inspecção visual. No entanto, a utilização dos dados provenientes destes sistemas de monitorização não é ainda feita de um modo eficiente e integrado. As principais razões para isso parecem ser: (1) a quantidade e variedade de dados recolhidos, que dificulta a definição de procedimentos padrão para extracção de conhecimento útil; (2) incertezas relacionadas com o real comportamento das estruturas nomeadamente, propriedades dos materiais estruturais, condições ambientais e de carregamento; (3) o destinatário da informação a fornecer, se a um nível operacional, táctico ou de gestão, o qual dita o nível de complexidade do processamento requerido para os dados recolhidos.

Com base nas observações anteriormente referidas, as seguintes prioridades foram estabelecidas para o desenvolvimento da dissertação: (1) enunciar, descrever e pormenorizar as principais fases da implementação de um sistema de monitorização integrado, vocacionado para longo prazo, numa ponte de grandes dimensões; (2) desenvolver e integrar técnicas de engenharia num novo software, com o objectivo de tornar os dados da monitorização mais legíveis a um nível de gestão; (3) modelar com rigor a estrutura monitorizada com recurso a Modelos de Elementos Finitos com o

objectivo de aferir a qualidade das medições obtidas pelos sensores; (3) analisar e discutir com detalhe as medições obtidas de modo a ter confiança nos mesmos para a sua efectiva utilização na gestão de pontes com base nas técnicas de engenharia desenvolvidas e implementadas.

Os dados recolhidos por um sistema de monitorização integrado instalado numa ponte de grandes dimensões recentemente construída em Portugal – a Ponte da Lezíria – suportam todo o trabalho desenvolvido. Focando o principal objectivo que consiste no apoio à gestão da estrutura ao longo da sua vida útil, a utilidade dos dados recolhidos é aqui demonstrada.

Palavras-chave: Pontes de betão; sistemas de monitorização integrados, processamento de dados, retracção, fluência, temperatura, análise numérica, vida útil de estruturas, gestão.

CONTENTS

LIST OF FIGURES

LIST OF TABLES

NOTATIONS

Capital Latin letters

AN	Acquisition Node
BD	Bearing Displacement
BWIM	Bridge Weight-In-Motion
CAN	Central Acquisition Node
CD	Concrete Deformation
CT	Concrete Temperature
CT_{AVG}	Average of the concrete temperatures
CUR	Curvatures
E_c	Tangent modulus of elasticity
$E_{c,ref}$	Modulus of elasticity at a reference age
EC2	European code Eurocode 2
EDA	Exploratory Data Analysis
E.P.	Estradas de Portugal
F(x)	Cumulative distribution function
FEM	Finite Element Model
FHWA	Federal Highway Administration
GF	Gage Factor
H	Distance between two layers

H_0	Null hypothesis
JB	Junction Box
K	Wobble coefficient
LC1	Load Case 1
LC2	Load Case 2
LVDT	Linear Variable Differential Transformer
$P^n(x)$	Polynomial function of 'n' degree
PAN	Provisional Acquisition Node
R_p	Return period
S	Section
SCB	Signal Connection Box
SD_{AVG}	Average of the shrinkage deformations
SG	Strain Gauge
SHM	Structural Health Monitoring
SPR	Statistical Pattern Recognition
$T_{lifetime}$	Structure lifetime
T_{max}	Maximum shade air temperature with an annual probability of being exceeded of 0,02 (equivalent to a mean return period of 50 years)
T_{min}	Minimum shade air temperature with an annual probability of being exceeded of 0,02 (equivalent to a mean return period of 50 years)
T_0	Initial temperature when structural element is restrained
VD	Vertical Displacement
VI	Virtual Instrument
VIF	Variance Inflation Factor
V14S	South Viaduct 14
V1N	North Viaduct 1

V1S	South Viaduct 1
V2N	North Viaduct 2
V3N	North Viaduct 3
Y_0	Threshold value for the strain amplitude

Small Latin letters

$c_{j,p}$	Polynomial coefficient ‘p’ of the polynomial ‘j’
$f(x)$	Probability density function
f_{ck}	Characteristic compressive cylinder strength of concrete at 28 days
f_{cm}	Mean value of concrete cylinder compressive strength
$f_{cm,cyl}$	Concrete cylinder strength at the age of 28 days
$f_{cm}(t)$	Compressive strength at a given age t
$k_{cc,0}$	Adjustment parameter for creep at infinite time
$k_{cc,t}$	Adjustment parameter for creep evolution
$k_{cs,0}$	Adjustment parameter for shrinkage at infinite time
$k_{cs,t}$	Adjustment parameter for shrinkage evolution
k_s	Subgrade reaction module
k_0	Sensitivity parameter
k_1	Load length correction
$k_2(t)$	Modulus of elasticity correction at a given age t
s	coefficient which depends on the type of cement
w_i	Weight coefficient
$x_{measure,i}(t)$	Time series of the independent variable ‘i’
$y_{measure}(t)$	Time series of the dependent variable
$y_{model}(t)$	Prediction model

Capital Greek letters

Δt	Elapsed time
ΔT	Linear temperature difference
$\Delta T_{M,cool}$	Linear temperature difference component (cooling)
$\Delta T_{M,heat}$	Linear temperature difference component (heating)

Greek case letters

α_c	Coefficient of linear expansion of concrete
α_{wire}	Coefficient of linear expansion of the strain gauge's wire
$\beta_s(t)$	Time factor for shrinkage/creep strain
δ	Bridge deflection
ε	Error
ε_{ca}	Autogenous shrinkage strain
ε_{cc}	Creep strain
ε_{cd}	Drying shrinkage strain
ε_{ci}	Instantaneous deformation
ε_{cs}	Total shrinkage strain
$\varepsilon_{c,\infty}$	Nominal coefficient for shrinkage/creep strain
ε_{cT}	Concrete strain due to temperature
$\varphi(t,t_0)$	Creep coefficient, defining creep between times t and t_0, related to elastic deformation at 28 days
κ	curvature
μ	Coefficient of friction between the tendons and their ducts

θ	Rotation
σ_c	Compressive stress in the concrete
τ	Observation period

“Where There's A Will,

There's A Way.”

Unknown author

1. INTRODUCTION

1.1. BRIDGES, AFTER ALL WHAT ARE THEY?

Since the first log fell across water, people have been fascinated with bridges and their power to bring together what had been separated by nature. Bridges can evoke exhilaration, triumph, and fear, sometimes simultaneously (Figure 1.1). Bridges span history. They have been built, burned, defended, crossed by athletes, as well as by those of us who commute to work each day. Their story has been shaped by the elemental barrier of water and by the cities that grew up along the world's great waterways. Their many sizes and silhouettes reflect the unfolding of mankind's knowledge of technology and building materials, as well as the influence of military conquest, religious belief, and economics (Dupré 1997). Bridges appear to ordinary people as works of art, stimulus for contemplation, theme of creation and dreams. From the engineering point of view, they are often associated with moments of scientific innovation and technological advance, as they impose increasing challenges as far as grandeur and simplicity are concerned (Azeredo and Azeredo 2002).

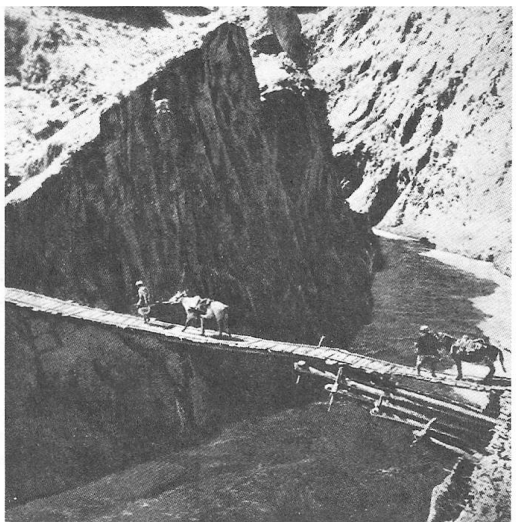

Figure 1.1 : Wooden bridge in India (photo SETRA cited in (Bernard-Gely *et al.* 1994)).

1.2. HISTORICAL NOTE ON LARGE-SCALE BRIDGES IN PORTUGAL

1.2.1. BEFORE THE REVOLUTION OF 1910 [2]

Portugal, along its history, has been gifted in what concerns to bridges. Namely, since the Industrial Revolution in the XIX century, the enchantment by that material so called steel have been produced the most extraordinary transformations in the construction systems. Since then, large-scale bridges have marked the Portuguese history in an irreversible manner and contributed for the change of the socio-economic paradigm.

With the political revolution of 1820[3], it was recognized the inexistence of lines of communication, which later in 1852 resulted in a governmental program to modernize strategic areas to foster development. One of the focuses of this program was to improve significantly the railway and roadway networks, which at that period and comparing with other countries of Europe, Portugal was significantly undeveloped. For that purpose, Portugal asked for external funds. However, they were extremely difficult to achieve for roadway projects because they were not seen as a profitable investment.

In this context, the railway network took advantage in a first stage, with a vigorous debate concerning two possible connections: (i) Lisbon-Porto line, to connect the two major cities of Portugal and (ii) Lisbon-Badajoz line, in order to restore the international status of the Lisbon harbour (it is interesting to observe that recently this same discussion was performed concerning the TGV network project).

During the second half of the XIX century and without precedents in Portugal, a large number of bridges, tunnels and stations were built. In 1859, the company *Companhia Real dos Caminhos de Ferro*[4] was formalized, which brought an important dynamism for this huge project. The employment and labour market had changed irreversibly, with the shift of farmer workers for the sector of the public works (Saraiva *et al.* 1983). During this period of the XIX century, the erection of two large-scale bridges has marked the country – *D. Maria Pia Bridge* and *Luiz I Bridge*.

[2] The revolution of 1910 was a republican coup d'état that occurred in Portugal on 5 October 1910, which deposed King Manuel II and established the Portuguese First Republic.
[3] The Liberal Revolution started with a military insurrection in the city of Porto that quickly and peacefully spread to the rest of the country, resulting in the return of the Portuguese Court to Portugal from Brazil in 1821. The movement's liberal ideas had an important influence on Portuguese society and political organization in the nineteenth century.
[4] The first public company that was responsible for the management of the Portuguese railway network.

- **D. Maria Pia Bridge**

D. Maria Pia Bridge was the first large-scale railway bridge built in Portugal, more precisely in the city of Porto (Figure 1.2). With this bridge, the construction of the fifth section of the north and east railway network was concluded. The connection of the two major cities – Porto and Lisbon – was finally achieved with the construction of this magnificent steel structure, designed by the French engineering Gustave Eiffel (1832-1923).

On the morning of November 5, 1877, the city woke up with flags and blankets in the windows while bandstands and podiums were flagged to receive the people for the opening celebrations of the new bridge. More than 300 boats decorated with streamers and pennants were floating and coiling on the River Douro full of spectators. During that day, more than 50 000 people were in the river hills, to admire the new bridge, which seemed to them more as a fantastic creation than an effective reality. For the official inauguration ceremony, more than 1 000 guests of honour were present in the *Devesas*[5] station at 11 h waiting for the train that would cross the bridge for the first time. Ministers from England, Austria, Germany, and Italy were among the special guests (Diario de Noticias 1877). The first to cross the new bridge were the royal family and some of the honour guests in a train of six carriages and a salon-car. The train left the station under saluting music and during the 55 seconds that took to cross it, the thousands of people spread around the bridge expressed their happiness waving white hankies and saying effusive *Viva!*[6]. Afterwards, a second train of 24 carriages, with a total length equivalent to 2/3 of the span length, crossed the bridge with more than 1 200 passengers. Even with the long train heavily loaded, the passengers did not fill any oscillation or crackles that were usual to ear in this type of structures, which seemed more as solid rock. After the official inauguration, a banquet for 600 people was prepared for the guests. In the streets, the population had to face the increase of bread price that more than tripled, from the 15 to 50 *reis*[7]. Curiously, during the banquet, Gustave Eiffel saw the opportunity to present to the royal family its project for the future *D. Luiz I Bridge*. Kindly, they accepted the project for appreciation (O Commercio do Porto 1877). However, Gustave Eiffel would not succeed in its intention for this new bridge, which would substitute the Pensil one.

[5] The first station, at that time, in the south side of the River Douro.
[6] A typical Portuguese expression for saluting.
[7] The unit of currency of Portugal from around 1430 to 1911.

At the end of that day, at 21 h, a firework show of almost 2 h 30 m closed the inauguration ceremonies. It was an unforgettable festival night with the riversides and the *Serra do Pilar* Church illuminated, offering an astounding view for those that were present and lived this astonishing event (O Commercio do Porto 1877).

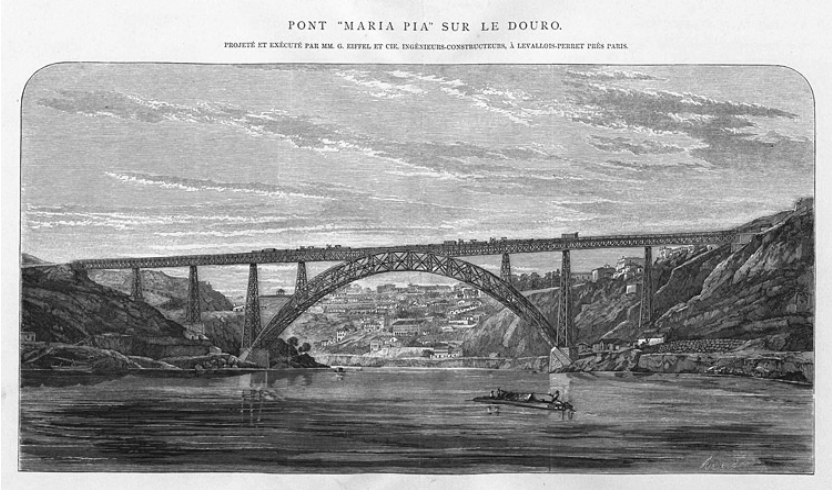

Figure 1.2 : D. Maria Pia Bridge (Eiffel 1879).

- **D. Luiz I Bridge**

As aforementioned, the funds for roadway projects were scarce in those days. Consequently, the construction of large-scale bridges for this type of infrastructures was rare. One notable exception was the construction of the roadway *Luiz I Bridge*, which was, in a certain way, a consequence of the construction of *D. Maria Pia Bridge* nine years before (Saraiva *et al.* 1983). Designed by Téophile Seyring (1843-1923), a co-worker of Gustave Eiffel, *Luiz I Bridge* was one of the most flamboyant bridges of its time. It was contracted on November 28, 1881, to the Belgian company Willebroek S.A. by the amount of 369 000 *reais*, excepting expropriations and complementary works (Diário de Notícias 1886).

On the opening date of the upper span deck[8], October 31, 1886, and similar to *D. Maria Pia Bridge*, the bridge was fully decorated with flags and pennants and the houses near the

[8] The inferior span deck was only opened to traffic later.

bridge had their windows decorated with blankets and flags with the presence of their house madams. The daily edition of the newspaper *O Commercio do Porto* wrote enthusiastically how the modern engineering was winning to what it seemed to be insurmountable (Figure 1.3).

O Commercio do Porto.

XXXIII ANNO — PREÇO DA ASSIGNATURA — FUNDADORES H. C. E MIRANDA E M. S. CARQUEJA — PREÇO DOS ANNUNCIOS — NUMERO 270

SEGUNDA-FEIR 1 DE NOVEMBRO DE 1886

PORTO, 1 DE NOVEMBRO

REVISTA POLITICA

Inauguração da ponte Luiz I

Gloria, pois, é sciencia inexgotavel! Gloria á engenharia moderna, para as quaes não ha difficuldades que as não vençam, precipicios que não as transponham, aoudibeiras que não se abram á passagem triumphal dos grandes vahiculos da civilisação!

INTERIOR

PROVINCIAS

Figure 1.3 : Newspaper edition of *O Commercio do Porto* of October 31, 1886.

At 4 h 29 m, a procession from the Porto bank to the Gaia side was performed to inaugurate the bridge. When the procession reached to the middle of the bridge, cardinal D. Américo gave his blessing and on that precisely moment, shots were fired by the artillery and the bells of the *Serra do Pilar* church and the *Santa Clara* Monastery blew effusively. With the bridge officially inaugurated, people marched across the upper span deck enthusiastically. Amidst the generated fuss, a temporary moment of panic append due to a small oscillation of the upper deck. People ran chaotically and screaming in view of possible collapse. However, shortly after everything returned to the normality and the bridge safety was never put in danger. Unknown at that time, these oscillations were induced by resonance derived from the people crossing that led to a dynamic response of the structure. In that day, the traffic was not allowed due to the thousands of people that wanted to cross the bridge (O Commercio do Porto 1886). Curiously, tolls were in practice from the bridge opening to 1943.

- **The most significant changes**

Despite the scarcity of funding for roadway projects, Minister Fontes Pereira de Melo (1819-1887) of the Ministry for Public Works fostered the construction of both networks with modern and bold solutions. Perhaps, *D. Maria Pia Bridge* and *Luiz I Bridge* were the highest expression during this period. In 1854, the extension of the railway network was as short as 36 km long, while the public roadway network had a mere 218 km in 1852. Curiously and ironically, these poor communication networks allied with rigorous winters were an advantage for the country during the French invasions in the first half of the XIX century (Tormenta and Fiéis 2005). During the following forty years, 2 000 km of railway lines were built, reaching a total extension of 3 407 km in 1934, while as far as the roadway network was concerned, 200 km/year were built during the following 30 years, leading to a total length of 11 754 km in 1907. These numbers are in fact impressive.

From another perspective, these numbers represented an utmost significant transformation of the Portuguese society that some called as the *train revolution*. Some of the most significant transformations were: (i) the Lisbon population more than doubled between 1864 and 1890, from 160 000 habitants to 391 000 habitants; (ii) the transportation facilities increased the commercial value of farming products – whose trade volume quadruplicated, from 663 000 ton to 2 316 000 ton – and the number of passengers has tripled, from 2.1 million to 6 million (Saraiva *et al.* 1983). The construction of *D. Maria Pia Bridge* and *Luiz I Bridge* were without any doubt vital infrastructures for the country development.

1.2.2. AFTER THE REVOLUTION OF 1910

After the advances achieved during the XIX century, the instability that the country lived in the beginning of the XX century, due to the end of the monarchy in 1910, led to a stagnation of the country. A new impulse was only made in 1935, when the Portuguese government implemented a program so called *Lei da Reconstituição Económica*[9]. An amount without precedents of 6 500 millions *escudos*[10] was applied in several fields

[9] National project that focussed the retool of the Army and the recover of the economy.
[10] The unit of currency of Portugal from 1911 to 2002.

namely in the construction of new roadway and railway lines, bridges, airports, schools, dams, etc. In what regards the roadway network, which had no progress since 1910, its extension grew from the 13 000 km to 32 000 km in the 60s, with the construction of 392 new bridges between 1926 and 1966 (Saraiva *et al.* 1983). Among all these bridges, two of them deserve distinction by their engineering innovations and large-scale – *Arrábida Bridge* and *25 de Abril Bridge*.

For that, a new structural material so called concrete that appeared in the beginning of the XX century had contributed in an irreversible manner for the bridge construction. The firsts bridges made with this material were arch bridges due to its high compressive strength and low resistance to axial tension forces. *Arrábida Bridge* is one of those examples. However, its application to bridge construction exploded only after the World War II (Fernandez Troyano 2004).

- **Arrábida Bridge**

In the decade of 1930, half-century afterwards the inauguration of *Luiz I Bridge*, a new bridge was demanded to relief the traffic between the cities of Porto and Gaia. This new bridge was officially reported on the *Plano de Melhoramentos*[11] *in 1956* (Portugal - Ministério das Obras Públicas 1956), and it was part of the motorway project that would link the cities of Porto and Lisbon (nowadays labelled as A1). The first's kilometres of this connection were built at south, 37 km between Lisbon and Vila Franca de Xira. A new dimension of the national roadway network was being achieved, which was only possible with the construction of a new bridge crossing the River Douro – *Arrábida Bridge*.

The bridge construction was a hard job order due to the adverse environmental conditions. During that time, the workers had to face rigorous winters with low temperatures, strong winds and long periods of rain, with several events of suspended works due to adverse climate conditions. This fact was highlighted by the president of the *Junta Autónoma das Estradas*[12], General Flávio dos Santos, referring how difficult it was always to transpose the River Douro since the roman invasions (137 b.c.). Curiously and ironically, a boat that

[11] Program implemented by the Portuguese government in 1956 to regenerate the construction and urbanism of the Porto city.
[12] Public company owned by the Government of Portugal that existed from 1927 until 1999 and was responsible for the development, planning and maintenance of the roadway network of Portugal.

by chance was so called Eiffel (name of the designer of *D. Maria Pia Bridge*), crashed to the falsework structure that supported the arch construction (O Seculo 1963).

The constructive process was complex, in part due to the properties of this recent material concrete. Particular emphasis was given to the positioning and ripping of the metallic falsework, the concreting of the arch and the respective close segment (Figure 1.4). Thousands of people witnessed these operations with the international press speculating the possibility of the biggest arch made of concrete, ever built at that time, might crash during its construction. For the first time, an arch was concreted over a deformable metallic falsework of 2 200 ton, where the elastic deformations of this support system was carefully taken into account. Regarding the close segment, a meticulous geometric control was performed due to the effects of the sun exposure and the wind speed on the edge faces of the arch-consoles. The close segment was precisely positioned with a space-gap of only 30 cm (O Seculo 1963). All these aspects were studied and supervised by the bridge designer Edgar Cardoso (1913-2000), one of the most brilliant Portuguese Civil Engineer.

On the opening day, June 22, 1963, several distinguished guests, of the engineering technical and scientific communities, were present such as professor Hubert Ruesch from Munique, professor Carlos Fernando Casado from Madrid, professor Ives Guion from Paris, A. L. L. Baker from London, professor Franco Levi from Turim, professor Georg Wastlund from Stockholm and professor Fritz Stussi from Zurique (O Seculo 1963).

Again, the inauguration of this new bridge brought together the Portuguese people, where 250 vehicles of fire brigades from all parts of the country were presented to participate in the ceremony. More than 1 000 bridge workers were also present to be decorated with honour medals offered by the Portuguese government through the hands of the president of the Portuguese Republic. Even the seven mortal victims during the construction were remembered in that day. Four widows received the respective honour medals, in a moment of great commotion. At the end, the president crossed the bridge by walking from Porto to Gaia, and when he reached to the mid-span, he approached to right balcony to enjoy the magnificent panorama. In that precise moment, the trumpets of some vessels sounded in a prolonged way[13]. As the President reached to the south side, at the Gaia city, thousand of pigeons were released to mark the bridge opening (O Seculo 1963).

[13] Traditional salutation, in that epoch and in some countries of Europe.

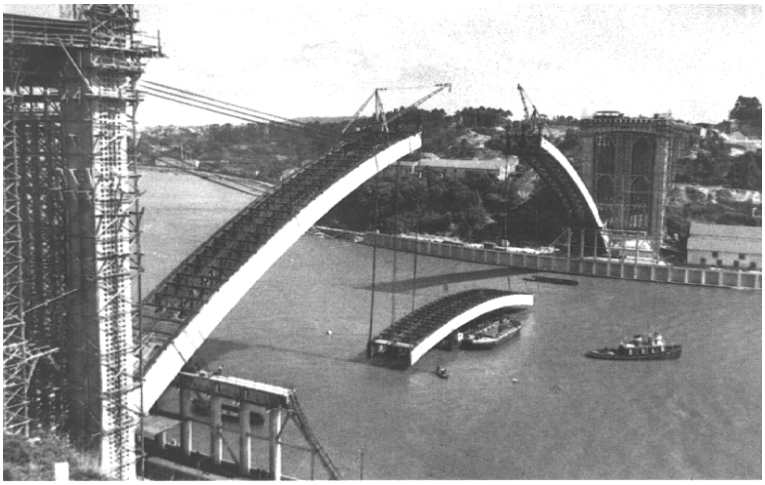

Figure 1.4 : Arrábida Bridge – positioning of the metallic falseworking (Azeredo 1998).

- **25 de Abril Bridge**

During this period, Porto was three bridges ahead of Lisbon in the construction of large-scale bridges. However, and almost a century after the initial aim, the bridge over the Tagus became a reality and the dream of Miguel Pais[14] (1825-88) was finally achieved.

In 1933, the Minister of Public Works Ministry, Duarte Pacheco (1900-1943), created a commission to analyse the request for the construction of a bridge over the River Tagus at Lisbon. The commission reported in 1934, the intention to build a road and rail bridge. Bids were obtained however, due to the Europe instability because of World War II, this proposal was subsequently put aside in favour of a bridge crossing the river at 35 km north of Lisbon, in Vila Franca de Xira. Nevertheless, in 1953 a new government commission was created that, in 1958, recommended again the construction of the bridge over Tagus in Lisbon. One year later, the international tender for the project received four bids. The winning consortium was announced in 1960, the American company United States Steel Export Company, which curiously had submitted a bid in 1935. The construction started in November 5, 1962, and the bridge was erected during the following 45 months (Figure 1.5).

On the opening day, August 6, 1966, Roger M. Blought, chairman board of the United States Steel Export Company, referred that this bridge represent the work capacity of

[14] Portuguese engineering of the XIX century that for the first time had suggested the construction of a bridge over the River Tagus linking the cities of Lisbon and Montijo.

different people, from two different hemispheres, carrying on the closest collaboration of hundreds of people during long years. This collaboration, supervised by Eng. Canto Moniz, the office director of the bridge construction, was a great success, with the construction ending six months ahead of the construction deadline. The whole government was present in that day near the tolls. One hundred million of Europeans saw by television the opening ceremony of the biggest and beautiful bridge of the Old Continent. The expectation of the population, namely of the south bank of Almada city, was so huge that thousands of people were present to see the bridge opening. José da Glória Pacheco, mayor of Almada, highlighted proudly how the best beaches of Portugal, at Costa da Caparica, would benefit with this bridge, allowing people from Lisbon to access them in less than 20 min, something impossible before this bridge became a reality.

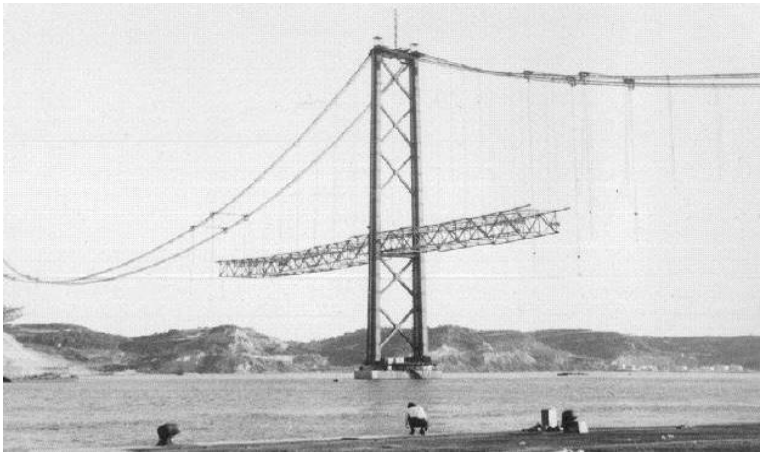

Figure 1.5 : 25 de Abril Bridge (ambiente2008 2009).

The bridge inauguration plate states that more than 3 000 workers were involved in the construction with reference to the names of the four mortal victims, names were referred, one by one, by Eng. Canto Moniz during the opening ceremony. Again, as in *Arrábida Bridge*, the Head of State rewarded those that anonymously collaborated in this gigantic bridge.

The population expectation was so huge that during the first hour, 10 000 vehicles crossed the bridge, carrying approximately 50 000 people. The importance of this new bridge was so huge that three days of celebrations were pronounced to commemorate this new national jewel (O Seculo 1966).

1.2.3. AFTER JOINING IN THE EUROPEAN ECONOMIC COMMUNITY IN 1986

More recently, after joining the European Economic Community in 1986, the construction of large-scale infrastructures has registered an exponential increase. European structural funds gave a new impulse in the modernization of the country, where the national roadways network had largely benefit with the construction of new motorways and consequently, the construction of a high number of bridges.

The design of these new bridges took into account the evolution of concrete technology. The combination of concrete and high strength steel has increased the structural capabilities, namely the resistance to bending forces. Prestressed concrete emerged as the main structural material for bridge construction. With this perfect mix, new thinner shapes, longer spans and shorter time schedules became possible and, once again, the bridge construction paradigm in Portugal was changed.

- **Vasco da Gama Bridge**

The greatest bridge ever built in Portugal was, until now, *Vasco da Gama Bridge*. With a total length of 18 km, this bridge brought a new connection in the oriental zone of Lisbon (Figure 1.6). This huge bridge, with various political promoters, was a product of 250 people that collaborated in the project design (Diario de Noticias 1998). This bridge was part of the requalification project of the oriental zone of the city, and was one of the ex-libris built for the EXPO'98.

To make this bridge a reality, seven building sites supported its erection, which metaphorically implied the setting up of authentic villages to support the bridge construction. Due to the bridge extension, precast elements were used to partially build the girder deck. In fact, precast elements began to be increasingly applied in bridge construction to render larger bridge extensions possible, which was only possible by using prestressing concrete. Construction was practically all over water and, for that, 30 boats, mostly tugboats, supported the construction. Among them, a boat called *Rambiz* was crucial in the positioning of 150 beams with 80 m of length each. This boat and the 3 000 workers that collaborated in the construction were the heroes of this construction. With the technological evolution since the last decade of the XX century, this bridge presented some

interesting innovations, namely: (i) the 87 video cameras that were installed to supervise traffic in all bridge length, (ii) the 37 SOS call boxes positioned every 400 m, (iii) the two weather stations in order to prevent potential accidents due to environmental effects and (iv) variable message panels to give real time information to the users (Diario de Noticias 1998).

Figure 1.6 : Vasco da Gama Bridge (Top 10 Places 2012).

Again, the inauguration was celebrated with the Portuguese people, where a giant meal was prepared and served over the girder deck, in a table with 5 050 m length for 15 000 people. A Guinness Book registered world record. The international press cover was significant, with newspapers from Brazil, France, Germany or television channels such as TVE or BBC for examples (Diario de Noticias 1998). Again, Portugal was in the mouth of the world due to its remarkable bridges. Since April 4, 1998, when it was inaugurated, Portugal has, until now, the longest bridge in Europe.

- **Lezíria Bridge**

Lezíria Bridge, with 12 km, is the latest large-scale bridge built in Portugal (Figure 1.7). The fourth bridge crossing the estuary of the River Tagus is one of the longest bridges in the world, the second largest bridge of Europe, after *Vasco da Gama Bridge*. During 23 months, the Portuguese Engineering erected one of the greatest constructions of the XXI century. With a cost of approximately 200 millions of euros, this bridge opened to traffic in

July 7, 2007, making it possible to travel by motorway from north to south and east to west without passing through Lisbon and releasing the city from outside traffic.

Figure 1.7 : Lezíria Bridge at May 2007 (© F. Piqueiro / Foto Engenho).

Besides the video cameras, SOS call boxes, weather station and variable message panels, this bridge introduced two important innovations: (i) it was the first to have a 'free flow' tolling system in Portugal. This system allows tolling with the vehicles at full speed. Nowadays this system is commonly used in several motorways; (ii) Another relevant innovation concerns a system that was installed to assess the health of the bridge along its lifetime. Almost 400 sensors were spread along the bridge delivering measurements capable of providing relevant information regarding its maintenance, thus avoiding the development of malfunctions.

1.2.4. SUMMARY OF THE MOST EMBLEMATIC LARGE-SCALE BRIDGES IN PORTUGAL

Figure 1.8 resumes the location and inauguration dates of all the bridges previously referred, as well as some others that by their socio-economic relevance are also briefly pointed:

- *Freixo* and *S. João* bridges as well as *Infante D. Henrique Bridge*, are the other three large-scale bridges built in Porto over the Douro that changed profoundly the life habits of the population;
- *Miguel Torga Bridge*, located in the vineyard region of the famous O'Porto wine;
- *Edgar Cardoso Bridge*, located at Figueira da Foz, is a fairly tribute to the engineering talent of Edgar Cardoso;
- *Salgueiro Maia Bridge* at Santarém is a tribute to one of the most prominent officers involved in the Carnation Revolution of April 25, 1974 and;
- *Sado Bridge*, recently built in Alcácer, as part of the requalification of the high-speed railway network;
- *Guadiana International Bridge* that establish the link between Portugal and Spain in the tourist region of the Algarve.

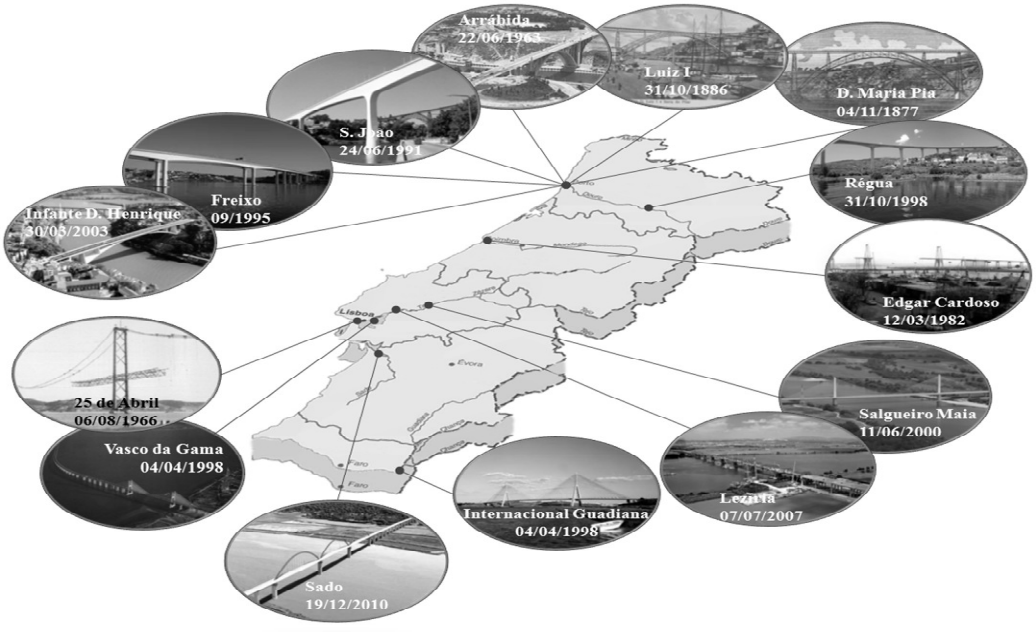

Figure 1.8 : Emblematic large-scale bridges in Portugal.

1.2.5. BRIDGE ACCIDENTS

More than one and a half century have passed since the construction of *D. Maria Pia Bridge*, in 1877, and the infrastructure park has grown exponentially, and inevitably has been subjected to progressive ageing. Moreover, ageing, if not controlled, most likely leads to extreme scenarios including failure.

Eventually, the worst memory related to bridge disasters has occurred not so long ago. In March 4, 2001, the second bridge built over River Douro – *Hintze Ribeiro Bridge* (1888) – collapsed (Figure 1.9). More than the economic costs, the 59 mortal victims, some of them never found, and the suffering of their families showed the magnitude of this sad tragedy. At that time, several causes were pointed as reasons for the collapse namely: (i) the water level and velocity, (ii) the river flood, (iii) the bridge aging, (iv) the traffic weight that was much higher than its initial, (v) the sand dredging, (vi) the constructive process (Jornal de Notícias 2001b). Since then, the surveillance and maintenance procedures have been reinforced. A national inventory of the existent bridges, similar to the collapsed *Hintze-Ribeiro Bridge*, was ordered by the authorities (Jornal de Notícias 2001d). However, and unfortunately, *Hintze Ribeiro Bridge* was not an isolated case. In the same year, the centenary *Lavandeiras Bridge*, located at Montemor-o-Velho, collapsed due to the river floods (Jornal de Notícias 2001c). On September 7, 2003, a pedestrian passage over the motorway IC19 in Lisbon also collapsed hurting two people.

a) aerial view (infopédia 2001).

b) closer view (Monumentos Desaparecidos 2009).

Figure 1.9 : Collapse of Hintze-Ribeiro Bridge (March 4, 2001).

Other bridges with anomalies were also reported during the first decade of the XX century. The bridge that crosses the River Tagus in Constância, Santarém, was identified as

problematic in 2001. The 4 000 vehicles per day, much of them concerning heavy traffic, the bridge age of 150 years and the single lane for traffic circulation were critical aspects that were taken into account to proceed a detailed inspection of the bridge health (Jornal de Notícias 2001f). In fact, the bridge was closed for rehabilitation in July 21, 2010 and it was only opened to traffic in March 2011, even though with prohibition for heavy traffic (Jornal de Notícias 2011). *Portimão Bridge* in Algarve was another similar case. Closed to traffic in 2007 due to problems in the piers foundations, the cost of repair and strengthening of all piers was estimated in 3 millions euros (Sol 2007).

Besides these two cases, other bridges were inspected due to their age. *Pinhão Bridge*, built in the beginning of the XX century and located in the heart of the DOC[15] vineyard region, is another important bridge crossing the River Douro that was recently rehabilitated. The degradation and oxidation that the structure exhibited in addition to the heavy traffic, namely due to the wine production, were determinant aspects to proceed with the structure rehabilitation (Jornal de Notícias 2001a). *Arrábida Bridge* was also recently rehabilitated. A study performed by Júlio Appleton and Manuel Carvalho, for *ICOR – Instituto para a Construção Rodoviária*[16], referred that in spite the good health of the bridge, degradation signs concerning structural aspects were identified as a result of ageing. It was recommended to replace the joint displacements as well as the drainage system (Jornal de Noticias 2001). Another emblematic bridge that was repaired and strengthened was *Luiz I Bridge*, in part to be capable to receive the subway transportations (Jornal de Notícias 2001e).

The bridges previously referred are a small sample of Portugal's large set of infrastructure assets. In 2007, *Estradas de Portugal*[17] was responsible for the management of 5 625 bridges, where 415 of them were identified as exhibiting anomalies. For the year 2007, this company estimated an investment of 26 millions euros to be applied in the bridge rehabilitation (Sol 2007). A similar example is concerned with the privately held BRISA[18]. This company was responsible for the management of 1 600 bridges in 2004,

[15] Portuguese abbreviation for "Denomination of Controlled Origin".

[16] Public company that existed between 1999 and 2002, responsible for construction of new roadways and tunnels, repair and rehabilitation of existing roadways and bridges, supervision and technical assistance in the implementation and execution of roadway projects.

[17] Private company with public funds, created in 2007, responsible financing, maintenance, operation, improvement and extension of roads that make up the National Road Network and secondly, the conception, design, construction, financing, maintenance, operation, improvement and widening of roads that make up the National Road Network Future.

[18] Private company, created in 1972, responsible for construction and operation of toll motorways.

which has increased for 2 661 bridges in the current year of 2011 (source BEG[19], 2011). This represents an increase of 66 % only in seven years.

To sum up, and based on the Portuguese case herein journalistically reported, bridges are more than they appear to be. They are (i) means of crossing rivers, behaving as ground over water saving time and money to travelling people; (ii) they are also a landscape object, with a unique capability of beautifying and promoting the regions to which they belong; (iii) but they do also reflect the result of an engineering work, where knowledge of the materials behaviour and their resistance is the fundamental key; (iv) finally, they reflect human heritage, because they transport history, they become monuments of their regions and purposes of tourism activities (Fernandez Troyano 2004).

In this context, since the beginning of the XXI century bridges with malfunctions have become a serious problem, where the attention concerning the health of the bridges was never so focussed by the media and the society. Therefore, it is a moral, social and economic responsibility to watch, preserve and supervise these unique infrastructures – bridges – and, more than ever before, to exert, efficient vigilance and perform adequate maintenance became mandatory procedures and are to be continuously developed and effectively implemented.

1.3. RESEARCH BACKGROUNG

Currently, Structural Health Monitoring (SHM) is one of the topics with greater development among research activities in civil engineering. Several guidelines focussing this theme have been published worldwide (BRITE/EURAM 1997; Mufti 2001; Bergmeister *et al.* 2002; Aktan *et al.* 2003; Andersen and Fustinoni 2006; Rucker *et al.* 2006). Drawing an analogy with the medical diagnosis of human diseases (Figure 1.10), today's engineers need to be able to check on the prevailing condition of bridges and structures. Medical doctors use specialized equipment to check a patient's health parameters, and thereby monitor the patient's health. Civil engineers use specialized sensors embedded in a structure to take a reading on the structural health of that facility. If

[19] Brisa Engenharia e Gestão.

a patient's blood pressure is too high, the doctor prescribes corrective medicine. Similarly, in SHM, if the data flowing from the sensors indicates excessive stress on the structure, the engineer can act appropriately to correct the situation. In both cases, immediate action prevents catastrophic consequences. Annual check-ups by a personal doctor are now a routine form of preventative maintenance. Similarly, SHM of infrastructure is going to be commonplace in the not too distant future to provide check-ups as a form of preventive maintenance. It is an emerging technology of great value to those responsible for the safety and well-being of civil engineering structures (Mufti 2001).

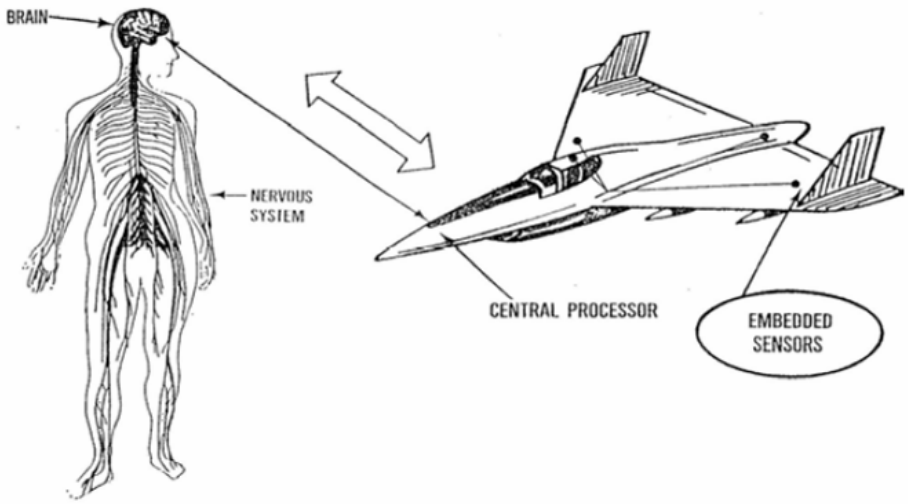

Figure 1.10 : Analogy between the nervous system of man and a structure with SHM (ROGERS 1993) (cited in (Balageas *et al.* 2006)).

Historically, SHM is a recent field of research that matured in the final decade of the last century. The need for conferences totally devoted to SHM gave birth in 1997 to the International Workshop on SHM (IWSHM), created by Professor Fu-Kuo Chang (Balageas *et al.* 2006). However, the earlier steps towards proper SHM (although not expressed like this at the time) possibly dates back much earlier than the 1980s when this specific terminology was created. Indeed, it may date to the origins of structural engineering (Boller *et al.* 2009). SHM is a multidisciplinary domain, mainly applied to aerospace, mechanical and civil engineering fields, where researchers and engineers from various classical disciplines – such as structural vibration analysis, structural control, non-destructive evaluation, material science, signal processing, sensors/actuators technology – work together with the aim of assessing and monitor structural health (Balageas *et al.*

2006; Farrar and Worden 2007). The booming in the development of sensing technology – with sensors constantly decreasing in size and cost –, and their combination – with microprocessors with increasing power and enhanced materials design and manufacturing (in terms of functional materials or even electronic textiles) – have opened avenues in merging structural design and maintenance with those advanced sensing, signal processing, and materials manufacturing technologies. Taking advantage of such wide integration is what SHM is about (Boller *et al.* 2009).

At present, long-term monitoring systems are becoming mandatory in major civil engineering structures such as bridges, tunnels and dams. These systems begin to be seen as much an integral part of the structures they incorporate as their concrete and/or steel components. Generally, they monitor a set of physical, chemical and mechanical parameters in critical sections of the structure by incorporating appropriate sensors.

The actual structural state can be evaluated by measurements of strain, deflection, curvature, inclination, temperature or other parameters, taken on selected locations. This may result in conclusions about pathologies of various forms, e.g. foundation settlement, global changes in stiffness, loss of continuous beam effect etc. (Rucker *et al.* 2006). For example, vibrations, temperature and settlements can typically lead to damages such as fatigue, cracks and deformations. The detection of these damages can be carried out by advanced computer analysis of the data collected by the Structural Health Monitoring Systems (SHMS) (Andersen and Fustinoni 2006). These data have shown high potential. In fact, the less we know about the operational conditions of a structure and the performance of materials and structures, the higher the safety factor will have to be. This illustrates the risk and dilemma of Structural Engineering design (Boller *et al.* 2009). Therefore, the potential knowledge that is inside of the monitoring data can contribute for a better understanding of the structural behaviour and therefore, to more efficient structural design and management.

Even an expert analyst may not be able to replicate actual bridge behaviour through mathematical models due to the non-consideration of certain aspects with direct influence in structural behaviour. There is no better way to understand the shortcomings of the mathematical models used for the design or evaluation of bridges than to compare the analytical predictions with the observed behaviour. As an example, in Ontario, Canada, the Structures Research Office of the Ministry of Transportation has conducted for many years

a program of field-testing of bridges. Several significant *surprises* encountered during bridge testing in Ontario have been reported, where the instruments sometimes seem to *lie*. It is tempting to disregard such readings as being the result of an instrument malfunction. In most cases, however, it was found that the unexpected readings from the instruments were in fact caused by unexpected bridge behaviour (Mufti 2001). Thinking rationally, sensors do not know how to *lie*. Moreover, the collected monitoring data can be also useful for future structures.

An interesting case is reported concerning the monitoring data of *Humber Bridge* (1981) in the United Kingdom. This data was subsequently used for validating the modelling procedures for simulating wind-induced response of the performance of a proposed 3300 m span for the Stretto di Messina (Strait of Messina) suspension bridge (Andersen and Fustinoni 2006).

However, multiple sensory systems, with different sampling rates, are commonly used for the same SHM project and therefore, the automatic processing of the measurements is mandatory, especially when the technology is constantly evolving. It is important that the system be able to process in an intelligent way the data from all inputs and relate it to a common reference such as a reference signal timing for example (Mufti 2001; Rucker *et al.* 2006).

The degree of complexity of the data processing will be dependent of the final target (Andersen *et al.* 2005): (i) in an operational level, the monitoring system must be supervised with data being continuously stored and automatic actions should be carried out such as dangerous wind speeds, traffic accidents, ship impact, etc.; (ii) at a tactical level, monitoring activities can be planned and the results analysed with the generation of statistical information; (iii) at a strategic level, information with relevance for management purposes should be delivered, which typically corresponds to aggregated data, the information not being required in real time. Figure 1.11 shows a scheme concerning the hierarchical organization of structural monitoring data.

In this context, the SHMS can act as an integrated part of the management system, similar to the inspections procedures. However, it shall be emphasized that one should not rely fully on the data and results from a SHMS, but on the combination of monitoring with inspections and data analysis done by experts (Andersen and Fustinoni 2006).

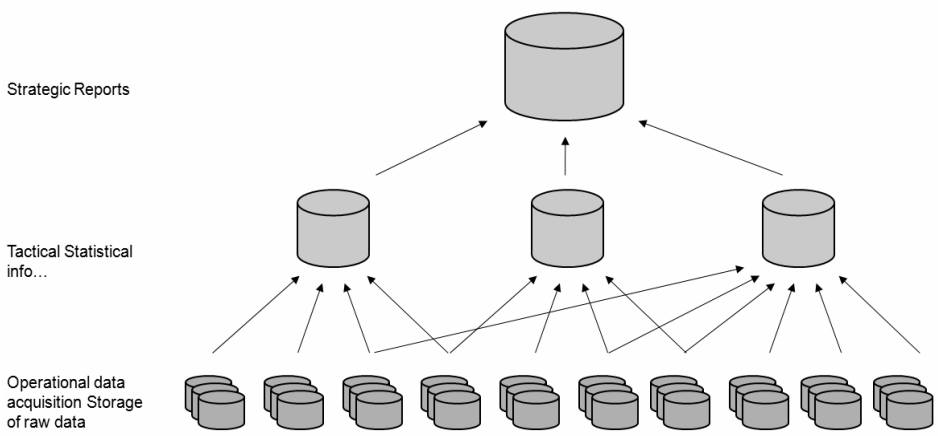

Figure 1.11 : Organizational levels of monitoring data (Andersen and Fustinoni 2006).

Moreover, the recent Model Code 2010 (FIB Commission on Practical Design 2010b) recommends for some situations the systematic monitoring of parameters allied to the planned periodic inspections. This confirms that the bridge management might in fact benefit with these systems in the long-term planning of preventive maintenance and in the day-to-day corrective maintenance.

However, the decision to invest on a SHM system for a given structure requires that the system provide a payback to the owners or to society in terms of reduced maintenance costs, overall lifetime costs, and/or increased structural safety. Establishing the cost *versus* benefit of a sensor system can be a nontrivial exercise (Huston 2011).

1.4. MOTIVATION AND RESEARCH OBJECTIVES

The usefulness and benefits of structural monitoring data may be recognized by many bridge stakeholders, such as designers, researchers and the authorities. In general, verification monitoring can be divided into three groups (Andersen and Fustinoni 2006): (i) *a priori* design verification – by validating modelling procedures for simulating loadings and responses through tests with mock-ups before construction or by measuring critical parameters on structures similar to the design under consideration (namely for designers); (ii) construction verification – useful to build the *history* of the structure and the construction work; (iii) *a posterior* design verification – classic use of structural

monitoring, stochastic load parameters and structural responses in comparison with the calculated response can be verified (namely for authorities and researchers).

However, the application of monitoring data for bridge management is not yet a straightforward exercise. The main reasons appear to be:

- The amount and variety of the collected data makes it difficult to establish standard procedures to analyse and extract objective information;
- Uncertainties concerning the effective behaviour of the structure, material properties, environmental conditions and loading, render the task even more difficult;
- Final target, if operational, tactical or management purpose, which dictates the level of complexity of the data processing.

In this context, the author believes that data-based engineering techniques that are being developed worldwide must be continuously improved, by taking advantage of the continuous evolution in technology, and stronger integration, in order to achieve procedures with higher levels of efficiency.

In fact, being it true that all sets of monitoring data enclose potential knowledge, it is even truer that, if such potential knowledge is not unveiled in a timely fashion, the collected data ceases to be useful. The size of databases grows continuously and without proper data management techniques, the collected data has the risk to be roughly analysed and therefore, the usefulness of this data can be questionable in the context of the bridge management. This has been recognized as future development by some researchers (Fraser 2006; Dimande 2010; Figueiredo 2010).

Classically, the condition assessment of a given structure might be performed by comparing monitoring results against Finite Element Models (FEM) that describe the predicted structural behaviour. FEM have been widely employed because they allow calculating the long-term behaviour of bridge structures, considering the influence of material properties, loading and environmental effects. Although this approach is the most reliable for the comprehension of the structure behaviour, the detailed analysis through FEM is a time-consuming process where some variables are difficult to simulate. A complementary approach for condition assessment can be made by using statistical and simplified mathematical models to discover regularities among the monitoring data and

trigger subsequent actions, such as classification, in order to establish alarm procedures if those health patterns change without apparent reason (Bishop 2006; Boller *et al.* 2009).

The advanced methods will typically be based on FEM, which can be calibrated and continuously updated based on the data collected by the SHMS, while complementary, but not less useful, engineering techniques will be used to find patterns in statistical and chronological data indicating damage at a structural section or component on the structure. With these potentialities, the development of new engineering techniques based on data collected by monitoring systems presents a promising future, which allied to the contributions of classical FEM analysis, will be the next step in the effective use of monitoring data for bridge management.

According to Rucker *et al.* (2006), during condition monitoring of structures, global and local structural properties can be evaluated based on continuously measured values with the aim of evaluate the current condition and to predict the future development and to identify and record gross changes in the structural behaviour.

Based on the previously enounced, the central theme of this thesis is to foster and reinforce the effective application of monitoring data for bridge management. In support of this work, a large-scale bridge – Lezíria Bridge – was equipped with an integrated monitoring system devoted to long-term analysis. The achievement of this purpose can be enounced in the following manner:

- To enumerate, describe and detail all the main phases of the implementation of an integrated monitoring system in a large-scale bridge regarding its life-cycle management;
- To develop and integrate the required data-based engineering techniques in a software system able to illustrate the implementation of the suggested approach;
- To build a detailed and rigorous FEM enabling the evaluation and discussion of the quality of the monitoring data extracted;
- To analyse and discuss the monitoring data in order to generate confidence for its effective use in the bridge management, based on the developed and implemented engineering techniques.

With these goals fulfilled, the author aims to show that the data collected by the monitoring system can be effectively used for the management of bridges and, specifically in this work, for Lezíria Bridge.

1.5. RESEARCH STRATEGY AND OUTLINE OF THE THESIS

The structure of this present thesis has been organized to be the result of a structured compilation of previously submitted papers. Indeed, six manuscripts were submitted beforehand for publication in international scientific journals in the field of civil engineering some of which have been already accepted or published. Each manuscript deals with a specific theme related with the monitoring of bridges, duly presented with the application to Lezíria Bridge. One advantage, of such an outline, is the possibility of almost independent reading of any specific chapter. Beyond the present introduction, which intends to give a higher consciousness concerning bridges as well as the definition of the main goals of this work, and a closing chapter that presents the main conclusions, this thesis is organized in seven chapters.

Chapter 2 presents the long-term monitoring system installed in the new Lezíria Bridge over the River Tagus in Portugal. The system was developed to control some aspects of the construction process and to survey the service life of the structure. A set of structural, durability and environmental parameters defining the bridge condition are remotely assessed in real time via an embedded fibre optic network. Aspects like architecture, installation and functionalities of the monitoring system are discussed, and the innovative aspects of the implementation are highlighted. In this context, the main goal of this chapter is to present the long-term monitoring system of Lezíria Bridge, sharing the experiences, the solutions and the procedures adopted, given their potential usefulness in implementing similar projects.

Chapter 3 presents the MENSUSMONITOR software, developed to assist in the data interpretation of structural behaviour using the records obtained from monitoring systems in an efficient manner. At present, monitoring systems are programmable and data obtained from the sensors can be automatically organized in computational data files. However, one of the main difficulties faced in this venture, is the processing of records

obtained from these systems without using specific engineering techniques. This is a time-consuming activity and, generally, the collected information is deficiently interpreted due to extensive tasks that are necessary to perform in order to produce an accurate analysis. Moreover, the size of the information obtained from these systems, generally, becomes extremely large. The available knowledge that can be obtained is enormous. However, in general, the interpretation of these results is very difficult and time-consuming. Due to the large data size, some results are not conveniently taken into account and therefore, some information is wasted. The application to the records derived from the monitoring system applied to full-scale bridge, namely the results from the load tests, is presented in this chapter to appraise the software performance.

Chapter 4 presents the appraisal of a statistical procedure for the long-term assessment of the structural behaviour. This procedure is based on prediction models, which establish the normal correlation patterns between environmental and material parameters (such as concrete temperature and shrinkage strains), and the observed structural response in terms of strains, rotations and movements of expansion joints. The calculation of the normal correlation pattern comprehends the minimization of a square error. By applying the prediction model to the structural response measured in the south approach viaduct of Lezíria Bridge, it was found that this methodology is a feasible tool for real time damage detection in bridges. The procedure was implemented in MENSUSMONITOR, improving the flexibility in the data handling and a faster data processing, with capabilities of real time visualization.

Chapter 5 focuses the deflections in bridge decks. The vertical displacements are one of the most desirable parameters to be assessed because their information reflects the global response of the bridge span. However, the implementation of systems to continuously and directly observe vertical displacements presents well-known difficulties. On the other hand, strain gauges and inclinometers are easier to install, but their measurements only provide indirect information regarding the bridge deflection. In this context, taking advantage of the information collected through strain gauges and inclinometers, and the present computer processing capabilities, a procedure to calculate deflections in bridge decks based on polynomial functions is presented. A beam model test and two full-scale bridges are used as case studies to evaluate the presented procedure. Finally, aiming at the assessment of bridge deflections based on measurements of strains and rotations, some

recommendations for future instrumentation plans are described based on the results analysis herein presented. The procedure was also implemented in MENSUSMONITOR.

Chapter 6 focuses the assessment of traffic load events and the structural effects. Current acquisition systems devoted to the monitoring of civil infrastructures allow reading sample rates up to 1 kHz, which allow for the detection of live different loads, such as traffic events – Bridge Weight-in-Motion (BWIM). Several technical and scientific publications have been made available for BWIM concerning railway bridges but have found no correspondence in road bridges. This chapter intends to make a contribution towards the latter. A procedure has been developed and fully detailed to support the assessment of traffic parameters such as load levels, speed and travelling direction based on strain gauge measurements and the Weibull distribution. Finally, extreme traffic loads are extrapolated for the lifetime of bridges. Numerical models, previously developed to evaluate the structural behaviour and to validate the sensors readings, are used to predict the bridges response to those extreme traffic loads, which are then compared to the alarm levels established by the bridge designers in order to assess the structural safety level. The results demonstrate the importance of the representativeness of the observation periods to accurately estimate extreme traffic loads. Again, the procedure was implemented in MENSUSMONITOR.

Based on the measurements collected by the monitoring system, chapter seven and eight presents the analysis strategy adopted to compute the long-term behaviour based on FEM. The long-term assessment of large civil infrastructures such as prestressed concrete bridges is a challenging task. The real time history related to the phased construction, the influence of the adopted constructive method, the characterization of the employed concrete and the environmental conditions are crucial aspects for accurate predictions based on FEM. Data from long-term monitoring systems have been used to improve the quality of those predictions, namely to validate the design assumptions, to calibrate the structural model, and to update the safety coefficients. A detailed scanning of all information with relevance for the structure behaviour was performed. A full discussion concerning the real long-term behaviour is made, focussing the differences between the measurements and the results obtained with the numerical model, namely the trends due to shrinkage and creep and the variations due to the temperature. Finally, concerning to the structure lifetime, the predicted values for the measured parameters are updated, since the predictions based on

the European standard rules presents significant bias to be used as reference values regarding the structure surveillance.

Finally, a statement of the main conclusions, which have evolved from this work, closes the thesis. Special reference to the most relevant results is made, and some possible directions for extending the scope of the work in the future are pointed out.

2. DESIGN AND IMPLEMENTATION OF A MONITORING SYSTEM – LEZÍRIA BRIDGE

2.1. INTRODUCTION

One current major concern related to large infrastructures is their increasing age and the implied inspection and maintenance costs. A major focus regarding this matter has been awarded to bridges and high-rise structures (Van der Auweraer and Peeters 2003). Bridges, in general, are experiencing accelerated deterioration and are becoming more and more exposed to wear and tear as time progresses because they were designed when the demand for transportation facilities was not as high as it is today. The vehicles' weight and the increase in traffic are critical aspects (Minchin *et al.* 2006). The maintenance works related to structural problems such as joints and bearings are critical because experience has shown that these are the items that suffer from premature wear, thus requiring careful and regular maintenance procedures (De Brito *et al.* 2002). Another common problem in bridges is the loss of sediments around and under the bridge footings due to scour, which can lead to excessive pier movement, creating unwanted stresses in the bridge structure that may eventually lead to failure or collapse (Minchin *et al.* 2006). Human error is also a critical issue in the structure's health. In Korea, several man-made disasters were registered in the 1990s, as a consequence of the country's modernization without a corresponding integrative moral basis (Chang *et al.* 2009).

In the case of long-span bridges, the effectiveness of visual inspection in reaching all the critical locations and finding all the possible defects becomes especially questionable. In the United States, a study by the Federal Highway Administration (FHWA) revealed that at least 56% of the average condition ratings were incorrect, with a 95% probability from the visual inspection (2001). It follows that if health monitoring could be designed and implemented as a complement to visual inspection, to enhance its effectiveness and

mitigate its shortcomings, bridge owners would decide to take advantages of this new paradigm (Pines and Aktan 2002).

Structural Health Monitoring (SHM) is a subject of major international research. While in the past this topic was mainly addressed from the angle of sensors, now the practical implications regarding the acquisition, collecting and processing of data are being addressed (Van der Auweraer and Peeters 2003). Today it is possible to monitor highly instrumented structures continuously and remotely, with a high degree of automation. Present solutions are versatile enough to allow for surveillance tasks to be realized remotely with sound cost-effectiveness (Bergmeister and Santa 2001). This is performed by measuring a set of physical and chemical parameters with appropriate sensors, which allow the permanent control of critical parameters through a compatible acquisition and communication system, allowing automatic and remote storage in a database, often accessible through the Internet. In general, continuous measurement at low frequencies over a long time (e.g. hourly measurements) would be needed to capture the trends in climate- and weather-related inputs, changes in ground and soil, the movements of the foundations and the superstructure. Programmed, as well as triggered, intermittent measurements would be needed for shorter periods at higher frequencies for capturing the operational and corresponding structural parameters (Pines and Aktan 2002). Over the past decade there have been several full-scale demonstration projects that have involved varying degrees of SHM technologies for short- and long-span bridges (Pines and Aktan 2002). In a European research project, *Smart Structures* (BRITE/EURAM 1997), innovative and inexpensive probes for monitoring existing concrete structures were developed, tested and integrated into a monitoring system to reduce inspection and maintenance costs and the traffic delays (Van der Auweraer and Peeters 2003). In Hong-Kong and China, SHM is currently included as a standard mechatronic system in the design and construction of most large-scale and multi-disciplinary bridge projects (Wong 2007).

In this context, it is important that new bridges are equipped with monitoring systems from the beginning of their operation. It is envisaged that the cost of the monitoring system and the perpetual cost of its maintenance are expected to protect the much higher investment in the bridge construction and its operating costs (Pines and Aktan 2002). Monitoring the

condition of an existing motorway bridge structure helps to ensure its safety with regard to life extension and replacement strategies (Bergmeister and Santa 2001).

This chapter presents the monitoring system implemented in a recent bridge built in Portugal: Lezíria Bridge. The main scope is to show how a complex process, related to the implementation of a monitoring system, was guided to obtain the intended solution. After a general description of the bridge, the monitoring system is detailed in three main parts:

- **The process**, where issues related to sensor type, acquisition systems and communication with a remote database are described;
- **The installation**, with reference to laboratory works and some of the most complex and particular field works associated with the sensors' installation;
- **The records**, referring the reading procedures adopted and how this information is organized and delivered to the bridge owner.

2.2. LEZÍRIA BRIDGE

2.2.1. THE SOCIO-ECONOMIC CONTEXT

Lezíria Bridge, built between 2005 and 2007, forms part of the A10 motorway from Bucelas to Carregado (A1)/IC3 (A13). With a total length of 39.9 km, this road forms an outer boundary to the Lisbon metropolitan area. It benefits those who wish to travel to or from Alentejo or the Algarve (A2 motorway) and Spain (A6 motorway), without having to cross the portuguese capital. In addition, this new bridge will improve accessibility between Vila Franca de Xira and the Samora Correia/Benavente locations, substantially relieving traffic on the national roads EN10 and EN118 (Oliveira 2006).

2.2.2. THE STRUCTURE

The 11 670 m total length of Lezíria Bridge is realized by three substructures: (1) the north approach viaduct with 1 700 m long; (2) the main bridge substructure, crossing the River Tagus, with a total length of 970 m; (3) and the largest substructure, the south approach viaduct, with a total length of 9160 m. Figure 2.1 illustrates the construction of the three substructures.

a) Aerial view of Lezíria Bridge – May 2007 (© F. Piqueiro / Foto Engenho).

b) north approach viaduct.

c) main bridge.

d) south approach viaduct.

Figure 2.1 : Lezíria Bridge.

- **North approach viaduct**

The north approach viaduct provides the connection to the A1 motorway. It has three elementary girder viaducts, with spans of 33 m, except where it crosses a railway line,

where the largest span is 65 m and is partially formed by a box girder. The viaduct deck is supported by piers on piles with length that can in some cases are 40 m deep (Figure 2.1-b). The railway line that crosses the north viaduct and the existence of an electric power plant and a neighbouring substation were constraints considered in the project (Oliveira 2006).

- **Main bridge**

The main bridge structure is formed by eight spans and seven piers supported on pilecaps over the river bed. The spans are 130 m long except the end spans, which are 95 m, and two of the middle spans that differ in 3 m due to a change in a pier implementation leading to spans with 127 m and 133 m of length. The bridge deck is realized by a box girder of variable inertia which is about 10 m wide and has a deep varying between 4 m and 8 m. The box girder core construction was made by segmental construction using a movable scaffolding, whereas the side consoles were subsequently constructed, supported by a different movable scaffolding and metal struts fixed in the bottom slab of the box girder, as it is illustrated in Figure 2.1-c. The concrete piers are formed by four walls with constant thickness and variable width, and are supported on pilecaps (8 piles in general and 10 in the two pilecaps adjacent to the navigation channel).

- **South approach viaduct**

The south approach viaduct has 22 elementary viaducts with extensions ranging from 250 m to 530 m. It has a span length of 36 m, with exceptions due to the existence of irrigation canals and dykes in the Lezíria fields. The deck floor is supported by precast beams cast on site, where an industrial precasting unit was specifically set up, being the precast elements monolithically linked to the piers. The viaduct deck is formed by precast slabs, supported on the precast beams, and serves as formwork for the in situ top concrete layer. As with the north viaduct, the viaduct deck is supported by piers on piles varying from 35 m to 60 m deep, given the need for crossing alluviums with variable properties (Figure 2.1-d).

2.2.3. THE MAIN CONCEPTS OF THE MONITORING SYSTEM

A project such as the long-term monitoring system for Lezíria Bridge is complex and has a broad scope. Nevertheless, it may be unfolded in a sequence of three main stages:

- **The process**, which includes all the development stages up until execution, ending with the document for execution – *Executive Project*;
- **The installation**, which includes all the work tasks that allows the full implementation of the *Executive Project*;
- **The records**, organized as a database representing the final product.

In the area of bridge monitoring, the long-term monitoring system of Lezíria Bridge presents a number of innovative aspects in comparison with other bridge monitoring projects. The structural and durability monitoring project is part of the bridge design tasks from the beginning, through a specific project volume entitled *Structural and Durability Monitoring Plan* (COBA-PC&A-CIVILSER-ARCADIS 2006). As part of that project volume, the long-term monitoring system was subjected to successive versions with the participation of different entities, such as the bridge owner, the designer, the contractor, various consultants and SHM experts in order to bring together and coordinate a variety of interests and points of view. The final version of the monitoring system project, the *Executive Project*, through its organization, contents and objectives, is a reference document for structural and durability bridge monitoring in Portugal. Following the specification and process definition phase, the installation of the monitoring system began. Over a period of approximately 18 months, a highly specialized team had a long journey of installation tasks. The key to the successful installation of the monitoring system resulted from the know-how, dynamism, flexibility, adaptability and common understanding qualities of the team.

The obtained results are an essential source of knowledge which in its present state provides a valuable basis for further research in the domain of structural monitoring. That source of knowledge represents a great potential for both the damage prevention and management of the monitored bridge.

2.3. MONITORING SYSTEM OF LEZÍRIA BRIDGE - THE PROCESS

The Executive Project of the Structural and Durability Monitoring Plan was fully defined as a set of structured documents. Those documents, although prepared in advance, were finished during the implementation phase, following a so called *opening drawers* process (Figueiras *et al.* 2007a). Each document has a defined objective and a chronological relationship with the other documents as specified in Table 2.1.

Following this concept, the process evolved in a timely manner and it was completed step by step, with a set of clear intermediate objectives, until final handcover to the owner. The process organization took into account some special features of these systems, especially issues related to its conclusion. The finalization of such a process does not necessarily coincide with the installation of all equipments, cables and devices. Operational conclusion effectively occurs only after a certain period after the physical installation. In that time, the installed monitoring system is submitted to a meticulous validation process.

The monitoring system integrates all the electrical/electronic components, sensors, automatic acquisition system and data treatment/management through an optical fibre communication network that also enables remote access. Such system has a high degree of complexity, which has three main components: a) sensorial component, b) communication component, and c) data treatment and management component (Figure 2.2). This architecture offers the client a set of continuous and simultaneous records of the observed parameters, with capabilities for surveillance and prevention of structural safety and durability (Figueiras *et al.* 2007a).

The document "*A – Project brief*" (Figueiras *et al.* 2007b) contains a detailed description of the adopted monitoring system, with special attention paid to the selection of sensors and acquisition systems, the communication network, the integration of all systems, the data treatment and the management software (Table 2.1)

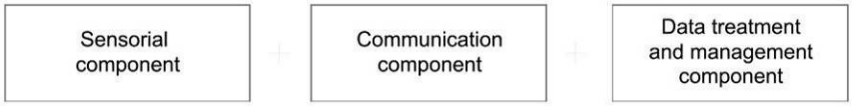

Figure 2.2 : Components of the monitoring system for Lezíria Bridge.

Table 2.1 : Executive Project organization.

Document	Objective	System installation		
		Before	During	After
Presentation Document	Project Executive organization; description of objectives of each document.	✓		
Project brief	Monitoring system definition and specifications, namely: sensors, acquisition systems, communication network, data treatment and management software.	✓		
Contract drawings	Plan and section drawings of the monitoring system implementation, namely: the instrumented sections, sensors, acquisition nodes, cables path.	✓		
Specifications and Procedures	Definition, sequence and description of a set of tasks to consider during the monitoring system installation.	✓		
Observation reports - Bridge construction	Bi-weekly reports with the records obtained during the bridge construction through time series graphs and summary tables with the mainly statistical results.		✓	
Final report	Verification of compliance of the monitoring system as installed, including: detailed location of the sensors installed in each section, table of calibration constants by sensor to convert the electrical or optical signal to the physical parameters intended to measure, sensor reference readings on which all measurements will be based.		✓	
Technical compilation	Detailed technical specifications of each type of sensor, their guarantee and certificates of conformity provided by the manufacturers.		✓	
Operations manual	Software and hardware descriptions of the monitoring system with: alert levels defined by the designers, operational mode in terms of service, maintenance plan, recommendations regarding good practice, procedures to detect and correct possible failures.		✓	
Observation reports - Service life	Semestral reports with the records obtained during the service life of the bridge through time series graphs and summary tables with the main statistical results.			✓

2.3.1. SENSORIAL COMPONENT

Considering the structure to be monitored, and what is intended to measure, a number of critical points are selected for monitoring a set of parameters. In this context, the sensorial component is based on the installation of, on the one hand, appropriate sensors to perform the measurements and, on the other, compatible acquisition systems to perform the signal processing and store the readings.

In the case of Lezíria Bridge, the instrumentation consisting of those sensors and acquisition systems is distributed over a number of structure zones as follows: two zones on the north approach viaducts, the whole of the main bridge length and four zones on the south approach viaducts. A set of instrumented sections defines a monitored zone and the corresponding acquisition system to interrogate the sensors is called an Acquisition Node (AN). A set of sensors is installed in each section to measure the intended parameters. Suitable cables connect the sensors to the acquisition systems, with the connection nodes made in Junction Boxes (JB) and Signal Connection Boxes (SCB) as shown in Figure 2.3 (Figueiras *et al.* 2007b).

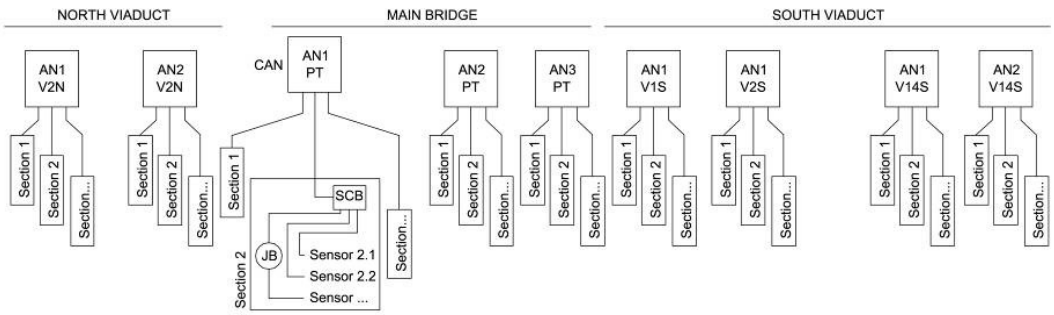

Figure 2.3 : Architecture of sensorial component.

Figure 2.4 illustrates the sensorial component. It identifies the measured parameters, shows the project symbols and abbreviations used and the types of the acquisition systems adopted to interrogate the signals from the sensorial component.

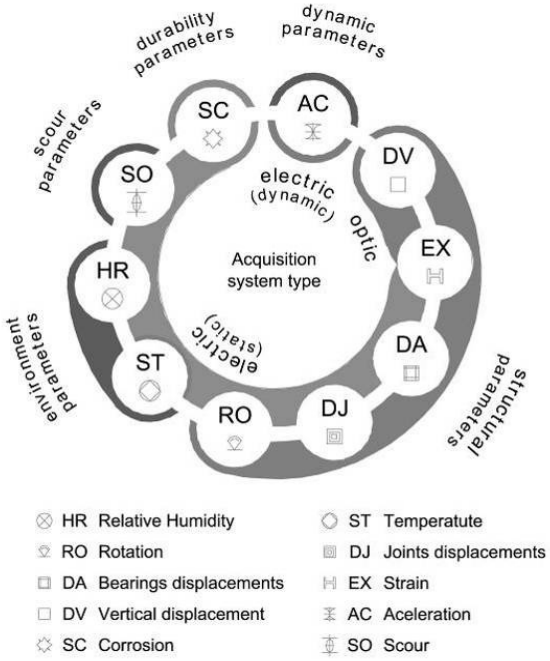

Figure 2.4 : Constituents of sensorial component.

- **Static acquisition system**

The static acquisition system interrogates 80 % of the total number of the installed sensors. Consequently, the monitoring system adopted for Lezíria Bridge is oriented towards long-term monitoring. Strains, rotations, displacements, corrosion, scour, and environmental parameters are those considered for static monitoring (Figure 2.4). The obtained records can be used to analyse the structure from the point of view of its behaviour with respect to environmental effects (e.g. temperature, relative humidity), time-dependent effects (e.g. shrinkage, creep and loss of prestress) and the interaction between the structure and the surrounding soil.

All these sensors are interrogated by the same acquisition system group, where it is possible to define reading procedures, with options available for defining the acquisition frequency of each sensor, for ordering the records sequence and storing those records in data files.

- **Dynamic acquisition system**

The number of sensors interrogated by the dynamic acquisition system represents about of 5 % of the total number of installed sensors. The main goal of these sensors is to monitor the accelerations induced in the structure and surrounding soil caused by earthquakes or by boats collisions. The adopted configuration means it will be possible to analyse the energy transmitted from the soil to the structure and its dissipation effects on the structural elements. The possibility of identifying the occurrence of those events with the dynamic system can provide valuable information for the interpretation of the long-term behaviour when changes in the pattern of evolution over time can be justified by those events.

Triaxial accelerometers are used to measure the accelerations at a specific point (structure or soil). Those sensors measure and record the accelerations in three orthogonal directions, being connected to the acquisition system by armoured cables, specifically manufactured for this type of devices. An acquisition system supplied by the same manufacturer performs the sensors' interrogation. The software managing the dynamic acquisition system allows the alarm levels definition to each sensor and/or measurement axis, and such alarms can be sent to a particular address as IP message.

- **Optical acquisition system**

The last decade has witnessed huge developments in the application of optical fibre sensors, in particular Bragg grating sensors in civil engineering structures (Maaskant *et al.* 1997; Inaudi 1999; Fernando *et al.* 2003). With recognized advantages such as immunity to electromagnetic fields and low signal losses, and also due to the application of multiplexing techniques – where signals of multiple sensors can be sent through a single optical fibre –, Bragg sensors represent one of the most promising sensing technologies for use in civil engineering structures (Bergmeister and Santa 2001). With this technology, it is possible to encapsulate long lengths of optical fibres carrying the signals of various sensors to one acquisition system located at a specific point (Figueiras *et al.* 2007b).

Considering the properties referred to and the socio-economic importance of Lezíria Bridge, it was decided to install an optical acquisition system based on the aforementioned Bragg grating sensors. The sensors, specifically developed for this purpose (Figueiras *et al.*

2010), are an integral part of the structural and durability monitoring system. They account for the remaining 15 % of the total number of sensors installed for measuring vertical displacements, strains and temperatures (Figueiras *et al.* 2007b).

The sensors' interrogation is performed by a compatible acquisition system. The management software for the readings of the optical sensors was developed based on the software of the manufacturer's acquisition system (Figueiras *et al.* 2007e). The optical acquisition system aims to expand the information about the structural behaviour of the main bridge and also to compare the efficiency of this system with the electrical monitoring system (Figueiras *et al.* 2007b).

2.3.2. COMMUNICATION COMPONENT

Because of the length of this bridge, the Acquisition Nodes (AN) of the monitoring system are physically distant from each other. For example, the distance between the two extreme ANs is about 8 km. Consequently, a local communication network was installed, allowing for the integration and centralization of the information recorded by the different ANs in a single place, so called as the Central Acquisition Node (CAN). Opting for a local communication network has simplified remote access to the monitoring system by allowing access to every device in the system through a single CAN. The communication network, also using optical fibres, has two rings with nine nodes (one for each of the nine instrumented zones) matching the various ANs and is shown schematically in Figure 2.5.

Lezíria Bridge is part of the motorway network operated by BRISA. It is, accordingly, included in BRISA's sophisticated communications network covering the whole of its motorway system. In order to enable remote access to the bridge monitoring system, a link was established between the local communication network and BRISA's communication network. A dedicated server installed at BRISA's Operations Control Centre manages this link and allows for direct and permanent communication with the CAN (Figure 2.5).

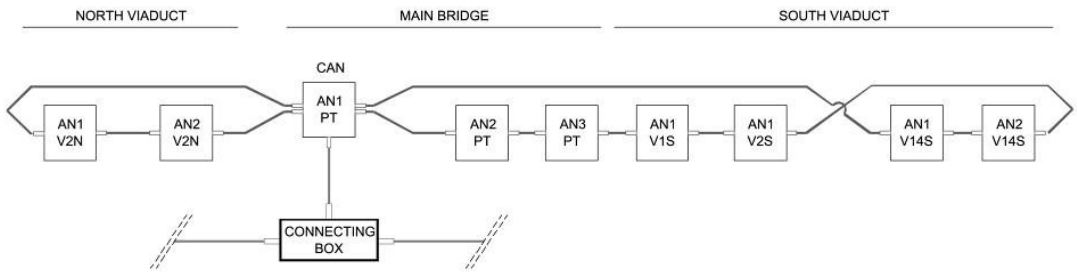

Figure 2.5: Communication network integrating the various ANs in the CAN.

2.3.3. DATA TREATMENT AND MANAGEMENT

A dedicated software module was developed for data treatment and management purposes. It also provides the main database updating functions and enables the visualization of results. In addition, the system has a consultation module covering the technical information about the installed system (Figueiras *et al.* 2007b).

In terms of data treatment, the data updating module distinguishes durability and dynamic parameters from the remaining ones, with a specific procedure available for each case (Figueiras *et al.* 2007b).

After selecting the sensors, the visualization module delivers results in both tabular and graphic forms. The graphics allow the observation of the time pattern of the sensors selected, individually or grouped by monitored sections.

The consultation module provides all the technical information about the monitoring system installed, such as the location of the instrumented sections, and a description of the sensors installed in each one.

It is also possible to create data files in text format for external processing as well as to generate reports automatically with the intended graphical results. Moreover, the software is prepared to notify the bridge owner by e-mail if the values measured by the sensors exceed the threshold values previously defined by the bridge designer (Figueiras *et al.* 2007b).

2.4. MONITORING SYSTEM OF LEZÍRIA BRIDGE - THE INSTALLATION

The guidelines for the installation of the monitoring system were the documents of the Executive Project: "*A – Project brief*" (Figueiras *et al.* 2007b), "*B – Contract Drawings*" (Figueiras *et al.* 2007c) and "*C – Specifications and Procedures*" (Figueiras *et al.* 2007d). Document C was specifically developed to guide the installation works, taking into account the size and complexity of the monitoring system. This project document, prepared to anticipate and organize a set of tasks to be carried out during the installation works, covered aspects such as: (1) organization of laboratory tasks in order to minimize the field works; (2) sequence and the interdependence of in situ work to minimize repetition of procedures; (3) phasing of construction tasks in order to anticipate scenarios, optimize allocation of resources and minimize human input.

2.4.1. PREPARATION AND ORGANIZATION OF LABORATORY WORKS

The success of the in situ installation heavily depends on the preparatory work carried out in the laboratory. To prepare the equipment and organize cables and accessories, it is essential to have a strong laboratory team. A set of normalized verification procedures has to be applied to all equipment, cables and accessories, and no material should leave the laboratory without passing through these. Figure 2.6 illustrates normalized procedures considered in the preparation and organization of laboratory work, including (a) calibration and verification of sensors; (b) setup of interfaces for the in situ installation of sensors, and (c) preparation, identification and protection of cables.

a) sensor verifications. **b) sensor holders.** **c) cable preparation.**

Figure 2.6 : Laboratory preparation work.

2.4.2. BRIDGE INSTRUMENTATION

To monitor a concrete bridge during its service life, the system installation may be implemented in two separate steps: firstly, all the embedded sensors are installed during the concreting phases, and, secondly, upon completing of the concreting works, all the complementary work to conclude the installation. However, in the presence of a monitoring requirement during the bridge construction, the installation of Provisional Acquisition Nodes (PAN), in addition to the embedded sensors, is compulsory. Moreover, cabling rails and connections for the construction phase are also provisionally placed. Thus, a truly temporary monitoring system is put in place, as part of the first installation step.

Given the importance of Lezíria Bridge, the monitoring process covered the construction period. With that proposal, three of the nine instrumented zones were monitored during the bridge construction. This fact required a great commitment from the installation team to follow the rhythm imposed by the construction works (often 24 h/day), and, at the same time, to obtain successful recordings. From the above, it becomes evident that monitoring projects addressing construction phases imply greater complexity and demand higher commitment from the installation teams than when monitoring service life only. Figure 2.7 illustrates some of the first monitoring works, performed during the construction of Lezíria Bridge, in particular (a) the embedded sensors installation, (b) the PANs installation, (c) the provisional cables path, and (d) provisional connections. It is mandatory for the anticipation and preparation of all necessary procedures to guarantee a robust installation that will stand up to the aggressiveness of the concreting operations.

Independently of the bridge being monitored during construction, the installation of the embedded sensors is followed by a short period for the implementation of the permanent monitoring system, which generally coincides with the finishing works of the bridge. As shown in Figure 2.8, the monitoring system implementation requires, additionally, (a) the installation of the external sensors, (b) the definitive installation of the ANs, (c) the cables passing through the technical rails and pipes, and (d) the provision of the connections boxes.

Bridge finishing is the most intensive working period, with the simultaneous presence of multiple work teams to fulfil all sorts of diversified works that must be finished before the inauguration date. This fact leads to increased pressure upon the installation works, thus

forcing longer daily working periods. At this stage, capabilities such as dynamism, flexibility, adaptability and integration are crucial to the success of the system installation. More details concerning practical aspects taken into account for the system installation can be found in Appendix A.

a) embedded sensors. **b) Provisional Acquisition Node (PAN).** **c) cables path.** **d) provisional connections.**

Figure 2.7 : First installation step of the monitoring system.

a) external sensors. **b) permanent Acquisition Node (AN).** **c) permanent cables path.** **d) permanent connections.**

Figure 2.8 : Second installation step of the monitoring system.

Given their particular complexity or special features, the installation of some sensors deserves a special mention. That is the case of (1) pile strain gauges, (2) soil accelerometers, (3) sonar in pile heads, and (4) the vertical displacement system.

- **Pile strain gauges**

Twelve strain gauges were installed inside a pile of the main bridge in a rather remarkable fashion. After the pile driving, the installation was carried out in three main phases: (1) installation of the vibrating wire strain gauges using steel bars with an appropriate fixing system to place the transducers inside the holes left for cross-hole acoustic tests at three different levels (1 m, 5 m and 35 m); (2) after the initial works for the pile head execution, the strain gauges were tested immediately before the holes were sealed; (3) the cables

previously placed at the pile top (to avoid connections inside the concrete) were routed through the pile head up to the pier base. Figure 2.9-a shows the placement of one of these sensors in the hole.

- **Soil accelerometers**

The accelerometers installed in the soil were inserted in a borehole through an inclinometer tube and positioned at different depths (over a range of 1 m to 40 m), with final cement sealing in order to achieve a good connection with the surrounding soil (Rudaz *et al.* 2006; Figueiras *et al.* 2007b; Figueiras *et al.* 2007c). This installation was particularly difficult because the sensors were installed with the total cable length necessary to reach the AN on the bridge deck. This option had the advantage of avoiding additional wire connections, but required the cables to be passed through the inclinometer tube to the acquisition system node beforehand. To illustrate the effort involved, the longest cable was > 300 m long and its pathway developed, sequentially, trough (1) a cable trench, (2) a pipe installed over the height of a pier, (3) along the technical paths of the border deck, and, finally, (4) inside the box girder of the main bridge up to the acquisition system. Figure 2.9-b illustrates the placement of one of those inclinometer tubes in the borehole, with the accelerometer rigidly positioned at the end of the tube in advance.

- **Sonar devices**

The sonar devices were installed after the bridge construction due to the particular conditions during the construction period in the piles head (placement of scaffolding and the backrest of boats to support the construction). In order to prevent the impact of objects floating in the river or boat collisions, the mechanical protection of the sensor and its maintenance were crucial aspects considered in the installation. The sonar devices were installed at the bottom of the pile head on the upstream side. To place it in its resting position, the sonar device was fixed to the extremity of a metal tube inserted in stainless steel section specially designed to protect the sonar setup. Figure 2.9-c shows the positioning of one of the sonar devices inside the stainless steel tube.

- **Vertical displacement system**

A liquid levelling system was installed along the entire length of the main bridge to allow the measurement of vertical displacements (deflections and settlements). For that purpose, a specialized team installed a hydraulic circuit after the main bridge box girder was finished. After installation, the pile system was filled with water and purged for possible air inside the hydraulic circuit. Finally, the sensors were installed and connected to the hydraulic circuit, after which a calibration routine was performed by varying the circuit water level to ensure the adequate performance of the system. Figure 2.9-d illustrates one of the containers fixed to the girder wall as well as the hydraulic circuit and the reference sensor.

a) strain gauges in pile. **b) soil accelerometer.** **c) sonar protection.** **d) hydraulic circuit.**

Figure 2.9 : Particular tasks of the monitoring system installation.

2.4.3. TESTING AND FINAL CHECKS

Before delivering the monitoring system to the owner, a series of final tests and checks were performed in order to verify its full performance. Those tests and final checks are crucial for the identification and correction of any anomalies that might have occurred during installation, given the well-known aggressiveness of construction environments. Several tests are performed, namely: (1) signal verification of all sensors; (2) verification of cable integrity; (3) verification of the acquisition systems up-state; (4) verification of communication and data transmission to the Operations Centre. After the conclusion of the tests and final verification, the monitoring system was considered ready to operate in full mode.

2.4.4. IMAGE MANUAL, WATERPROOFING AND SEALING

At this stage, it was possible to produce, an image-based manual. The layout of this manual aims to offer a comprehensive view and provide an easy understanding of all equipment in the monitoring system. Moreover, it facilitates future intervention in the system, as described in (Figueiras *et al.* 2007c). The so called Image Manual is a set of identification plates, plastic sheets and user manuals. The connection boxes were all waterproofed to maximize system up state and durability. Finally, the entire system was sealed to prevent and trace any unauthorized intervention that would otherwise not be easily detectable. Figure 2.10 illustrates some finishing works, in particular (a) the identification plates provided for an external sensor sheltered by a protection box, (b) plastic sheets with useful information about the monitoring system inside an AN box, (c) waterproofing the tubes entering in an AN, and (d) sensor sealing to prevent unauthorized access.

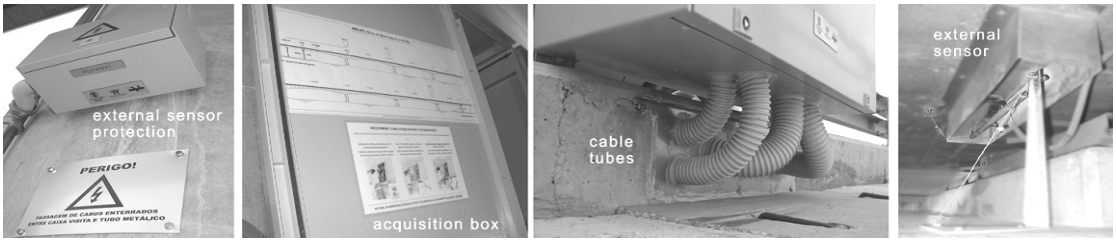

a) identification plates. **b) user manuals.** **c) waterproofing.** **d) system sealing.**

Figure 2.10 : Image manual, waterproofing and sealing.

2.5. MONITORING SYSTEM OF LEZÍRIA BRIDGE - THE RECORDS

2.5.1. READING PROCEDURES

The records obtained so far are defined by reading procedures previously established according to the project objectives. For the static parameters resulting from interrogation by the electrical acquisition system, the sampling rate adopted is one sample every 3 hours in normal mode. In alarm mode, the acquisition frequency can be increased to one sample per minute. In the case of the dynamic parameters, the accelerometer sampling rate is

established in 200 Hz by default and the system is permanently alert, with the sensors' readings continuously saved in a ring buffer. If an alarm level is reached, an event occurs and the system creates a set of files with the respective sensors' readings and a warning message. For the optical sensors, the sampling rate adopted is one sample every 3 hours in normal mode. In alarm mode, the acquisition frequency can be increased up to 500 Hz in the case of the fibre-optic strain sensors (Figueiras et al. 2007e). Table 2.2 shows the parameters monitored and also sensor type, acquisition system type, sample rate acquisition, bridge zones where sensors are installed and their purpose, and the thresholds for surveillance and alarm levels defined by the bridge designer (COBA-PC&A-CIVILSER-ARCADIS 2006). The threshold values for some parameters have not been initially defined (n/d in Table 2.2): their evaluation based on the first years of observation.

2.5.2. MONITORING RECORDS

As aforementioned, the Lezíria Bridge monitoring system has been operating since the installation of the first sensors, thus enabling monitoring of the structural behaviour during construction. During this period, it was possible to monitor some construction operations, such as concreting operations, prestressing, falseworks disassembly and movements of the movable scaffolding used for segmental construction (main bridge), application of forces at the closing sections (main bridge), precast beams positioning (south viaduct) and load tests for structural behaviour conformity upon at completion of construction (Figure 2.11). After the bridge was finished and with the monitoring system in full operation, some effects concerned with the service life of the structure have been monitored, namely: environmental effects, shrinkage and creep evolution, and traffic load effects.

a) concreting. **b) prestressing.** **c) precast beams positioning.** **d) load test.**

Figure 2.11 : Construction operations.

Table 2.2 : Characteristics and locations of measured parameters.

Parameter	Acquisition system	Measuring Frequency	Objective	Instrumented zones					Threshold	
				Soil	Piles	Piers	Bearings	Deck	Surveillance *a)	Alert *b)
Strain	Electrical/ Optical	Static / Dynamic	Concrete deformation		✓	✓		✓	n/d	
Relative horizontal displacement	Electrical	Static	Relative displacement between pier and deck and at expansion joints				✓		275 mm *c) 520 mm *d) 315 mm *e)	350 mm 675 mm 380 mm
Rotation	Electrical	Static	Rotation of structural elements					✓	n/d	
Temperature	Electrical/ Optical	Static	Environment and concrete temperatures		✓	✓		✓	n/d	
Relative Humidity	Electrical	Static	Environment relative humidity					✓	n/d	
Scour	Electrical	Static	Scouring			✓			-9.8 m *f)	-13.5 m
Durability	Electrical	Static	Corrosion potential in reinforcing steel near concrete surface			✓		✓	* g)	
Acceleration	Electrical	Dynamic	Accelerations in three orthogonal directions in soil and structure	✓		✓		✓	0.05 g	0.10 g
Vertical displacement	Optical	Static	Vertical displacements of main bridge					✓	50 mm *h)	100 mm

* a) The surveillance levels are determined for the frequent combination of actions, with a limit of L/2500 (COBA-PC&A-CIVILSER-ARCADIS 2006).
* b) The alert levels are determined for the characteristic combination of actions, with a limit of L/1200 for the main bridge and L/1000 to L/600 for the approach viaducts (COBA-PC&A-CIVILSER-ARCADIS 2006).
* c) Maximum values allowing for joint expansion in north approach viaduct.
* d) Maximum values allowing for joint expansion in main bridge.
* e) Maximum values allowing for joint expansion in south approach viaduct.
* f) Maximum values, considering as reference the riverbed elevation at the end of the bridge construction.
* g) The alarm is triggered when the penetration of aggressive agents can predict that the depassivation of the reinforcements will occur in half of the remaining lifetime of the structure, with a minimum of 10 years.
* h) Maximum value allowing for the longest spans of the main bridge.

The contract called for a set of periodic observation reports to be delivered to the bridge owner twice a week during the construction phase. Those reports included (1) drawings with the positioning of all installed sensors; (2) the main events organized as a schedule; (3) time series charts of the recordings and (4) summary tables with the main statistical results. Figure 2.12 illustrates the information included in the periodic observation reports delivered twice a month during the bridge construction. This task allowed for a closer check of the monitoring system during its installation and has proved to be useful in evaluating the structural response during the construction process, which is one of the most important stages of a structure's life. Since opening to traffic, an observation report, including all the sensor records and main statistical information, is delivered every semester in order to be analyzed and accounted for.

Although the bridge maintenance includes comprehensive visual inspections every six years, the sensor readings represent extra knowledge to help in the interpretation of damage identified in the visual inspections. Moreover, the monitoring system provides information about the bridge performance permanently, thus enabling the owner to organize an extraordinary visual inspection to facilitate an interpretation of the situation if abnormal values are read at any time between those campaigns every six years. Likewise, if during a regular visual inspection any given pathology is noticed, the owner can resort to the model and to the history of measured data in order to promote a better interpretation of the actual situation.

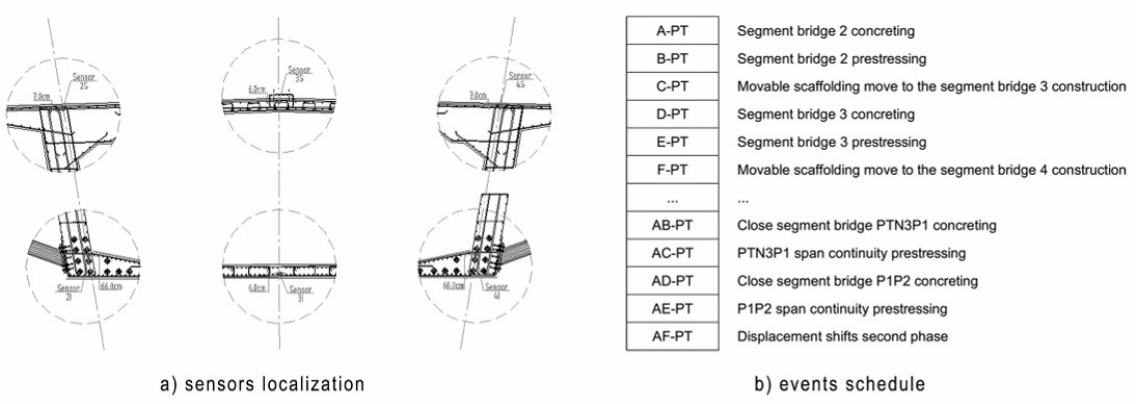

A-PT	Segment bridge 2 concreting
B-PT	Segment bridge 2 prestressing
C-PT	Movable scaffolding move to the segment bridge 3 construction
D-PT	Segment bridge 3 concreting
E-PT	Segment bridge 3 prestressing
F-PT	Movable scaffolding move to the segment bridge 4 construction
...	...
AB-PT	Close segment bridge PTN3P1 concreting
AC-PT	PTN3P1 span continuity prestressing
AD-PT	Close segment bridge P1P2 concreting
AE-PT	P1P2 span continuity prestressing
AF-PT	Displacement shifts second phase

a) sensors' localization. **b) events schedule.**

Figure 2.12 : Information included in the periodic observation reports during the bridge construction.

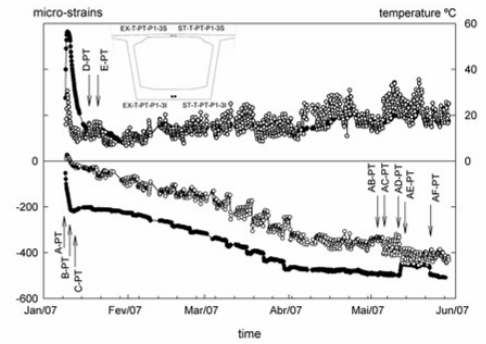

Sensor	Sampling (31/07/06 at 07/07/07)	$y_{initial}$ (31/07/06)	$y_{min.}$ (occur)	$y_{máx.}$ (occur)	y_{final} (07/07/07)
EX-T-PT-P1-3I	3422	-1με (08/01/07 22:00)	-565με (05/07/07 3:00)	0με (8/01/07 21:00)	-565με (05/07/07 3:00)
EX-T-PT-P1-3S-1	3307	-1με (09/01/07 3:00)	-501με (05/07/07 3:00)	+28με (9/01/07 15:00)	-501με (05/07/07 3:00)
ST-T-PT-P1-3I	3425	21.7ºC (08/01/07 22:00)	+8.4ºC (29/01/07 11:00)	+56.4ºC (9/01/07 17:00)	+21.9ºC (05/07/07 0:00)
ST-T-PT-P1-3S-1	3323	16.5ºC (09/01/07 3:00)	+6.7ºC (24/01/07 12:00)	+35.5ºC (18/05/07 16:00)	+24.7ºC (05/07/07 0:00)

d) time series graph. **d) statistical information.**

Figure 2.12 : Information included in the periodic observation reports during the bridge construction. (cont.)

2.6. CONCLUSIONS

The present chapter described in detail the procedures related to the design and installation of a concrete bridge monitoring system spanning from construction to life-cycle surveillance. The project's complexity and its scale were thoroughly illustrated adopting a hands-on approach and reflecting an understanding of implementation. Several hierarchical stages had to be crossed to turn this system into a physical and manageable reality, with emphasis on three fundamental phases:

- A conceptual design based on a set of structured documents. Due to the system's complexity, these documents were crucial for the subsequent work stages. The definition of intermediate objectives was an efficient strategy, with full detail of all work steps involved from the preparatory works to the desired measurements in the form of graphs and tables. It is fundamental to have a full advance vision of the system that integrates different systems (static, dynamic and optical systems) and components to anticipate potential difficulties and/or problems at the implementation stage.
- Installation works that were performed during the bridge construction. Document "*C – Specifications and Procedures*", elaborated in the previous phase, was an important guide for the installation works, i.e. for a better mutual understanding between the contractor and the monitoring team, providing all the necessary conditions for the implementation of the system. The monitoring requirement during the bridge construction led to the installation team exploring capabilities such as dynamism,

flexibility, adaptability and integration, to follow the rhythm imposed by the construction works (often 24 h/day). After installation, several tests were needed to consider the system ready and operational in full mode. In a monitoring system like that of Lezíria Bridge, it is vital to waterproof and seal all the connection boxes and sensors in order to maximize the system robustness and durability in a long-term management process.

- Data acquisition and treatment was conceived to supply the management authority with the required graphs and statistical tables. The reading procedures for normal and alarm modes were established according to the project requirements, and the collected measurements are stored in a remote database linked to the field system via fibre-optic cables. The fact that the monitoring system has been operating since the installation of the first sensors has the advantage of a closer check of the construction process as well as the evaluation of the structural response from the beginning of construction. Since being opened for traffic, the monitoring system has been working in full mode, and periodical reports are delivered to the owner. The possibility of combining information with the visual inspections can certainly benefit the surveillance and management of the bridge.

3. SOFTWARE FOR TREATMENT AND ANALYSIS OF MONITORING DATA – MENSUSMONITOR

3.1. INTRODUCTION

In the last years, Structural Health Monitoring (SHM) has been one of the topics with higher improvement among research activities in Civil Engineering. It has been intensively used to conceive the predicted structural behaviour during the design process and to collect data related to the real behaviour of structures.

At present, monitoring systems are programmable and data obtained from the sensors can be automatically stored into computational data files. However, one of the main difficulties faced in this course of action is the processing of the data obtained with these systems, if specific engineering techniques are not used. If made *manually*, this is a time-consuming activity and, generally, the collected information is deficiently studied due to the extensive tasks that are necessary to perform in order to produce an accurate analysis. Moreover, the size of the information obtained with these systems, generally, becomes extremely large. The knowledge that can be extracted is vast however, in general, the interpretation of this type of data is difficult and time-consuming. Due to the large data size, some results are not conveniently taken into account and therefore, some information might be wasted.

Devoted software to process and analyse this type of data is the best way to achieve high levels of efficiency (Barcina and Mato 1997; Calado *et al.* 2007). Common worksheets of EXCEL type and/or generic numerical tools as MATLAB are two examples of software commonly used to process monitoring data. If not the case, when a user develops specific numerical tools, generally they are built to answer a specific problem without regarding its integration with complementary tools already developed. Moreover, because it is normally

developed for personal use, the graphical interface is many times not very user-friendly and consequently they are difficult to be used by others (Caetano and Cunha 1996).

The manufacturers of equipments devoted to SHM develop their own software with specific functions and user-friendly interfaces for easy data visualization and processing (GEOSIG 2009; SMARTEC 2009). Although the usefulness of these type of software, they are normally available as a final product with no access to the source code and therefore, the implementation of new functionalities are not possible in order to improve the user needs. Considering the expertise and specificities of the SHM, the author advocates the need of specific numerical tools to process efficiently the collected data.

Nowadays, the software development with the implementation of specific numerical tools benefits from a wide range of programmable platforms, specifically devoted for the construction of stand-alone applications such as C++ (Stroustrup 1997), LABVIEW (Beyon 2001) and MATLAB (Math 1992). Moreover, to allow the code assembly from different programming languages into a single run application, communication protocols between those programming languages have been developed (Cezzar 1995). In fact, currently it is possible to develop software based on assembly concepts, where a set of numerical applications written with different programming languages can be set into a unique application supported on these communication protocols. Consequently, the specificities and advantages of each programming language can be combined for a purpose of higher level.

The focus of this chapter is to present a software, which was developed to give answers to some difficulties in the handle of monitoring data – MENSUSMONITOR. Firstly, the main motivations for the software development are enounced, where some features of the SHM field are described with some illustrative examples. Secondly, regarding the optimal choice of the programming languages to be used in the software project, a historical reference is made focussing the evolution of programming concepts. Thereafter, the programming languages adopted for the software project are enounced, highlighting the main advantages of each one and how they might be complemented. The software project is then presented, namely the adopted framework and the principal functionalities are enounced. Finally, a practical application is presented in order to show the flexibility and functionalities of MENSUSMONITOR. The main conclusions close the chapter.

3.2. SOME ISSUES ABOUT STRUCTURAL HEALTH MONITORING

SHM activity has a strong experimental component, which means that the collected data is highly liable to effects such as:

- the parameters that are under observation,
- the quality of the monitoring system installation,
- the specificities of the sensors and the data acquisition equipments used in the observation process,
- specific aspects related to the monitored structure such as materials, constructive process and structural behaviour,
- environmental effects in the measurements, namely due to the temperature and the relative humidity variations.

Generally, these effects require extra work that delays the principal task – the study of the material and structural behaviour based on the monitoring data. In the next subchapters, the main tasks related to these aspects are described, which must be performed before any calculations based on the monitoring data.

3.2.1. ERRORS IN THE SENSOR READINGS

In some cases, the collected data exhibits disturbances due to specificities of the monitoring system setup, which normally do not have any correlation with the phenomena under observation. For example, the electromagnetic interference is perhaps the most common disturbance, which adds a noisy signal to the sensors' measurement. This effect is practically inevitable due to the electric nature of the equipments. Besides this type of interference, others exist that are not possible to avoid, and are caused by intrinsic characteristics of the measuring systems and/or phenomena under observation. This type of interference is characterized by an oscillation of the signal around the mean value, and in function of the magnitude of that interference, it can mask completely the phenomenon that is being measured. Most of these interferences are difficult to avoid during the measuring

processes however, they always make difficult the perception of the values of interest and the pre-treatment is required in order to remove or, at least, mitigate them.

Figure 3.1 presents the measurement of a vertical displacement supported by the method of liquid levels. In the second half of the register, interferences in the measurement process are clearly visible, which were originated by vibrations induced in the hydraulic circuit that supported the measurement system. Without any correlation with the structural behaviour, a pre-treatment was necessary (by using a proper signal filter) before any data analysis.

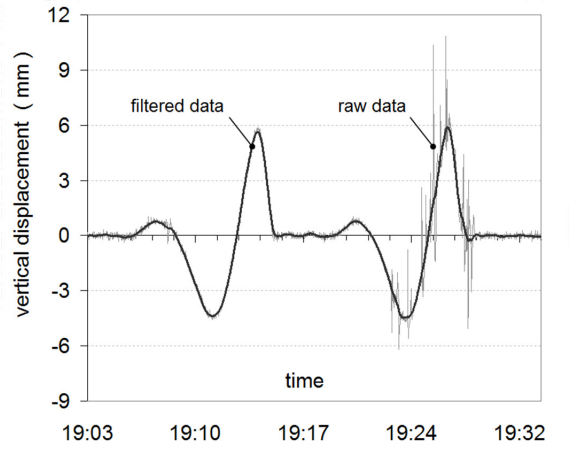

Figure 3.1 : Interferences in the sensors' measurement.

3.2.2. OPERATIONAL CONDITIONS OF THE SHM

The sensors' measurements might not directly represent what it is being observed, namely in their magnitudes and absolute values. All measurements have a conversion expression that correlates the parameter effectively used for the measurement procedure (generally an electric or optic signal) and the intended physical parameter – signal conversion. However, in some situations additional corrections are needed besides the signal conversion. For example, considering again the vertical displacement measurements obtained by the method of liquid levels, all measurements depend from a reference of the hydrostatic level. As in the previous case, this reference is normally established with a sensor, reference sensor, positioned at a location where the vertical displacement might be considered practically null. Consequently, all sensors' measurements must be corrected to the reference, which can be a non-zero result. This task must be made before any data analysis.

As an example, Figure 3.2 plots two vertical displacements, where one of the measurements respects a mid-span section while the other one refers to a section over a pier, this last used as reference. Performing the correction, the final value obtained for the vertical displacement of the mid-span section is 7 % lower than the measurement obtained by the respective sensor.

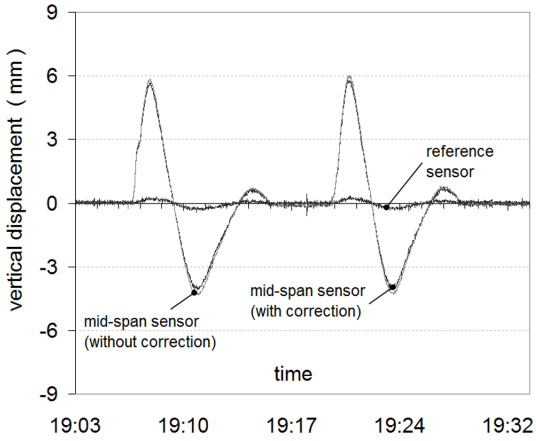

Figure 3.2 : Correction of the vertical displacements obtained by the method of liquid levels.

3.2.3. ENVIRONMENTAL EFFECTS

Some of the sensors available in the market are susceptible to temperature effects, in other words, the measurements performed by these sensors can be unfolded in two components due to the:

- temperature effects over the sensor,
- phenomena under analysis.

For some type of sensors, the elimination of the temperature effect is automatically performed through an internal system. However, a considerable number of sensors are not provided with these internal systems and therefore, the correction have to be posteriorly made. Commonly, this is made by using a temperature measurement that is positioned near the sensor that is being used to perform the intended observation. Hence, tables containing pairs of measurements, measured parameter and the respective temperature, are necessary

to be organized in order to allow the measurement correction. Once again, this task has to be made before any data analysis.

As an example, Figure 3.3 plots the concrete deformation (CD) measured by a strain gauge installed in a deck girder of a concrete bridge and during a load test. Additionally, the temperature evolution is plotted, which was obtained by a temperature sensor that was installed near the strain gauge. This sensor does not have any internal system to automatically perform the correction due to the temperature effect. However, the temperature effect is clearly visible in the strain measurement by a non-linear trend, which is clearly correlated with the temperature measurement. Using the temperature measurement, the temperature effect can be removed, remaining only the effect due to the applied loads during the load test, as it is illustrated in Figure 3.3.

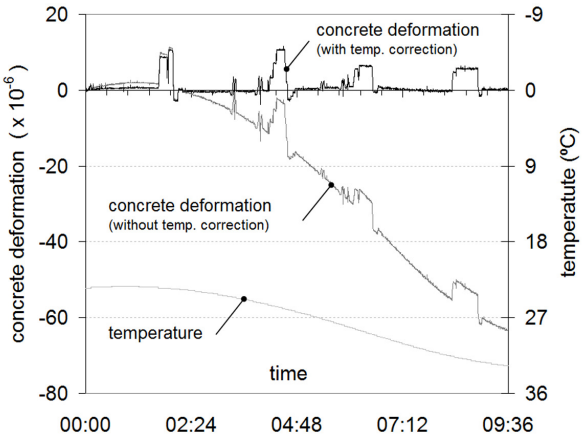

Figure 3.3 : Removing the temperature effect in a strain measurement.

3.2.4. DATA MANAGEMENT

As aforementioned, the current acquisition systems used in civil infrastructures for structural monitoring are programmable and capable of generating output data files with the sensors' measurements. However, those data files have specific formats, set by the equipments' manufactures and therefore, a standard data format does not exist for this type of records. In this context, data collected by a monitoring system that integrates a set of different acquisition equipments, i.e. from different manufactures, requires a pre-organization of the collected data. The standardization of all data must be previously done,

and only after that, the data access and its study can be made based on standard procedures, independently of the data source. Moreover, if made manually, this might be a time-consuming task in order to get the optimal organization, sort and identification into a standard format.

On the other hand, the respective databases can easily attain considerable sizes. In fact, these monitoring systems allow sampling rates that can reach to 200 Hz, depending on the sensor's type, their number and the characteristics of the acquisition system. Hence, the database consulting with the aim of extracting information of higher knowledge can be a difficult task with significant time-consuming if made without specific numerical tools.

The potential knowledge that exists within the collected data is high however, it is also important to reach to that knowledge in productive time for an effective use, regarding the management of civil infrastructures based on monitoring data (Sousa *et al.* 2008). As an example, the monitoring system of Lezíria Bridge has approximately 400 sensors connected to nine acquisition nodes, which are equipped with three different sorts of acquisition systems where the sampling rate can reach to 200 Hz. On average, the database grows 3 200 measurements pear day, which lead to one million of measurements pear year. No doubt that, without automatic tools, the data consulting and analysis is almost impracticable.

3.3. PROGRAMMING LANGUAGE REVIEW

Programming languages have constantly evolved in an increasingly and dynamic way since their birth. Curiously, as the society has evolved, the capabilities and potentialities offered by these languages have been growing up in order to satisfy the society needs, or in other words, to satisfy the complex requirements of the computer science and monetize the effort invested in the software conception.

There is a theory, Turing machine, that says that any programming language can do anything that any other language can, in the limit, by simulating the other language if needed (unless for some unlikely reason a simulator of the other language cannot be written). However, the cost associated with this option is clearly reflected in the time and effort spent (Cezzar 1995). Therefore, the choice to use a certain programming language

should take into account the purposes that the developers intend to reach, according to the project requirements.

3.3.1. HISTORICAL REFERENCES

The evolution of the programming languages can be described through paradigms that are supported by them (Rodrigues *et al.* 2005).

ALGOL (for ALGOrithmic Language) is one of the earliest languages, being mentioned due to its historical interest. Main contributions were concepts of recursion and block structure. As it name implies, ALGOL has been influenced by ordinary algebraic notations, and it placed emphasis on numerical data processing involving array manipulations. With general clarity and elegance, ALGOL heavily influenced the structure of PL/1 and later versions of FORTRAN. ALGOL is one of the earliest compiled languages. Due to dynamic referencing, which requires considerable run-time storage allocation, ALGOL programs are not as efficient as FORTRAN programs. This is one reason why, as a static language where everything is known before execution, FORTRAN still dominates in scientific computations. ALGOL programs are composed of a main program and a set of subprograms organized into blocks. This is the essence of block structure in high-level languages (Cezzar 1995).

APL (for A Programming Language), published in 1962 by Kenneth Iverson, was intended for applications involving heavy use of data in the form of tables, matrices and vectors. A typical APL implementation is based on a purely software-interpreted program execution, hiding not only the hardware details but also the operating system environment. A stack for subprograms activation records and heap for array storage is maintained. Arrays are stored with full run-time description, which makes manipulations flexible. APL is quite restricted in data typing and structuring. The expressions are sometimes perplexing but compact. APL is one of the less strongly typed languages, but it is still considered a very efficient language in expression evaluation (Cezzar 1995).

The first version, referred to as Modula, was designed to support the systems programming requirements of Lilith's software development in Europe. This version was never widely implemented. During the time of standardization efforts for Pascal by both ANSI and ISO,

Niklaus Wirth developed a new language called Modula-2 (successor of Modula) in response to the perceived shortcoming of Pascal, in 1978. This language was an answer, in adequate and efficient manner, to the development of software projects with some complexity. A program in Modula-2, called a module, has two main divisions. The first division starts with the keyword MODULE and consists of a series of IMPORT declarations. IMPORT declarations involve the external modules and variables to be used. The other main division consists of block statements enclosed within BEGIN and END keywords. The structure is similar to Pascal. One important characteristic of Modula-2 is the reuse of already developed and working pieces of code (Cezzar 1995).

PL/1 (for Programming Language), was announced by IBM in 1963, combining the functionalities of the FORTRAN, ALGOL and COBOL (Beyon 2001). PL/1 is a multipurpose programming language. It was designed for the use by both scientific and commercial applications, by teams and task forces set up from Share organization of FORTRAN users. PL/1 consists of one or more separately compiled program modules. Each external procedure is constructed from units that are grouped as: (1) simple statements, (2) compound statements, (3) DO groups, (4) BEGIN blocks, and (5) internal procedures. Thus, PL/1 can be characterized as a blocked structured language, with logical organization of program components (Cezzar 1995).

SNOBOL (for StriNg Oriented symbolic Language) was designed in 1962 by a research group lead by R. Griswold at Bell Laboratories as an aid to other internal projects in symbolic formula manipulation. It is based on pattern-matching principles for solving string-manipulation problems. The concepts are primarily on manipulation of regular expressions. Many of those have been incorporated into text editors, filtering utilities, lexical analyzers, and parsers (Cezzar 1995).

More recently, C language was developed by D. M. Ritchie of the AT&T Bell Laboratories in 1972, and C++ by B. Stroustrup also of the AT&T Bell Laboratories in the early 1980's. This last one is based on the latest paradigms in text-based programming language: object-oriented programming languages (Beyon 2001).

In order to summarize the programming languages' evolution, Table 3.1 presents the main generations of programming languages with reference to the period of their appearance and a brief description of each one.

Table 3.1 : Generations of programming languages (Rodrigues *et al.* 2005).

Generation (decade)	Programming paradigms that support	Examples	Description
1ª (50's and 60's)	Unstructured	Cobol, Fortran, Basic	Instructions using a pseudo-natural language: English words, such as PRINT or DISPLAY; All code written in a single program.
2ª (70's)	Procedural	Pascal, C language	Problem decomposition in a necessary number of procedures; use of algorithms most appropriate that it intends to implement; supported a limited set of control primitive.
3ª (80's)	Modular	Modula II	Based on the principle of data encapsulation; decomposition of the program in modules, so that the data being hidden in them.
4ª (80´s)	Data types abstraction	ADA	Defining the kind of data that it is needed and the creation of a specific set of operations and comprehensive intended exclusively to them.
5ª (80's and 90's)	Object-oriented	Smaltalk, C++, Java	Choice of classes or types of objects that it is needed; provide these classes with a full set of operations; making explicit recognized common characteristics between classes, through mechanisms of inheritance of classes; use of methods polymorphisms between objects of derived classes.

3.3.2. C++ PROGRAMMING LANGUAGE

The name C++ was introduced by Rick Mascitti in the summer of 1983. The name signifies the evolutionary nature of the changes from C, through the concatenation of letter C with the increment operator: ++. Thus, the evolution of the C resulted in the current one known C++. The Company AT&T Bell Laboratories made a major contribution to this, by allowing Bjarne Stroustrup to share drafts of revised versions of the C++ reference manual with implementers and users (Stroustrup 1997).

C++ is used by hundreds of thousands of programmers in essentially every application domain. This use is supported by about a dozen independent implementations, hundreds of libraries, hundreds of textbooks, several technical journals, many conferences and innumerable consultants. Training and education courses at a variety of levels are widely available (Stroustrup 1997).

Early applications tended to have a strong systems programming essence. For example, several operating systems where developed in C++ and many more have key parts done in

C++. Bjarne Stroustrup considered uncompromising low-level efficiency essential for C++. This allows the users of C++ to develop device drivers and other software that relies on direct manipulation of hardware under real time constraints. C++ was designed so that every language feature is usable in code under severe time and space constraints (Stroustrup 1997).

It is quite common to find an application that involves local and wide-area networking, numeric, graphics, user interaction and database access. Traditionally, such application areas have been considered distinct, and they have most often been served by distinct technical communities using a variety of programming languages. However, C++ has been widely used in all of those areas. Furthermore, it is able to coexist with code fragments and programs written in other languages. The areas in which C++ is applied are wide, such as banking, trading, insurance, telecommunications and military applications (Stroustrup 1997).

C++ is widely used for teaching and research, although C++ is not the smallest or cleanest language ever designed. It is, however (Stroustrup 1997):

- clean enough for successful teaching of basic concepts,
- realistic, efficient, and flexible enough for demanding projects,
- available enough for organizations and collaborations relying on diverse development and execution environments,
- comprehensive enough to be a vehicle for teaching advanced concepts and techniques,
- commercial enough to be a vehicle for putting what is learned into non-academic use.

The most important thing to do when learning C++ is to focus on concepts and not get lost in language-technical details. The C++ supports a variety of programming styles, however, programmers coming from different language (say C, FORTRAN, Pascal, etc.) should realize that to gain the benefits of C++, they must spend time learning and internalizing programming styles and techniques suitable for C++. It is possible to write in the style of FORTRAN, C, Pascal, etc., but doing so is neither pleasant nor economical in a language with a different philosophy (Stroustrup 1997).

C++ has no built-in high-level data types and high-level primitive operations. For example, the C++ language does not provide a matrix type with an inversion operator or a string type with a concatenation operator. If a user wants such operator type, it can be defined in the language itself. In fact, defining a new general-purpose or application-specific type is the most fundamental programming activity in C++. A well-designed user-defined type differs from a built-in type only in the way it is defined, not in the way it is used (Stroustrup 1997).

The C++ mainly seats in the programming oriented to objects paradigm. In other words, it consists in the classes' choice or objects type that the programmer needs. Provide those classes with a full set of operations, making explicit recognized common characteristics between them, through classes' inheritance mechanisms, and use of methods polymorphisms between objects of derived classes (Rodrigues *et al.* 2005). Table 3.2 summarizes the fundamental concepts of the object-oriented programming.

Table 3.2 : Fundamental concepts of object-oriented programming.

Concept	Description
Class	Set of objects representation with similar characteristics.
Object	Class instance. An object is capable of storing states through its attributes.
Attributes	Object information of their class.
Methods	Definition of skills of objects.
Heritage	Mechanism by which a class (sub-class) can extend another class (super-class), using their behaviours (methods) and possible states (attributes).
Polymorphism	Principle by which two or more classes derived from the same super-class can invoke methods that have the same signature (list of parameters and return) but distinct behaviours, specialized for each derived class, using either a reference to an object of a kind of super.

This programming philosophy converge to what Bjarne Stroustrup referred as a need to achieve higher levels of code recycle, so that much of the work for a given purpose, may be used in other objectives, without constantly be *reinvented the wheel* (Stroustrup 1997).

It should be noted however, that C++ has some disadvantages, such as (Stroustrup 1997):

- the current compilers do not always create the most optimized code as well as in speed and on the application size;
- normally requires a long period of learning;

- because of its great flexibility, it is recommended the use of programming methods more frequently than in other languages.

3.3.3. MATLAB PROGRAMING LANGUAGE

The name MATLAB stands for matrix laboratory. MATLAB was originally written to provide easy access to matrix software developed by the LINPACK (collection of FORTRAN subroutines that analyze and solve linear equations and linear least-squares problems) and EISPACK (collection of FORTRAN subroutines that compute the eigenvalues and eigenvectors of several classes of matrices) projects. Today, MATLAB engines incorporate the libraries LAPACK (routines in Fortran 90 for solving systems of simultaneous linear equations, least-squares solutions of linear systems of equations, eigenvalue problems, and singular value problems) and BLAS (routines to perform basic linear algebra operations such as vector and matrix multiplication), embedding the state of the art in software for matrix computation (MathWorks 2007).

MATLAB has evolved over a period of years with input from many users. In university environments, it is the standard instructional tool for introductory and advanced courses in mathematics, engineering, and science. In industry, MATLAB is the selected tool for high-productivity research, development and analysis. It collects a family of add-on application-specific solutions called toolboxes. Very important to most users of MATLAB, these toolboxes allow learning and applying specialized technology. Toolboxes are comprehensive collections of MATLAB functions (M-files) that extend the MATLAB environment to solve particular classes of problems. Areas in which toolboxes are available include signal processing, control systems, neural networks, fuzzy logic, wavelets, simulation, and many others.

In this context, MATLAB is a high-performance language for technical computing that integrates computation, visualization, and programming in an easy-to-use environment where problems and solutions are expressed in familiar mathematical notation. Typical uses include (MathWorks 2007):

- math and computation,

- algorithm development,
- data acquisition,
- modelling, simulation, and prototyping,
- data analysis, exploration, and visualization,
- scientific and engineering graphics,
- application development including graphical user interface building.

This ambitious program contains hundreds of commands to do mathematics namely, graphical functions, solving equations, statistical tests, and much more. It is a high-level programming language that can communicate with FORTRAN, C and LABVIEW. MATLAB is more than a fancy calculator; it is an extremely useful and versatile tool (Hunt *et al.* 2001). In the early versions, all variables were double precision matrices, but now many other useful data types are available. For example, integration with Java is standard, and Java classes can appear in MATLAB code. The MATLAB language now has its own object-oriented features. These changes have made clear code writing more important and more challenging (Johnson 2011).

More recently, MATLAB has been used to make Exploratory Data Analysis (EDA). The idea is to explore data sets with statistics and data analysis, often using methods from descriptive statistics, scientific visualization, data tours, dimensionality reduction, and others. It is mostly a philosophy of data analysis where the researcher examines the data without any pre-conceived ideas in order to discover what the data can tell about the phenomena that is being studied (Martinez *et al.* 2010). Undoubting, these are useful tools in order to extract new knowledge from the monitoring data regarding a better understanding of the real behaviour of civil infrastructures.

3.3.4. LABVIEW PROGRAMMING LANGUAGE

In 1986, the National Instruments introduced a new programming language paradigm with LABVIEW 1. Initially, it was a big program devoted to data acquisition with very limited functionalities. Since then, its functionalities and programming potentialities have been

grown, and LABVIEW has now become one of the most used applications among engineers, researchers and scientists. Contrasting with text-based programming languages, which normally require a learning period to get into the syntax and all the language details, the programming concept in LABVIEW is visually intuitive and user-friendly due to graphical representations instead of the lines of code. A new concept was created and a new expression appeared, G-language (Graphical). While for conventional programming languages text files are used to write the source code with pre-defined formats, in LABVIEW those text files are replaced by files so called Virtual Instrument – VI (Beyon 2001). Two levels of code access exist in the LABVIEW, namely a:

- high-level, where the user manipulates pre-defined VIs and/or others created by the programmer;
- low-level, where the VIs are compiled (not accessible to the programmer user).

The insertion of a VI into a software project is made in a front panel where the graphical interface is implemented, and a block diagram where the relations between the different objects (respecting to the graphical representations in the front panel) are established with connecting wires.

Figure 3.4 illustrates a trivial example of the sum of two numbers, ‘x’ and ‘y’, which is displayed into the object ‘z’. In more detail, Figure 3.4-a presents the front panel where the graphical interface implemented by the user is displayed, while Figure 3.4-b shows the block diagram where connecting wires are used to establish ‘z’ as the sum of ‘x’ and ‘y’.

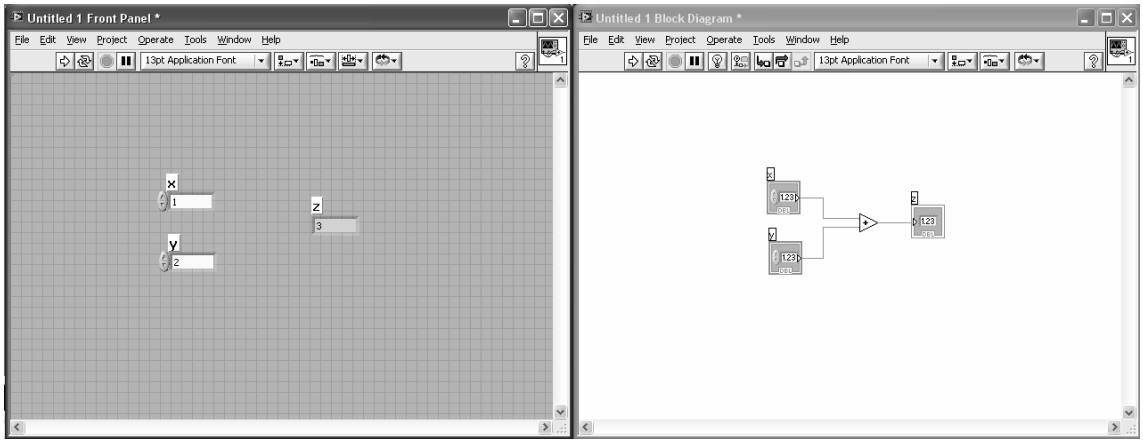

a) front panel. **b) block diagram.**

Figure 3.4 : LABVIEW programming environment – trivial example of adding two numbers.

As aforementioned, the front panel is a simple and inviting mean for software projects with high requirements for graphical interface. The programmer does not have to write lines of code, and on the other hand, the graphical aspect in the block diagram with wires linking objects increases the interpretation of the source code. Summarizing, the programming environment of LABVIEW is set by two windows – front panel and block diagram as illustrated in Figure 3.4. The concept of a pre-defined sort, such as for example *from left to right* does not exist in LABVIEW due to the non-existence of a text file with code lines. Therefore, parallel processing can be explored. For example, two VIs without variables dependence can be processed in parallel, making the applications fasters comparatively with projects developed in other programming languages (Beyon 2001).

LABVIEW, if compared with programming languages based on lines of code, presents the following advantages (Beyon 2001):

- the learning period is lower,
- the graphical environment makes easier the code interpretation,
- the time spent in the implementation phase is lower,
- a set of built-in tools are available for graphical interface (GUI) to be easily used.

Despite of these advantages, the following aspects must be taken into account (Beyon 2001):

- minor changes in the code may require a new restructuring of the project software namely, when a new variable/procedure is created, which obligates to reconnect wires and symbols to restore the full functioning;
- commonly, more variables than the strictly necessary are introduced, which might lead to an increase of the execution time.

3.4. INTEGRATED PROJECTS IN LABVIEW\MATLAB\C++

For complex projects, programming with subroutines, where each subroutine can be written in a specific programming language, might exhibit some advantages from the

developer's perspective. Moreover, the subroutines assembly can take profit of the potentialities of the low-level and high-level characteristics of the used languages. The *failures* of each programming language may be partially, or even totally, compensated by the advantages of the remaining programming languages. To make this possible, specific communication protocols, by which two languages must obey, have to be used. Generally, mixed-language programming involves one high-level language, which is used as the main language responsible for calling subprograms, subroutines, procedures, and functions developed in other(s) language(s) (Cezzar 1995).

For example, if a programmer has a set of tools already developed and validated in C++, they can be recompiled into DLL (Dynamic Link Library) extension. This allows that those tools might be called, for example, from LABVIEW environment through the communication protocol that exists for these two languages communicate correctly. The recompilation of the existing C++ code into DLL does not involve a significant effort, where the main aspect to take into account is the coherent definition of the input variables and the output results with what it is respectively defined in the LABVIEW environment.

Taking into account the characteristics previously described of LABVIEW, MATLAB, and C++, Table 3.3 summarizes the main potentialities offered by each one.

Table 3.3 : Principal potentialities of the C++, LABVIEW and MATLAB.

LABVIEW	MATLAB	C++
Graphical programming environment	High-performance language for technical computing	Hardware access (low level)
A set of built-in tools devoted to data visualization	Wide range of functions devoted to complex mathematical calculations	Object-oriented programming: classes and objects
Assembly of C++ programs through DLL's extension	Interface with LABVIEW (Math script, "*m-files*")	Interface with LABVIEW (extern C)

3.5. MENSUSMONITOR

The term MENSUSMONITOR is the link of two basic words:

- *Mensus*, a Latin verb that means measure, assess, evaluate, judge;

- *Monitor*, a noun that can mean equipment that transmits information through images or an auxiliary of the professor.

Hence, MENSUSMONITOR allows the visualization of monitoring data and the extraction of information of superior level through specific engineering techniques, which were, and are being, developed with the purpose of supporting the SHM process. In other words, it is an auxiliary (the software), of the professor (the user), for his evaluations, judgements and decisions based on the sensors' measurements. Figure 3.5 shows the positioning of MENSUSMONITOR in the SHM process.

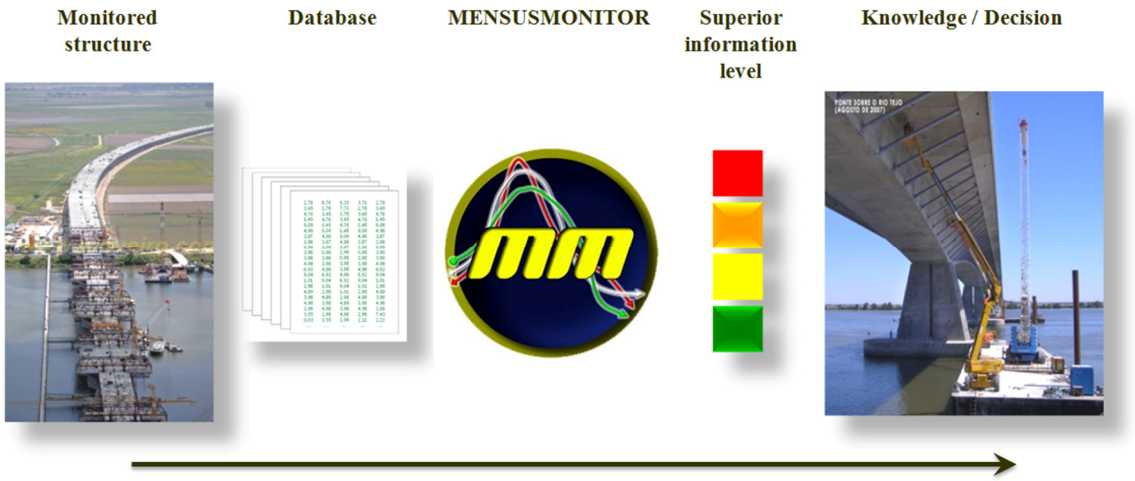

Figure 3.5 : Positioning of MENSUSMONITOR in the SHM process.

3.5.1. MAIN GOALS

MENSUSMONITOR intends to reduce, significantly, the time spent in data input, consulting and knowledge extraction. In fact, in a first stage, the tasks previously described in the sub-chapter "*3.2 Some issues about Structural Health Monitoring*" were the main motivations for the firsts numerical tools implemented in MENSUSMONITOR. Therefore, the presented software offers the following competences:

- a library of numerical tools – engineering techniques – specifically developed for the treatment and analysis of data collected by monitoring systems, devoted for civil infrastructures and based on the authors' experience;

- information extraction of higher level of knowledge, and its presentation through graphics, tables and colour indicators;
- vehicle to promote academic and/or professional work of the authors.

3.5.2. SOFTWARE DESIGN

Two fundamental aspects characterize MENSUSMONITOR:

- efficient calculus procedures in order to allow an easy handling, treatment and knowledge extraction from input data;
- intuitive graphical interface in order to achieve high levels of efficiency.

The MENSUSMONITOR framework was implemented in LABVIEW, the high-level programming language, taking advantage of the available built-in tools for the implementation of the graphical interface. As far as the modules that comprise the software are concerned, they were developed using three different programming languages:

- LABVIEW for the implementation of algorithms with basic requirements and without relevant complexity.
- MATLAB for the implementation of algorithms with some mathematical complexity, by taking advantage of the available functions.
- C++ for the implementation of algorithms with specific aim and/or high computational complexity.

The programming structure of MENSUSMONTOR is shown in Figure 3.6. The main advantage offered by this structure is the possibility to integrate numerical tools developed by different programming languages. Therefore, MENSUSMONITOR benefits from the principal advantages of each programming language, which in a certain way, compensate the limitations of each one. Moreover, the programmers that usually develop their numerical tools in one of the languages do not have to re-write the source code in order to be possible their integration in the software project.

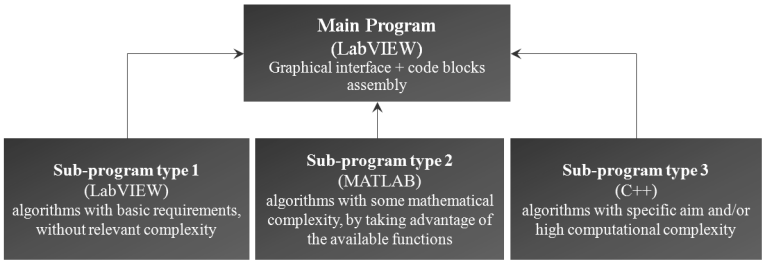

Figure 3.6 : Programming structure of MENSUSMONITOR.

Regarding the main scope of MENSUSMONITOR – knowledge extraction from monitoring data by using proper engineer techniques devoted to SHM – five independent modules were defined, namely (Figure 3.7):

- "*Data Entry*" module, which manages the data input,
- "*Numerical Tools*" module, which is responsible for the management of the numerical tools library,
- "*Auxiliary Tools*" module, which offers a set of functionalities for data preparation focussing the application of a specific numerical tool,
- "*Export Results*" module that allows the exportation of the output results,
- "*Help*" module, in html format with all the relevant information concerning the proper use of the software.

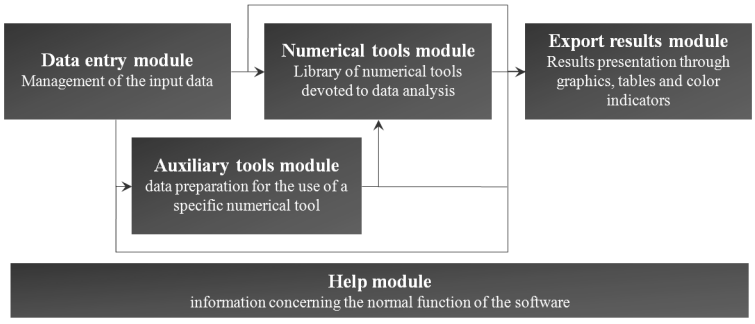

Figure 3.7 : MENSUSMONITOR modules.

This modulation allows MENSUSMONITOR to evolve with higher flexibility. In fact, the modular structure offers unique advantages namely, it turns possible modify/add/remove

part of the code source without needing to change the program structure. For instance, the implementation of a new numerical tool can be performed without change the "*Data Entry*" and "*Export Results*" modules because these last two are already implemented. Another example is the implementation of an algorithm in order to get access to data files generated by a new equipment for data acquisition. This might be done by simply updating the "*Data Entry*" module without modify the remaining modules. Thus, it is possible to have a program team working together and simultaneously focussed on different targets. The work dependency between them is low and the sharing of different experiences, with different programming languages, may lead to solutions more robust.

3.5.3. MODULES AND FUNCTIONALITIES

The five modules presented in Figure 3.7 have different but complementary functions. Global input and output variables are the main key to establish the link between these modules. For example, the "*Data Entry*" module produces an output variable with data in a standard format, which afterwards is used as input variable for the "*Numerical Tools*" and/or "*Auxiliary Tools*" modules.

- **"*Data entry*" module**

The supported format, for input data, was one of the main aspects taken into account in the software project. The appeal to use a new/specific software is strongly influenced by the way that raw data is accessed, i.e. directly and without intermediate steps. Therefore, taking into consideration the data acquisition systems commonly used for civil engineering infrastructures, the data access can be done by two means:

  - direct access to acquisition systems, by collecting and storing the sensors' measurements into the memory of the current working session namely, equipments of the following manufactures: *Data Taker*, *Micron Optics*, and *National Instruments*;

- access to data files created by acquisition systems namely, equipments of the manufactures: *Data Taker*, *Micron Optics*, *GEOSIG* and *National Instruments*.

Nevertheless, the software also supports files with extensions *txt* and *xls*. In this case, and for a correct interpretation of the data contained in those files, the user has only to be aware to fulfil a specific standard format that is detailed in the "*Help*" module. Additionally, for extreme cases of massive data, MENSUSMONITOR is also capable to access to databases of *mySQL* type, locally or remotely via IP address.

- **"*Numerical tools*" module**

This is the core module of MENSUSMONITOR, where the numerical tools are allocated. As aforementioned, different programming languages (LABVIEW, MATLAB or C++) were (and are) used, depending on the specific requirements of each case.

Table 3.4 resumes the numerical tools currently available, which are the outcome of their authors' experience, namely from handling with monitoring data. Hence, this module joins a set of functionalities, which results from a collective experience with its inherent benefits.

Table 3.4 : "*Numerical tools*" module.

Name	Functionalities	Programming language
mensus sampling rate change	Reduction/increment of measurement sampling with decimation / interpolation techniques.	MATLAB
mensus filter	Removal of undesired effects in the sensors' measurements with a set of signal filters.	LABVIEW \ C++
mensus fitting	Adjustment of shrinkage and creep models of Eurocode 2 to experimental data.	C++
mensus correlation	Identification of correlation patterns for pairs of sensors' measurements.	LABVIEW
mensus deflection	Assessment of structure deflections based on measurements of deformations and rotations.	C++
Mensus traffic	Evaluation of traffic parameters based on strain measurements namely: velocity, travelling direction and loading.	C++
Mensus prediction	Prediction of a sensor response based on others sensors' measurements.	LABVIEW \ MATLAB

- **"*Auxiliary tools*" module**

For an efficient use of the tools provided by the "*Numerical tools*" module (Table 3.4), the data management becomes a critical aspect. For example, during the same working session, it might be useful to store the output results obtained by a numerical tool, for later use as input data into another numerical tool. Another example might be a set of sequential data files, for which it might be desirable the data assembly into a single matrix before any calculations. Conversely, in the presence of a long data set, it might be desirable the creation of smaller matrices for subsequent calculations.

In order to become possible this kind of operations, i.e. a flexible data handling, four auxiliary tools were implemented. Table 3.5 resumes the main functionalities, which offer higher potentialities in order to use more efficiently the software features.

Table 3.5 : "*Auxiliary tools*" module.

Name	Functionalities	Programming language
Data selector	Data sub selections, both in rows and columns. Possibility to define/store event windows for flexible data sub-selection.	LABVIEW
Data manipulator	Corrections and/or adjustments in data, namely:	
	Sensors calibration: Conversion of the measured electrical/optical parameter into the desired physical parameter.	LABVIEW
	Merge signals: Merge of two consecutive data sets, into a single data set.	LABVIEW
	Offset compensation: Removal of linear and non-linear effects in data measurements.	C++
	Linear combination: Linear combination of two data sets.	LABVIEW
	Outliers: Removal of unmeaning samples.	LABVIEW
	Match peaks: Offset of the abscissa scale of data sets.	LABVIEW
Data memory	Data storage and management. Possibility of data backup or, conversely, data importation to restore the working point of a prior working session.	LABVIEW
Data viewer	Simultaneous visualization of measurements and video footage.	LABVIEW

- **"*Export results*" module**

The author's experience says that when a software without proper output interface is used, subsequent formatting work is always necessary in order to get the required layouts for graphics and tables. In fact, this is common for sophisticated software, which normally throws out a set of results as unformatted text files, however, this output format is not the desirable to be used for documents publishing. Hence, for these cases, spreadsheets such as EXCEL type, for example, are normally used to arrange the intended layouts with tables and graphics in order to be used in official documents such as reports, thesis, articles and/or presentations.

In this context, an "*Export results*" module was implemented in MENSUSMONITOR, with a set of output styles so that this intermediated step might be avoided, namely:

- data files, which can be helpful for future calculation procedures;
- image files, which can be helpful to be inserted in text documents;
- html file, which can be helpful in a subsequent data consulting by avoiding the need of recalculating a same scenario;
- data storage into databases of MySQL type.

- **"*Help*" module**

Despite of all precautions taken in the implementation of the graphical interface, in order to make the software use intuitive, a "*Help*" module was developed and incorporated in the software project. Here, all relevant information for a correct use of the software is illustrated. This module provides a wide-raging guide with step by step illustrations of the main functionalities for a correct use of the software. Besides this function, the "*Help*" module sponsors the authors' work, which is also one of the main goals of this software project, as abovementioned. This strategy has a pedagogic effect on the numerical tools' developers, because it stimulates the development of their work focussing the final user. Therefore, a final package more robust and equilibrated is attained. Figure 3.8 shows a print-screen of the entering page of the "*Help*" module.

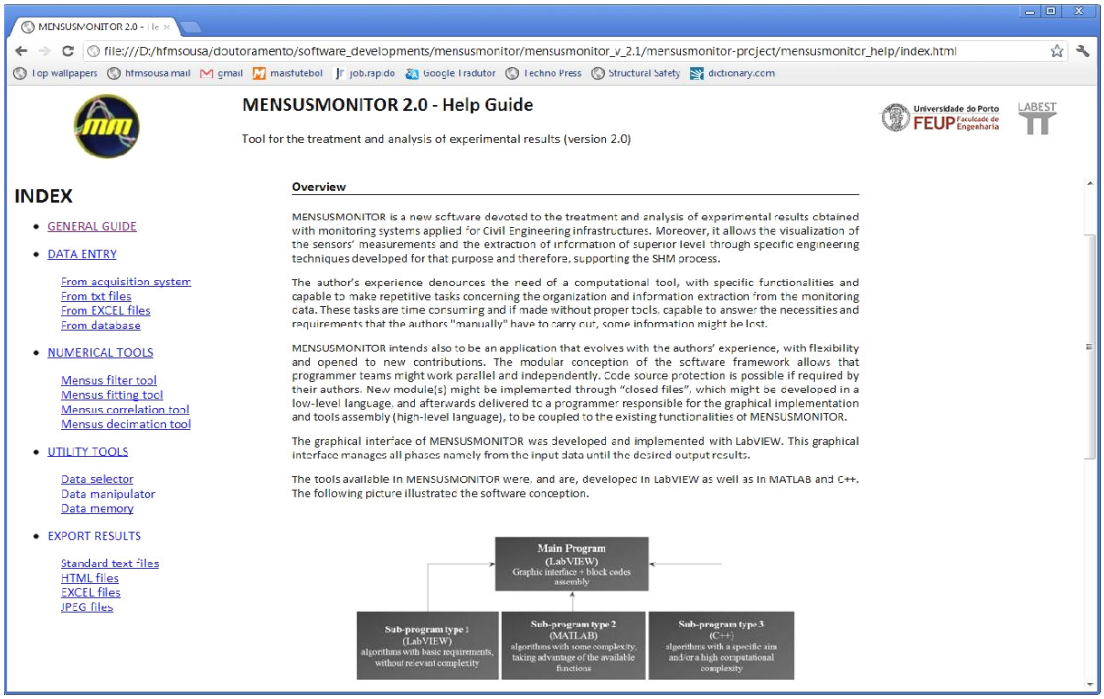

Figure 3.8 : "*Help*" module.

Finally, Figure 3.9 shows the entry point of MENSUSMONITOR, i.e. the initial front panel when the application is prompted. The modules previously detailed might be accessed through the menu bar at the top. Meanwhile, two additional modules were implemented: (i) "*Operate*" module to manage the program settings, and (ii) "*Demonstration*" module focussing future features that are currently under development.

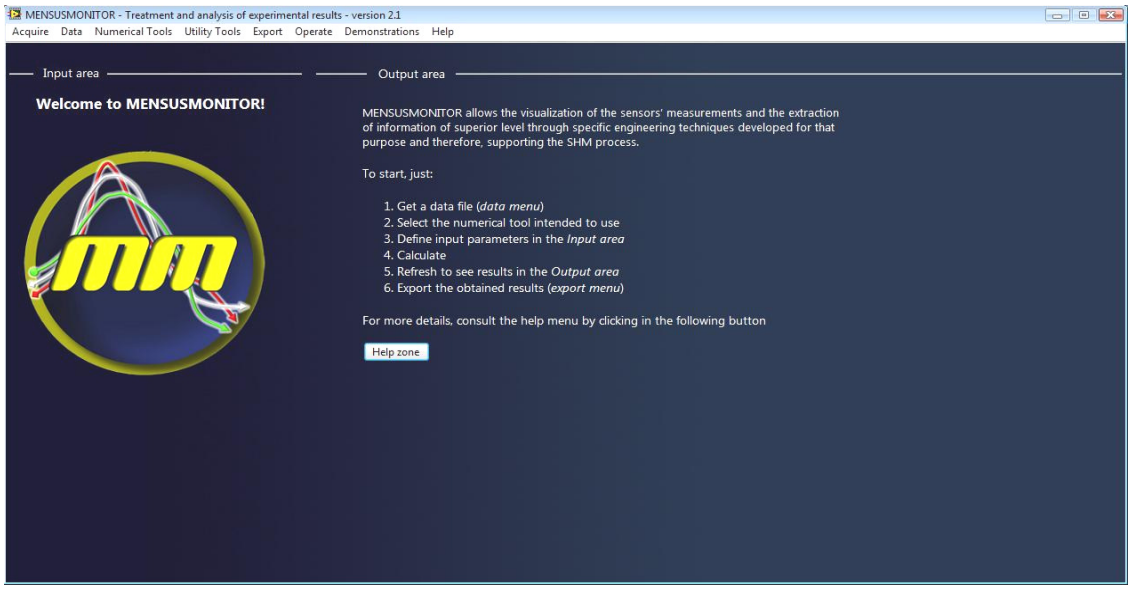

Figure 3.9 : Front panel of MENSUSMONITOR.

3.6. PRATICAL APPLICATION

In order to show the functionalities of MENSUSMONITOR and its flexibility in data processing, a practical application is presented in this subchapter. In more detail, this case regards the observation of the load test of a concrete bridge – Sorraia Bridge – that is equipped with a monitoring system (SMARTE 2004; Sousa *et al.* 2005). At the end of the load test, the data size collected by the referred monitoring system was considerable and the data processing became a non-trivial task.

The objective herein is to use MENSUSMONITOR features in order to organize, treat and produce the final graphics to be included in the observation report, which will be the essential information in future analyses.

3.6.1. THE STRUCTURE

Sorraia Bridge, located at Salvaterra de Magos, is inserted in the motorway A13 that links Almeirim to Marateca. It has a total length of 1 666 m composed by two parallel and identical structures – east and west decks (GRID 2003). Three substructures of prestressed concrete materialize the structure: (i) north viaduct, main bridge and south viaduct with 487 m, 270 m and 909 m, respectively. The main bridge is the focus for the current example (Figure 3.10). This substructure of three spans was constructed by the cantilever method: two end spans with 75 m and a central span with 120 m. The bridge section is a box girder with section height ranging from 2.55 m (at mid-span) to 6.00 m (near the support piers). The piers with 7.5 m high have sliding guided bearings positioned on their top that enable the deck supporting. Pilecaps of five piles each support the piers. Piles have 2 m diameter and are approximately 30 m deep.

Figure 3.10 : Sorraia Bridge – Load test.

3.6.2. THE MONITORING

A long-term monitoring system is installed in the east deck of Sorraia Bridge, which was developed under the scope of a consortium project between BRISA S.A. and two R&D institutions, LABEST-FEUP and INESC-PORTO, which was partially supported by AdI – Innovation Agency (SMARTE 2004). Regarding the load test, this system registered the structural behaviour of the bridge by collecting measurements concerning concrete deformations and temperatures by embedded sensors in a set of sections as well as the environmental temperature and relative humidity. Additional to this system, another one was installed to observe and register additional parameters during the load test namely, vertical displacements and rotations (Sousa *et al.* 2005). This additional data was useful to calibrate and validate the permanent monitoring system that was permanently installed. Figure 3.11 shows the location of the instrumented sections whilst Table 3.6 summarizes the instrumentation plan.

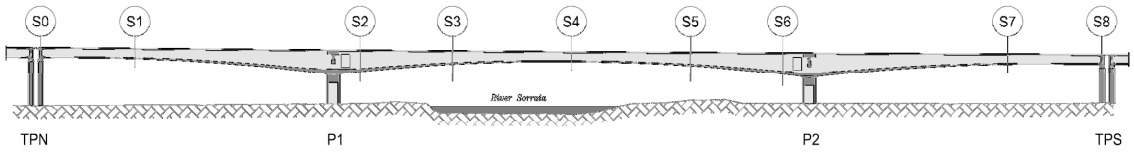

Figure 3.11 : Location of the instrumented sections in Sorraia Bridge.

Table 3.6 : Instrumentation plan.

Parameter	S0	S1	S2	S3	S4	S5	S6	S7	S8
Vertical displacement	-	1	3	1	1	1	3	1	-
Horizontal displacement	2	-	1	-	-	-	1	-	2
Rotation	-	-	1	-	-	-	1	-	-
Deformation	-	6	12	4	12	4	12	8	-
Temperature	-	-	-	-	-	2	2	-	-
Relative humidity	-	-	-	-	-	-	2	-	-

The load test lasted approximately 4 hours, for which five acquisition nodes equipped with three different acquisition systems supported the data storage. Each acquisition system allowed different signal sampling rates, with frequency readings that reached to 200 Hz. At

the end of the load test, more than 20 data files were created with the measurements collected by the 83 sensors installed in the bridge.

Focussing the relevant information for the observation report, this information must be organized through systematic procedures and during the shortest period possible. As a result, the results were organized in a set of graphics, with the sensors readings properly identified and grouped by load cases. Moreover, for each graph, a summary table with the most relevant statistical information is also plotted namely, minimum and maximum values and the respective instants of occurrence as well as the number of samples. Despite of the importance of this information for the observation report, the collected measurements are also important for future FEM analysis and therefore, it is very important to have the data properly treated and organized.

3.6.3. DATA TREATMENT

- **Access to the data files**

The 20 data files generated by the acquisition systems were directly accessed by MENSUSMONITOR, by means of the "*Data Entry*" module (Figure 3.12). Different access types were used because different acquisition systems were used during the load test as aforementioned. Always that a data file is accessed, the user is informed about the file size, which is always useful to know the amount of data that is going to be handled, and the number of sensors' measurements that the data file contains, i.e. the number of columns. Usually, these data files contain a header with information about the adopted reading procedures, namely the columns' label that might be useful to edit correctly the name of the data columns. This step is crucial to avoid mistakes and confusions between measurements in the following processing steps.

After the data upload into MENSUSMONITOR, the information was stored in the session memory through the "*data memory*" tool from the "*Auxiliary tools*" module (Table 3.5), which allowed the sequential access to the 20 data files without loosing the information

previously uploaded. At the end, the data contained in the data files was finally available in the current working session of MENSUSMONITOR as it is presented in Figure 3.13.

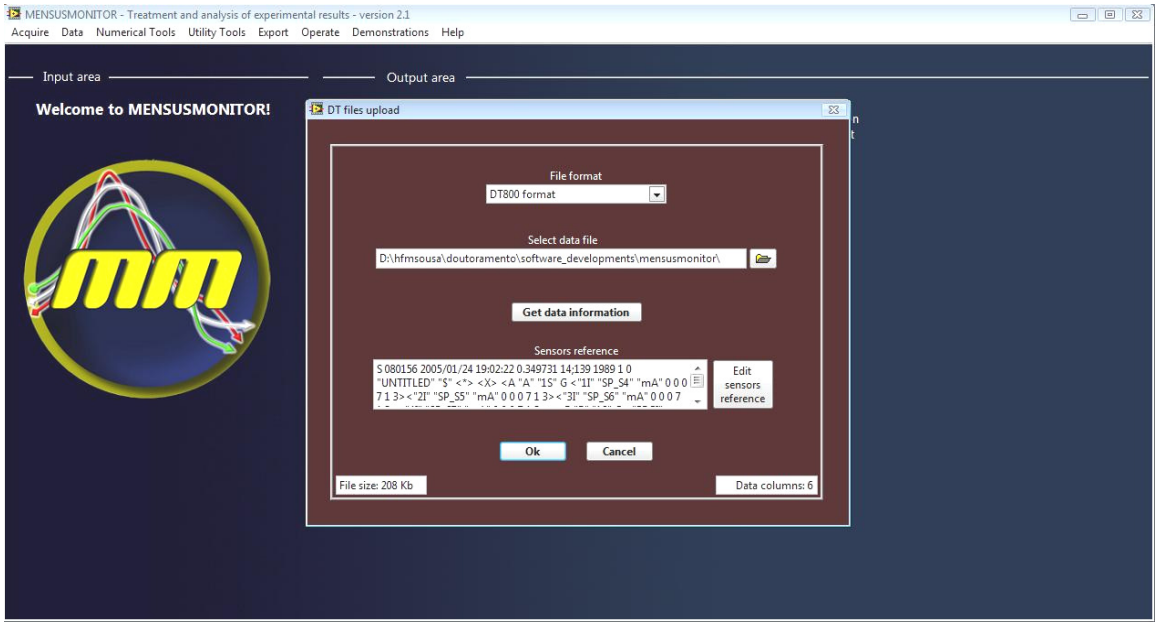

Figure 3.12 : Data file access and upload ("*data entry*" module).

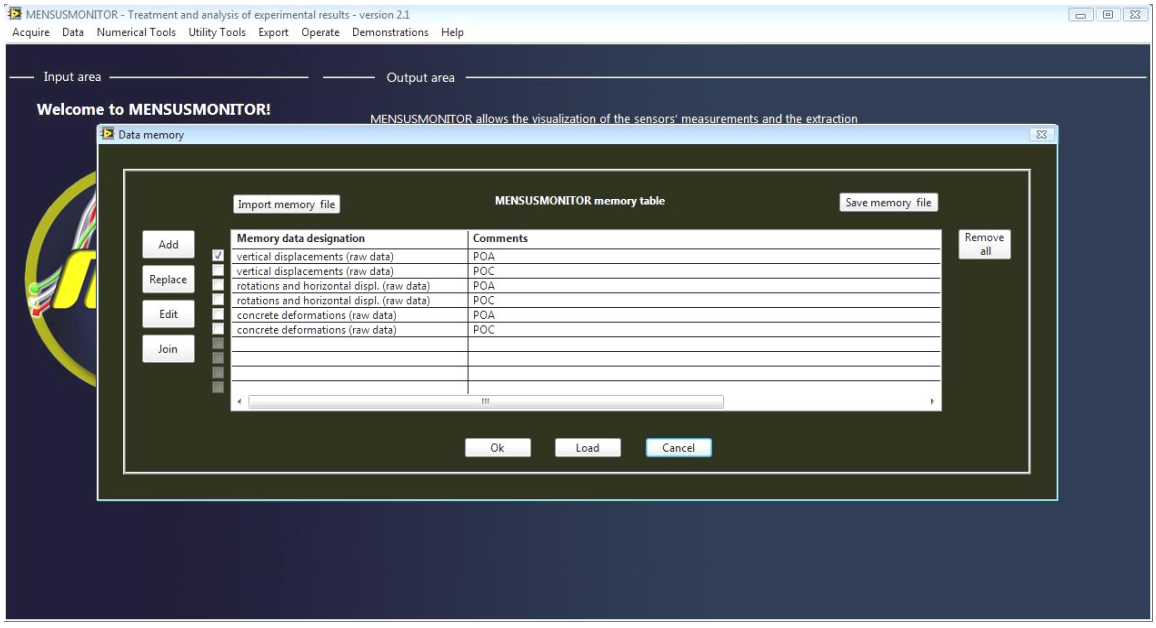

Figure 3.13 : Data storage into the current working session ("*data memory*" tool).

- **Data pre-treatment**

The conversion of the sensor signal, from the electrical signal to the respective physical parameters of interest, was the first task performed after the data upload. This procedure was performed by using the "*sensor calibration*" operation that is available in the auxiliary tool "*data manipulator*" (Table 3.5). A set of converters are available that takes into account the sensors type commonly used in SHM. Figure 3.14 illustrates the conversion performed for the measurement concerning the vertical displacements of section S4 (Figure 3.11).

Figure 3.14 : Data conversion ("*Data manipulator*" tool).

Some atypical measurements and not null trends were encountered in the data, namely caused by temperature variations during the load test. In the case illustrated in Figure 3.14, it is notorious the existence of atypical values in the sensor's measurement. Therefore, after the signal conversion, the atypical measurements were eliminated with the "*outliers*" operation, whilst the environmental effects were removed by using the "*offset compensation*" operation, both available in the auxiliary tool "*data manipulator*" (Table 3.5).

- **Definition of window events**

Figure 3.15 shows the auxiliary tool "*data selector*" active, where it is presented the measurements of seven vertical displacements (VD), in correspondence to the sections S1 to S7 (Figure 3.11 and Table 3.6).

Two slow passages were registered, as it can be observed by the repetition of the measurements' pattern. These two slow passages were split in two independent data sets, which might be useful for posteriorly overlapping of both passages in order to evaluate the linear elastic behaviour of the bridge. With that purpose, two event windows were defined and used to slice the measurements into the two data sets. The tool "*data selector*" from the "*Auxiliary tools*" module (Table 3.5) supported the definition of those two event windows – "*Slow passage 1*" and "*Slow passage 2*". This information was stored in the memory of the current session to make possible the data access whenever intended.

The flexibility of this feature allied to the "*data memory*" tool deserves to be highlighted. The "*data memory*" tool allowed the data management, which was used in function of the desired graphic, while the concept of event windows was an efficient strategy to support and organize the required graphics.

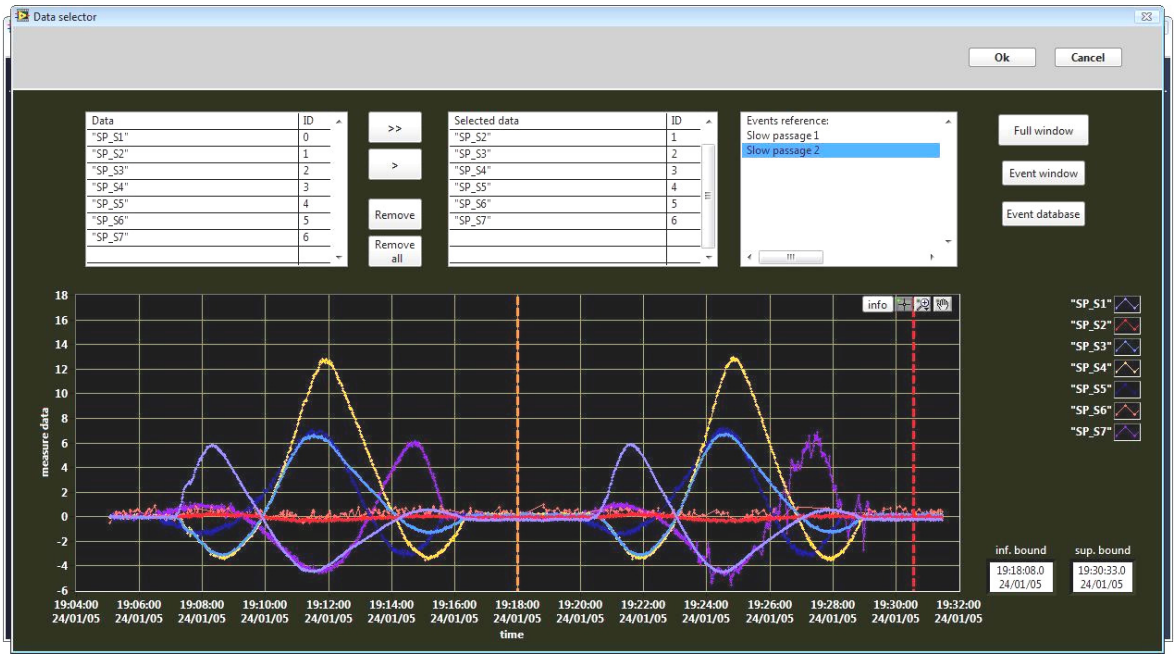

Figure 3.15 : Definition of event windows.

- **Data treatment**

As aforementioned, even though the measurement quality is highly influenced by the characteristics of the monitoring system setup, the in situ conditions are also an important aspect. Commonly, measurements exhibit some noise, which in fact occurred in this load test. To improve the results quality, the tool "*mensus filter*" of the "*Numerical tools*" module (Table 3.4) was applied to improve the quality of the measurements.

Figure 3.16 shows the MENSUSMONITOR front panel with the "*mensus filter*" tool active. Two different areas can be identified:

- On the left side, the input variables can be defined namely, measurement selection, filter type and its parameters' values;
- The remaining area shows the output results by graphics and tables. Raw and filtered data as well as the main statistical information are shown in order to support the judgment about the smoothness quality.

Regarding the case illustrated in Figure 3.16, a Savitzky-Golay filter type (Savitzky 1964) with a movable window of 15 points of equal weight was applied to smooth the vertical displacement measured in section S7 (see Figure 3.11). Particularly for this case, the complete data set is presented, i.e., "*Slow passage 1*" and "*Slow passage 2*", in order to testify how it is possible the data recover by using proper filtering techniques.

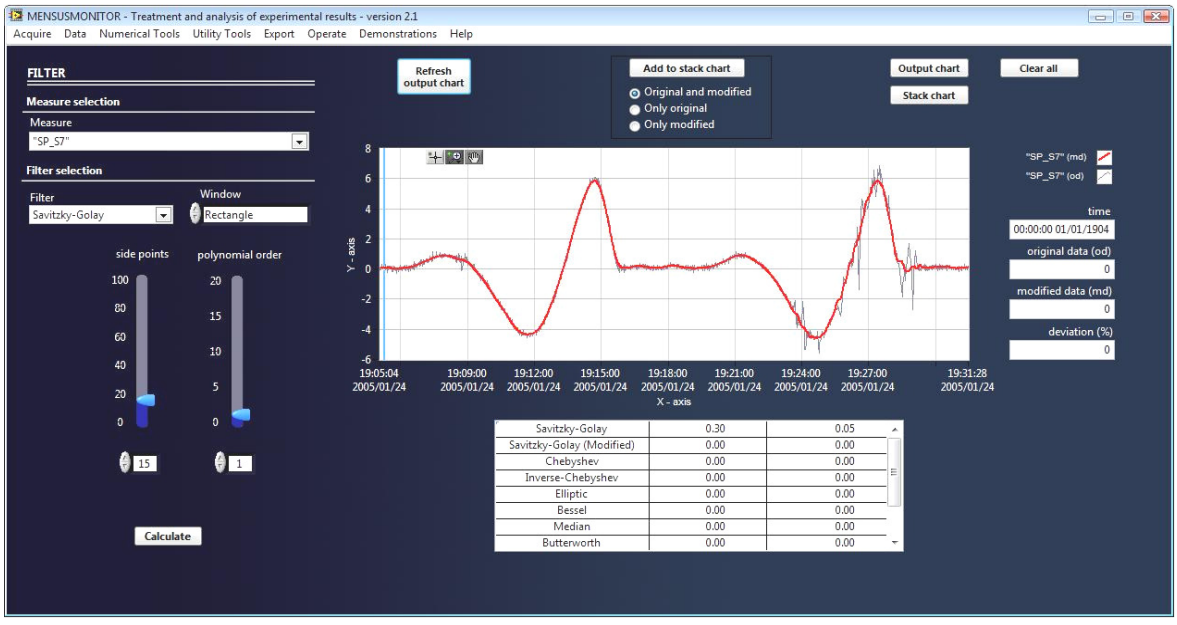

Figure 3.16 : Smoothness of the measurements with the "*mensus filter*" tool.

Generally, this filtering procedure was applied to all the remaining measurements. However, in order to construct a set of filtering results, the option "*add to stack chart*" available in the "*mensus filter*" tool (Figure 3.16) was used, which allowed the construction of graphics and tables with several filtering results. In other words, when a suitable filtering result is obtained, this result can be added to a stack that collects the optimal results. This stack might be viewed in form of graphics and/or tables that contain the relevant statistic information about the optimal filtering.

- **Export results**

Finally, the desired results were exported as images files of *JPEG* format, in order to be included in the observation report. With that intention, the resources available in the "*Export Results*" module was used, more precisely the operation "*JPEG images*" that allowed the creation of images with the final graphics and tables. Figure 3.17 shows the final graphic of the vertical displacements concerning the "*Slow passage 1*" for the sections S1, S3, S4, S5 and S7 (see Figure 3.11). During this operation, the graphic layout is editable by using some of the in-built tools of LABVIEW such as lines' and background colours, references and format of the axis and measurements' labels.

Figure 3.17 : Exporting a final graphic as JPEG image.

3.7. CONCLUSIONS

The present chapter focuses the development and presentation of a new software devoted to SHM – MENSUSMONITOR –, which intends to give answers to some difficulties in the data handling from monitoring systems applied to civil infrastructures. Based on the results herein presented, some relevant conclusions could be drawn:

Comparing with other commercial solutions, such as worksheets of EXCEL type and generic numerical tools as MATLAB, with features for treatment and analysis of monitoring data, MENSUSMONITOR offers the following advantages:

- A set of numerical tools specifically designed and prepared to give adequate responses in the essential steps concerning the monitoring data processing and analysis;
- The available numerical tools results from the practical experience of their authors, who have a high experience in the SHM field and therefore, efficient and optimized solutions are attained;
- It is a evolving software, with a conceptual design prepared to integrate new modules and/or to update the existing ones;
- It is an executable software, which can be installed in any computer without specific requirements.

However, some limitations have to be referred, which are in fact the present motivations for the release of the next version that is under construction:

- The number of numerical tools available are not large and therefore, the software gives answers just to some of the countless issues of the SHM field;
- It requires a learning period, as it happens to any new software that appears to give answers to a new paradigm.

As a final remark, it should be mentioned that is relatively easy to develop software projects with specific functionalities and at the same time with user-friendly interfaces. Nowadays, the available programming languages offer several tools already prepared to build desirable graphical interfaces in order to satisfy specific requirements, as the LABVIEW example. Moreover, the profit that can be attained by using more than one programming language is high. In some way, the advantages of one of them are the extra

profit that is needed to minimize the disadvantages of the others as it was illustrated in the present chapter with the MENSUSMONITOR project.

4. LONG-TERM ASSESSMENT OF A PRECAST VIADUCT BASED ON PREDICTION MODELS

4.1. INTRODUCTION

Structural monitoring is an issue that receives more and more research interest and Bridge Health Monitoring Systems (BHMS) has been a subject of increasing international relevance. While in the past attention was focussed on sensors, the emphasis is shifting to the practical implications regarding the acquisition, collecting and processing of data (Van der Auweraer and Peeters 2003). Today it is possible to continuously and remotely monitor highly instrumented structures, with a high degree of automation. Present solutions are versatile enough to allow for surveillance tasks to be remotely carried out in a cost effective manner (Bergmeister and Santa 2001; Chang *et al.* 2009).

The condition assessment of a given structure may be performed by comparing monitoring results against numerical models that describe the predicted structural behaviour. Finite Element Models (FEM) have been widely employed in those calculations. FEM make it possible to calculate the long-term behaviour of bridge structures, considering the influence of concrete creep and shrinkage, temperature and imposed loads. Accurate estimates of the actual structural behaviour can only be obtained if the relevant concrete properties (creep, shrinkage and modulus of elasticity) are determined through adequate tests and the real temperature history is known. However, this information is not always available. Moreover, the detailed analysis through FEM, considering the real sequence of construction, is a time-consuming process.

An alternative approach for condition assessment can be made by using the data collected by the monitoring systems to establish the statistical models which describe the normal correlation pattern between non-structural parameters (such as temperature and shrinkage strains) and the observed structural response (strains, rotations and movements of

expansion joints). Some authors have already followed this path. Indeed, the long-term monitoring of the Cogan and Grangetown viaducts (UK) were studied by Howells et al. (Howells *et al.* 2005) and Barr et al. (Barr *et al.* 1997). These authors found that a linear relationship could be established between the observed strains and temperatures, although these temperatures differ slightly, depending on the season and the segment location within the span. Ni et al. (Ni *et al.* 2007) have also analyzed the relationship between observed temperatures and bridge response. However, unlike the former, whose study was based on environmental temperatures, Ni et al. used temperatures measured inside the bridge cross sections. This enabled the authors to establish a normal correlation pattern between temperatures and structural response. The correlation model was used to establish alarms to detect future monitoring data that disobey the normal pattern. In this authors' study, the analysis of the structural response was focused on the movement of the expansion joints, envisioning the scheduled interval for replacement of expansion joints.

The long-term behaviour of structures such as the south approach viaduct of Lezíria Bridge, in Portugal, is complex. In fact, it is well known that significant stress redistributions occur over the service life, due to concrete creep and shrinkage deformations and the evolution of the structural system during the construction phases. Therefore, a monitoring system was implemented to follow the structural behaviour since the beginning of the construction.

In this paper, the above-mentioned structure is briefly described and the implemented monitoring system is presented. Then, the main steps involved in the treatment of the experimental data are exposed.

At that stage, the comparison between the experimental results and the outcome of FEM is addressed. It was concluded that FEM are able to provide approximate estimates of the long-term behaviour if detailed information about the material properties and the construction procedure are available. However, the analysis procedure is time-consuming and the FEM results hardly match the observed values with a high degree of accuracy, because the definition of the material properties, the environmental parameters, the structure geometric characteristics and the applied loads always involve some degree of approximation.

Therefore, a real time assessment procedure was developed to calculate the expected value of the monitored parameters at a given time. The developed approach is based on

prediction models, which establish the normal correlation patterns between non-structural parameters and the observed structural response. That correlation pattern is established in the first years after construction, assuming that the structure has a healthy behaviour in that period. For later ages, the expected values can then be compared with the observed ones, so that anomalies can be detected if the difference exceeds a given threshold limit. One of the strengths of this methodology lies in the fact that it provides quick calculation results with minimum time and computational efforts. Moreover, it is suitable for implementation in automatic monitoring systems, which trigger an alarm if unexpected values occur. In this context, this work aims at contributing to the development of systems devoted to the management and maintenance of bridges.

4.2. THE PRECAST VIADUCT

Lezíria Bridge, an 11 670m long structure, is composed of three distinct substructures: (i) the north approach viaduct; (ii) the main bridge crossing the River Tagus; (iii) and the longest one, the south approach viaduct, with a total length of 9 160m. The south approach viaduct is a partially precast structure and is composed of 22 elementary viaducts, whose total length (i.e., distance between expansion joints) ranges from 250 m to 530 m. The most common span length is 36 m.

Each elementary viaduct is composed of a continuous deck monolithically connected to the piers. The foundation is provided by piles, which have the same cross section as the piers, thus forming a pier-pile element. Transition piers were adopted to establish the connection between the different elementary viaducts. In the transition, one of the elementary viaducts is connected to the transition pier by means of fixed pot bearings whereas the other is supported by sliding guided bearings.

The deck slab, which is 29.95 m wide, is made up of four 1.75 m high, precast, U-shaped girders and a 0.25 m thick slab. The girders are prestressed by means of pretension strands and were made in a factory specifically build at the construction site. The prestress release was carried out approximately 12 hours after casting.

The slab is composed of precast planks and a cast-in-place layer. The monolithic connection between spans is established through a cast-in-place diaphragm and continuity

reinforcement. Moreover, in the region above the piers, the deck slab is prestressed by straight post-tensioning cables. The continuity diaphragm is also monolithically connected to the piers, which have a circular cross section and a diameter of 1.5 m. On the top of the pier, there is an octagonal capital whose maximum dimension reaches 1.7 m, so that the girders can be positioned without conflicts with the pier reinforcement. In the transverse direction, a precast beam connects the capitals of each two piers. The piles cross alluviums with variable constitution, and the maximum deepness reached by each pile varies between 35 m and 60 m. The concrete piles were cast inside steel tubular elements, which were installed by using a vibratory pile hammer (COBA-PC&A-CIVILSER-ARCADIS 2006).

Figure 4.1 depicts an aerial view of the viaduct as well as a set of images with some details of its construction.

a) aerial view (© F. Piqueiro / Foto Engenho).

b) precast factory.

c) precast positioning.

d) precast planks positioning.

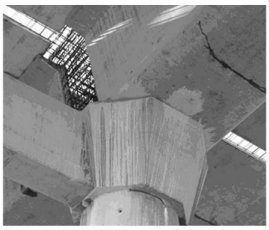

e) diaphragm construction detail.

Figure 4.1 : Precast viaduct.

4.3. THE MONITORING SYSTEM

The decision to monitor this structure was motivated by two main reasons. Firstly, it is a very long structure, made with a repetitive precast solution; consequently, the actual performance of the structural solution can be observed by monitoring part of the structure; in this way, the bridge owner can be aware of the long-term structure performance, spending a reduced value with respect to the overall structure cost. Secondly, important stress redistributions occur in these structures, due to the employed construction sequence and the concrete creep and shrinkage properties. Therefore, the monitoring results of this complex behaviour are expected to provide valuable data for the validation of a proper numerical model.

Two out of the 22 elementary viaducts were monitored: the V1S and the V14S (Figure 4.2). Before the start of the construction, a monitoring plan was developed, which indicates the parameters of interest and the critical cross sections that were selected for monitoring (Figueiras *et al.* 2007a). These viaducts were extensively instrumented, namely with vibrating wire strain gauges to measure concrete deformations (CD), thermistors and resistive temperature detectors to measure concrete temperature (CT), inclinometers to measure girder rotations (RO), displacement transducers to measure bearing displacements (BD) as well as temperature and humidity sensors to measure environmental conditions (TE, RH). Figure 4.2 presents the elevation of the monitored viaducts, with indication of the cross sections in which embedded sensors were installed, as well the external sensors location, while Figure 4.3 illustrates the distribution of the embedded sensors along the two typical cross sections: mid-span and support cross sections. Some of the embedded sensors are labeled in Figure 4.3 for future reference in the paper.

Eight concrete prisms, with dimensions 15 cm × 15 cm × 55 cm, were cast for measurement of shrinkage deformations. These prisms were instrumented with strain gauges and temperature sensors and subjected to the same curing conditions of the monitored structural elements, to achieve as a realistic representation as possible, of the deck concrete shrinkage. Four prisms were made with girder concrete and were subjected to the curing procedure applied to the precast beams; the other ones were made with slab concrete (from the mid-span region of the second span). For each concrete composition, half of the prisms were subjected to the surrounding environmental conditions (although

sheltered from rain), whereas the others were kept in the interior of the box girder since the pouring of the second-span slab of each viaduct.

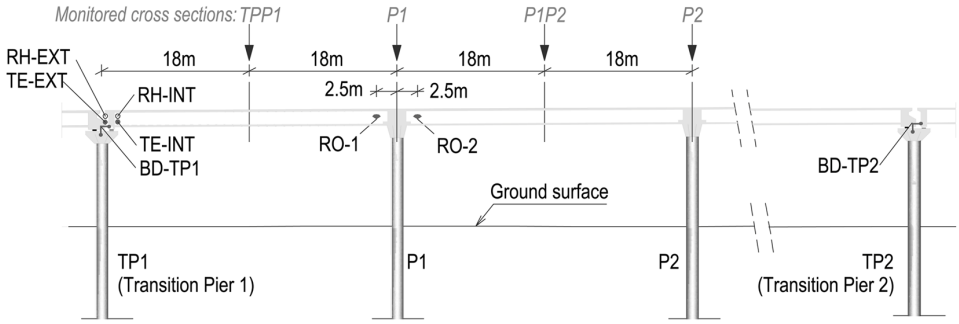

a) V1S viaduct.

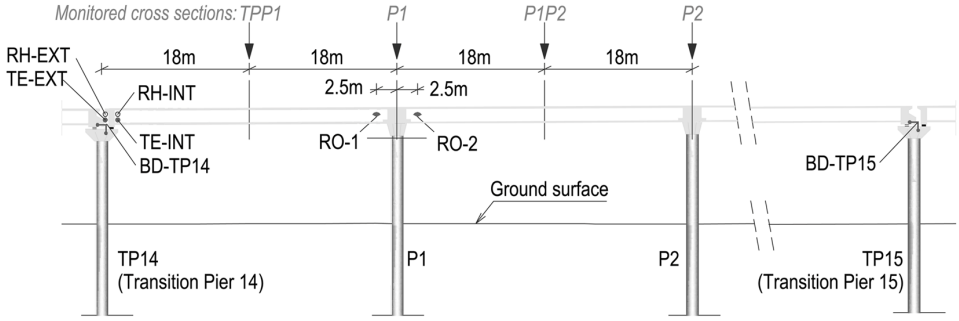

b) V14S viaduct.

Figure 4.2 : Elevation of the monitored viaducts V1S and V14S.

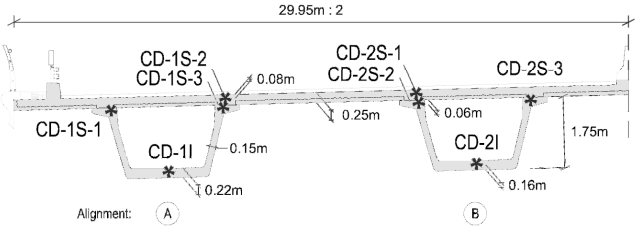

a) mid-span cross section.

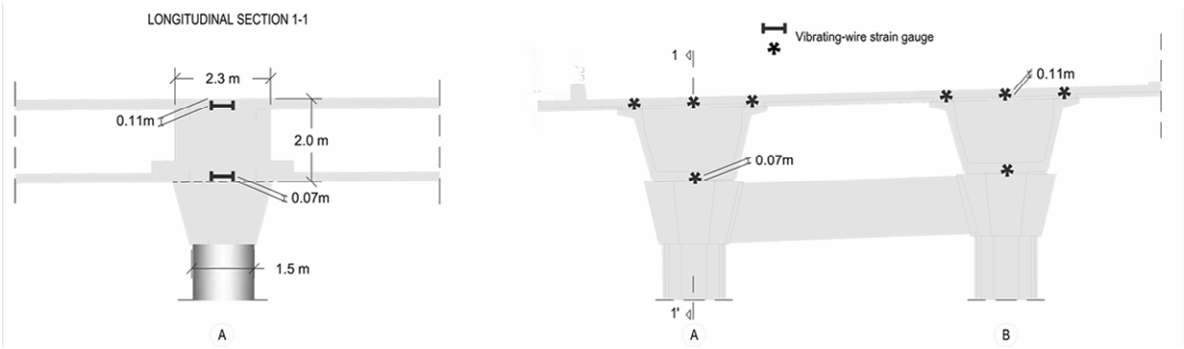

b) support cross section.

Figure 4.3 : Strain gauges location in the monitored cross sections.

Given the aggressiveness of the concreting operations, the embedded sensors (vibrating wire strain gauges and temperature sensors) were fixed to the reinforcement, near the concrete surface, by using square steel bars, which allowed a robust installation (

Figure 4.4-a). In general, measurements started before the concreting operations. Consequently, it was necessary to install cables through provisory and safe paths and acquisition systems in adequate protection boxes, to prevent potential damaged due to the construction works. The available time for these works was always short. For that reason, the installation of all the embedded sensors was a demanding task. The bridge deck instrumentation comprised two main phases: (i) the instrumentation of the precast girders, which started in the precast plant; (ii) the instrumentation of the deck slab, which started before the *in situ* concreting.

The external sensors were installed after the structure was cast. Inclinometers with great inertial sensitivity were employed to measure the deck rotation about the horizontal axis. These sensors were rigidly attached to a metallic base, which was previously fixed to the precast girder surface and properly leveled (

Figure 4.4-b). The metallic base is provided with a mechanism allowing the leveling of the sensor without removing it. Both temperature and humidity sensors were installed in two different environments: (i) inside the box girders; (ii) outside the precast girders, sheltered from rain. Given that it is not possible to access the interior of the box girders after the end of the construction, internal sensors were fixed to a movable sealed device, so that the sensors could be accessed in case of malfunctioning or for maintenance operations. Linear Variable Differential Transformers (LVDTs) were installed to monitor the bearing displacements of the viaducts. These sensors were installed after the expansion joint was placed. The installation was made by fixing one sensor end to the pier top, and the other to the lateral face of the girder that is supported by sliding guided bearings. In order to prevent damage and to guarantee the appropriate mechanical protection, all the external sensors were encapsulated in a protection box (ventilated in the case of the environmental parameters measuring). In the case of the LVDT, the mechanical protection was performed by a stainless steel shelter (

Figure 4.4-c).

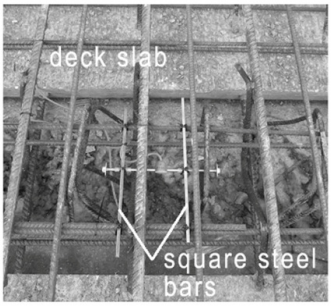

a) strain gauge.

b) inclinometer and protection box.

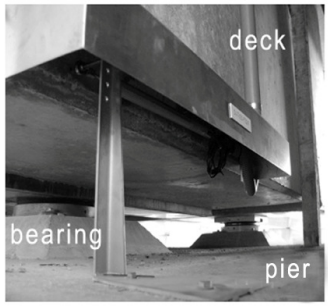

c) displacement transducer and stainless steel shelter.

Figure 4.4 : Sensors' installation.

4.4. INTERPRETATION OF CONCRETE STRAINS

A large number of vibrating wire strain gauges were employed to evaluate concrete strains. The results obtained with these sensors must be carefully interpreted. According to Eq. (1), the strain reading, obtained by direct correlation with the wire vibration frequency, may be decomposed into three basic components: (i) the instantaneous deformations that occur at specific instants of time, t_0, caused by events such as loadings or prestressing operations, $\varepsilon_{ci}(t_0)$; (ii) the delayed deformation due to long-term effects such as creep and shrinkage, $\varepsilon_{cs+cc}(t)$; the deformation due to temperature variations, $\varepsilon_{cT}(t)$.

$$\varepsilon_c(t) = \sum_i \varepsilon_{ci}(t_0) + \varepsilon_{cs+cc}(t) + \varepsilon_{cT}(t) \tag{1}$$

4.4.1. INSTANTANEOUS DEFORMATIONS

If the cause of a given instantaneous deformation, $\varepsilon_{ci}(t_0)$, is not known, then it is not possible to interpret correctly the corresponding results. This is even more complicated in a structure that was built across different construction phases. For this reason, information about all the relevant construction events was recorded and compiled in the quality control report (TACE 2007). This document allows the identification of the construction event that matches a given instantaneous deformation.

4.4.2. TIME-DEPENDENT DEFORMATIONS

The time-dependent deformations are mainly due to the concrete creep and shrinkage. The relaxation of prestressing steel is also responsible for long-term deformations, however both the magnitude and the variability of this phenomenon are significantly less important than those due to creep and shrinkage are. In this context, shrinkage was measure in eight prisms, as mentioned before.

Figure 4.5 depicts the monitored strains in the shrinkage prisms of the V14S viaduct without the temperature effect (analogous results were obtained in the other monitored viaduct). In these two figures, the shrinkage estimated according to the Eurocode 2 (Standardization European Committee 2004) is also shown, and it was based on the concrete compressive strength measured in cubes (TACE 2007), considering a notional cross section size of 150 mm, and taking into account the fact that the concrete is made of high strength rapid hardening cements. Two different values were considered for the relative humidity (RH = 70 % and RH = 90 %), which correspond to the average observed values in the exterior and interior environments.

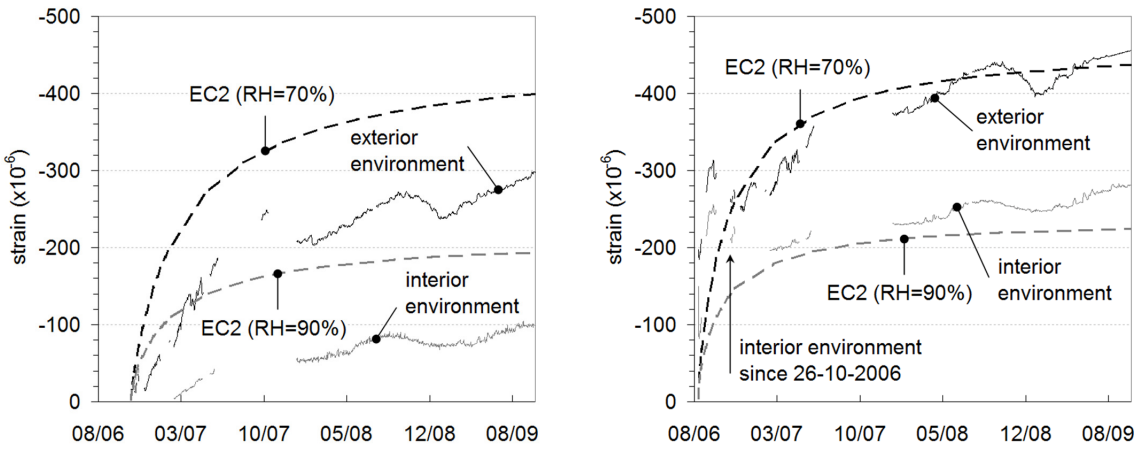

a) slab concrete **b) girder concrete**

Figure 4.5 : Shrinkage strain of the concrete applied on the V14S viaduct.

These figures show that the shrinkage prisms provide relevant information to support the interpretation of the monitoring results, as the code estimates do not precisely follow the observed values:

- even though the Eurocode 2 estimates might yield similar results for both concretes, there are significant differences between the actual shrinkage development in both materials, due to their different compositions and curing conditions;
- the girder concrete exhibits high shrinkage values in the first days after casting, which is not observed in the slab concrete, for which the Eurocode 2 overestimates the deformations;
- the observed shrinkage curves exhibit a seasonal variation, which has already been detected by other authors (Santos 2002; Santos 2007); shrinkage increases in the warm and dry months and decreases in the winter, but, again, this effect is not taken into account by the code estimates;

4.4.3. TEMPERATURE EFFECT ON DEFORMATIONS

Sensors used to measure concrete deformations are influenced, in general, by concrete temperature variation. Vibrating wire strain gauges are sensitive to both the wire and the concrete temperatures. Therefore, these sensors are usually provided with an internal thermistor, so that the temperature influence can be taken into account. The concrete strain can thus be obtained through the following equation:

$$\varepsilon_c(t) = GF \cdot \left(f_2{}^2 - f_1{}^2\right) + k \cdot \Delta T \tag{2}$$

where GF is the sensor gauge factor, f_1 and f_2 represent the initial and the actual (at the time t) vibrating wire frequency respectively and ΔT is the temperature variation. If the total concrete deformation is to be obtained, then only the wire temperature-dependent deformation must be compensated. In this case, the parameter k takes the value:

$$k = \alpha_{wire} \tag{3}$$

where α_{wire} represents thermal dilation coefficient of the wire. The manufacturer usually gives this value and it takes the value 11 με/ºC for the sensors used in this work (Gage Technique International 2011). However, it is often more convenient to obtain a strain reading which does not include the free thermal deformation. This can be achieved by taking the following parameter *k:*

$$k = (\alpha_{wire} - \alpha_c) \tag{4}$$

where α_c represents the thermal dilation coefficient of the concrete. If the temperature compensation is carried out in this way, then the obtained strain $\varepsilon_c(t)$ only includes stress dependent deformations (i.e., deformations caused by concrete stresses) and shrinkage strains. The strain obtained through this compensation procedure is suitable for comparison with the results of numerical models.

The accurate evaluation of the temperature effect depends on the correct estimate of the parameter α_c. For this reason, a set of prisms (made with the same concrete that was used in the structure and instrumented with the same type of transducer) was tested in a climatic chamber. The test procedure consisted in applying different temperature cycles. The temperature variation was slow, so that a uniform temperature distribution could be obtained in the prisms. The temperature ranged from 5 ºC to 40 ºC, which broadly corresponds to the range of temperatures observed in the structure. The results obtained for the parameter $k = (\alpha_{wire} - \alpha_c)$ that eliminates the sensitivity to the free thermal deformation are characterized by an average value μ = 3.1 με/ºC and a standard deviation σ = 0.3 με/ºC (Sousa and Figueiras 2009a).

Figure 4.6 presents the results obtained in one typical concrete prism. The evolution of both the concrete temperature and the climatic chamber temperature is also represented in this figure. These results reveal that the thermal dilation coefficient of the employed concrete is approximately equal to 7.9 με/ºC. This value is similar to that obtained by other authors (Kada *et al.* 2002; Santos 2007).

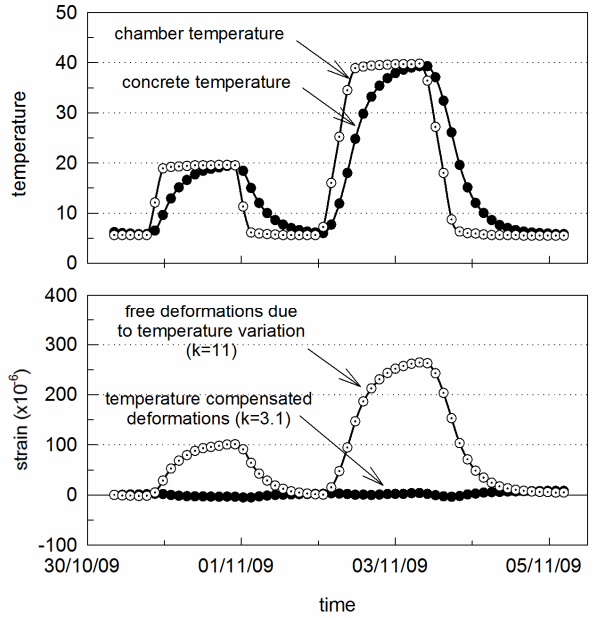

Figure 4.6 : Chamber climatic test.

4.5. COMPARISON BETWEEN MONITORING AND FEM RESULTS

A finite element analysis of the V14S viaduct was carried out, aiming at evaluating whether a detailed numerical model could provide similar results to the ones that were experimentally obtained. A good agreement between field measurements and FEM results validates the monitoring procedures and encourages the effective use of this information in surveillance and assessment tasks. Two different analyses were performed: (i) a time-dependent phased analysis of the viaduct response, comprising both construction and service phases; (ii) a linear-elastic analysis of the structural behaviour during the load test.

The time-dependent analysis was carried out through a FEM with beam elements. A phased analysis was performed, in which the actual construction sequence was modeled, according to the recorded sequence of construction events (TACE 2007). In this analysis, the constitutive model adopted to describe the concrete behaviour allows for the consideration of the creep, shrinkage and cracking effects. The definition of the material properties was also based on the information collected during the quality-control procedures (TACE 2007). Furthermore, the shrinkage variation was described by curves that were determined through a curve fitting procedure based on the results of the shrinkage prisms. Given that no creep measurements were available, the strain results observed in one of the precast girders before its erection was used to obtain additional

information regarding the long-term behaviour of the girder concrete. This was carried out by means of a retro-analysis procedure.

A 3D FEM with brick elements was used to analyze the local behaviour of the connection between the deck and the piers during the load test. This is a zone of strong geometric discontinuity and consequently, the strains that were monitored in this region (see Figure 4.2 and Figure 4.3) cannot be directly compared with results calculated by means of finite element beam models. Furthermore, modelling the whole viaduct with 3D brick elements would give rise to a complex and large model. Consequently, the following analysis strategy was adopted. The global analysis of the different load cases was carried out by a FEM with beam elements. Then, the local 3D model was used to determine the strains in the sensor locations when the corresponding cross section is subjected to a given bending moment. Note that the local 3D model comprises half a span, so that the boundary conditions can be properly simulated.

In this chapter some relevant and illustrative results are presented. A comprehensive description of the employed numerical models and the obtained results can be found elsewhere (Sousa *et al.* 2009a; Sousa *et al.* 2012).

4.5.1. SHORT-TERM ANALYSIS (LOAD TEST)

Four different load positions were considered in the load test to maximize the stresses in each monitored cross section.

Figure 4.7 depicts the results of the load test for the 12 sensors that are located at upper level in the four monitored support cross sections. The calculated results are also plotted in this figure (note that the dashed lines do not correspond to the exact variation of strain between points; they are only represented to clarify the interpretation of the results). From the analysis of this figure, one may conclude that the strain distribution through the deck slab is not uniform. This is a consequence of both the geometric discontinuity due to the support diaphragm and the shear lag effects, which lead to lower strains in the transducer located on the symmetry axis. In Figure 4.7, this effect is evident in both the experimental and the numerical results. Moreover, there is a remarkable agreement between the

calculated and the observed results and a good repeatability of measurements in corresponding locations.

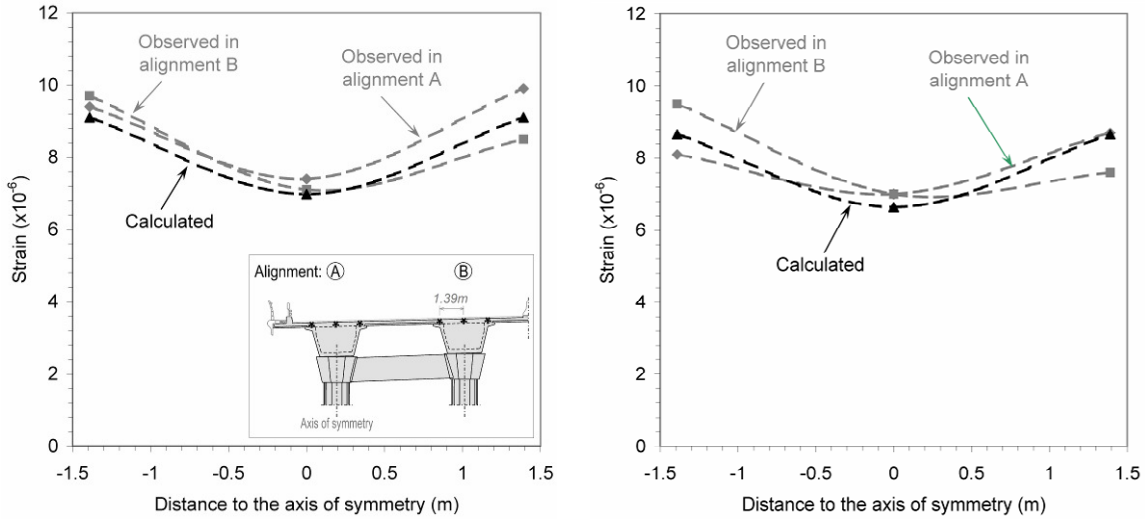

a) cross section above P1. **b) cross section above P2.**

Figure 4.7 : Deck slab strains at the support cross sections, during the proof load test.

4.5.2. LONG-TERM ANALYSIS

Figure 4.8 presents the strain results for one of the monitored mid-span cross sections, V14S-TPP1 (see Figure 4.2) during the construction and the first years in service. Some relevant construction stages are identified in this figure and the observed values (at 6 a.m.) are represented by symbols that identify the location of each point. Note that measurements started before the precast girder was cast and the strain values do not include the free thermal deformation.

This figure also depicts the results of two FEM analyses: (i) continuous lines represent calculations in which the concrete properties were based on monitored parameters (results of concrete cube tests, shrinkage measurements and retro-analyses for identification of the creep properties) (Sousa *et al.* 2012), and (ii) dashed lines present the outcome of calculations in which the concrete properties are based on the Eurocode 2 estimates and the design specifications. Figure 4.5 had already shown that the measured shrinkage deformations were significantly different from the code estimations. Therefore, it is not surprising that calculations based on estimated concrete properties lead to results

significantly different from the observed ones. Differences are particularly important in the first weeks after casting the precast girder and before casting the continuity connection, because the deviation between the actual creep and shrinkage deformations and the estimated values are significantly higher in this period. In the long-term, the agreement between measurements and calculations is improved, namely in the case of the girder strains. In the case of the deck slab, important differences exist even in the long-term, because the actual slab shrinkage strains are lower than the estimated values (Figure 4.5-a).

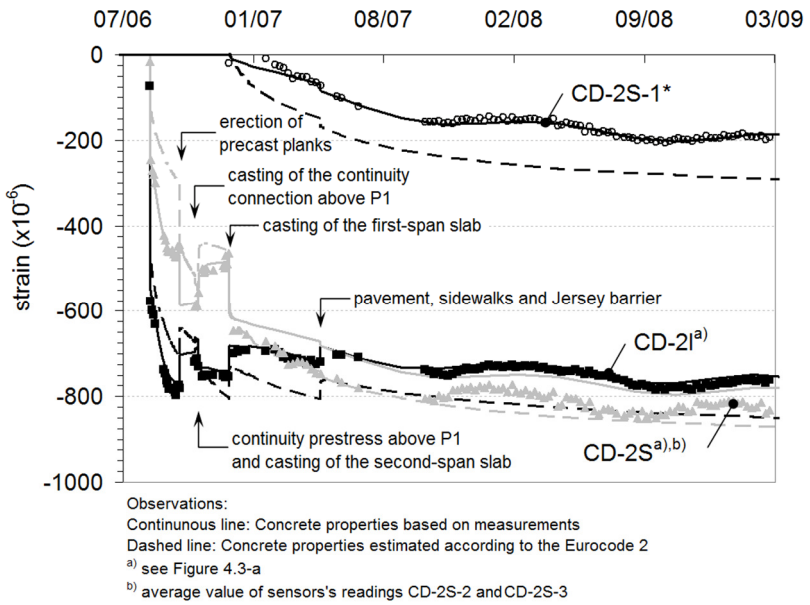

Figure 4.8 : Comparison between numerical and experimental results (strains in the mid-span cross section of the first span, alignment B).

Conversely, the outcome of the detailed analysis with concrete properties based on measured parameters closely agrees with the observed strains. Therefore, important conclusion could be taken from the calibrated FEM analyses: they revealed that the actual structure behaviour is in accordance with the expected response, and the good agreement and correlation between the different measured parameters gives confidence in the monitoring system. FEM analyses proved to be relevant for validation of the measured values. However, detailed analyses are time-consuming and a lot of detailed information is necessary for the accurate calculation of the long-term structure response. Thus, the use of simpler approaches for real time long-term assessment of the structure performance is encouraged and justified.

4.6. PREDICTION MODELS

4.6.1. MODEL DESCRIPTION

A possible approach for real time assessment of the structure condition was evaluated within the scope of the present work. This procedure consists in obtaining the normal correlation pattern between the structural response (strains, rotations and movements of expansion joints) and basic information provided by environmental and material parameters (such as concrete temperature and concrete shrinkage measurements). If the new structure has a healthy behaviour in the first years after construction, it is possible to determine the normal correlation pattern between different measurements. These correlations can be regarded as prediction models, which can be used to assess the adequacy of the structure behaviour in the future.

The proposed model is described by Eq. (5), where the model prediction $y_{\text{model}}(t)$ for a given parameter (strains, rotations or movements of expansion joints) at a given time t is estimated from a linear combination of measurements $x_{\text{measure},i}(t)$ weighted by w_i. The predictor parameters $x_{\text{measure},i}(t)$ must comply with the following conditions: (i) the structure response must be sensitive to the value of this parameters; (ii) they must not depend on the soundness of the structure behaviour, i.e., they must represent material properties or environmental characteristics; (iii) minimal correlation should exist between the predictor parameters. It is desirable that these parameters correlate highly with the dependent ones, but the existence of high correlation between the predictors (multicollinearity) leads to imprecise determination of the coefficients w_i, inaccurate estimates and inexact tests on the regression coefficients (Montgomery and Runger 2003). In this work, the predictor parameters consist of concrete temperature and concrete shrinkage measurements, for the reason that these variables strongly affect the time variation of the structure response.

$$y_{\text{model}}(t) = \sum_{i=1}^{k} w_i \cdot x_{\text{measure},i}(t) \tag{5}$$

$$y_{\text{measure}}(t) = y_{\text{model}}(t) + \varepsilon \tag{6}$$

The problem unknowns consist of the set of weights w_i. The problem is solved by calculating the value of the weights w_i which minimize the differences, ε, between the actual measurement $y_{measure}(t)$ and the model prediction, $y_{model}(t)$, as represented by Eq. (6). The optimal solution is the one that minimizes the function R, which represents the sum of the squared errors, as represented by Eq. (7). The minimum of the function R is found by setting the gradient to zero. This problem has a unique solution because R is a quadratic function, $y_{model}(t)$ being a linear combination of a set of measurements.

$$R = \sum_{i=1}^{n} \left(y_{measure}(t_i) - y_{model}(t_i) \right)^2 = \sum_{i=1}^{n} \varepsilon_i^2$$

$$R_{\min} \Rightarrow \left. \frac{\partial \left(\sum_{i=1}^{n} \varepsilon_i^2 \right)}{\partial w_j} \right|_{w_0, w_1, \ldots, w_k} = 0 \quad j = 1,2,\ldots,k \tag{7}$$

The observation period (i.e., the set of times t_i) over which the minimization problem is formulated must also be established. In this type of problems, it is common to use a fraction of the total available period of observation, a so called *training window*. The appropriate size of the training window can be determined by making several calculations with increasingly larger dimensions. The adequate time window is the one that lead to the same set of weights w_i that would be obtained if larger training windows were considered.

It is worthy of note that the size of the training window depends on the phenomena under analysis. If the prediction model is devised for long-term structural analyses, then a minimum size of one year might be necessary, for the reason that the concrete temperatures and delayed deformations have a seasonal variation with a yearly period.

Once the set of weights is determined, the model may be used to calculate the expected structure response $y_{model}(t)$ for the remaining time window. If the structure has a normal behaviour, the magnitude of the error ε shows the robustness of the prediction model.

This algorithm was implemented in an existing software devoted to structural monitoring – MENSUSMONITOR. Its user-friendly interface and capacity to connect to MySQL databases enabled efficient data handling and simple calculation procedures. Figure 4.9

shows the front panel with the "*mensus prediction*" tool active (see Table 3.4). More details about this software can be found elsewhere (Sousa *et al.* 2009b).

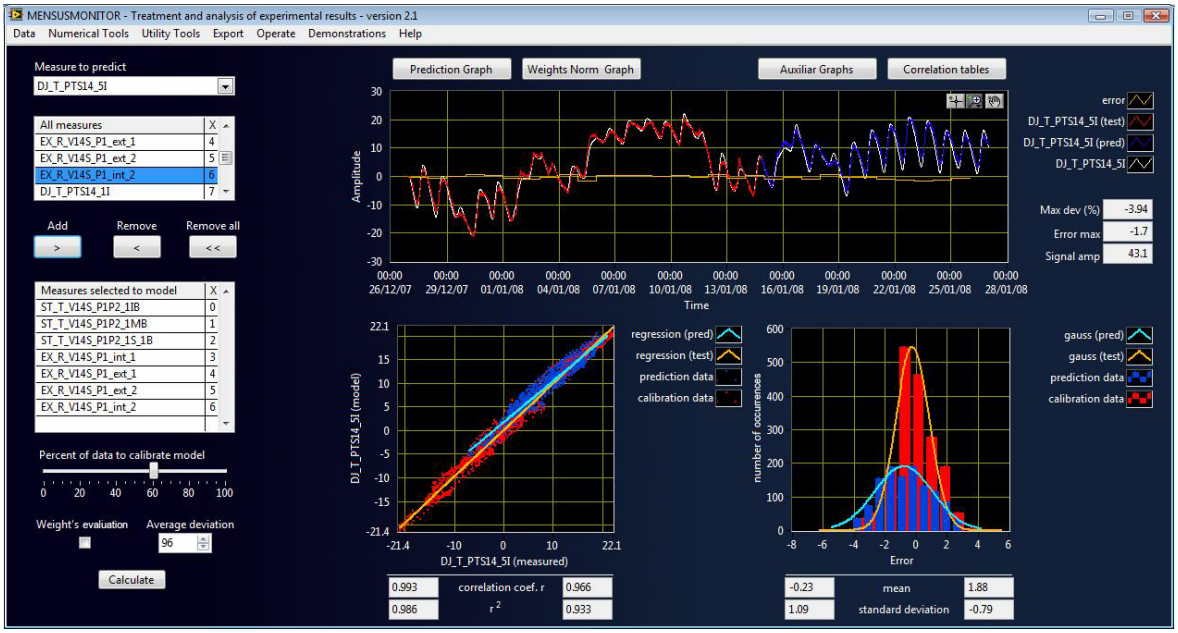

Figure 4.9 : Front panel of MENSUSMONITOR with the "*mensus prediction*" tool active.

4.6.2. APPLICATION TO THE PRECAST VIADUCT

- **Problem description**

The prediction model was used to analyze the outcome of 24 transducers (12 from viaduct V1S and 12 from V14S): 4 (2+2) bearing displacements *BD*; 4 (2+2) deck rotations *RO*; and 16 (8+8) concrete deformations *CD*, of four mid-span cross sections (Figure 4.2 and Figure 4.3). The predictor parameters $x_{\text{measure},i}(t)$ were shrinkage deformations *SD* observed in concrete prisms and concrete temperatures *CT*. Figure 4.10 shows the location of the temperature sensors, which are positioned in three mid-span cross sections.

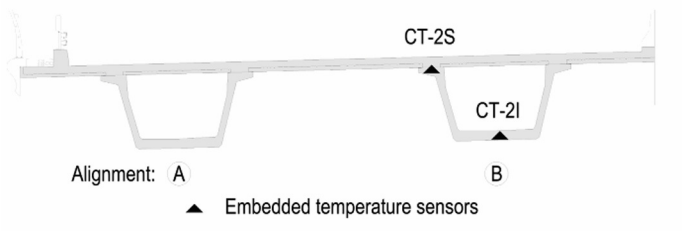

a) V1S-PTP1.

b) V1S-P1P2.

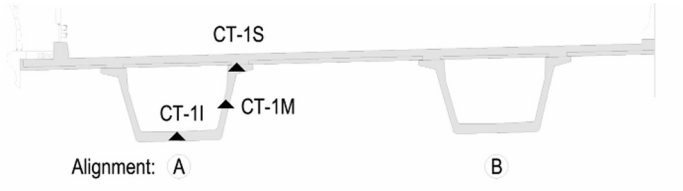

c) V14S-P1P2.

Figure 4.10 : Embedded temperature sensor locations.

Table 4.1 and Table 4.2 present the correlation coefficients R^2 for all the measurements that are candidates to be used as predictor parameters, for viaducts V1S and V14S, respectively. These tables show that high correlation exists within the subsets of temperatures and shrinkage measurements, with R^2 always higher than 0.95. This indicates a strong collinearity between measurements of each data set. Consequently, instability problems would occur in the calculation of the problem unknowns (the set of weights w_i) if more than one temperature and one shrinkage strain were taken as predictor parameters.

Therefore, only two independent variables were considered: the average of the shrinkage deformations SD_{AVG} and the average of the concrete temperatures CT_{AVG}. The correlation coefficients between these variables are -0.281 and -0.542 for viaducts V1S and V14S, respectively. These correlations lead to Variance Inflation Factors (VIF) of 1.1 and 1.4, respectively, which are clearly lower than 10 (the threshold value for multicollinearity) and robust model predictions can thus be achieved (Montgomery and Runger 2003). In this way, the prediction model given by Eq. (5) is expressed by Eq. (8).

For this study, the observation period ranges from 24/12/2007 to 05/10/2009, with one sample per day, at 6 a.m.

$$y_{\mathrm{mod}\,el}(t) = w_1 \times SD_{AVG}(t) + w_2 \times CT_{AVG}(t) \tag{8}$$

Table 4.1 : Correlation coefficient R^2 for the independent measurements in V1S.

	SD_{IN1}	SD_{IN2}	SD_{EX1}	SD_{EX2}	CT_{1I}	CT_{1S}	CT_{2I}	CT_{2S}
SD_{IN1}	1	0.997	0.970	0.977	-0.232	-0.212	-0.234	-0.210
SD_{IN2}		1	0.980	0.979	-0.288	-0.269	-0.290	-0.267
SD_{EX1}			1	0.983	-0.414	-0.393	-0.415	-0.391
SD_{EX2}				1	-0.259	-0.238	-0.260	-0.236
CT_{1I}					1	0.995	0.990	0.994
CT_{1S}						1	0.995	0.999
CT_{2I}							1	0.994
CT_{2S}								1

Table 4.2 : Correlation coefficient R^2 for the independent measurements in V14S.

	SD_{IN1}	SD_{IN2}	SD_{EX1}	SD_{EX2}	CT_{1I}	CT_{1M}	CT_{1S}
SD_{IN1}	1	0.962	0.980	0.966	-0.573	-0.572	-0.556
SD_{IN2}		1	0.953	0.991	-0.628	-0.628	-0.612
SD_{EX1}			1	0.958	-0.439	-0.438	-0.422
SD_{EX2}				1	-0.595	-0.593	-0.580
CT_{1I}					1	0.999	0.995
CT_{1M}						1	0.995
CT_{1S}							1

- **Results and discussion**

Figure 4.11 to Figure 4.13 present the model predictions for three measurements: a concrete deformation, a deck rotation and a bearing displacement. For each measurement, the first graphic depicts the time variation of measured values and model predictions. The training window size was taken as one year, which corresponds to 60 % of the complete time range. However, the influence of this size is discussed below. The time variation of

the error ε, i.e. the difference between measurements and model predictions, is also depicted in the graph. A second graphic for each measurement shows histograms of the calculated errors, for both the training window and the remaining time window. The Gaussian distribution that best fits these histograms is also plotted.

The quality of the predictions for the different measurements can be compared by using the relative error concept, which is defined as the ratio between the calculated error at a given time t and the range of variation of measurements over the complete time window (see e.g. Figure 4.11). It was observed that the smallest relative errors occur in the case of the bearing displacement. For this parameter, the maximum relative error is 4.6 %, and 95 % of the calculated errors are lower than 3.2 %. Moreover, the error average takes the value 0.45 mm, which corresponds to 0.5 % of the signal amplitude. This small value reveals that the models prediction follows the actual measurements and the error has a random nature. The correlation coefficient between predictions and measurements equals 0.99, which confirms a good correlation.

The poorest performance of the prediction model was observed in the deck rotation, for which the maximum relative error is 20.3 %. However, even in this case, the error mean is approximately equal to zero. As for the concrete deformation, the maximum error takes the value 10.8 %. It is not surprising that the best agreement between measurements and predictions occur in the case of the bearing displacement. This is a global measurement that is influenced by the deformation of a large portion of the structure. Therefore, a good correlation between this parameter and the average values of temperature and shrinkage measurements was expected. On the other hand, local measurements such as concrete deformations are very sensitive to the local concrete behaviour, which does not correlate so well with the adopted average predictor parameters.

The occurrence of errors is also justified by the fact that the structure response is also sensitive to other variables that were not considered as predictor ones: traffic loading, wind, insolation, rainfall, among others with minor importance. This is why the prediction of the deck rotations was the poorest one: this transducer is the most sensitive to traffic loadings. However, the fact that the mean error is approximately equal to zero shows that the adopted predictor variables play a key role in the long-term structure response. If the long-term performance is to be evaluated, then it is logical to analyze the average error over a certain period, so that the relevance of random deviations due to the ignored effects

is reduced. Table 4.3 to Table 4.5 display the maximum relative error for weekly and monthly averages. It is possible to conclude that the error significantly decreases, if averaged values are taken into account. The most significant reduction occurs for the deck rotation when the training window is equal to 60% of the observation window, a fact that is justified by the aforementioned reasons.

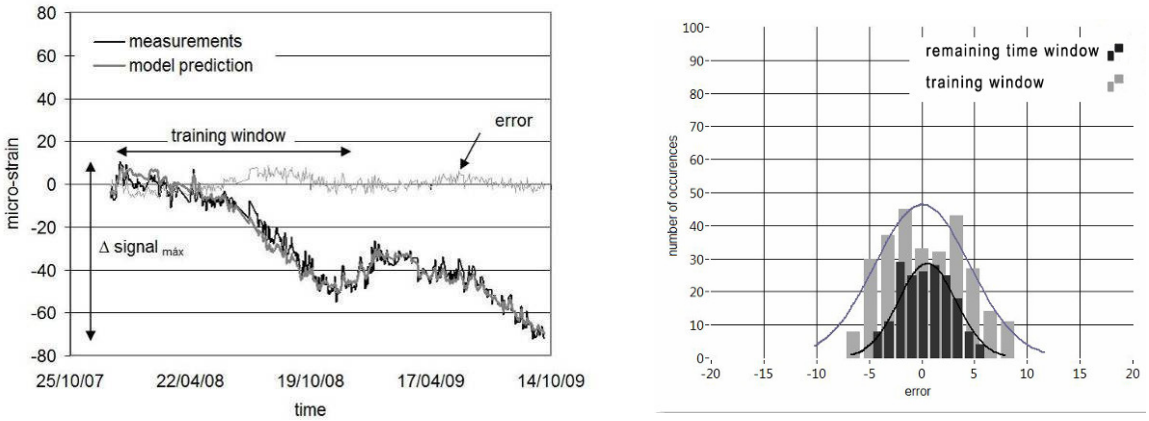

a) measured values and model prediction. **b) statistical distribution of the error.**

Figure 4.11 : Concrete deformation at the bottom slab of the cross section TPP1 of viaduct V1S.

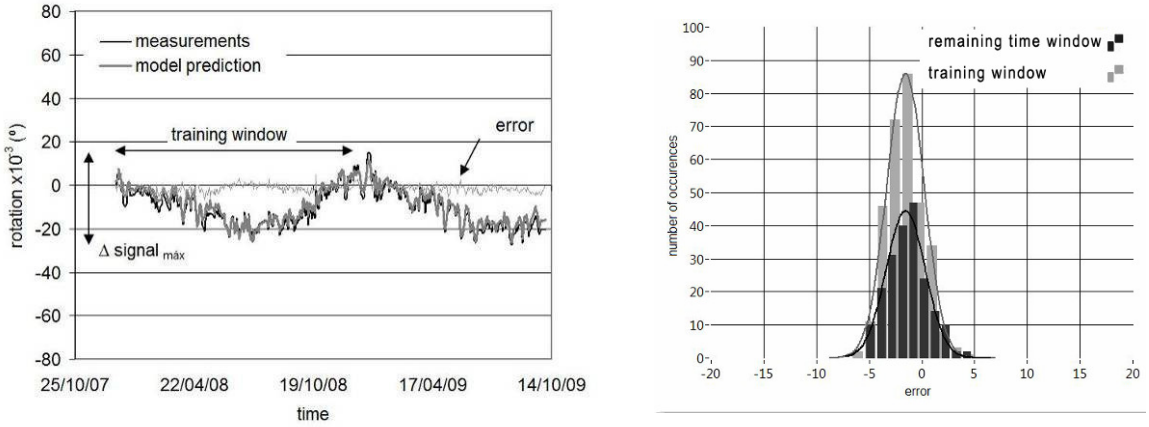

a) measured values and model prediction. **b) statistical distribution of the error.**

Figure 4.12 : Deck rotation RO-2 of viaduct V14S.

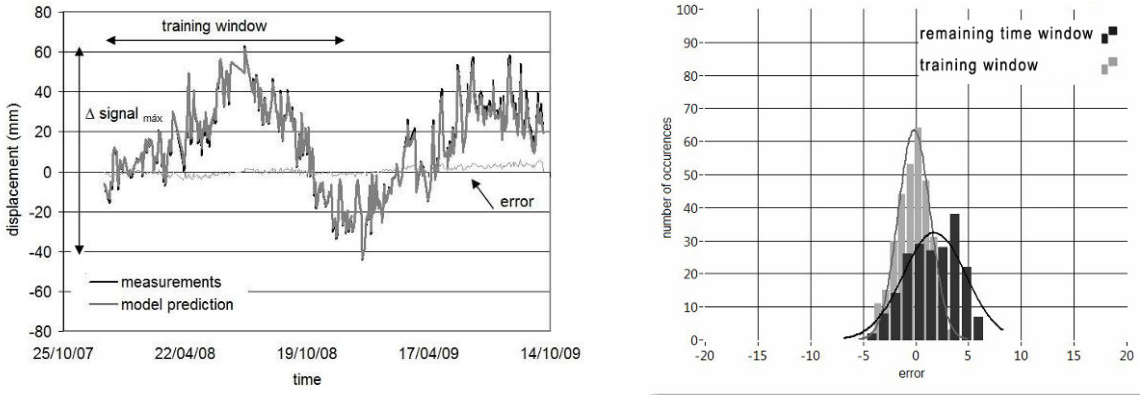

a) measured values and model prediction. **b) statistical distribution of the error.**

Figure 4.13 : Bearing displacement at the transition pier TP14 of viaduct V14S.

- **Discussion of the training window size**

Table 4.3 to Table 4.5 show the variation of the maximum relative error as the training window size increases (taking values of 30 %, 45 % and 60 % of the observation time window), for the three transducers under analysis. Besides the maximum individual error and the weekly and monthly averages, these tables also present the maximum error for a probability of occurrence of 95 %.

Table 4.3 : Maximum relative error for the concrete deformation at the bottom slab of TPP1 (V1S).

Maximum relative error	Training window size (percentage of the observation window)		
	30%	**45%**	**60%**
Without averages	39.9 %	20.2 %	10.8 %
Weekly average	36.3 %	16.1 %	7.5 %
Monthly average	26.9 %	12.8 %	6.5 %
P>95%	47.2 %	19.1 %	8.6 %

Table 4.4 : Maximum relative error for the deck rotation RO-2 (V14S).

Maximum relative error	Training window size (percentage of the observation window)		
	30%	**45%**	**60%**
Without averages	26.5 %	17.9 %	15.6 %
Weekly average	22.8 %	14.8 %	8.4 %
Monthly average	20.2 %	12.5 %	6.4 %
P>95%	23.9 %	14.7 %	11.5 %

Table 4.5 : Maximum relative error for the bearing displacement at TP14 (V14S).

Maximum relative error	Training window size (percentage of the observation window)		
	30%	**45%**	**60%**
Without averages	5.4 %	4.8 %	5.5 %
Weekly average	5.0 %	3.2 %	2.7 %
Monthly average	3.7 %	2.0 %	2.1 %
P>95%	2.2 %	3.0 %	3.1 %

In general, the maximum errors decrease as the training window size increases. In the case of the deck rotation, similar results are obtained for window percentages of 45 % and 60 %. As regards the bearing displacements, the training window size seems to have a minor influence on the calculation results. The influence of the training window size can be more clearly understood by analyzing Figure 4.14, which depict the evolution of the set of weights w_i (the problem unknowns) when the training window size varies from 1 % to 100 % of the total period. The figure shows that a very small training window (~10% of the observation time) guarantees a good estimate of the weights w_i for prediction of bearing displacements. This conclusion conforms to the fact that these global displacements are well correlated with the predictor variables: averages of the measured concrete temperatures and shrinkage strains. On the other hand, large training windows are required for the prediction of local concrete deformations as well as for deck rotations, because of lower correlation with the predictor variables. An extensive study was also performed for the remaining sensors and similar conclusions were gathered.

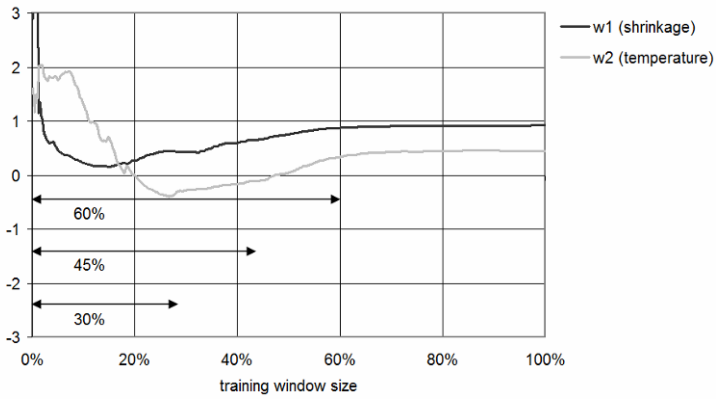

a) concrete deformation at the bottom slab of TP1P1 (V1S).

Figure 4.14 : Calculated weights w_i as a function of the training window size.

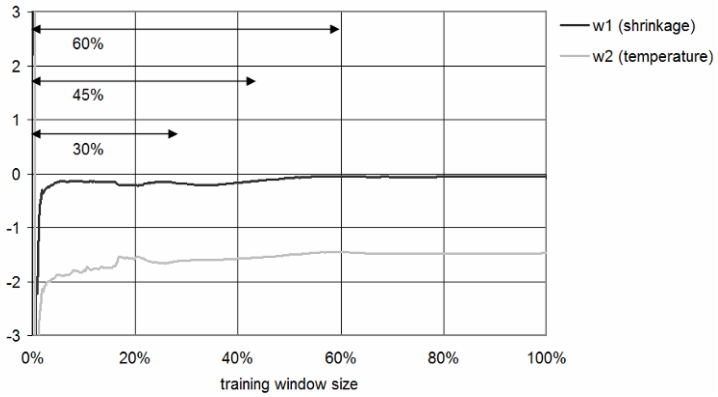

b) deck rotation RO-2 (V14S).

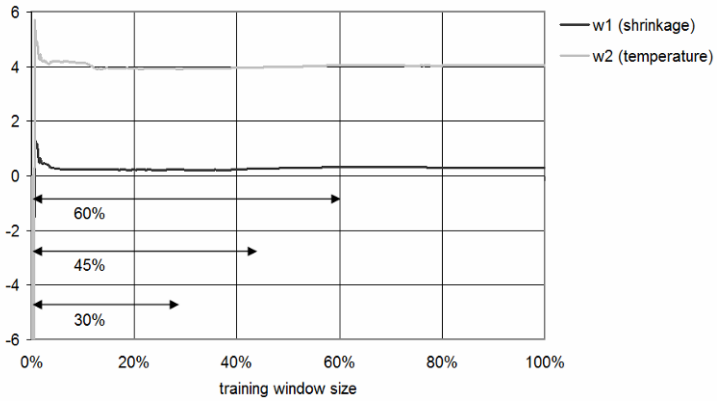

c) bearing displacement at TP14 (V14S).

Figure 4.14 : Calculated weights w_i as a function of the training window size. (cont.)

- **Example of anomaly detection**

The usefulness of the prediction model can be demonstrated by the following real example. Figure 4.15 shows the time variation of measurements and model predictions for one of the monitored bearing displacements. The time variation of the calculated error (difference between measurements and predictions) shows an abrupt variation at a specific time (09/05/2008 6 h a.m.), which indicates some anomaly. After searching for possible explanations for this occurrence, it was found that this instant of time corresponded to maintenance operations that forced a temporary removal of the LVDT. Upon removal and replacement of the transducer, the reference was lost, which justifies the detected deviation in the graphical representation of the error.

This maintenance operation was carried out without communication with the authors. It could only be detected after the prediction model has been applied to the results of this

transducer. Therefore, the usefulness of the prediction model is not restricted to the detection of structure deficiencies; it also detects anomalies in the monitoring results.

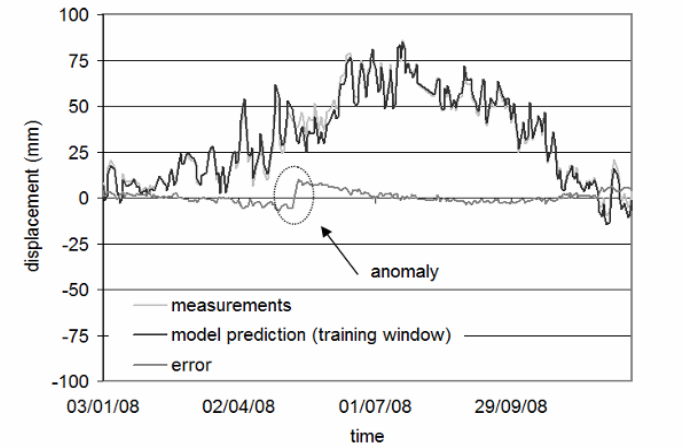

Figure 4.15 : Anomaly detection in bearing displacement BD-TP15 (V14S).

- **Global analysis of measured results**

Given the large number of the installed transducers, a subset of 24 sensors was selected for presentation in this work, as previously mentioned Figure 4.16 shows the calculated maximum relative errors, for a training window of 60% of the total period of observation. The label of each concrete deformation, CD, includes the cross section as indicated in Figure 4.2, the sensor location within the cross section, as shown in Figure 4.3, and the identification of the viaduct. The position of each rotation and displacement measurements is shown in Figure 4.2.

These results conform to the ones discussed before. Predictions of bearing displacements (with maximum relative errors lower than 4 % for a probability of occurrence of 95 %) are significantly better than the model estimations for concrete deformations and deck rotations. However, it is worthy to note that the relative errors are calculated with respect to the time variation in the observation period under analysis. If the total range of variation was considered, then significantly lower relative errors would be obtained. Figure 4.8 shows that the maximum strain variation in the precast girder amounts to ~850 microstrain. Therefore, the relative error with respect to the total range of variation is approximately ten times lower than the one with respect to the range of variation in the period of observation (~80 microstrain for the transducer in Figure 4.11).

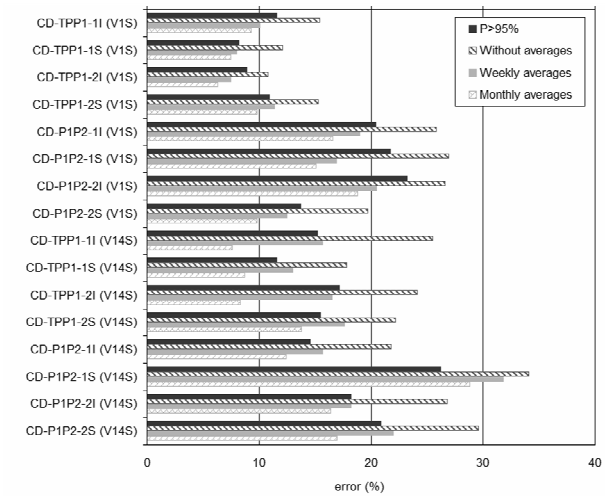

a) concrete deformations.

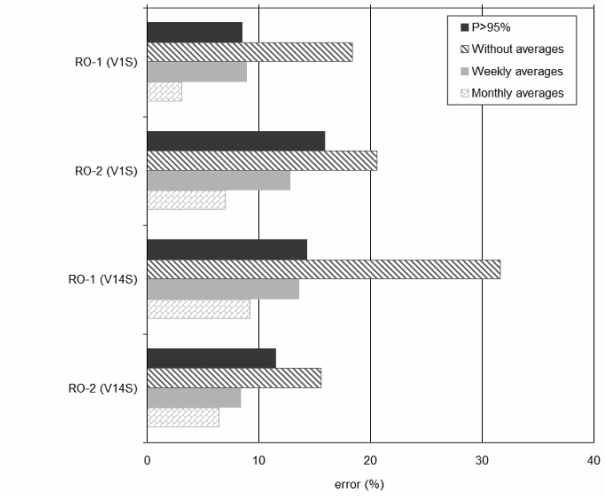

b) deck rotations.

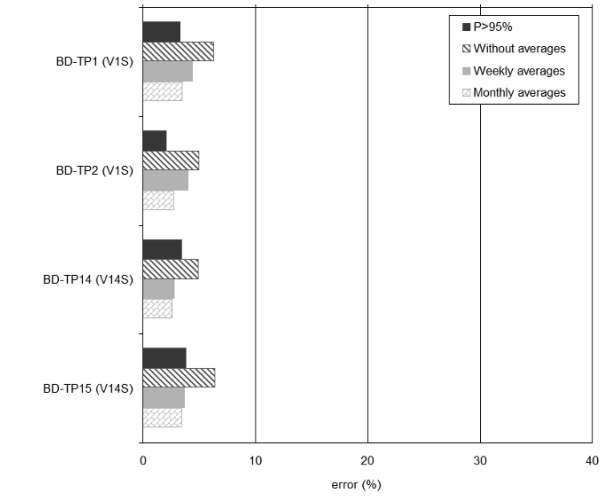

c) bearing displacements.

Figure 4.16 : Differences between actual measurements and predictions.

4.7. CONCLUSIONS

The present chapter focuses the monitoring and assessment of the long-term structural behaviour of continuous viaducts made with precast girders. A real structure, which was recently built in Portugal, has been monitored since the beginning of its erection. The monitoring system was carefully planned, installed and protected so that it could provide long-term reliable results. This chapter describes the viaduct, presents the monitoring system, and discusses the procedure employed to assess the structure's behaviour. This procedure is based on FEM calculations and regression models. Some relevant conclusions could be drawn:

- The measurement of the time variation of relevant concrete properties and the identification of the timing of the various construction events provided relevant information for the development of accurate FEM analysis. This conclusion stems from the difference between the actual time variation of the concrete deformations and those resulting from the design code predictions and also from the fact that the construction sequence strongly affects the structural behaviour.
- The good agreement between field measurements and FEM results validates the monitoring procedures and encourages the effective use of this information in surveillance and assessment tasks.
- The prediction model presented might be applied to establish normal correlation patterns between material and environmental parameters (such as temperature and shrinkage strains) and the observed structural response (strains, rotations and movements of expansion joints). The problem unknowns are determined by considering an initial time window in which healthy behaviour is assumed. The model can then be employed to calculate the expected response of the different transducers, for each point in time. The existence of abnormal differences between the expected values and the actual measurements reveals changes in the structural behaviour or deficiencies in the monitoring system.
- The choice of the predictor variables and the size of the time window used are of relevance and their calculations were presented and discussed.

- The use of prediction models involves minimal time and computational efforts, if the algorithm is implement in dedicated software, such as MENSUSMONITOR, with direct access to the measurements database.
- The usefulness of the prediction model was demonstrated through a real example in which a maintenance operation with implications in the monitoring results was detected.
- The best agreement between measurements and model predictions were obtained for transducers, which are not very sensitive to variables other than the employed independent (i.e., predictor) variables. In this case, the best results were obtained for the relative displacements at the expansion joints.

5. BRIDGE DEFLECTIONS BASED ON STRAIN AND ROTATION MEASUREMENTS

5.1. INTRODUCTION

Structural monitoring has received an increasing interest within scientific and technical community. At the same time, Bridge Health Monitoring Systems (BHMS) have been applied more intensively worldwide. Firstly, attention was focused on sensors applications. However, recently the emphasis has been shifting to the practical implications regarding the acquisition, storage and data processing (Van der Auweraer and Peeters 2003). Nowadays, it is possible to monitor continuously and remotely heavily instrumented structures, with a high degree of automation. Present solutions are versatile enough to carry out remote surveillance tasks with moderate costs (BRITE/EURAM 1997; Van der Auweraer and Peeters 2003).

In the last years, the concept of *smart structures* has increasingly been gaining the interest of the civil engineering community (BRITE/EURAM 1997). Full-scale structures equipped with sensors, processing units and communication networks are a reality all over the world, and these complex systems might become a powerful instrument to support the surveillance and maintenance tasks inherent to bridges.

Current monitoring systems applied on concrete bridges consist of strain gauges to measure local deformation, inclinometers to measure rotations, accelerometers to measure accelerations and transducers to measure displacements. Vertical displacements are in fact one of the most desirable parameters to be known for short and long-term observation. Bridge deflections reflect a global response of the structure giving essential information about the performance in service. However, it is well known how difficult it is to implement a measuring setup to observe vertical displacements in a bridge. Solutions

currently available to measure vertical displacements are often tedious to use and require specialized operators. For example, traditional transducers need a reference base and they are not suitable for several situations, e.g., on the river bed. One of the most widely used methods to measure vertical displacements on river bed is the levelling system. However, it has disadvantages such as the possible loss of reference marks and its cost in comparison with other methods. Attempts have been made to apply GPS technology to monitor displacements however, this approach are still far from being practical and effective. Therefore, there is a need of an alternative and expeditious approach to determine vertical displacements in bridges.

It is a fact that strain gauges and inclinometers are easier to install than a system to measure vertical displacements. Nonetheless, deformations and rotations are indirect information about the bridge deflection and therefore, to get a full understanding of the bridges' behaviour too many sensors would be necessary, and that would be costly. Nevertheless, taking advantage of the data collected with these sensors and the processing capabilities of the current computers, some authors have tried to estimate the vertical displacements based on concrete deformations and rotations. Vurpillot et al. presented in (Vurpillot *et al.* 1998) one of the first attempts to estimate the vertical displacements using measurements collected by strain gauges and inclinometers. Considering the Bernoulli beam theory, the authors presented a formulation based on a polynomial function to approximate the beam deflection. The strain and rotation measurements worked as constraints to the polynomial function. The methodology was tested in a laboratorial load test and in a full-scale bridge under daily temperature variations during 24 hours. A similar application, in which only strains are used, is presented in (Chung *et al.* 2008). A prestressed concrete girder was instrumented with long optical strain gauges, and using the geometric relation between curvature and vertical deflection in a simple beam the deflection curve of the girder was estimated. Analogously, Hou et al. used only measurements of inclinometers to estimate the bridge deflection (Hou *et al.* 2005). Another example of estimating the bridge deflection based on measurements of inclinometers can be found in (Burdet and Zanella 2000). Considering these previous studies, the aim of this chapter is to discuss the performance of the polynomial approach to estimate the deflection curve of full-scale concrete bridges. Measurements obtained through monitoring systems devoted to surveillance and maintenance are used, mainly composed by inclinometers over the supports and strain gauges at mid-span and near the supports. The main purpose is to

evaluate the suitability of these systems to estimate the bridge deflection. Short-term observations, obtained during load tests, are the focus of the analysis. An automatic procedure was developed and implemented in a software devoted to the management, treatment and analysis of monitoring results – MENSUSMONITOR (Sousa *et al.* 2009b). This option offered more flexibility in the data handling and a faster data processing with capabilities of real time visualization, with the advantages of being simple and applicable to monitored bridges. Firstly, the procedure to estimate the bridge deflection, detailing the main steps, is presented. Then, its application to a prestressed concrete beam is carried out in order to appraise its performance in laboratorial conditions. Afterwards, the results obtained for two full-scale bridges – Sorraia Bridge and Lezíria Bridge – are shown and discussed in detail. Finally, some recommendations are made in order to optimize the monitoring plans with the intention of estimating bridge deflections with strain gauges and inclinometers measurements.

5.2. PROCEDURE TO ESTIMATE BRIDGE DEFLECTIONS

5.2.1. INTRODUCTION

For a period between $t_{initial}$ and t_{final}, it is assumed a database with a set of experimental registers, where each register contains the measurements performed by a set of sensors. The database contains measurements of concrete deformations and rotations of the most critical sections of the bridge deck. Those critical sections – S_i, i = 1, 2..., n – are generally located at the mid-span and near the bridge supports (Figure 5.1).

During the service life, it is expected a linear elastic behaviour and therefore, the bridge deflection can be accurately estimated with simple mathematical models.

Considering the Bernoulli hypothesis – plane sections after deformation – the deflection curve of an uniformly loaded beam of 'm' spans is expressed as a sequence of 'm' fourth degree polynomials, $P_j^4(x)$. Each span is considered with constant inertia, uniformly loaded, and subjected to end forces and moments (Massonnet 1968). However, for full-scale bridges, the materials properties as well as the cross section may vary along its

length. Furthermore, the Bernoulli hypothesis is not observed near the supports neither in regions where concentrated loads are applied. Hence, the function that expresses the bridge deflection is in fact rational, namely because of the variability of the mechanical properties and the cross section inertia along the bridge length.

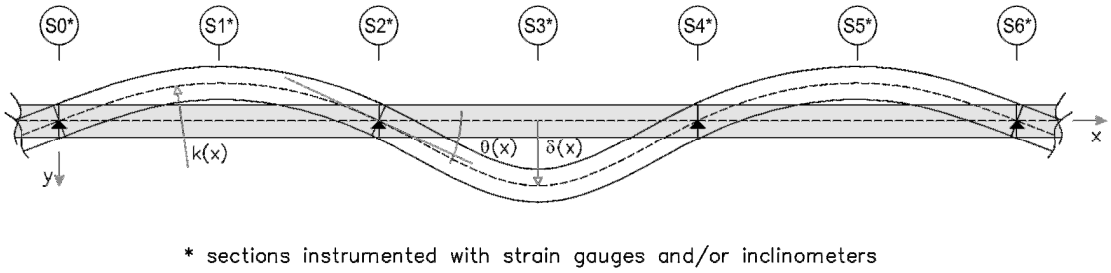

Figure 5.1 : Bridge deflection based on the monitoring of instrumented sections.

However, for moderate loads, the bridge deflection is a smooth curve, where the vertical displacements are considerably low if compared with the spans length, even for failure scenarios. In this context, it is reasonable to approximate the bridge deflection with a polynomial function and therefore, a polynomial approach will be adopted.

The procedure adopted herein calculates a polynomial function based on two types of information previously known: (i) intrinsic characteristics of the bridge behaviour, namely null vertical displacement over the supports and null curvature over the outer supports and (ii) curvatures and rotations based on measurements taken with strain gauges and inclinometers, respectively. In this context, the problem is solved according with the following steps.

5.2.2. CALCULATION STEPS

- **Sections curvature**

The curvature, $\kappa(x)$ is a function of the bridge deflection, $\delta(x)$, and is expressed by Eq. (9) (Massonnet 1968). As before referred, the vertical displacements are generally very small

if compared with the beam length, which results in small values for $d\delta(x)/dx$. Therefore, the value of $(d\delta(x)/dx)^2$ can be considered negligible and the denominator of Eq. (9) becomes unitary, leading that the curvature might be expressed by Eq. (10).

$$\kappa(x) = \frac{\dfrac{d^2\delta(x)}{dx^2}}{\left[1+\left(\dfrac{d\delta(x)}{dx}\right)^2\right]^{3/2}} \quad \Leftrightarrow \tag{9}$$

$$\Leftrightarrow \kappa(x) = \frac{d^2\delta(x)}{dx^2}, \left(\frac{d\delta(x)}{dx}\right)^2 \cong 0 \quad \textit{for small displacements} \tag{10}$$

For pure bending, the neutral axis is known a priori, and the curvature of a cross section can be calculated through Eq. (11), where $\varepsilon(x)$ represents the deformation of the layer that distances 'y' from the neutral axis.

$$\kappa(x) = \frac{\varepsilon(x)}{y} \tag{11}$$

However, if the beam is not restricted to bending, the curvature can be calculated based on the deformations of two different layers. This can be achieved by using appropriate strain gauges placed in the bottom and top layers, denoted as, 'SG-bot' and 'SG-top' respectively (Figure 5.2). Then, the curvature of the instrumented section can be calculated by Eq. (12), where 'H' represents the distance between those two layers.

$$\kappa(x) = \frac{\varepsilon_{bot}(x) - \varepsilon_{top}(x)}{H(x)} \tag{12}$$

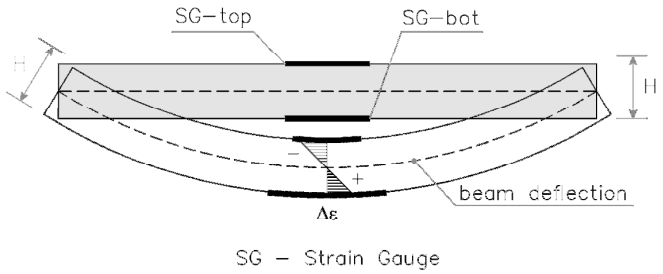

Figure 5.2 : Calculation of the section curvature based on strain gauges measurements.

As expressed by Eq. (13), a second-order constraint of the deflection curve is found by replacing Eq. (12) in Eq. (10). In other words, cross sections instrumented with strain gauges allow the curvature calculation providing thus, a second-order boundary constraints for the polynomial function of the deflection curve.

$$\frac{d^2\delta(x)}{dx^2} = \frac{\varepsilon_{bot}(x) - \varepsilon_{top}(x)}{H(x)} \tag{13}$$

- **Sections rotation**

Eq. (14) expresses the relation between the deflection curve, δ(x), and the rotation θ(x). However, the rotation of any cross section is considerably small, normally in the order of 10^{-3} of degree, because of the small magnitude of the vertical displacements if compared with the span length. Hence, Eq. (14) results in Eq. (15).

$$\theta(x) = arctg\left[\frac{d\delta(x)}{dx}\right] \quad \Leftrightarrow \tag{14}$$

$$\Leftrightarrow \theta(x) = \frac{d\delta(x)}{dx} \quad , \quad \textit{for small rotations} \tag{15}$$

Consequently, the measured rotations can be directly considered as a first-order constraint of the polynomial function that is intended to be estimated.

- **Polynomial function setting**

For each span a polynomial function is estimated, which means that 'm' polynomials are calculated for the 'm' bridge spans. This option allows a flexible *modus operandi* in the data handling and enough versatility to apply on a bridge with any number of spans. The process is repeated in a *while-loop* as many times as the number of spans. As previously mentioned, the polynomial function is calculated based on boundary constraints. Figure 5.3 shows a generic scheme of a bridge span, where the span deflection is represented, highlighting the constraints at mid-span and support sections. However, for real cases, some constraints may not exist, depending on the instrumentation available for each span.

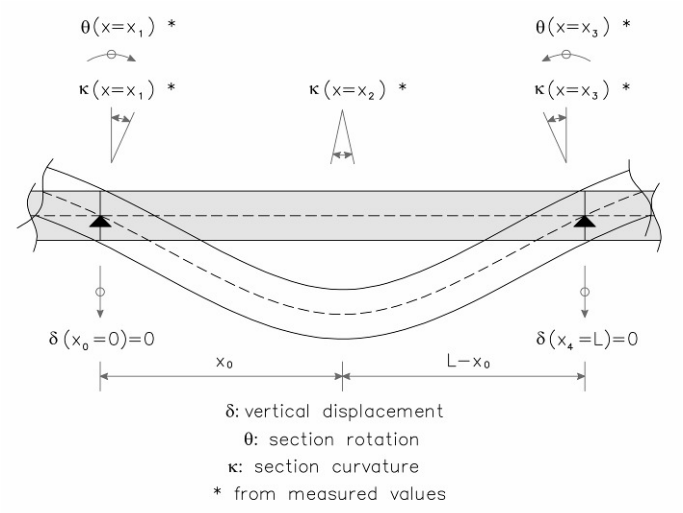

Figure 5.3 : Span deflection and boundary constrains.

Generally, if 'n + 1' boundary constraints are known, a 'n' degree polynomial function, as expressed by Eq. (16), can be fitted. For the generic case of Figure 5.3, seven boundary constraints are known and consequently a sixth order polynomial function could be used. This is the maximum degree for the polynomial function that can be reached.

One of the advantages of using one polynomial function for each span is that high degree functions are avoided, if compared with a unique polynomial function for all bridge length, and therefore, problems of overfitting are prevented (Björck 1996).

$$y_j(x) \cong P_j^n(x) = \sum_{p=0}^{n} c_{j,p} \cdot x^p \quad , \quad j - span \tag{16}$$

The parameters $c_{j,p}$ in Eq. (16), are the unknowns that are calculated by imposing the boundary constraints previously referred, namely: (i) null vertical displacements over the supports and null curvatures over the outer supports; (ii) curvatures and rotations based on the sensors readings. Therefore, based on 'n+1' boundary constraints that are known for a bridge span 'j', a system of linear equations can be established as expressed, in the matrix format, by Eq. (17).

$$[A]_j \cdot \{c\}_j = \{b\}_j \tag{17}$$

The matrix [A] depends only of the span geometry, namely the location of the instrumented sections, x_i, and the span length, L. The reason for the dependency of the span length is due to numerical aspects. The section location is normalized by x/L, leading to possible locations ranging between zero and one. In this context, the matrix coefficients are homogenous, preventing potential instability in the calculation. The vector $\{c\}_j$ contains the problem unknowns – the polynomial coefficients – and the vector $\{b\}_j$ the boundary constraints. The problem solution is given by Eq. (18). It must be assured that the matrix [A] is not singular, which can be done by considering linearly independent constraints.

$$\{c\}_j = [A]_j^{-1} \cdot \{b\}_j \tag{18}$$

- **Calculation of bridge deflection**

Finally, a set of 'z' sections is chosen to calculate the vertical displacements, δ. With the problem solved, the polynomial functions are perfectly known and therefore, the vertical displacement can be calculated using Eq. (19) for any bridge section, $S_{x=x_k}$, by solving P(x = x_k). Moreover, rotations, θ, and curvatures, κ, can also be calculated by simply taking the derived functions P′(x = x_k) and P″ (x = x_k) as expressed, respectively, by Eq. (20) and (21).

$$\delta:\ P_j(x_k)=\sum_{p=0}^{n} c_{j,p}\cdot x_k^p \quad , \quad k=1,2,...,z \tag{19}$$

$$\theta:\ P_j'(x_k)=\sum_{p=1}^{n} p\cdot c_{j,p}\cdot x_k^{p-1} \quad , \quad k=1,2,...,z \tag{20}$$

$$\kappa:\ P_j''(x_k)=\sum_{p=2}^{n} p\cdot(p-1)\cdot c_{j,p}\cdot x_k^{p-2} \quad , \quad k=1,2,...,z \tag{21}$$

5.2.3. SOFTWARE IMPLEMENTATION

The steps previously detailed were implemented in an existing software, specifically devoted for the treatment, processing and analysis of data concerning the Structural Health Monitoring of structures – MENSUSMONITOR (Sousa *et al.* 2009b). The data access through database consulting and the data pre-treatment, as well as real time visualization capabilities, are features already available in this software. Therefore, the implementation of the described procedure in this software makes its application easier and faster when compared with usual commercial tools such as spreadsheets. Figure 5.4 shows the front panel with the "*mensus deflection*" tool active (see Table 3.4). More details about this software can be found elsewhere (Sousa *et al.* 2008).

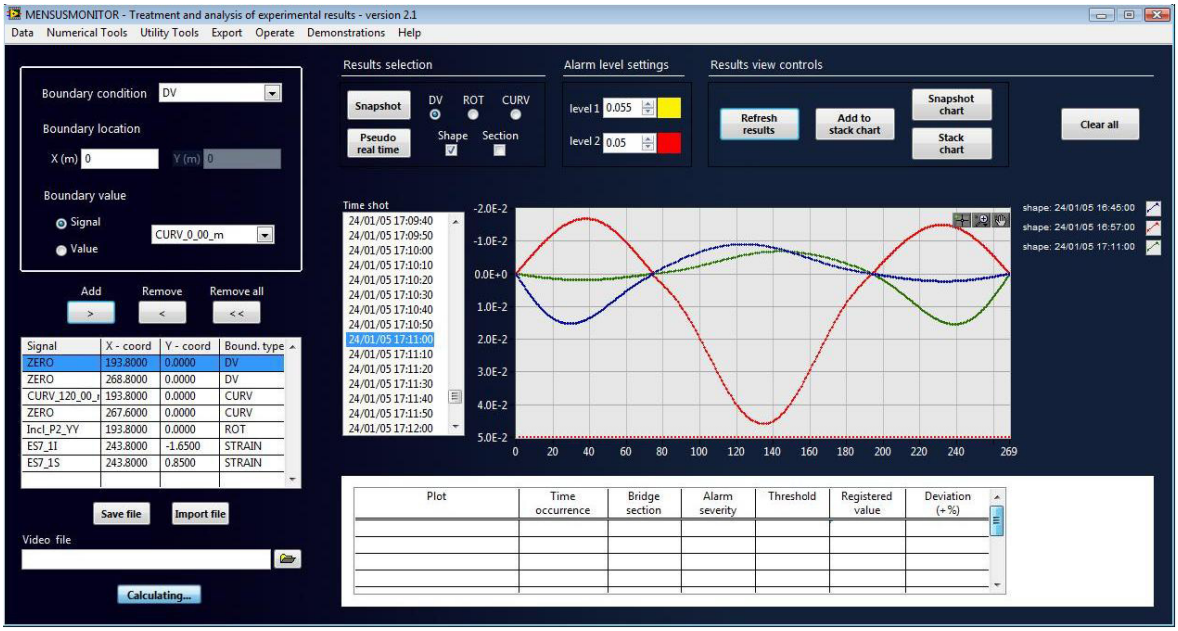

Figure 5.4 : Front panel of MENSUSMONITOR with the "*mensus deflection*" tool active.

Moreover, the calculation steps can be automatically extended, by a temporal cycle, for an observation period [$t_{initial}$,t_{final}], where a generic register occurred at instant t contains all sensors measurements, namely concrete deformations, ε, and rotations, θ. Figure 5.5 presents a flowchart of the calculation steps of the temporal cycle.

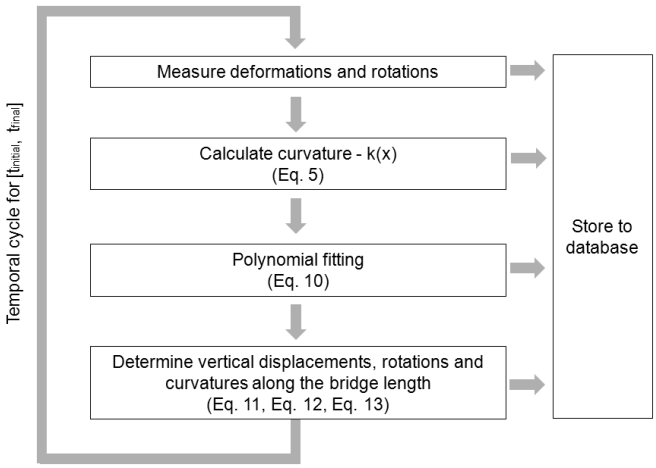

Figure 5.5 : Flowchart of the calculation steps.

5.2.4. VALIDATION ON A SIMPLY SUPPORTED PRESTRESSED BEAM

The methodology was firstly assessed on a prestressed concrete beam simply supported with 150 mm x 200 mm cross section and an effective span of 3.96 m (Figure 5.6). The applied materials were concrete of class C40/50 and steel of class A500. The longitudinal reinforcement is constituted by 4ϕ12 mm, while the transversal reinforcement is 2ϕ6 mm 10 cm spaced. Additionally, the beam was prestressed with a force of 172 kN, by using a seven-wire strand with a cross section of 1.40 cm^2 and yield stress of 1857 MPa (Sousa 2002).

As illustrated in Figure 5.6, three cross sections, S1, S2 and S3, are monitored with six electric strain gauges each, where two are embedded in concrete and the remaining four are bonded to the reinforcement bars. Additionally, the vertical displacements on sections SA, SB and SC, using LVDTs, and rotations at the two ends of the beam, using electric inclinometers, were observed. The environmental temperature was also measured. An

automatic acquisition system was provided to collect and register the values measured by all sensors (Sousa 2002; Cavadas *et al.* 2009).

The beam was loaded at the sections SA and SC, with two concentrated loads, F1 and F2, respectively, (Figure 5.6). The two load cases considered, combining F1 and F2, are shown in Table 5.1. The criterion of L/2000 was established as the maximum deflection, ensuring the elastic behaviour during the tests.

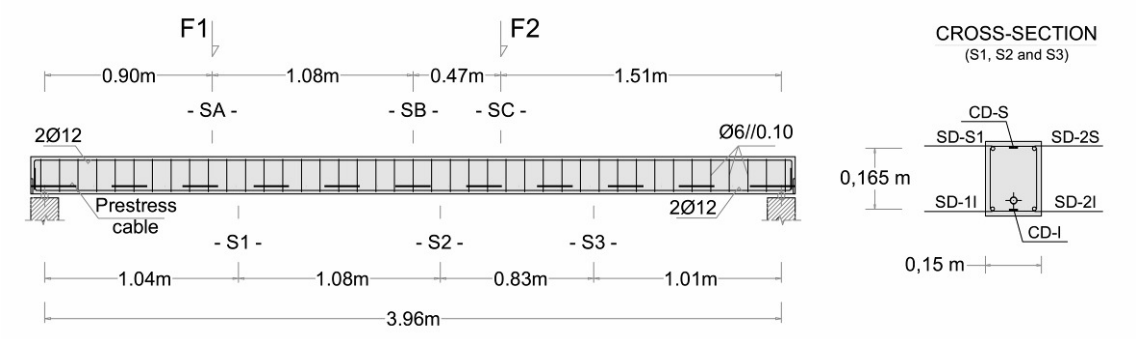

Figure 5.6 : Prestressed concrete beam.

Table 5.1 : Beam load cases (kN).

Load Case	F1	F2
LC1	4.42	0.19
LC2	0.97	3.79

Figure 5.7 shows the vertical displacements of the beam, for the LC1 and LC2, where the vertical displacements measured with LVDTs (grey circles) and the beam deflections calculated with the polynomial function (black line) are overlapped. A 4th degree polynomial function was used, based on the null vertical displacements and the measured rotations at the beam-ends and the curvature at section S2. A good conformity between the polynomial function and the measured displacements was found for both load cases, with a maximum relative error of 2.1 % at section SA (Figure 5.7-a) and 4.9 % at section SB (Figure 5.7-b) for LC1 and LC2, respectively. Nevertheless, it should be referred that the experimental tests were conducted with a different purpose (Cavadas *et al.* 2009).

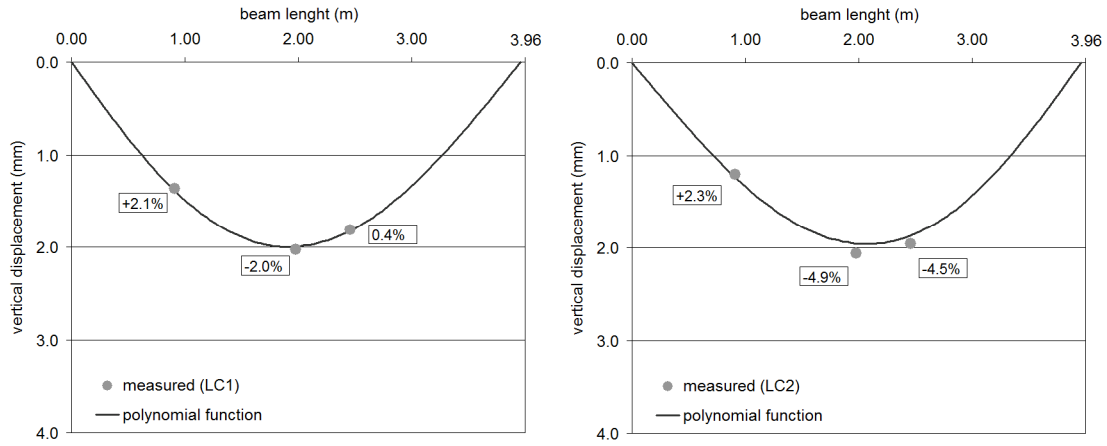

a) Load Case 1 (LC1). **b) Load Case 2 (LC2).**

Figure 5.7 : Beam deflection of the prestressed beam.

5.3. FULL-SCALE APPLICATIONS

5.3.1. INTRODUCTION

The deflection of a bridge span is highly influenced by the behaviour of sections located at the mid-span and near the support zones. A failure scenario in a bridge deck normally starts in these zones due to the high stress level. Generally, higher curvatures are measured for sections located at the mid-spans and near the support zones, while for rotations the higher values are measured for sections near the deck supports.

Two bridges – Sorraia Bridge and Lezíria Bridge – equipped with monitoring systems taking into account the previous considerations, were object of this study to evaluate the presented procedure in full-scale structures. These structures are inserted in two important motorways in Portugal, near the capital, Lisbon. Both bridges are equipped with monitoring systems devoted to aid the surveillance and maintenance operations. For comparison purposes, the vertical displacements were measured only at mid-span sections. However, to have a more comprehensive view of the bridge deflection, this study is also supported on results obtained by numerical models using the Finite Element Method (FEM). The vertical displacements predicted with the present methodology could be confronted, not only with the measurements taken on a limited number of sections, but also

along all the bridge length with the bridge deflection obtained from the numerical models. Thus, the results obtained with the polynomial functions can be analysed and discussed in more detail.

5.3.2. SORRAIA BRIDGE

As part of the Portuguese motorway A13, Sorraia Bridge, situated at Salvaterra de Magos, is a prestressed concrete structure composed by two parallel and identical structures – east and west bridges with a total length of 1666 m each (Figure 5.8). Focussing on the main bridge of the east side, this structure has a total length of 270 m, constructed by the cantilever process. The structure has three spans, two end spans with 75 m length and a central span with 120 m length (Figure 5.10). The bridge deck is a box girder whose height ranges between 2.55 m at mid-span and 6.00 m at the support region. The bridge deck is supported on piers, 7.5 m high, through unidirectional bearings. The piers are supported by pilecaps of five piles each, and each pile is 30 m long with 2 m diameter.

Figure 5.8 : Sorraia Bridge (© Brisa Engenharia e Gestão (BEG)).

As previously referred, a long-term monitoring system is installed in the east deck of the Sorraia Bridge, which was developed in the scope of a consortium project between BRISA S.A. and two R&D institutions, LABEST-FEUP and INESC-PORTO, partially supported

by AdI – Innovation Agency (SMARTE 2004; Perdigão 2006). The monitoring system was implemented during the bridge construction and it has allowed the long-term observation of the structural behaviour. The main instrumentation is based on (i) strain gauges, that encapsulates simultaneously electric and optical sensors (Figure 5.9-a) (Sousa 2006c), and (ii) temperature sensors in a set of cross sections. The environmental temperature and the relative humidity, namely inside and outside the box girder (Figure 5.9-b), are also monitored. These sensors are connected to Acquisition Nodes (AN) located inside the deck girder and above the piers P1 and P2 (Figure 5.9-c and Figure 5.10). Additionally, during the load test, a temporary monitoring system was placed to observe other important parameters, such as vertical displacements and rotations. Figure 5.10 and Table 5.2 illustrate and detail the location of the relevant instrumentation for this study.

The data collected by the temporary system was very useful to complement the measurements taken by the permanent monitoring system, in order to assess the bridge behaviour as well as to evaluate the performance of the permanent monitoring system through cross analysis of data.

Regarding the assessment of the bridge behaviour during the load test, a numerical model of Sorraia Bridge was built based on finite element techniques, considering the effective properties of the bridge materials and the loads applied during the load test. It consists in a two-dimensional model using beam elements in accordance with the Timoshenko theory to simulate the concrete elements of the bridge, which is a reasonable approach for the study of the structural global behaviour.

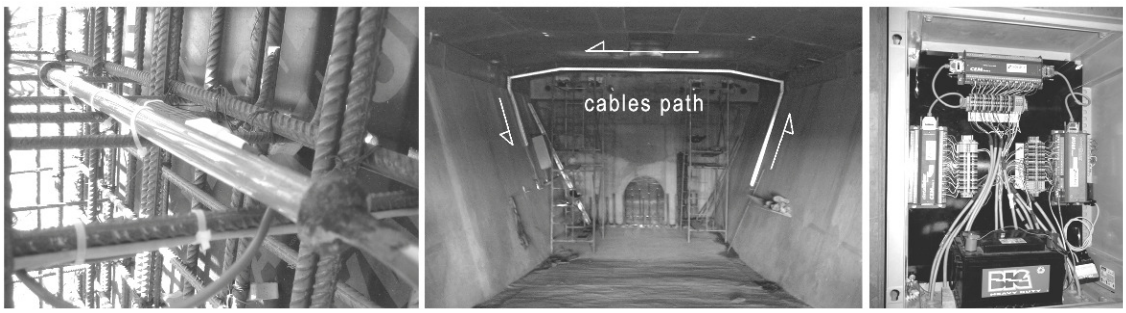

a) Electric/Optical strain gauge. **b) Interior of the box-girder.** **c) Acquisition Node.**

Figure 5.9 : Monitoring system of Sorraia Bridge.

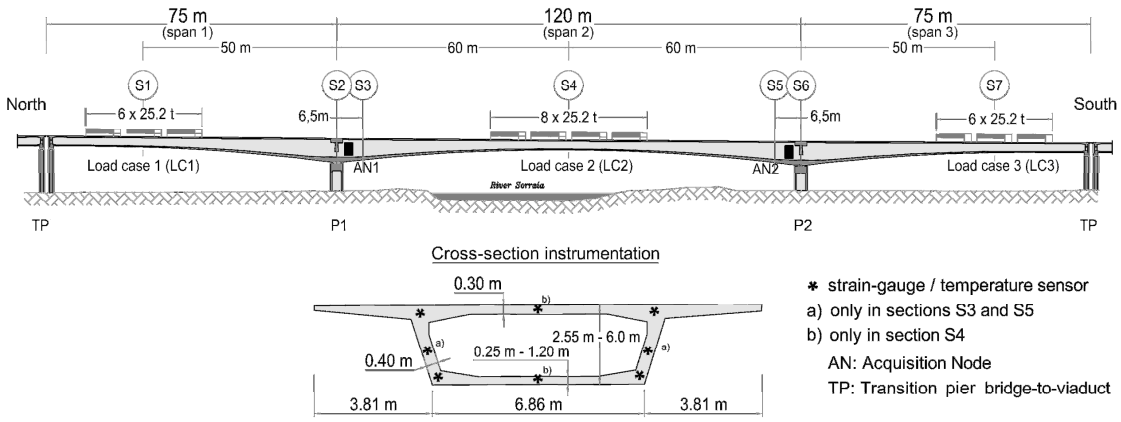

Figure 5.10 : Location of the instrumented cross sections in Sorraia Bridge.

Table 5.2 : Instrumentation typology and quantities – Sorraia Bridge.

Parameter	S1	S2	S3	S4	S5	S6	S7
Vertical displacement	1	-	-	1	-	-	1
Rotation	-	1	-	-	-	1	-
Deformation	4	-	6	6	6	-	4
Temperature	-	-	-	-	2	-	-

The estimation of the vertical displacements was made using the measurements collected during the load test performed at the end of the bridge construction. Trucks full charged, with controlled weight, were used to carry out the load tests without put in risk the elastic behaviour. Those tests comprised a set of configurations by immobilizing the trucks at specific positions of the bridge, corresponding to three load cases, Load Case 1, 2 and 3, which explored the maximum deformation in the critical sections, i.e. the three mid-span sections (Figure 5.10). The results presented bellow concern to these three load cases.

The polynomial functions were calculated based on the measurements and the intrinsic characteristics of the bridge, namely null vertical displacements above piers and null curvature at the end support of the outer spans (span 1 and span 3).

Figure 5.11-a shows the vertical displacements for the three load cases, namely the measured values (bullet marks), the deflection curves using the polynomial functions (continuous lines) and those obtained with the numerical model (dashed lines). In addition, the relative errors are also presented (text boxes), where the measured value was taken as reference. Comparing the predicted values with the measured ones, the best result corresponds to section S4, which was obtained with a 6^{th} degree polynomial function,

while for span 1 and 3 a 4th degree polynomial function led to poorer results. This result was expected, due to the higher number of instrumented sections in span 2 (see Figure 5.10). The error is less than 1 % for section S4, which is a good indicator, taking into account that it is assumed a simplified polynomial function for the real span deflection. However, for spans 1 and 3, the relative errors for sections S1 and S7 are greater than 10 %. For these spans, only the curvature and rotation of one of the span ends are known, contrasting with the span 2 where the rotations and curvatures at both ends are known (see Figure 5.10), which can explain the results obtained for these spans. For a better understanding of the results, Figure 5.11-b presents the rotation diagrams, according to Eq. (20), as well as the results obtained by the numerical model. It is clear that the higher deviations are observed in deck zones that are near the piers P1 and P2. For LC1 and LC3 the polynomial functions exhibit a higher rotation for spans 1 and 3 near the piers P1 and P2, leading to higher displacements, which results in the overestimated values for spans 1 and 3.

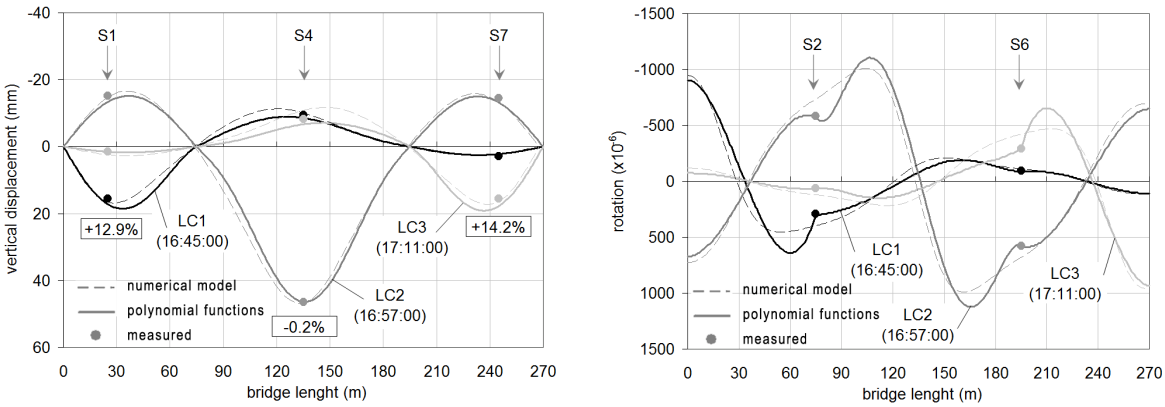

a) vertical displacement diagrams. **b) rotation diagrams.**

Figure 5.11 : Sorraia Bridge results for LC1, LC2 and LC3 (case 0).

5.3.3. LEZÍRIA BRIDGE

Lezíria Bridge is inserted in the A10 motorway in Portugal. With a total length of 39.9 km, this motorway is an outside bound to the Lisbon Metropolitan Area. The main bridge structure has a total length of 970 m (Figure 5.12), with 8 spans, 95 + 127 + 133 + 4 × 130 + 95 m and 7 piers supported by pilecaps over the riverbed (Figure 5.14). The bridge deck

is a box girder with variable inertia - approximately 10 m wide and height ranging from 4 m to 8 m. The box girder core was segmentally built using movable scaffolding while the side cantilevers were subsequently constructed with a specific movable scaffolding and metallic struts fixed on the bottom slab of the box girder. The concrete piers are formed by four walls with constant thickness and variable width and are supported by pilecaps.

Figure 5.12 : Lezíria Bridge – night view.

The bridge has an integrated monitoring system devoted to the management and surveillance of the structure (Sousa *et al.* 2011b). Several cross sections are instrumented with embedded and external sensors. The installed sensors measure a set of quantities such as static, dynamic and durability parameters. Among all the installed sensors, only the strain gauges (Figure 5.13-a), inclinometers (Figure 5.13-b) and displacement transducers (Figueiras *et al.* 2010) are considered for this study. Among the eight spans that compose the bridge deck, the first three spans between piers PTN3 and P3 were selected to carry out this study. These sensors are connected to Acquisition Nodes (AN) located inside the deck girder and above the piers P1 and P2 (Figure 5.13-c). Figure 5.14 illustrates, and Table 5.3 summarizes, the relevant information about the instrumentation plan for this study.

Regarding the assessment and surveillance tasks, a numerical model of Lezíria Bridge was built based on FEM. It consists in a two-dimensional model using beam elements in accordance with the Timoshenko theory to simulate the concrete elements of the bridge.

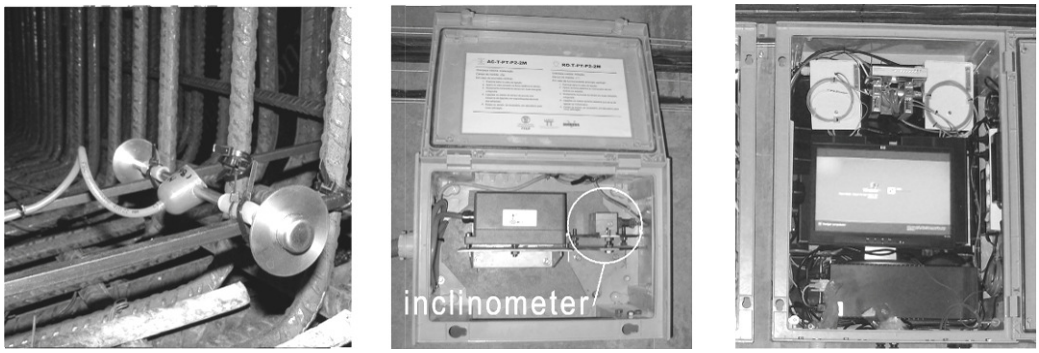

(a) Electric strain gauge. **(b) inclinometer installation.** **(c) Acquisition node.**

Figure 5.13 : Monitoring system of Lezíria Bridge.

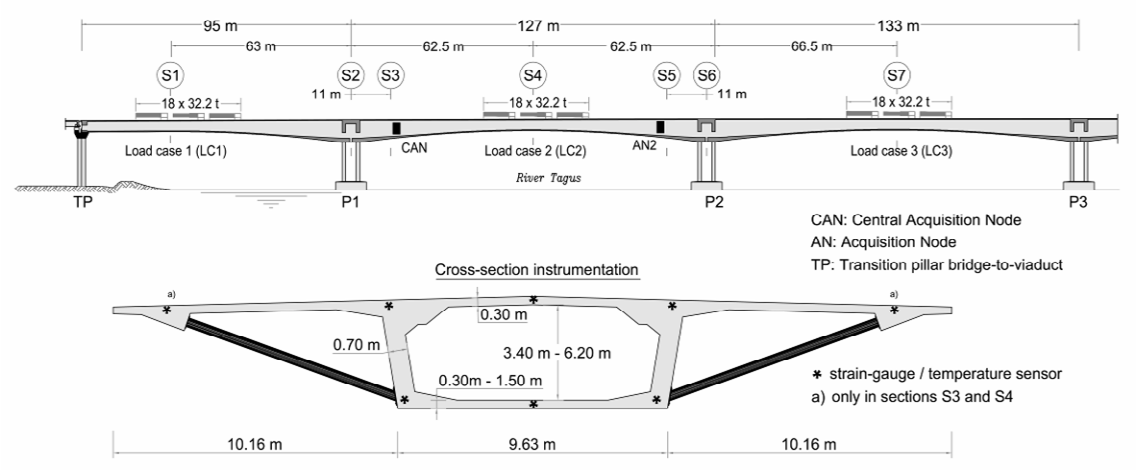

Figure 5.14 : Location of the instrumented cross sections in Lezíria Bridge.

Table 5.3 : Instrumentation typology and quantities – Lezíria Bridge.

Parameter	S1	S2	S3	S4	S5	S6	S7
Vertical displacement	1	-	-	1	-	-	1
Rotation	-	1	-	-	-	1	-
Deformation	6	-	8	8	6	-	6
Temperature	2	-	8	8	-	-	2

Similarly to what it was presented for the Sorraia Bridge, the vertical displacements were estimated using the measurements collected during the load test performed at the end of the bridge construction. To carry out the load tests, trucks full charged were used. Those tests comprised a set of configurations by stopping the trucks at positions that cause the maximum deformation in the critical sections, namely the three mid-span sections, Load Cases 1, 2 and 3 (Figure 5.14).

The polynomial functions were calculated based on the measurements and the intrinsic characteristics of the bridge, namely null vertical displacements above piers and null curvature at the end support of the outer span (span 1).

Figure 5.15-a shows the results for the vertical displacements. Comparing the predicted values using the polynomial functions with the measured ones, the estimation for section S4, with a 6th degree polynomial function, presents a good agreement, while for spans 1 and 3, the 4th and 3rd degree polynomial functions, respectively, the estimations give poorer results. The error for section S4 is less than 5 %, which is a good estimate considering that a 6th degree polynomial approach was used. Again, the available number of instrumented sections for each span can explain the deviations, where the differences increase as the polynomial degree decreases. Observing the rotation diagrams presented in Figure 5.15-b, the highest deviations are again observed near the piers P1 and P2. For LC1 and LC3 the polynomial functions exhibit a higher rotation for spans 1 and 3 near the piers P1 and P2, respectively, leading to higher displacements, which results in the overestimated values for spans 1 and 3 with error magnitudes above the reasonable. Moreover, the results obtained for span 3 are completely out of bound, which is namely explained by the few constraints that are known for the girder section above the pier P3. The results demonstrate that imposing only a null vertical displacement in this section is insufficient to obtain acceptable values. Therefore, without additional information concerning the girder behaviour over pier P3, it is not possible to estimate the bridge deflection for span 3 with acceptable accuracy.

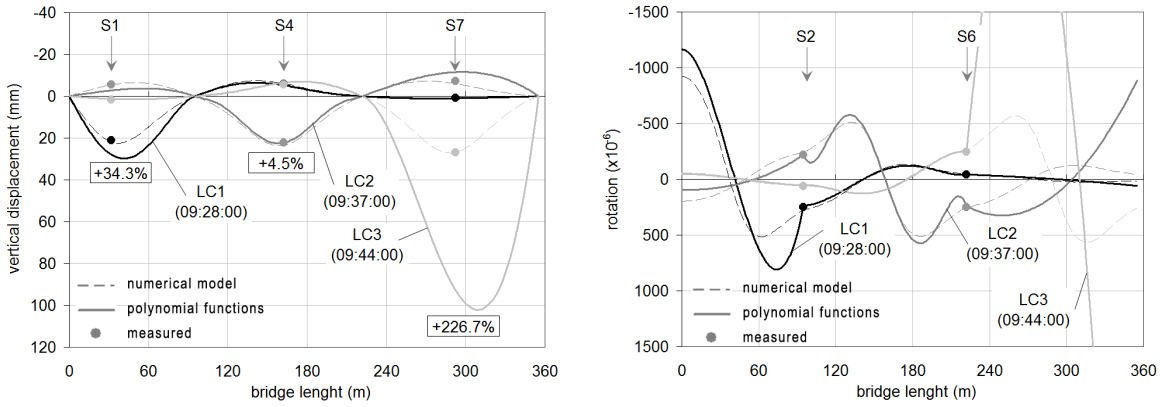

a) vertical displacement diagrams. **b) rotation diagrams.**

Figure 5.15 : Lezíria Bridge results for LC1, LC2 and LC3 (case 0).

5.4. STRATEGIES TO IMPROVE THE ESTIMATION OF THE BRIDGE DEFLECTION

5.4.1. BASED ON DATA EXTRAPOLATION OF CURVATURES

Observing carefully the bridge instrumentation in Figure 5.10 and Figure 5.14, the two girder sections instrumented near the piers, S3 and S5, are not exactly above the pier axis but inside of span 2. Since the deformation field of girder sections over the support (S2 and S6) does not follow the Bernoulli hypothesis, these sections are avoided to measure strains with the purpose of estimating section curvatures. This fact implies that only one section instrumented with strain gauges is available for span 1 and span 3, respectively. Despite a 4^{th} order polynomial function may be used to estimate the bridge deflection for these spans, as it was presented in Figure 5.11-a and Figure 5.15-a, the quality of the results obtained for spans 1 and 3 is significantly lower when compared with the ones obtained for span 2. Therefore, the knowledge of the curvature of sections near the pier support is essential to predict the deflection of these spans more accurately. To overcome this limitation, the curvature of these sections was estimated with the polynomial function obtained for the span 2 and therefore, the degree of the polynomial functions used for spans 1 and 3 could be incremented by one.

Using this additional information, Figure 5.16-a presents the results for Sorraia Bridge. With a 5^{th} degree polynomial function a significant improvement is obtained for spans 1 and 3, where the relative error for sections S1 and S7 decrease from + 12.9 % to - 4.5 % and from 14.2 % to - 1.9 %, respectively. Hence, the consideration of the curvatures of sections S2 and S6, calculated with the polynomial function obtained for the span 2, is essential. The deviations observed near the piers P1 and P2 diminished, which can be confirmed by comparing the rotation diagrams shown in Figure 5.11-b and Figure 5.16-b.

As far as Lezíria Bridge is concerned, the results for span 3 are not satisfactory due to the limited information about the deck behaviour over pier P3, as previously referred. Therefore, the use of the deck curvature over piers, obtained with the polynomial function of the span 2, is only applied for section S2 (span 1).

Figure 5.17-a presents the results of the vertical displacements, which are significantly better than the ones presented in Figure 5.15-a, with a reduction of the relative error from

+34.3 % to +3.3 % for section S1. The deviations observed near the piers P1 decreased, which is the main reason for the improvement of the results in section S1, as it can be confirmed by comparing the rotation diagrams of Figure 5.15-b and Figure 5.17-b.

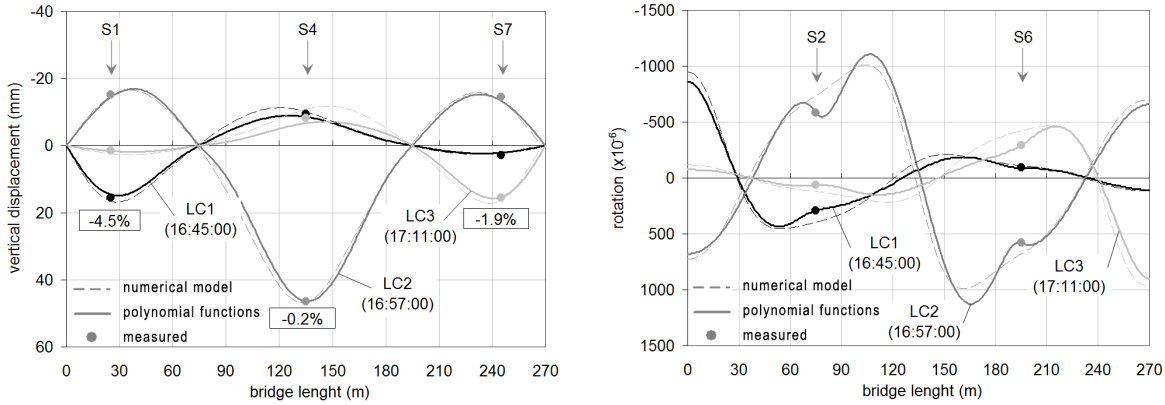

a) vertical displacement diagrams. **b) rotation diagrams.**

Figure 5.16 : Sorraia Bridge results for LC1, LC2 and LC3 (case 1).

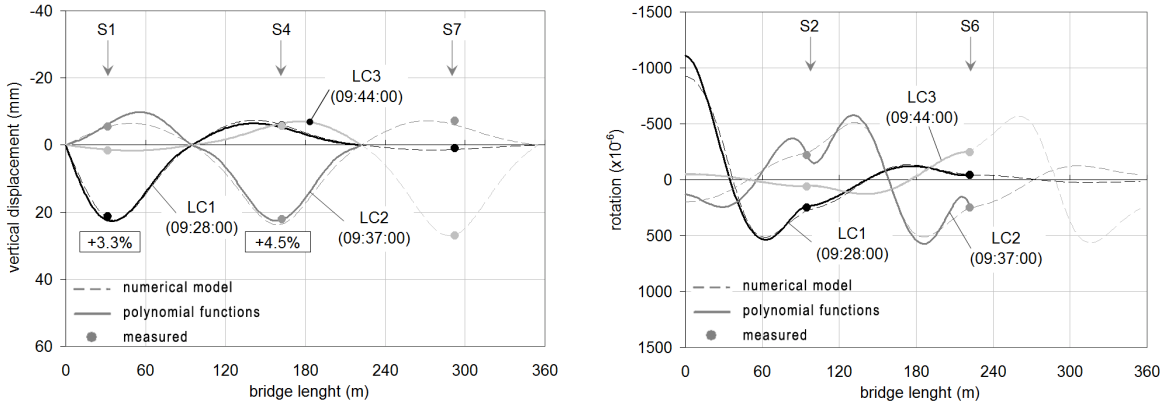

a) vertical displacement diagrams. **b) rotation diagrams.**

Figure 5.17 : Lezíria Bridge results for LC1, LC2 and LC3 (case 1).

The results presented both in Figure 5.16 and Figure 5.17 correspond to specific shootings among all that are contained in the observation period $[t_{initial},t_{final}]$. However, as previously referred, it is possible the visualization of the evolution of the deflection curve in a time sequence, with the results of all shootings stored in the referred observation period. Figure 5.18 shows the evolution of the vertical displacements at the instrumented sections calculated with the polynomial functions (continuous line) and the sensors measurements (marker shapes) during the load test. In general, the polynomial values exhibit a good

agreement with the measured ones, with relevance to the trend evolution that is clearly identical.

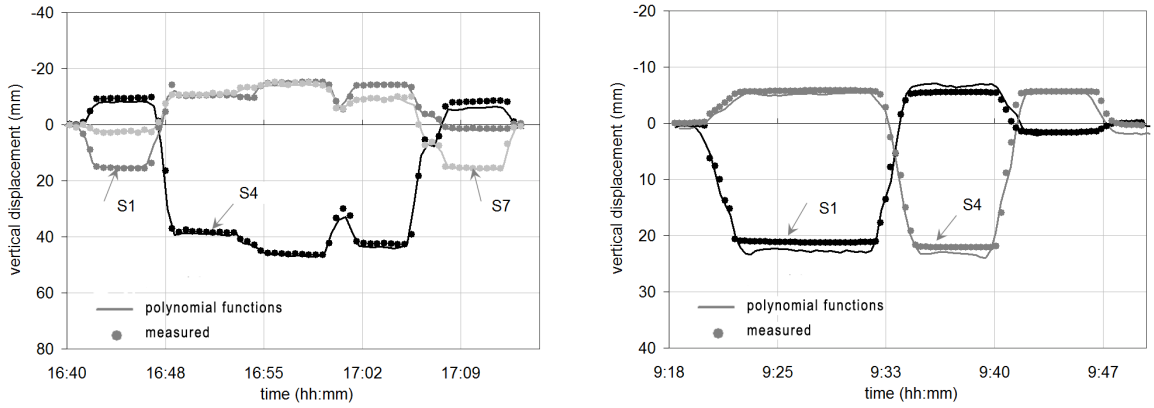

a) Sorraia Bridge. **b) Lezíria Bridge.**

Figure 5.18 : Vertical displacement time series during the load test.

5.4.2. BASED ON ROTATION MEASUREMENTS

Although the vertical displacements for the sections S1, S4 and S7 are satisfactory with errors less than 4.5 %, the same cannot be straightforward stated about the shape of the bridge deflection. In fact, observing the deflection shape near the inner supports P1 and P2 of both bridges (Figure 5.16-a and Figure 5.17-a), it is evident a deviation of the normal curvature evolution. The polynomial functions exhibit a higher curvature near the piers supports when compared with the numerical results, as shown in the rotation diagrams presented in Figure 5.16-b and Figure 5.17-b. For example, in the LC2 presented in Figure 5.16 and Figure 5.17, it is perfectly noticeable an inflection of the deformed shape above the pier P1.

On the other hand, the use of local strain measurements to estimate the bridge deflection is unreliable if cracks occur in the instrumented zone. It would be necessary to use long gauges to have an average deformation, which is not the case in the examples presented. Therefore, as an alternative, the installation of additional inclinometers could improve the quality of the estimated deflection shape. These sensors are easier to install when compared with the strain gauges, which are normally installed during the casting operations with a higher cost and effort, with embedded cables in concrete.

In this context, the calculation of the deck deflection considering only rotations is discussed. Due to the inexistence of additional rotation measurements in the experimental results, this study is supported in the numerical results obtained for the three load cases LC1, LC2 and LC3. In order to search the best solution for the bridge deflection, a parametric study was performed using four rotations in the case of the end spans and six rotations for the inner spans, as illustrated in Figure 5.19. The analysed configurations consider always, for each span, two rotations at the girder sections above the piers – fixed inclinometers – and, at variable positions, four inclinometers in the case of inner spans, and two inclinometers in the case of the end spans – movable inclinometers. The reason why a different configuration was adopted for the inner spans is related with the deck discontinuity of the end spans, which is an additional constraint for the problem resolution (null curvature at the outer span), and the shift of the section with maximum vertical displacement to the deck discontinuity side, which justifies the positioning adopted for the inclinometers. The movable inclinometers were successively moved 5 m apart in order to explore several possible configurations (Figure 5.19).

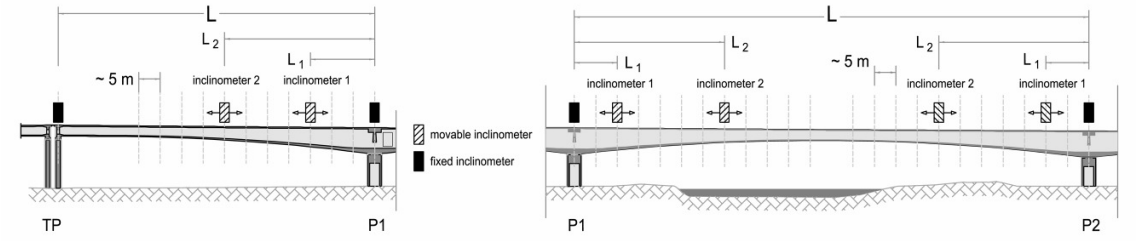

a) end spans. **b) inner spans.**

Figure 5.19 : Parametric study for the bridge deflection calculation based on rotations.

Figure 5.20 presents the results of the parametric analysis concerning Sorraia Bridge. For each span, the results show the average error committed, which is calculated as the quotient between: (i) the average of the absolute differences between the vertical deflection calculated by the polynomial function and the one given by the numerical model, and (ii) the maximum vertical displacement (Eq. (22)). For each entry of inclinometer 1 and 2, the column height represents the average error when the inclinometers are positioned at a distance of $\eta_1 \cdot L$ and $\eta_2 \cdot L$ of the pier, respectively (Figure 5.19).

$$e_j = \frac{\dfrac{\sum_{k=1}^{z}\left|\delta_{j,k} - \overline{\delta}_{j,k}\right|}{z}}{\max\left|\overline{\delta}_{j,k}\right|} \quad , \quad \begin{cases} \delta_{j,k} - \textit{polynomial function} \\ \overline{\delta}_{j,k} - \textit{numerical model} \end{cases} \tag{22}$$

The results shows that the optimal position for inclinometers 1 and 2 are at $L_1 = 0.14 \cdot L$ and $L_2 = 0.42 \cdot L$ for end spans, while for inner spans the positions that lead to the best results are at $L_1 = 0.12 \cdot L$ and $L_2 = 0.30 \cdot L$. For the three spans, the average errors are about 1 %, all of them related to a local minimum as it can be observed in Figure 5.20.

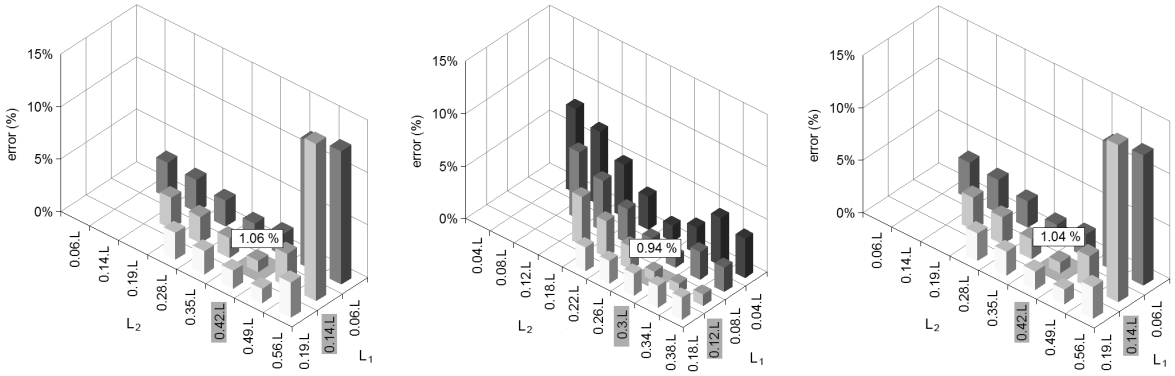

a) span 1. **b) span 2.** **c) span 3.**

Figure 5.20 : Results of the parametric analysis for Sorraia Bridge.

For these optimal positions of the inclinometers, Figure 5.21-a shows the bridge deflection where an almost perfect agreement is observed. The rotation diagram presented in Figure 5.21-b exhibits also a good agreement, with slight deviations near the piers P1 and P2, which can be again explained by the higher variation of inertia of the deck in these zones. For sections S1, S4 and S7, the relative error, between the value predicted by the polynomial function and that by the numerical model is less than 2 %.

In what it concerns to Lezíria Bridge, the results of the parametric analysis are shown in Figure 5.22. The optimal position of the inclinometers 1 and 2 are at $L_1 = 0.15 \cdot L$ and $L_2 = 0.41 \cdot L$ for end spans, while for inner spans the best positions are at $L_1 = 0.11 \cdot L$ and $L_2 = 0.31 \cdot L$. For the three spans, the average errors are approximately 1.4 %, which all of them correspond to a local minimum, as it can be observed in Figure 5.22.

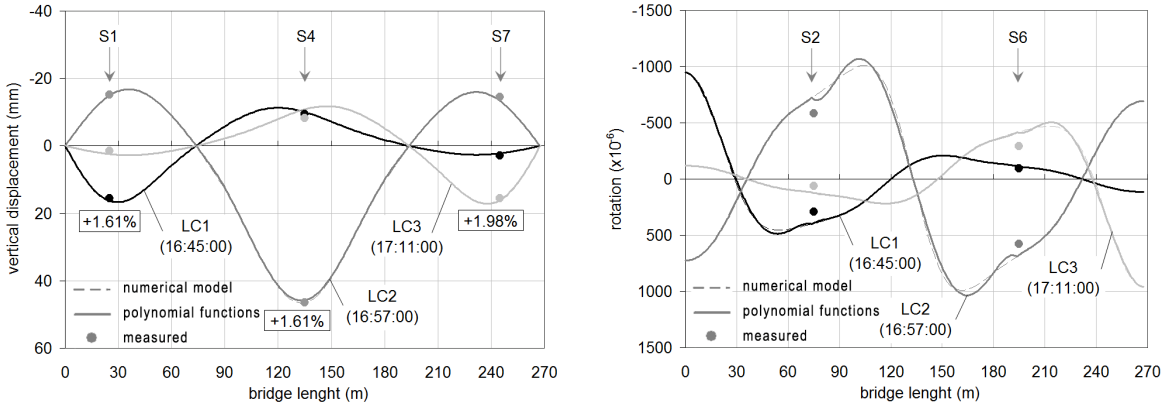

a) vertical displacement diagrams. **b) rotation diagrams.**

Figure 5.21 : Sorraia Bridge results for LC1, LC2 and LC3 (case 2).

Figure 5.23-a presents the solution obtained for the bridge deflection, considering these optimal positions for the inclinometers, and an almost perfect agreement is observed. The rotation diagram presented in Figure 5.23-b exhibits also a good agreement, with slight deviations near the piers P1 and P2, which can be again explained by the higher variation of inertia of the deck in these zones. For sections S1, S4 and S7, the relative error, between the value predicted by the polynomial function and that by the numerical model is less than 3 %, which reveals that this option is the one that leads to the best results.

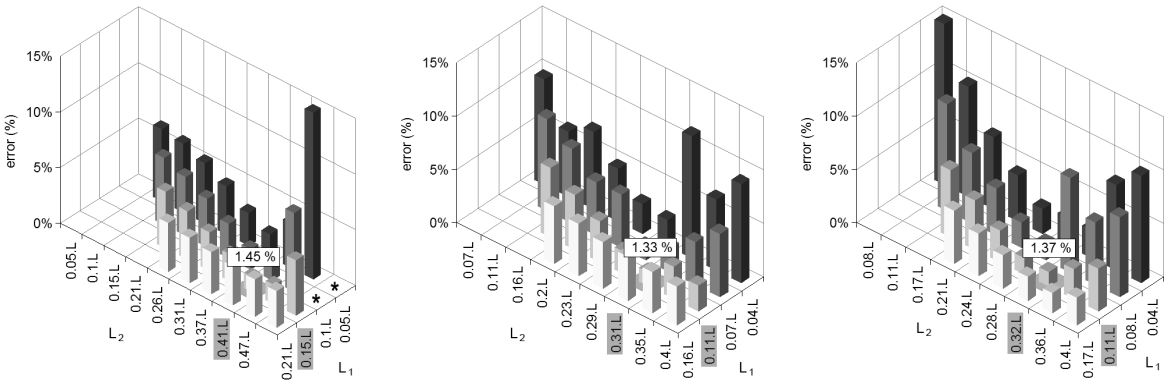

*** error > 15 %**

a) span 1. **b) span 2.** **c) span 3.**

Figure 5.22 : Results of the parametric analysis for Lezíria Bridge.

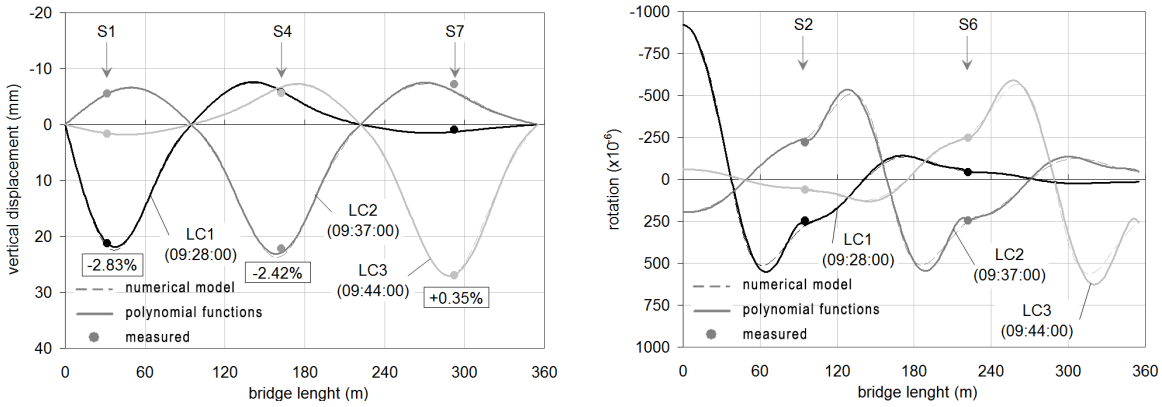

a) vertical displacement diagrams. **b) rotation diagrams.**

Figure 5.23 : Lezíria Bridge results for LC1, LC2 and LC3 (case 2).

The most relevant improvement with this option is the perfect agreement that is achieved for the bridge deflection calculated with the polynomial functions and the numerical results. Another relevant aspect is that if the results of both bridges are compared, the relative location of the movable inclinometers is practically the same for both bridges. Therefore, taking into account the results obtained in two different bridges, Figure 5.24 draws the optimal configuration for the inclinometers positioning, considering four inclinometers for end spans and six inclinometers for inner spans with the purpose of estimating the bridge deflection by the methodology herein exposed.

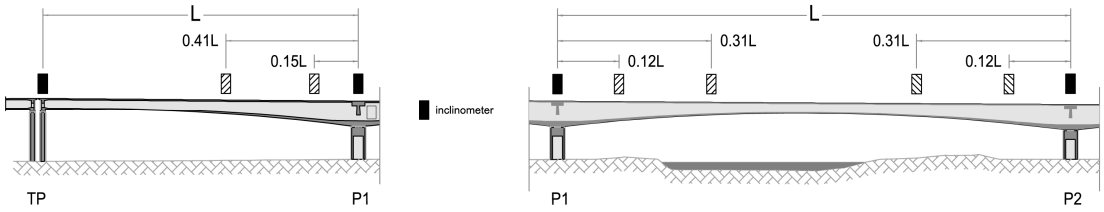

a) extreme spans. **b) inner spans.**

Figure 5.24 : Optimal positioning of the inclinometers to estimate the bridge deflection.

5.5. CONCLUSIONS

The present chapter focuses on the estimation of bridge deflection based on polynomial functions using strain and rotation measurements. The procedure to estimate the bridge deflection is presented and applied to a prestressed concrete beam and in two full-scale

bridges – Sorraia Bridge and Lezíria Bridge. The results are compared with measured values as well as the ones obtained with the corresponding numerical models. Some relevant conclusions can be drawn:

- The data processing is computationally heavy, namely if it is intended to handle long periods of observation. However, a numerical implementation, such as that made in an existing software, MENSUSMONITOR, revealed to be efficient and flexible in the data input/output. The time spent in the data handling was significantly shortened, when compared with traditional tools as spreadsheets. Besides that, it also has the advantage of making possible the real time visualization by connecting directly to the acquisition systems.
- The methodology was firstly applied to a simply supported prestressed beam, where two load cases were tested with satisfactory results. The maximum relative error was 4.9 %.
- Concerning the full-scale bridges, the spans with higher instrumented sections exhibit the best results with errors less than 4.5% in the mid-span sections. For both bridges, this corresponded to the span 2, with three sections instrumented with strain gauges and two sections instrumented with inclinometers. For the other two spans, it was observed that the knowledge of the curvature of the both end sections is essential for accurate results.
- The results obtained for spans 1 and 3, considering the curvatures above piers P1 and P2 extrapolated from the polynomial function determined for span 2, led to an improvement of the results quality with relative errors less than 4.5 % in the sections where the vertical displacement was measured.
- The bridge deflections calculated with the polynomial functions deviates slightly from that obtained with the numerical model. The main deviations occur at zones of the bridges near the support piers, because the aim of the instrumentation plans adopted was not the estimation of the deflection curves with the polynomial functions. Furthermore, the real bridge deflection is a rational type function instead of polynomial. Near the supports, the high variation of inertia can distrust the approximation with a polynomial function. However, in a global evaluation, the

deflections present a satisfactory agreement with the ones obtained with the numerical models.

- An alternative approach using rotation measurements only was numerically tested. A parametric study was performed, with several configurations that comprised four inclinometers in the end spans and six inclinometers in the inner spans. The optimal solution conducted to a maximum relative error less than 3 % and a perfect agreement was achieved between the bridge deflection calculated with the polynomial functions and the ones obtained by the numerical models.
- The results obtained for both bridges allowed the definition of the relative position of the inclinometers, regarding the estimation of the bridge deflection based on rotation measurements.

6. ASSESSMENT OF TRAFFIC LOAD EVENTS AND THEIR STRUCTURAL EFFECTS BASED ON STRAIN MEASUREMENTS

6.1. INTRODUCTION

Civil infrastructure projects are often large-scale investments undertaken to improve the quality of life for entire communities. Nonetheless, after the first investment it is necessary to accompany the life-cycle of these projects. In recent years, there has been an increasing interest in structural monitoring within the scientific and technical communities. Moreover, the development of Bridge Health Monitoring Systems (BHMS) and their application has become more frequent worldwide. Although initially attention was focused on sensor applications, recent concerns are shifting their emphasis to the practical implications regarding the acquisition, collection and processing of data (Van der Auweraer and Peeters 2003). Nowadays, it is possible to remotely monitor highly instrumented structures, with a high degree of automation. In fact, present solutions are sufficiently versatile to carry out remote surveillance tasks with moderate costs (Bergmeister and Santa 2001; Chang *et al.* 2009).

Depending on the equipment and the sensors selected, the current systems devoted to the monitoring of civil infrastructures, such as bridges, allow the reading of sample rates up to 1 kHz. Furthermore, although the monitoring systems deployed in bridges aim to help both the structural integrity assessment and the management and maintenance/repair operations of large groups of structures, they can also be used to characterize the crossing traffic, if designed for that intent as well. In fact, if the bridge is equipped with a suitable monitoring system and assuming a linear elastic behaviour under normal operation conditions, the system can act as a weighing device and therefore quantify traffic parameters. This concept is known as bridge weigh-in-motion, commonly identified with the acronym BWIM

(Karoumi *et al.* 2005). One of the first works related with the detection of traffic loads on bridges based on strain gauges measurements was presented by Moses (Moses 1979). The weight-in-motion analysis is an inverse-type problem where the structural response (bending moment for instance) is measured and the traffic load causing this moment is unknown. It has been shown that good correlation may be found between gross load and peak strains (Moses 1979; Liljencrantz *et al.* 2007; Liljencrantz and Karoumi 2009). This fact may contribute to a better knowledge of the effective traffic loads on bridges. Moreover, an approach that considers the traffic load and volume statistics for a specific bridge site provides a more accurate representation of the actual loading conditions and can be cost saving, namely by preventing unnecessary bridge rehabilitation and replacement (Getachew and Obrien 2006). Several technical and scientific publications have been made available for BWIM concerning railway bridges, either for metallic or concrete structures, but they do not have correspondence in road bridges. The following main reasons can be pointed out for this fact: (i) on railway lines the vehicles, hence the loads, travel along a well-defined path; (iii) railway vehicles have always two wheels per axle; (iii) and probably the most important, the rails of the track stand as excellent candidates to host instrumentation systems capable of providing reliable data. In this context, studies on road bridges, equipped with appropriate monitoring systems, emerge as crucial to explore the potential knowledge about the real traffic events that take place in these bridges and therefore, evaluate in more detail the effective structural safety when subjected to traffic loads.

In this chapter, a comprehensive study about the quantification of traffic loads and its structural effects in two road bridges – Lezíria Bridge and Pinhão Bridge – is reported.

Firstly, it is presented: (i) the structures, the monitoring systems implemented and the Finite element Models (FEM) specifically developed to calibrate and validate the measurements obtained by the monitoring systems; (ii) a probabilistic approach based on the Weibull distribution is proposed to describe the real traffic loads and extrapolate higher load levels, which was developed and implemented in a software devoted to the management, treatment and analysis of monitoring data – MENSUSMONITOR (Sousa *et al.* 2009b).

Afterwards, a detailed description of the selected sensors for this study is made. The main results are presented and discussed. Regarding the bridges lifetime, the characteristic load

levels achieved with the Weibull distribution are used to numerically evaluate the bridges response, and compare with the alarm levels established by the bridge designers with a discussion concerning the safety level. Finally, a comparative discussion is made focussing the different results achieved for both bridges, followed by the main conclusions. The work aims to contribute to a deeper knowledge and understanding of the effective traffic loads on road bridges, with emphasis on the development of intelligent systems for the efficient management and maintenance of these structures.

6.2. BRIDGES MONITORED WITH AUTOMATIC AND PROGRAMMABLE SYSTEMS

The following two road bridges support this study, namely: (a) Pinhão Bridge and (b) Lezíria Bridge (Figure 6.1 and Figure 6.2). These structures, built in Portugal, cross the two major rivers in Portugal namely, the River Douro and the River Tagus, respectively. It deserves to be highlighted that these bridges, built in different centuries, exhibit distinct structural solutions and traffic features. Remote and automatic monitoring systems were installed in these structures by LABEST-FEUP.

Figure 6.1 : Pinhão Bridge – landscape view of the vineyard region.

Figure 6.2 : Lezíria Bridge – sunset view.

6.2.1. PINHÃO BRIDGE

This structure, which crosses the River Douro in the DOC vineyard region where the famous Porto wine is produced, is a crucial infrastructure of the national road network, operated by Estradas de Portugal (E.P.), the Portuguese company responsible for the administration of the national road network. Pinhão Bridge comprises three main metallic spans, simply supported and 68.95 m long. A tragic collapse of an older bridge crossing the same river occurred in the year of 2001 (Jowell 2001). At the time, the authorities engaged a thorough inspection of the structure as well as a viability study that led to its strengthening and rehabilitation.

A sensing network with 32 strain gauges, 8 temperature sensors, 6 displacement transducers and 2 tiltmeters composes the permanent electric observation system installed in this bridge (Figure 6.3-a and Figure 6.3-b). Additionally, two acquisition units support the sensing network (Figure 6.3-c) with the ability of scanning the sensors' signal with a maximum frequency of 100 Hz, well suited for recording the structure dynamic response (Costa *et al.* 2009).

Pinhão Bridge was included in this study for two main reasons: (i) it was important to assess the conformity of the posted limits for speed and load; (ii) the bridge presents a single lane along its deck and therefore, its crossing is made alternately. Consequently, the design of the monitoring system was made in order to take advantage of the unique features of this bridge, focussing the traffic characterization.

(a) sensors installation. **(b) sensor SG-13B.** **(c) local observation station.**

Figure 6.3 : Monitoring system of Pinhão Bridge.

A numerical model was developed, based on finite element techniques, to appraise the bridge behaviour. The webs of the transversal and longitudinal I-beams were simulated by shell elements and the flanges modelled with bar elements, in order to capture simultaneously the torsion, shear and bending deformations. The concrete deck slab was also simulated with shell elements, and the medium plane was connected to the top of the beams grid with stiff bars to guarantee shear connection between them. All the remaining structure elements were modelled with bars, and a rigid joint behaviour was assumed for the connections, i.e. not allowing relative rotations between connecting bars at the nodes.

6.2.2. LEZÍRIA BRIDGE

Lezíria Bridge is located in the A10 motorway in Portugal. Its main structure has a total length of 970 m (Figure 6.2), with eight spans and seven piers supported by pilecaps over the riverbed. The spans length is 130 m except the end spans with 95 m, and two middle spans whose length differ in 3 m due to a change in a piers location that led to spans with 127 m and 133 m of length. The bridge deck is a box girder with variable inertia, with approximately 10 m of width and heights varying between 4 m and 8 m. The box girder core was segmentally built using a movable scaffolding system while the side cantilevers were subsequently constructed with specific movable scaffolding and metallic struts fixed on the bottom slab of the box girder. Four walls form the concrete piers with constant thickness and variable widths, which are supported by pilecaps (with 8 piles in general and 10 in the two pilecaps bounding the navigation channel).

The bridge has an integrated monitoring system devoted to the management and surveillance of the structure. Several cross sections are instrumented with embedded and external sensors. The installed sensors measure a set of quantities such as static, dynamic and durability parameters. For the present chapter, the 30 optical strain gauges (Figure 6.4-a), purposely developed for this bridge are the focus (Rodrigues *et al.* 2007a; Sousa *et al.* 2011b). They were installed in 15 cross sections along the bridge deck, from which seven of them are positioned near the support piers, and the remaining eight located at the middle of the spans. Two optical strain gauges were installed in each instrumented section (Figure 6.4-b). Each sensor was positioned in the bottom and upper box girder slab, respectively, aligned with the vertical symmetry axis of the section as well as with the longitudinal axis of the bridge. A local communication network allows the integration and centralization of the information recorded by the different Acquisition Nodes (AN) in a single location, called the Central Acquisition Node (CAN) (Figure 6.4-c). Lezíria Bridge is part of the motorway network operated by BRISA. It is, accordingly, included in BRISA's sophisticated communications network, covering the whole of its motorway system. A link established between the local communication network and BRISA's communication network enables the remote access to the bridge monitoring system (Sousa *et al.* 2011b).

The capability of the implemented monitoring system to acquire strain measurements at a high rate level, and consequently enabling the detection of traffic events, motivated its inclusion in the present study.

(a) optical strain gauge. **(b) cross section at mid-span.** **(c) acquisition node.**

Figure 6.4 : Monitoring system of Lezíria Bridge.

As in the case of Pinhão Bridge, a FEM was developed for Lezíria Bridge. Regarding the assessment and surveillance tasks, the FEM analysis was performed since the beginning of

construction, considering the effective chronological erection timetable as well as the real mechanical properties of the applied concrete and steel. A thorough scanning of the structure geometry was carried out supported in the final drawing plots, part of the bridge project. Considering the bridge length, a set of computational tools was developed to automate the scanning of the drawings and extract the relevant information for the input file that supports the numerical analysis (Sousa and Figueiras 2009b). The modelling approach is a two-dimensional model using beam elements to simulate the concrete elements of the bridge, which is a reasonable approach for the study of the global behaviour of the structure. The reinforcement steel and the prestressing cables embedded in the concrete were considered as reinforcement elements attached to the respective beam elements. These reinforcing elements have a stiffness contribution as well a restriction effect on the concrete deformations due to shrinkage and creep, which is important to consider for long-term analyses. The external prestressing cables were simulated with truss elements. Besides the mechanical properties, the time-dependent properties of concrete and steel are considered, namely the concrete hardening, shrinkage and creep of concrete as well as the prestressed steel relaxation.

6.2.3. DATA ANALYSIS TO EVALUATE THE EFFECTIVE TRAFFIC LOADS

The analysis of the collected time series of strain gauges, with high sampling rate, presented periodical strain peaks. Supported in a cross observation of the collected time series with video footages, these peaks have been correlated with traffic events. This fact enables that information about the effective live loads, due to traffic events, might be extracted from these time series, which can be useful to assess the real deformation level that the bridges are subjected. Therefore, a procedure is presented to characterize and quantify traffic loads on road bridges, taking into account specificities of their structural schemes, monitoring systems and traffic events. Afterwards, with these loads quantified, their structural effects can be studied supported by the numerical analysis.

6.3. CHARACTERIZATION OF TRAFFIC LOADS ON ROAD BRIDGES AND THEIR STRUCTURAL EFFECTS BASED ON SENSOR MEASUREMENTS

In order to characterize the traffic loads based on the time series collected by strain gauges, a set of main steps are sequentially followed. Starting from the sensor measurements to the desired traffic parameters, five main steps are considered, namely: (i) sensors selection and pre-treatment of the measurements; (ii) detection of local peaks in the time series; (iii) evaluation of speeds and travelling direction; (iv) estimation of loads correlated with the identified peaks; (v) probabilistic extrapolation of loads and assessment of their structural effects in the monitored bridges.

6.3.1. SENSORS SELECTION AND PRE-TREATMENT OF DATA

For the detection of traffic load events, it is required that sensors' readings must have a high correlation with this phenomenon. In other words, the local peaks of the sensors' readings must match up to traffic events with a high degree of correspondence. In general, strain measurements exhibit good properties due to their sensitivity to bending moments, and therefore, to the passage of vehicles. Several authors have used this type of measurements for detection of traffic events (Moses 1979; Liljencrantz *et al.* 2007; Liljencrantz and Karoumi 2009). Among all available sensors, a robust method for the selection of the best ones is using the influence line concept (Moses 1979; Liljencrantz *et al.* 2007; Liljencrantz and Karoumi 2009). Their response can be evaluated through a load test and/or through a FEM analysis. Higher amplitudes of the influence line denounce higher sensitivity for traffic load events. Moreover, the influence of the sensor's noise is reduced because its relative weight decreases when compared with the maximum value of the influence line. After checking all available sensors, two sensors are enough, in general, for the purpose.

However, before any calculations, the time series were pre-treated. In a first step, trends in the time series caused namely by environmental effects were removed. Afterwards, the time series were smoothened with a Savitzky-Golay modified filter. The particularity of

this modified filter is the capability of smoothing the stationary periods of the signal with negligible reduction of the peaks values (Savitzky 1964; Sousa 2006b).

6.3.2. RECOGNITION OF LOCAL PEAKS IN THE TRAFFIC EVENTS TIME SERIES

The identification of local peaks is performed by a threshold value, Y_0, which plays the role of lower threshold where all lower values are discarded. This procedure leads to a new time series with a set of time gaps, which allows, in a second step, the recognition of the local peaks by analysing the time difference between two consecutive measurements (Figure 6.5). In a straightforward manner, and considering two generic consecutive samples, if the elapsed time between both is not equal to the acquisition signal period (previously known), this means that a new local peak zone is found. While the elapsed time of two consecutive samples is equal to the acquisition signal period, the maximum value is searched and duly stored. At the end, the local peaks identified, and the corresponding instants of occurrence, are stored.

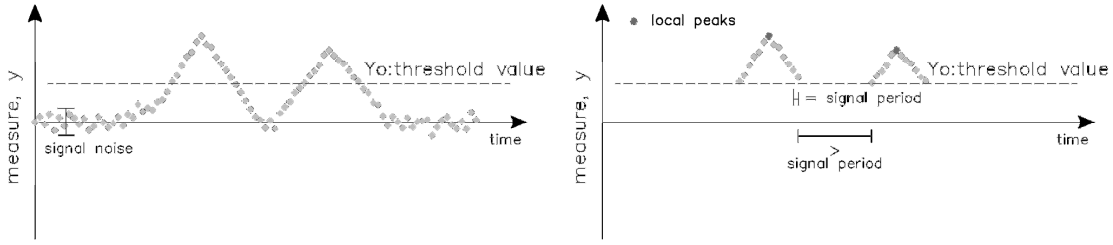

Figure 6.5 : Local peak values identification.

A careful inspection leads to the conclusion that the noise amplitude is the main criterion to fix the threshold value. The sensor accuracy, the cables length, the characteristics of the acquisition systems and the free vibration of the monitored structure can contribute for noise amplitude. These are the reasons why it is so important the measurements pre-treatment, in order to maximize the range of detectable local peaks, which, as aforementioned, is achieved with the reduction of the noise amplitude without significant decrease of the local peak values.

6.3.3. EVALUATION OF SPEED AND TRAVELLING DIRECTION

Considering the two sensor readings previously selected, if a traffic event occurs on the bridge, the ratio between the relative distance among sensors and the elapsed time between peaks might be considered an estimation of the average speed (Figure 6.6). However, some precautions must be taken into account, namely the relative distance between sensors. Firstly, it is desirable that the pairs of peaks are clearly visible when the two sensors readings are overlapped, as illustrated in Figure 6.6. Large distances between sensors compromise this objective and restrain the detection of traffic events. Secondly, the signal frequency influences the precision of the elapsed time between peaks, Δt, and consequently, the estimation of the average speed. For example, if a vehicle crosses a span with 70 m length at 50 km/h, it is required at least 50 samples, i.e. a reading frequency of 10 Hz to have an error less than 2 % for Δt.

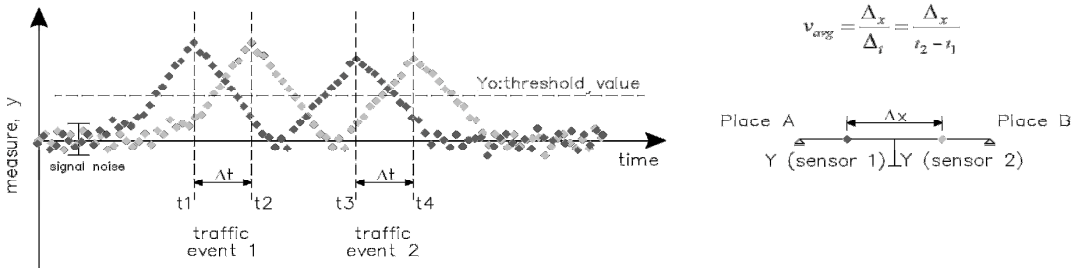

Figure 6.6 : Time gap identification between local extreme values of two sensors readings.

6.3.4. CALCULATION OF THE LOAD LEVEL

Studies concerning load models for bridge assessment carried out by Getachew and Obrien in (Getachew and Obrien 2007) and Cremona in (Cremona 2001) showed that the dominant heavy load trucks correspond to five-axle trucks. The trucks used for the load tests in both bridges, had three to five axles, which correspond to vehicles with lengths between 5 m to 12 m (Rodrigues *et al.* 2007b; Costa *et al.* 2008). These values are small if compared with the span length of Lezíria and Pinhão bridges (see sections *6.2.1* and *6.2.2*). Moreover, as it is presented later, the readings of the strain gauges exhibit one single peak for each detected traffic event, which proves that individual load axles are not traceable and consequently, a vehicle can be treated as a single load. Hence, the load level in

correspondence to a traffic event detected by a strain gauge can be achieved by Eq. (23), where P_i and $\varepsilon_{i,peak}$ are the estimated load and the measured strain peak at instant t, while k_0, k_1 and $k_2(t)$ are constants that depend on the problem specifications.

$$P_i(t) = k_2(t) \cdot k_1 \cdot k_0 \cdot \varepsilon_{i,peak}(t) \tag{23}$$

$$\begin{cases} k_0 = P_{ref} / \varepsilon_{ref} & (24) \\ k_1 = \varepsilon / \varepsilon_{ref} & (25) \\ k_2(t) = E_{c,ref} / E_c(t) & (26) \end{cases}$$

- **Sensitivity parameter – k_0**

Strain gauges measure an electric or optical signal. An accurate calibration must be made in order to correlate that signal with the deformation of the structural material. Normally, the sensors' manufacturer provides this information however, when a strain gauge is installed, uncertainties related with its alignment and position should not be disregarded in the calibration. These variations can have influence on the assessment of traffic load events based on the strain gauge measurements and consequently, a sensitivity parameter, k_0, was considered. The suitable way to get an accurate value for this sensitivity parameter is through a load test, in which the loads and their positioning are perfectly known. A direct correlation can be established between the strain gauge measurement and the load as expressed in Eq. (24). In order to attain higher confidence, the achieved values were validated by FEM analysis.

The loads applied during the load test are normally centred with the longitudinal axis of the bridge however, this is not the current case for operational conditions. Despite of this fact, the presented methodology focuses on long span bridges and for these cases, loads are mainly carried by bending and consequently, the torsion effects are normally negligible in the sensors' readings.

- **Load length correction – k_1**

For the load test, a specific number of trucks are positioned, with different configurations, in order to accurately evaluate the structural behaviour of the monitored bridges. Often, those configurations have a sequence of two, three or more trucks aligned one after the other. These configurations are not representative of the ordinary daily traffic loads, because they correspond to frequent or characteristic load combinations. In other words, most of the daily traffic loads are related with single passages. In this context, a correction must be made in order to consider the different load lengths used for the load test and the ordinary daily traffic. This correction can be made by using the referred influence lines of the strain gauges that were selected for this purpose. As expressed in Eq. (25), a coefficient k_1 is defined as the ratio between the strain produced by a point load of value 'Q' and the strain obtained with the same load 'Q', but in this case distributed along a specific length. Figure 6.7 illustrates an example of a load test with three trucks, where the strain magnitudes are calculated using the influence line.

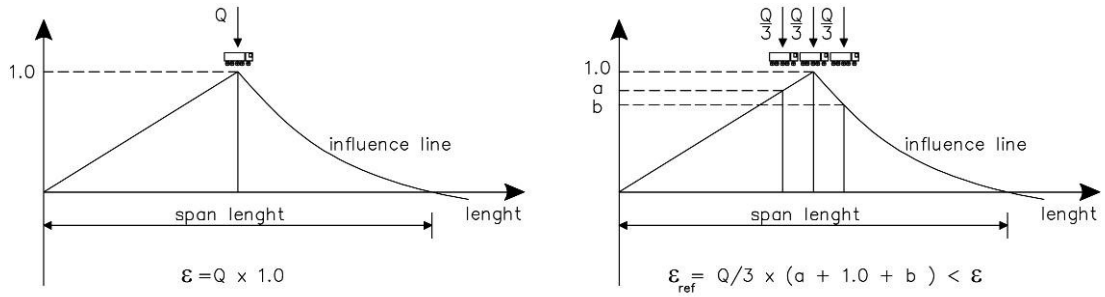

a) ordinary load traffic configuration. **b) load test configuration.**

Figure 6.7 : Load length correction supported by the influence line concept.

- **Modulus of elasticity correction – $k_2(t)$**

Concrete presents viscous-elastic behaviour and therefore, its modulus of elasticity increases with time. This means that, for the same load level, different deformations are expected for different ages. Bias can be mitigated, if a correction factor $k_2(t)$ is considered, expressing the ratio between the modulus of elasticity at the observation period, $E_c(t)$ and the modulus of elasticity at the age of the load test, $E_{c,ref}$, as expressed in Eq. (26).

6.3.5. PROBABILISTIC APPROACH AND EVALUATION OF THE STRUCTURAL EFFECTS

As aforementioned, all strain peaks, the calculated loads and the corresponding time of occurrence are stored in a matrix. However, matrices are not easily readable when hundreds of events are detected and consequently hundreds of rows are available for analysis. Therefore, the results are also presented in other formats namely, histograms and correlation graphs, which are in fact an easier output for reading and data consulting. Table 6.1 resumes the available graphical outputs in MENSUSMONITOR for results consulting and analysis.

Table 6.1 : Types of plots for the output results.

Description	X-axis	Y-axis	Information content
Load spectrum	Load	Frequency	Histograms with probability density function adjustment
Speed spectrum	Speed		
Traffic amount	Time	Frequency	Traffic evolution and intensity
Travelling direction	Time		
Load-speed correlation	Load	Speed	Load as a function of the speed with regression analysis
Load-travelling direction	Load	Travelling direction	Load level for each direction

Focussing on the spectrum histograms, they might be studied in more detail if probability density functions are used to fit data, which afterwards enables the extrapolation of higher values based on the fitted function. The speed spectrum histogram is fitted with the normal density function. As far as the load spectrum is concerned, the Weibull distribution is used. This function was chosen because the strains measurements are correlated with local extremes values, in which the cause for a specific peak is independent from the causes of the remaining peaks (Montgomery and Runger 2003). The Weibull distribution, as presented in Eq. (27), has high flexibility for data fitting through its two parameters β and δ. Analysing the probability density function, it can be perceived that when $\beta = 1$ the Weibull distribution matches the exponential distribution.

However, the methodology presented here can only detect strain peaks above the threshold value, Y_0, which means that only loads above x_0 can be detected. Consequently, the Weibull distribution is not representative for values below x_0 and therefore, values below

x_0 should be disregarded and the remaining area delimited by the function normalized, as presented in Eq. (28). Finally, a goodness-of-fit test procedure is performed, based on the chi-square distribution and the p-value to evaluate the null hypothesis H_0: the type of the load spectrum is a Weibull distribution (Melchers 1999; Montgomery and Runger 2003).

$$f(x) = \frac{\beta}{\delta} \cdot \left(\frac{x}{\delta}\right)^{\beta-1} \cdot e^{\left[-\left(\frac{x}{\delta}\right)^{\beta}\right]}, \quad x > 0\,;\, \delta > 0\,;\, \beta > 0 \tag{27}$$

$$\bar{f}(x) = \begin{cases} 0 & x \le x_0 \\ \dfrac{f(x)}{\int_{x_0}^{+\infty} f(x)dx} & x > x_0 \end{cases} \tag{28}$$

Based on the fitted Weibull distribution, different values, x, might be seen as the values to be exceeded with a probability α along a period τ in agreement with Eq. (29), with the value τ representing the observation period (Melchers 1999). This information can be very useful to build graphics with different traffic load events in correspondence to different return periods, with the main benefit of being based on real traffic loads.

$$R_p(x) = \frac{\tau}{\alpha} \quad , \quad \begin{cases} \tau - observation\ period \\ \\ \alpha = 1 - F(x) \end{cases} \tag{29}$$

However, characteristic values in correspondence with the structure lifetime are required, in order to be comparable with the design values, which can be extracted with Eq. (30). The characteristic value in correspondence to the upper quantile 0.05 is normally used for design purposes.

$$R_p = -\frac{T_{lifetime}}{\ln(1-\alpha)} \quad , \quad \alpha = 0.05 \tag{30}$$

Bridges are expected to exhibit an elastic behaviour along their lifetime, even though when subjected to extreme traffic load events. Therefore, the permanent loads and the characteristic load of a traffic event, previously calculated, are considered in the characteristic combination, according with the Eurocode 0 (Standardization European Committee 2002). Focussing the structure lifetime, this combined effect is afterwards used to evaluate the bridge response based on FEM analysis. Finally, the gathered results can be compared with the limit values established by the bridge designer, in order to evaluate the effective safety level of the bridge.

Finally, due to the difficulty in handling large databases in a single loop, such as in the present case, the previous first four steps (sections *6.3.1* to *6.3.4*) were repeated in a while loop, where each loop handles a smaller database in order to extract the desired information. The procedure herein described was fully implemented in MENSUSMONITOR software, taking advantage of its features namely, real time acquisition, database storing/querying and filtering data, which are fundamental for a flexible and efficient handling of data for this type of calculations. Figure 6.8 shows the front panel with the "*mensus traffic*" tool active (see Table 3.4). More details about this software can be found elsewhere (Sousa *et al.* 2009b).

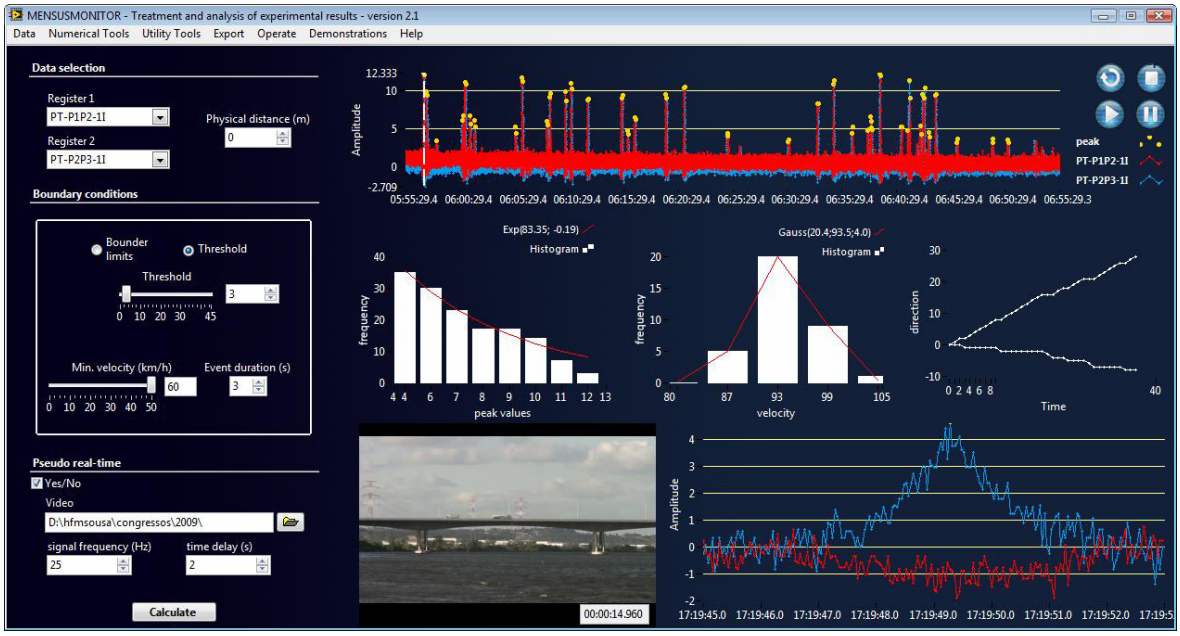

Figure 6.8 : Front panel of MENSUSMONITOR with the "*mensus traffic*" tool active.

6.4. RESULTS

6.4.1. PINHÃO BRIDGE

- **Observation procedures**

Three strain gauges were selected to support this study. The first sensor, labelled as "SG-13B", is located in the bottom flange of the mid-span transverse beam of the north span, in the section P1E1 (Figure 6.9). This gauge was selected taking into account the rehabilitation project, which revealed that the transverse beams are the most critical structural elements. Using the data collected by this gauge, and having as reference values the ones obtained during the load test, an equivalent load spectrum of moving vehicles was generated. This information was used for real traffic data by comparing the shape of the influence line for a single testing truck with the one gauged for each sensed vehicle. The factor that allowed this conversion was set based on results provided by the calibrated FEM, which allowed evaluating the loading length to the strain evolution for different vehicles carrying the same load. On the other hand, sensor "SG-13B" exhibits the highest sensitivity for the same traffic load event. The other two sensors, labelled as "SG-1B" and "SG-5B", are installed in the upstream lower chords of the trusses in the middle of the south and central spans, respectively (Figure 6.9). Readings from these gauges were used to estimate the vehicles average speed. During the 24 hours of the day September 14, 2008, the strain gauges were continuously interrogated with a sampling rate of 10 Hz.

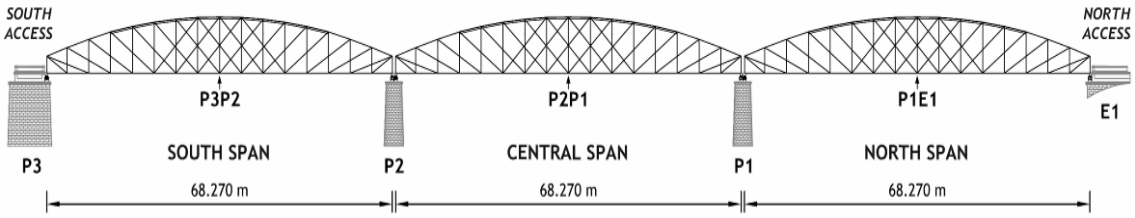

a) bridge elevation and location of the instrumented sections.

Figure 6.9 : Instrumentation plan of the Pinhão Bridge.

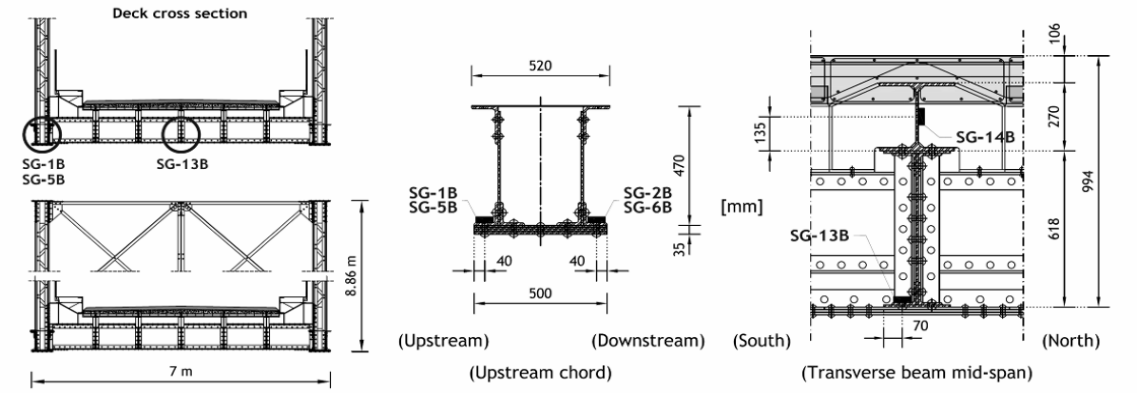

b) sensors' location in the mid-span cross sections.

Figure 6.9 : Instrumentation plan of the Pinhão Bridge. (cont.)

- **Traffic events detection**

The searching for local peaks is performed for small observation periods, which are defined as a fraction of the observation period. The observation period of 24 h was split into subsets of 1 h each. Hence, temperature effects could be removed from the sensors' readings with the subtraction of a linear trend function, which is acceptable for a time window of one hour.

Figure 6.10 presents the result for a period of approximately 50 minutes, highlighting the detected local peaks (black circles). The threshold value, Y_0 (Figure 6.5), was set to 4 με, taking into account the noise amplitude of the sensors' reading. This value is considerably low regarding the precision of the strain gauges, which is 1 με.

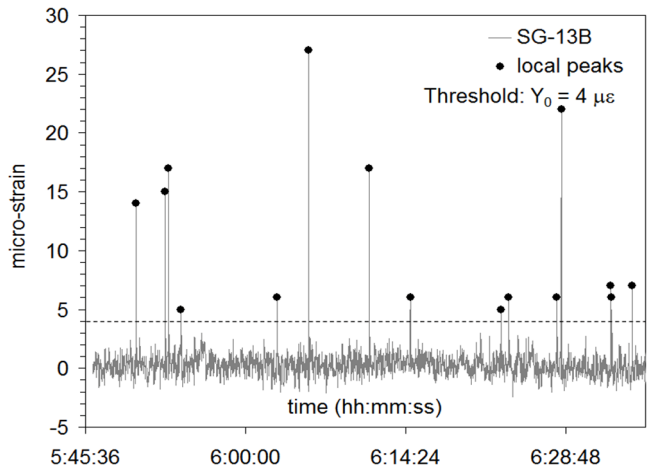

Figure 6.10 : Time series of the strain gauge "SG-13B".

- **Speed and travelling direction**

According to the procedure presented in Figure 6.6, Figure 6.11 shows the speed spectrum and a normal distribution fitting. The average speed is 37 km/h and the standard deviation is 4 km/h. The obtained average value is in accordance with the speed limit established for the heavy traffic in Portugal – 50 km/h in national roads. Moreover, based on these results, the suspicions raised during the rehabilitation project of heavy vehicles exceeding the speed limit were not confirmed.

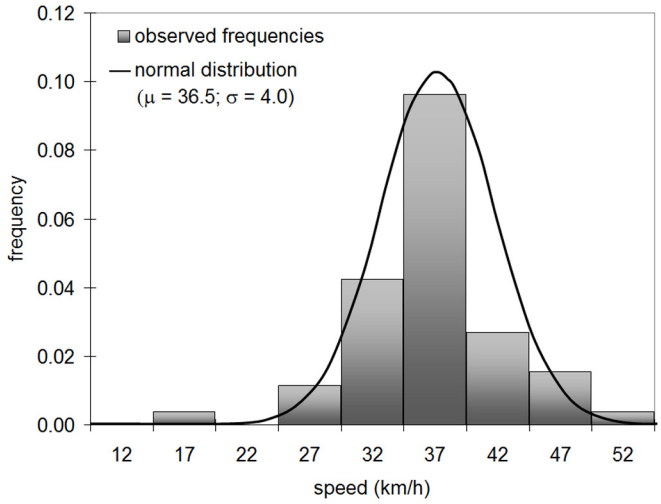

Figure 6.11 : Speed spectrum and normal distribution fitting – Pinhão Bridge.

Although the speed results presented in Figure 6.11 are naturally positive, the output results from the calculation procedures have positive or negative, depending the signal of Δt (Figure 6.6). Taking advantage of this fact, the counting of traffic events in each direction becomes possible. In the case of Pinhão Bridge, the travel directions were defined as North-to-South and South-to-North (Figure 6.9). Figure 6.12 presents the results for traffic load events above 9.5 tons, which denounces a clear trend towards the north-to-south direction, in a relation of four traffic events for each one travelling in the opposite direction. In this case, during the night period no traffic events were detected for loads above 9.5 tons.

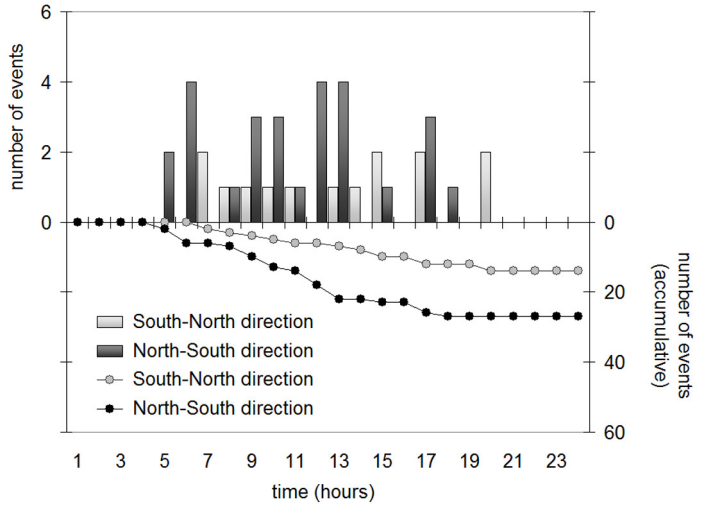

Figure 6.12 : Histogram of travelling directions (loads above 9.5 tons) – Pinhão Bridge.

- **Load spectrum**

Pinhão Bridge has a single lane along its deck, which means that the traffic loads are approximately centred with the longitudinal axis of the bridge and therefore, torsion effects are negligible. In this context, the sensitivity parameter, k_0, was set to 0.48 tons/με for the strain gauge "SG-13B (P1E1)" (Figure 6.9). This value was provided from the load tests performed after the rehabilitation and it was confirmed by the FEM analysis (Costa *et al.* 2008).

The influence of the trucks' length used in the load tests was considered with a value for k_1 equal to 1.23. Taking into account Eq. (23) and the value fixed for the threshold value Y_0 (Figure 6.10), traffic events loading more than 2 tons were detected. This load level suggests that the traffic events identified are related to medium to heavy vehicles, i.e. trucks.

The frequency of the detected traffic events were grouped in six load classes as presented in Figure 6.13. The histogram has an exponential form, which means that the main traffic in Pinhão Bridge is due to traffic events with loads less than 8.25 tons. It is also worth mentioning the fact that the load limit of 30 tons, established for the heavy vehicles was never surpassed.

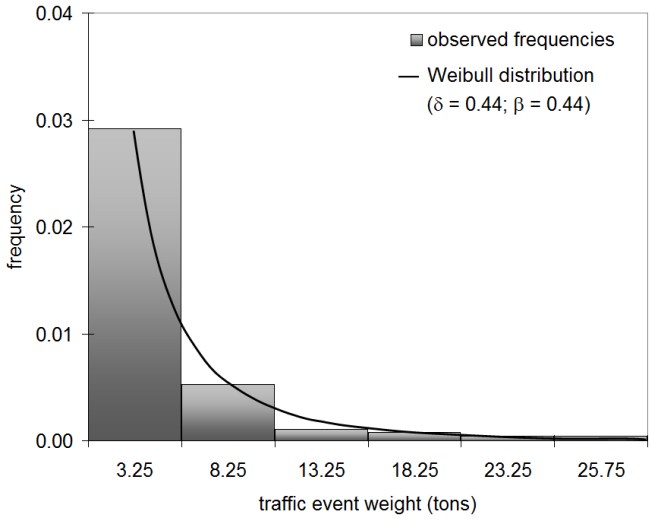

Figure 6.13 : Load spectrum – Pinhão Bridge.

- **Probabilistic analysis and evaluation of structural effects**

The frequencies of the load spectrum were adjusted with the Weibull distribution (Eq.(28)) and the result is plotted in Figure 6.13, overlapped with the results obtained for the load classes frequency. The p-value obtained for this adjustment was 0.37, which means that the null hypothesis "H_0: the form of the load distribution is Weibull" cannot be rejected for a significance level of 0.37. In other words, it means that there is a 37 % probability that any deviation from expected is due to chance only, which is statistically acceptable. Higher load levels were extrapolated with the fitted Weibull distribution, in order to estimate the characteristic value of traffic load events focussing the structure lifetime of 30 years, which was the design assumption for the bridge rehabilitation. Based on the FEM analysis, this characteristic load and the permanent loads were simultaneously considered to evaluate the bridge response for a period matching the bridge lifetime.

Among other parameters, the vertical displacement parameter is commonly used by the bridge designers to establish alarm levels. This parameter offers an overview about the structure behaviour, where its magnitude is easily correlated with the deformation level. Therefore, the first line of Table 6.2 presents the vertical displacement obtained for section P1E1 (Figure 6.9) for an observation period of one day, the characteristic load, and the safety level, established as the ratio between the project design value and the predicted value with the methodology.

Table 6.2 : Results of section P1E1 for a lifetime of 30 years.

Return period	Characteristic load (tons)	Vertical displacement (mm)		Safety level
		Project	Predicted	
1 day	158	48.7*	64.0	0.76
7 days	110		55.1	0.88
28 days	82		49.7	0.98
365 days	42		42.2	1.15

* Value determined for the characteristic combination of actions, with a limit of L/1200.

As it can be observed, the safety level achieved for Pinhão Bridge is clearly lower than one. However, this study was based on measurements collected during the vintage season, for which the heavy daily traffic experiences an increase, both in intensity and load magnitude. This means that the collected data during the 24 hours of observation is characteristic of the daily average traffic of the vintage month, and therefore, the possibility of the return period, related to the observation period, might be greater than one day is plausible. For example, if the observation period corresponds in fact to a return period of 28 days, which might be justified by the vintage month, the safety level almost reach the unit value. Consequently, the estimated safety values might be too conservative. In agreement with Table 6.2, Figure 6.14 plots different curves regarding the characteristic loads for traffic events, considering that the collected data has a return period superior to one day, namely one week, one month and one year. The differences are large, which means that further studies are required, with wider observation periods in order to accurate the safety level. Even so, it is possible to conclude for the safety of the structure.

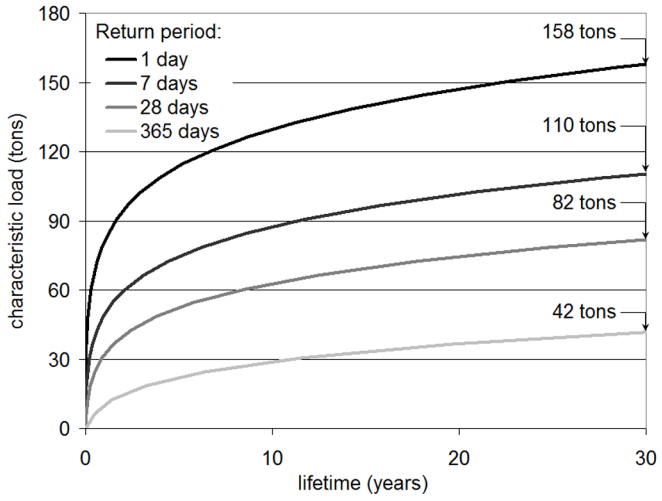

Figure 6.14 : Characteristic traffic load events for different return periods – Pinhão Bridge.

6.4.2. LEZÍRIA BRIDGE

- **Observation procedures**

From all instrumented sections, two mid-span sections were selected. Figure 6.15 shows the location of these two cross sections, labelled as P1P2 and P2P3. These two cross sections have optical strain gauge (SG) installed at the bottom slab of the box girder, labelled as "SG-3B", which are aligned with the vertical symmetry axis of the cross section. Similar to the procedure adopted for Pinhão Bridge, during the 24 hours of the day May 14, 2009, strain gauges were continuously interrogated with a sampling rate of 50 Hz.

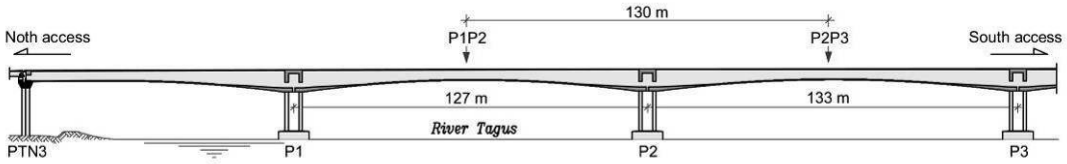

a) Bridge elevation and location of the instrumented sections.

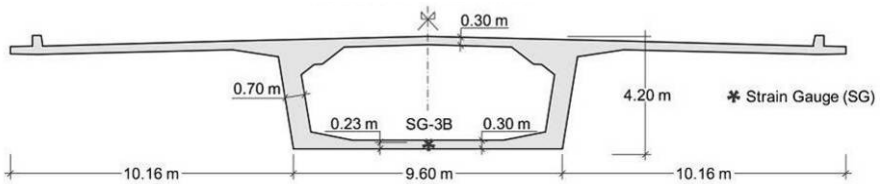

b) Sensor location in the mid-span cross section.

Figure 6.15 : Instrumentation plan of Lezíria Bridge.

- **Traffic events detection**

Similar to the procedure adopted for Pinhão Bridge, the observation period of 24 h was split into subsets of 1 h each. Figure 6.16 presents the data of a small period, approximately 6 minutes, highlighting the local peaks detected. The threshold value, Y_0 (Figure 6.5), was set to 3 με, which is a sufficiently low value, regarding the precision of the strain gauge, which is 1 με.

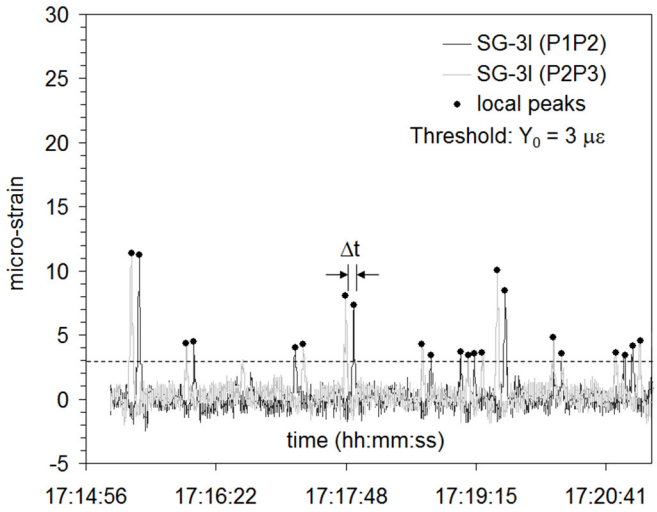

Figure 6.16 : Time series of the strain gauges "SG-3I" (P1P2) and "SG-3I" (P2P3).

- **Speed and travelling directions**

Pairs of local peaks, elapsed by Δt, are clearly identified in Figure 6.16. Following the procedure presented in Figure 6.6, Figure 6.17 presents the speed spectrum as well as a normal distribution fitting. The average speed was found to be 85 km/h and the standard deviation of 5 km/h. The obtained average value is in accordance with the speed limit established for the heavy traffic in the Portuguese motorway roads, whose value is 90 km/h.

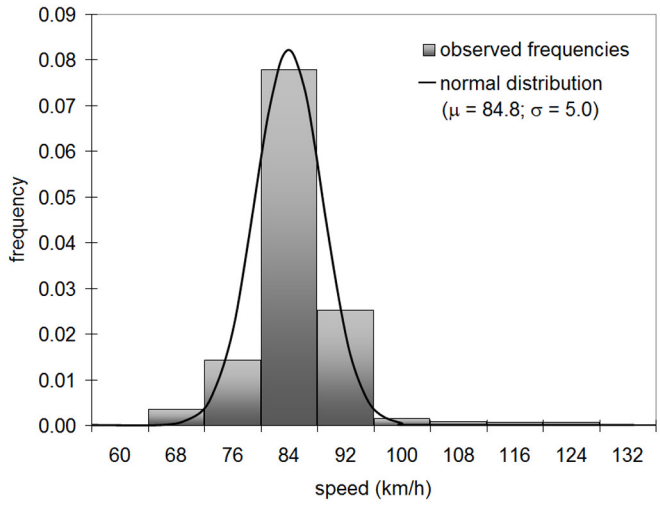

Figure 6.17 : Speed spectrum and normal distribution fitting – Lezíria Bridge.

Travel directions were defined as North-to-South and South-to-North (Figure 6.15). Figure 6.18 presents the counting of traffic events detected in each direction. It is shown that heavy traffic heading south is the most predominant, where 13 of the 24 observed hours reveal a higher intensive traffic in that direction. Only 7 hours of the recorded period present a more intense traffic in the north direction, mainly occurring during the afternoon between 5 h p.m. and 9 h p.m.. The representation of the accumulated traffic events confirms the predominance of the traffic heading south. It is also concluded that heavy traffic intensity diminishes significantly during the night (between 9 and 3 h a.m.).

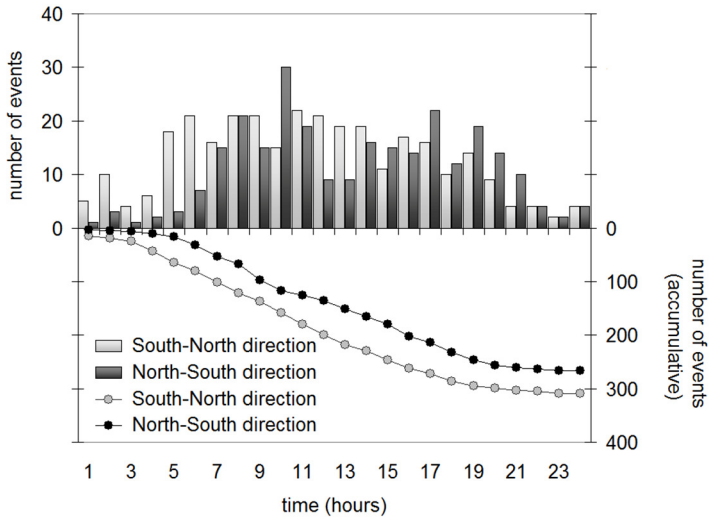

Figure 6.18 : Histogram of travelling directions – Lezíria Bridge.

- **Load spectrum**

The positioning of the optical strain gauges at the vertical symmetry axis of the cross section (Figure 6.15) and the outsized span length justify neglecting torsion effects. The sensitivity parameter, k_0, was set to 7.4 tons/με and 9.2 tons/με for strain gauges "SG-3I (P1P2)" and "SG-3I (P2P3)", respectively (Figure 6.15). These values were established based on the load tests performed during the construction (Rodrigues *et al.* 2007b), and validated by FEM analysis (Sousa and Figueiras 2010). The influence of the trucks length used in the load tests was considered with a value of 1.26 for k_1. As far as the modulus of elasticity correction is concerned, the parameter k_2 was set to 0.96, by taking the effective properties of the concrete used in the bridge construction (TACE 2007). Regarding Eq.

(23) and the value fixed for the threshold Y_0 (Figure 6.16), traffic events loading more than 18 tons were detected. These load levels suggest that the identified traffic events are related with heavy vehicles, i.e. trucks.

The detected traffic load events were grouped into six load classes as presented in Figure 6.19. In contrary with what it was observed for Pinhão Bridge, the first class exhibits a minor frequency when compared to the following two classes. This means that a larger spectrum of dominant traffic events exists for the Lezíria Bridge case, which ranges namely between 24 tons and 78 tons load classes. Events above 100 tons were also detected, perhaps related to the crossing of two or more heavy trucks simultaneously or, special transportations which is an ordinary event for motorway roads.

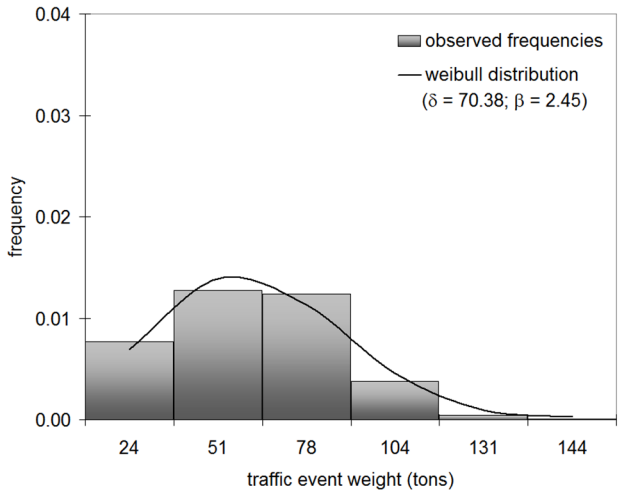

Figure 6.19 : Load spectrum – Lezíria Bridge.

- **Probabilistic analysis and evaluation of structural effects**

The load spectrum in Figure 6.19 was fitted with the Weibull distribution (Eq.(28)). The p-value achieved for this fit was 0.01. Although the adjustment achieved is not as confident as the one obtained for Pinhão Bridge, the fitting result exhibits an acceptable agreement with the observed data and therefore, it is assumed that the Weibull distribution describes the traffic load events spectrum. Based on this fitting result and focussing the structure lifetime of 100 years, higher load levels were extrapolated, namely to calculate characteristic values. Considering this characteristic load and the permanent loads for a

period equal to the structure lifetime, the bridge behaviour was numerically evaluated. Similar to Table 6.2, the first line of Table 6.3 presents the vertical displacements achieved for section P2P3 (Figure 6.15) related to the observation period of one day.

Table 6.3 : Results of section P2P3 for a lifetime of 100 years.

Return period	Characteristic load (tons)	Vertical displacement (mm)		Safety level
		Project	Predicted	
1 day	211	55*	44.8	1.23
7 days	198		43.9	1.25
28 days	188		43.1	1.27
365 days	166		41.7	1.32

* Value determined for the characteristic combination of actions, with a limit of L/1200.

The results show that Lezíria Bridge exhibits a safety level of 1.23, which indicates a safe response even when subjected to extreme traffic load events. Even though the representativeness of the observation period of one day might be questionable (p-value of 0.01), the bridge safety is clearly guaranteed. Similar to what it was done for Pinhão Bridge, Figure 6.20 plots different curves regarding the characteristic loads, considering the possibility of the load spectrum, plotted in Figure 6.19, might be representative of observation periods superior to one day. In this case, the load variability is not as pronounced as it is for the Pinhão Bridge case. Table 6.3 resumes the results obtained for the different return periods. For all scenarios, the bridge safety is not compromised.

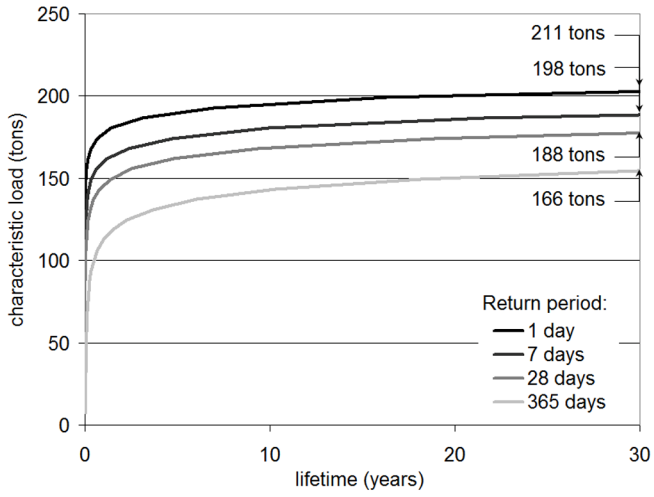

Figure 6.20 : Characteristic traffic load events for different return periods – Lezíria Bridge.

6.5. RESULTS COMPARISON AND DISCUSSION

If the extrapolated characteristic loads obtained for both bridges are confronted, it might be concluded that they are less variable for Lezíria Bridge. In fact, the load spectra results can explain these differences. While the load spectrum of Lezíria Bridge is broadened with a wider range of loads, approximately with the same significant contribution (Figure 6.19), the one obtained for Pinhão Bridge has a clear exponential form (Figure 6.13). To explain this fact two main reasons can be pointed out: Firstly, smaller loads are measured in Pinhão Bridge (a minimum of 2 ton against the 18 ton of Lezíria Bridge), which lead to a high frequency in the first classes of the spectrum. Secondly, the more exceptionally heavy traffic events are registered during the observation period, more elongated is the right side of the load spectrum and consequently, the end-right tail of the fitted Weibull distribution becomes also more elongated. These two facts together reinforce the exponential form obtained for Pinhão Bridge. In fact, as aforementioned, the observation period used for this bridge is concurrent with the vintage season, which means that a higher number of heavy vehicles had crossed the bridge when compared with the daily average of the year, which justifies the exponential form.

As far the safety level is concerned, Lezíria Bridge may be clearly rated as a safe structure, while for Pinhão Bridge the conclusion is not so straightforward. As referred, the data from Pinhão Bridge was collected during the vintage season, for which the heavy traffic experiences an increase and consequently, the computed characteristic loads are overestimated. Larger observation periods might resolve this problem, however, this was not possible yet. Hence, it is advised, if not mandatory, further studies with higher observation periods to evaluate with more accuracy the safety level.

Furthermore, the different construction ages, the applied materials and the traffic requirements might also contribute to explain the different results obtained. It is comprehensible that a centenary structure as Pinhão Bridge does not exhibit the same performance to traffic loads as the new Lezíria Bridge. In other words, it means that different periods have to be considered for the expected lifetime of both bridges, which is in fact considered, and consequently more frequent checking procedures are required for Pinhão Bridge as it was previously expected and the results herein presented have demonstrated.

6.6. CONCLUSIONS

The present chapter focuses the assessment of traffic loads based on strain measurements and their structural effects on road bridges. Based on the results herein achieved, some relevant conclusions could be drawn:

- In order to extract information related to traffic parameters, the data processing is computationally time-consuming, namely if large periods of observation are analysed. The implementation of automatic procedures for data processing in dedicated software, such as MENSUSMONITOR with direct access to the measurements' database, revealed to be efficient, time saving and flexible.
- The influence line concept is an accurate strategy to optimize the selection of the best sensors. In particular, measurements of strain gauges showed a high correlation with traffic events.
- The pre-treatment of sensors' readings is of utter importance. Environmental effects must be removed, and the strategy of considering smaller observation windows of one hour each revealed to be efficient, because linear trend offset is generally sufficient to remove those environmental effects, namely the temperature variation.
- In order to get an accurate estimation of the traffic loads based on the identified strain peaks, it is important to have a field calibration through a load test, taking into account the load length used in the test and the viscous-elastic behaviour of concrete.
- The major difference between the results obtained for both bridges is the magnitude of the detected traffic load events, which is mainly justified by the different values obtained for the sensitivity parameter, k_0. In other words, for the same load the strain sensitivity of Pinhão Bridge is higher than the one of Lezíria Bridge, which is in accordance with the expectations given the different structural typologies and design requirements for each case. In fact, the results demonstrate the ability of instrumented metallic structures to sense smaller loads, which are more sensible to local effects and prone to experience higher deformations for the same load level.
- The type and the load level related with the heavy traffic detected for both bridges are clearly different. While for Pinhão Bridge no more than five load events loading more than 25 tons were detected, that number is much higher for Lezíria Bridge with a ratio of 1 to 10 between them. The fact that one is inserted in a national road with only one

traffic lane while the other has 6 lanes of traffic (3 for each direction) and is located in a motorway justify the referred differences.

- The obtained load spectra reveal that for the Pinhão Bridge case the diagram has an exponential shape, while for the Lezíria Bridge case it was observed a minor frequency for the first class, when compared to the following two classes. This means that while for Pinhão Bridge the heavy traffic is due to load events less than 8.25 tons, for Lezíria Bridge a larger spectrum of dominant traffic events is observed which ranges between 24 tons and 78 tons. The greater flexibility of Pinhão Bridge and the insertion of Lezíria Bridge in a motorway explain these results.
- The fitting process for the load spectra with the Weibull density function shows good agreement, revealing a better performance for Pinhão Bridge with a p-value of 0.37.
- Regarding the structures lifetime, the expected loads for traffic events, based on the Weibull distribution, do not endanger the safety level of Lezíria Bridge, whereas the structural response of Pinhão Bridge at the end of its renewed lifetime the conclusions are not so straightforward. However, it must be taken into account that the used data for Pinhão Bridge was collected during a period for which the traffic has a considerable increase (vintage season) and therefore, the estimated extreme loads may be overestimated and the safety level under evaluated. In spite of that, if the obtained load spectrum is taken as representative of the entire vintage month, then the safety level reaches almost the unit.
- Due to the impossibility of having larger observation periods until the present date, and the observation period of Pinhão Bridge matched with the vintage season, as well as the low value of the p-value for Lezíria Bridge, it is recommended the collection of larger observation periods.
- The obtained results can be useful for structural safety analysis and not for vehicles identification purposes. Strain inducing load events are detected – events which led to measurable responses of the structure – and therefore, do not enable vehicles counting.
- Finally, the obtained results show potential for decision processes related with the management and surveillance of road bridges, namely in the adoption of restrictive actions to the traffic, viability studies and/or rehabilitation of structures.

7. MODELLING OF THE CONSTRUCTION AND LONG-TERM BEHAVIOUR OF A CONCRETE VIADUCT BUILT WITH A MOVABLE SCAFFOLDING SYSTEM

7.1. INTRODUCTION

The long-term assessment of large civil infrastructures such as prestressed concrete bridges is a challenging task. One of the most common and reliable strategies is the use of Finite Element Models (FEM). Based on information concerning the geometry and materials properties, the structural behaviour can be uniquely interpreted. Despite of the short-term behaviour, load tests for example, can be interpreted with FEM analysis with good accuracy, the long-term prediction of these large structures is not so straightforward. The new bridge designs, the materials evolution and the advances in the constructive methods employed in the civil engineering domain are aspects with direct influence in the long-term response. Therefore, and in addition to the geometric and materials properties, all other aspects with significance in the bridge behaviour must be taken into account in the analysis strategies in order to get predictions more reliable and reduce deviations. The real time history related to the phased construction, the influence of the adopted constructive method, the characterization of the employed concrete and the environmental conditions are some of those most relevant aspects.

As regard the constructive methods, one of the most commonly used in the construction of cast in situ concrete bridges, in Portugal, is the movable scaffolding system. A travelling steel structure, which supports the formwork that gives shape to the bridge, is the basis of this system. It is frequently applied to multi-span bridges over difficult terrain or water, where the launching girder moves forward span-by-span, supported on the piers. The application of this system is profitable for long bridges with spans ranging between 30 m to 55 m and a high degree of replication. The movable scaffolding is supported on the

bridge piers and therefore, an interaction between the girder and the bridge exists, which can lead to higher deformation and stress levels than the ones that will be installed during the service life. This is why the bridge behaviour during this transitional period must be controlled. Measurements obtained since early ages with appropriate sensors would be desirable to get a more comprehensive knowledge of the real behaviour of bridges constructed with these systems. However, databases with this type of information are scarce.

As far as the concrete properties are concerned, several studies show that long-term predictions differ significantly from the observed response, mainly due to the evaluation of shrinkage and creep at the design stage (Robertson 2005; Goel *et al.* 2007; Santos 2007).

Besides the rheological effects of concrete, the variability concerning the environmental conditions, namely the humidity and temperature, are also critical for an accurate evaluation of the effective long-term response (Roberts-Wollman *et al.* 2002; Li *et al.* 2004; Catbas *et al.* 2008).

Data from long-term monitoring systems have been supporting the aforementioned studies, which demonstrate the importance of these systems to improve the knowledge concerning the effective structural behaviour. Initially, these measurements were provided to detect in advance any possible risk factor during the construction of the bridge, and thus prevent any resulting accident (Chang *et al.* 2009). With the technology evolution, the monitoring systems have become more and more powerful, offering information on structural integrity, durability and reliability, and ensuring optimal maintenance planning and safe bridge operations (Ko and Ni 2005). In fact, monitoring data have been contributing to validate the design assumptions, to calibrate the structural models, and to update the safety coefficients.

The recent construction of a major bridge in Portugal, Lezíria Bridge, comprises a 1 700 m viaduct erected using a movable scaffolding system, which offered the opportunity to observe its long-term behaviour and compare with that obtained with a numerical model. The measurements were collected by a permanent monitoring system, installed in the bridge since the beginning of the construction, devoted to the bridge surveillance and maintenance (Sousa *et al.* 2011b).

This chapter presents the FEM implemented to the prediction of the long-term response of the viaduct, which was calibrated with measurements obtained during the construction phase and the load test. The effective mechanical and time-delay properties of concrete and

prestressing steel were considered, as well as the effective prestress forces and the real construction sequence. A full discussion concerning the real long-term behaviour is made, focussing the differences between the measurements and the results obtained with the FEM, namely the trends due to shrinkage and creep and the variations due to the temperature. Finally, concerning to the viaduct lifetime, the predicted values for the measured parameters are reviewed, since the predictions based on the European standard rules present significant bias to be used as reference values regarding the viaduct surveillance.

7.2. THE CONCRETE VIADUCT

The 11 670 m total length of Lezíria Bridge is materialized by three substructures: (i) the north approach viaduct 1 700 m long; (ii) the main bridge substructure, crossing the River Tagus, with a total length of 970 m; (iii) and the south approach viaduct, with a total length of 9 160 m (Figure 7.1). From the three substructures, the north approach consist of three elementary viaducts, V1N, V2N and V3N, with current spans of 33 m of length, except at the railway crossing in which the largest span is 65 m long and is partially formed by a box girder. The deck has a total width of 29.95 m, where 2 × 1.15 m is sidewalk technical paths. The expansion joints are approximately 560 m spaced to limit the deck expansion and control the maximum deformations imposed to the vertical elements (COBA-PC&A-CIVILSER-ARCADIS 2005a).

Figure 7.1 : Lezíria Bridge – construction stage at May 2007 (© TACE).

The viaduct deck is generally supported by four alignments of circular piers-pile with 1.5 m of diameter and lengths that can reach 40 m deep (Figure 7.2-a). The constructive process adopted for the viaducts' construction was based on a self-sustaining movable scaffolding supported on the piers. In a straightforward description, this movable structure was recurrently mounted and dismounted. After positioning, works related with reinforcement arrangement, metallic sheaths and anchorage systems installation were performed. Then, the span construction was followed by the concrete pouring. Finally, the prestressing cables were tensioned and the movable scaffolding was moved to the next span (Figure 7.2-b and c). The viaduct construction was finished with the concreting of the service sidewalks, the bituminous layer, positioning of expansion joints, exterior safety barriers, railings and border beams. Figure 7.3 presents the elevation of the viaduct under analysis, V2N, while Table 7.1 presents the time history of its construction.

a) piers. **b) deck.** **c) prestressing.**

Figure 7.2 : Construction views of the north approach viaduct.

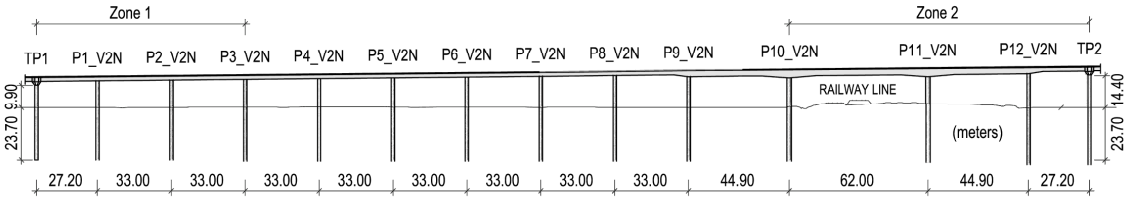

Figure 7.3 : Elevation of the V2N viaduct.

Table 7.1 : Time history of the V2N viaduct construction.

	2005				2006				2007			
	1st	2nd	3th	4th	1st	2nd	3th	4th	1st	2nd	3th	4th
Piles												
Columns												
Deck												

7.3. THE MONITORING SYSTEM

Lezíria Bridge is equipped with an integrated monitoring system to support the management of the structure. In what it concerns to the V2N viaduct, two zones were instrumented: (i) Zone 1, referring to the first three spans between piers TP1 and P3 and (ii) Zone 2, referring to the last three spans between piers P10 and TP2 (Figure 7.3). Cross sections were selected in these two zones to be instrumented with suited sensors.

Focussing the Zone 1, and in accordance with Figure 7.4, the installed sensors were vibrating wire strain gauges in three deck sections (P1P2, P2 and P2P3) to measure the concrete deformations (CD). Figure 7.5 depicts the typical instrumentation of girder sections, each section with four vibrating wire strain gauges, two in each alignment A and B. The strain gauges have an internal thermistor, which was used to measure the concrete temperature (CT). The strain values captured by the vibrating wire strain gauges were corrected by eliminating the effect of the free thermal deformation of the wire and the concrete. For this purpose, the thermal dilation coefficient took the value 11×10^{-6} ºC^{-1} in the case of the wire (given by the manufacturer) and 7.9×10^{-6} C^{-1} in the case of the employed concrete (Sousa and Figueiras 2009a). Sensors measurements were generally taken since the concrete pouring, and when this was not possible, reference readings were taken before the concreting.

The bearing displacements (BD) at the viaduct extremities were also monitored (see Figure 7.4), but only after the end of construction. The vertical displacements (VD) of sections P1P2 and P2P3 were measured during the load test, with reference to the soil as also presented in Figure 7.4. Two load cases, LC1 and LC2, are also indicated in Figure 7.4, which are used later in the results discussion. These load cases, with four trucks placed at the girder cross section, correspond to the maximum deflection of the spans P1P2 and P2P3, respectively.

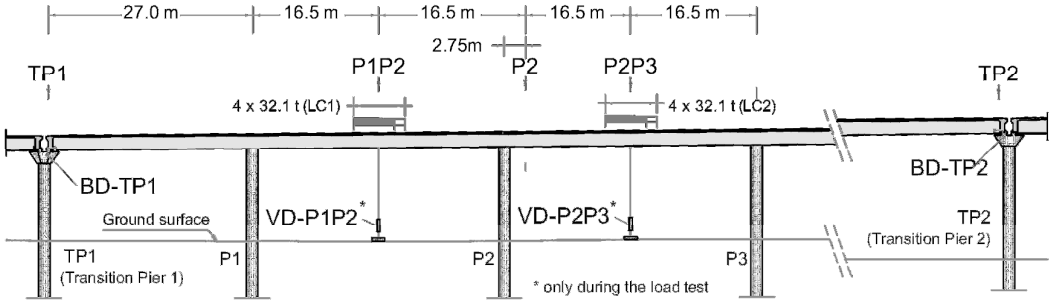

Figure 7.4 : Identification of the monitored cross sections (V2N – Zone 1).

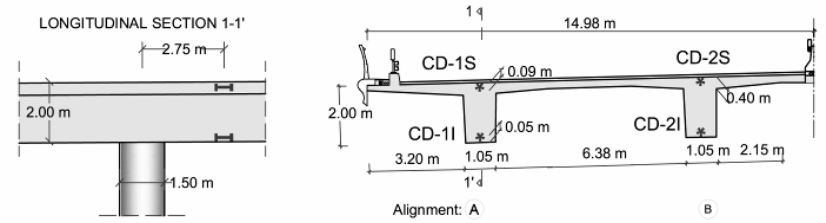

a) support zone.

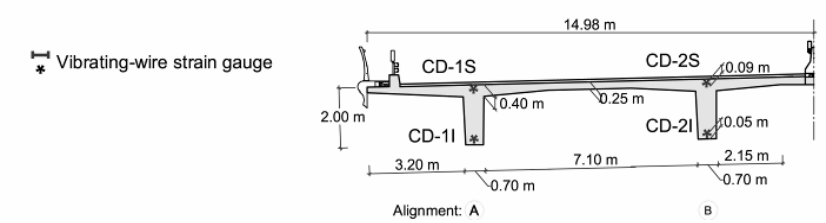

b) mid-span.

Figure 7.5 : Layout of the vibrating wire strain gauges positioning at cross section (V2N – Zone 1).

Regarding the long-term behaviour, strains and temperatures were also recorded in six prisms with dimensions of 15 cm × 15 cm × 55 cm, with two long faces unsealed. Four of these six prisms were used for shrinkage measurements while the other two were used for creep measurements. The prisms were cast with the same concrete of the girder and kept under to the same curing conditions. In order to get a more comprehensive characterization of the concrete employed in the deck girder, two shrinkage prisms were cast with concrete of Zone 2, while the remaining prisms (shrinkage and creep) were cast with concrete of Zone 1 (see Figure 7.3).

Additionally, the environment temperature, durability parameters and accelerations were measured. A complete description of the monitoring and data acquisition system installed in Lezíria Bridge can be found elsewhere (Sousa *et al.* 2011b).

7.4. FINITE ELEMENT ANALYSIS

7.4.1. GENERAL CONSIDERATIONS

A non-linear finite element analysis was conducted by using the general-purpose finite-element code DIANA (Witte 2005). Structural discretization was carried out using beam finite elements, in accordance with the Timoshenko theory. The elements are

numerically integrated along the beam axis and at the cross sections. Longitudinally, each beam element has three nodes and is based on an isoparametric formulation (Zienkiewicz 1971). The discretized beam elements are approximately 1 m long. Only one alignment of the girders, alignment A (see Figure 7.2), is modelled in the two dimensional analysis, as the loading and slab width over each alignment is similar. In this model, both geometry and loading are symmetric to the girder axis. The reinforcement, both ordinary and prestressed, was modelled using embedded reinforcement elements, whose deformation is calculated from the displacement field of the concrete finite-elements in which they are embedded. In this way, prestress losses due to concrete creep and shrinkage as well as relaxation of the prestressing cables are automatically accounted for. The piles-soil interaction was also modelled with elastic springs.

A phased analysis with 56 stages was performed, where the model was changed by including new elements and/or modifying the connection to the supports at each new stage. The sequence adopted in the analysis follows the real chronology observed during the construction (Table 7.1) (TACE 2007).

Errors are inevitable in the development of FEM devoted to large structures, namely due to data input (Catbas *et al.* 2007). To mitigate potential errors during the process, CAD tools were specifically developed to allow a full and detailed scanning of the drawing pieces with time-consuming benefits (Sousa and Figueiras 2009b). More information about these tools can be found in Appendix B.

7.4.2. STRUCTURAL MODELLING

The construction of the geometric model was based on the final drawings of the bridge project (COBA-PC&A-CIVILSER-ARCADIS 2005a). The structural elements, piles, piers and viaduct girder, were reduced to their axis as presented in Figure 7.6-a.

The ordinary reinforcement of all structural elements was taken into account with layers of reinforcement near the concrete faces. An additional reinforcement layer, matching the girder axis, was modelled to take into account the effect of the web reinforcement in the concrete delay deformations. The embedded prestressed cables in the girder concrete were precisely modelled with parabolic elements, in order to have a rigorous evaluation of the prestressing losses (Figure 7.6-b). To be possible the analysis of

the viaduct behaviour since early ages, the movable scaffolding system was also modelled with beam elements supported on the viaduct piers. Globally, the numerical model has 992 beam elements, 396 linear reinforcement elements (ordinary reinforcements), 60 parabolic reinforcement elements (prestress cables), 561 spring and 14 supports.

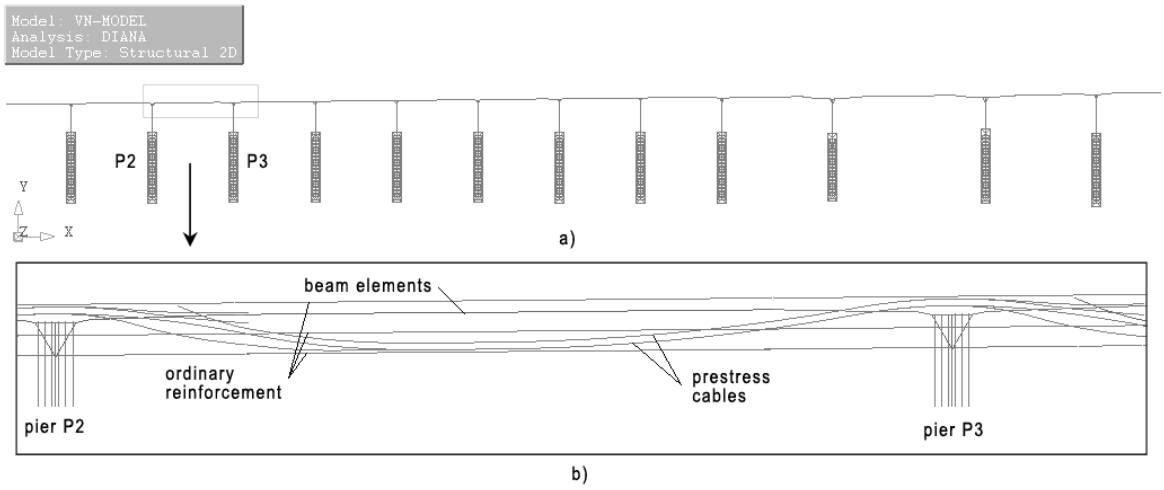

Figure 7.6 : FEM of the viaduct (DIANA output): a) general view, b) detailed view of span P2P3.

7.4.3. CONCRETE MODELLING

In concrete structures, to obtain a correct prediction of the structural behaviour, an accurate modelling of the material properties is required, namely for the concrete. Therefore, the definition of the mechanical properties of concrete were based on the tests of 150 mm cubes, which were performed during the construction (TACE 2007), and measurements taken from the reference concrete prisms to evaluate the shrinkage and creep.

The expressions proposed by the European code Eurocode 2 (EC2) were considered to describe the time variation of the concrete properties, namely the modulus of elasticity, creep and shrinkage (Standardization European Committee 2004). Whenever possible, the value of the parameters involved in those expressions was obtained from the measurements. Moreover, concretes with different mechanical properties were considered in the FEM analysis to take into account the phased concrete pouring performed during the viaduct construction.

- **Evolution of concrete compressive strength**

The consideration of the concrete compressive strength evolution is mandatory for a long-term analysis, since it is correlated with the evolution of the concrete modulus of elasticity. The concrete compressive strength was calculated based on compressive tests performed in 15 cm cubes. An extensive study was performed to characterize the compressive strength of different structural elements, namely piles, piers and girder. Since the cylinder strength was not experimentally evaluated, it was taken as 82 % of the observed cube strength as recommended by EC2 (Standardization European Committee 2004). Table 7.2 resumes the statistical information concerning the compressive strength at 28 days.

Table 7.2 : Compressive cylinder strength of concrete at 28 days (MPa) – statistical data.

Element type	Minimum Value	Maximum value	Mean value	Standard deviation	Coefficient variation
Piles (C35/45)	46.2	50.2	48.9	1.4	2.9 %
Piers (C30/37)	38.1	46.3	43.7	3.0	6.9 %
Deck (C35/45)	45.5	53.1	49.4	2.0	4.0 %

Based on these results, the compressive strength at a given age, $f_{cm}(t)$, is given in the EC2 by Eq. (31).

$$f_{cm}(t) = \beta_{cc}(t) \cdot f_{cm} \quad , \quad \beta_{cc}(t) = \exp\left[s \cdot \left(1 - \sqrt{\frac{28}{t}} \right) \right] \tag{31}$$

where t represents the concrete age in days, s is a cement-hardening coefficient that characterizes the evolution of the concrete strength, and f_{cm} is the mean value of the concrete compressive strength, at the age of 28 days. The parameter s was determined by a curve fitting procedure, which consisted in minimizing the mean square error between the cube test results (at different ages) and the Eq. (31). Figure 7.7 illustrates the curve fitting results for the concrete in the instrumented zone, namely of pile 2, pier 2 and deck

span P2P3 (Figure 7.3), whilst Table 7.3 resumes the values obtained for those parameters, grouped by different structural elements.

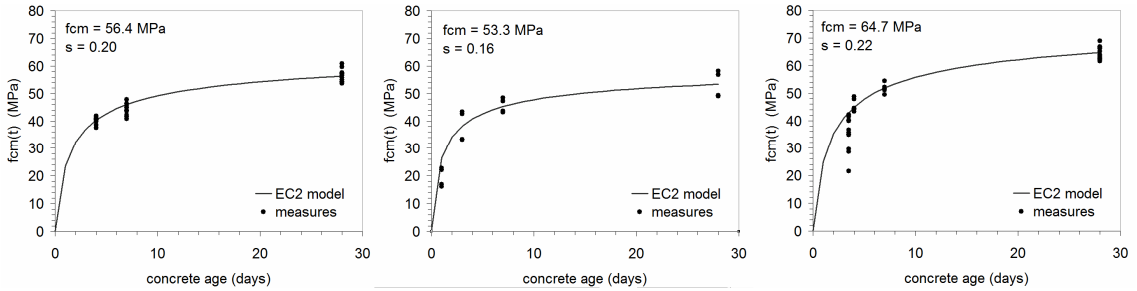

a) pile P2. **b) pier P2.** **c) deck P2P3.**

Figure 7.7 : Compressive strength evolution.

- **Modulus of elasticity**

The determination of the tangent modulus of elasticity, E_c, was based on the observed concrete compressive strength, by means of the Eq. (32).

$$E_c = 1.05 \cdot 22000 \cdot \left(f_{cm,cyl}/10\right)^{0.3} \qquad (E_c \text{ and } f_{cm,cyl} \text{ in MPa}) \tag{32}$$

where $f_{cm,cyl}$ represents the mean value of the concrete cylinder strength at the age of 28 days (Table 7.2). According with EC2, the evolution of the modulus of elasticity correlates to the time variation of the compressive strength (determined above), and is given by Eq. (33). Table 7.3 resumes the average values, depicted by structural element type.

$$E_c(t) = \beta_E(t) \cdot E_{c(28)} \quad , \quad \beta_E(t) = \exp\left[\frac{s}{2} \cdot \left(1 - \sqrt{\frac{28}{t}}\right)\right]^{0.5} \tag{33}$$

Table 7.3 : Mechanical properties of concrete - average values.

Element type	f_{cm} (MPa)	E_c (GPa)	s
Piles	48.9	37.2	0.20
Piers	43.7	35.9	0.18
Deck	49.3	37.3	0.20

- **Shrinkage**

The total shrinkage strain, ε_{cs}, is set by two parts as expressed in Eq. (34): the drying shrinkage strain, ε_{cd}, and the autogenous shrinkage strain, ε_{ca}. The drying shrinkage strain develops slowly, since it is a function of the migration of water through the hardened concrete, while the autogenous shrinkage strain develops during concrete hardening phase (Standardization European Committee 2004). The mathematical models given by EC2 for the drying and autogenous shrinkage are presented in Eq. (35) and Eq. (36), respectively, and they are expressed through a multiplicative model with a nominal coefficient, $\varepsilon_{c,\infty}$ and a time factor, $\beta_s(t)$.

$$\varepsilon_{cd}(t) = \varepsilon_{cd}(t) + \varepsilon_{ca}(t) \tag{34}$$

$$\varepsilon_{cd}(t) = k_{cs,0} \cdot \varepsilon_{cd,\infty} \cdot \beta_{ds}(t, t_s)^{k_{cs,t}} \tag{35}$$

$$\varepsilon_{ca}(t) = \varepsilon_{ca,\infty} \cdot \beta_{as}(t), \tag{36}$$

where t is the time (in days) since drying begins, t_s. Additionally, $k_{cs,0}$ and $k_{cs,t}$ were introduced in Eq. (35) so that the drying shrinkage model could be scaled and adjusted to the experimental results obtained from the concrete prisms (Santos 2002). In fact, the autogenous shrinkage was not considered in the fitting problem, because the major part develops in the early days after casting (Standardization European Committee 2004). However, the autogenous shrinkage was not neglected because the measurements collected from the concrete prisms had started since the concreting. Instead, its effect was removed from the measurements by subtracting a quantity expressed by Eq. (36) to allow the fitting process to the drying shrinkage model, and afterwards it was added. Therefore, the model

presented in Eq. (34) was fitted to the strain measurements performed in the concrete prisms.

Figure 7.8 presents the results achieved for the shrinkage prisms of Zone 1 and Zone 2 (see Figure 7.3). A more realistic model is obtained with the fitted EC2 model, being clear that the EC2 model overestimates the shrinkage deformations. The shrinkage deformations are almost equal for both zones, rounding the 300 με after almost 2000 days ($k_{cs,0} \cong 0.53$), while the evolution in the first ages are different ($k_{cs,t} = 0.50$ for prisms of Zone 1 and $k_{cs,t} = 1.73$ for the prisms of Zone 2). Moreover, the results respecting the Zone 2 are better adjusted for long-term while the results concerning the Zone 1 exhibit a better adjustment during the first ages. The scarce measurements obtained for the prisms of the Zone 2 during the first 250 days can explain the different fitting results.

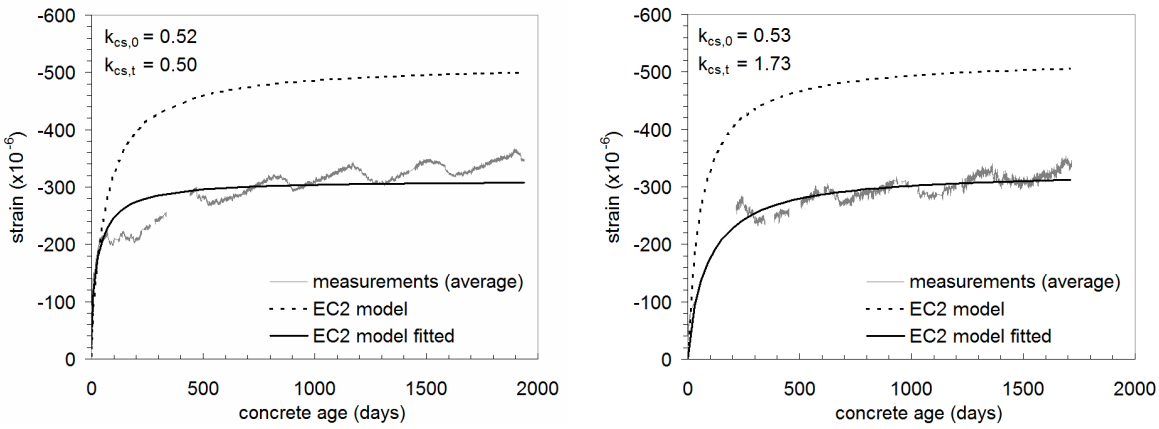

a) Zone 1. **b) Zone 2.**

Figure 7.8. Shrinkage strains of the deck concrete.

The cross-sectional shape influences the evolution of the shrinkage strains and this dependence is commonly expressed by the notional size (Standardization European Committee 2004). The notional size of the structural elements of the viaduct ranges between 360 mm to 680 mm, which is significantly higher than the shrinkage prisms that are 150 mm. The strategy employed in this work was to derive the shrinkage curves of the structural elements based on their effective notional size and the fitted curve obtained for the shrinkage prisms and presented in Figure 7.8. In addition, in order to take into account the beam thickness variation (see Figure 7.5), three different shrinkage curves were calculated with different notational size for each of the 13 spans and therefore, 3×13

shrinkage curves, as presented in Figure 7.9, were calculated in order to be considered in the input file.

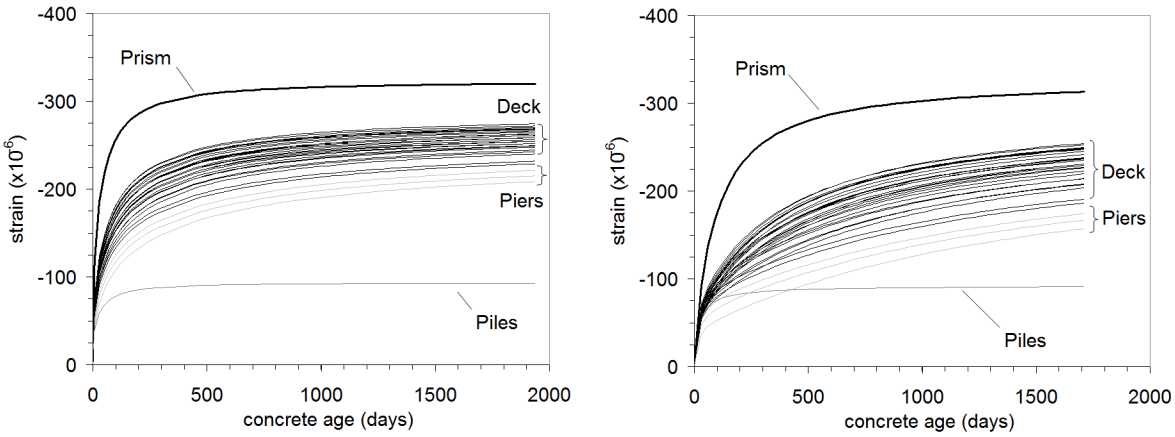

a) based on shrinkage prisms of Zone 1. **b) based on shrinkage prisms of Zone 2.**

Figure 7.9 : Shrinkage curves for the structural elements of the viaduct.

- **Creep**

According with the EC2, the creep deformations of concrete, $\varepsilon_{cc}(t,t_0)$ at a generic time t for a constant compressive applied stress at the age t_0 is given by Eq. (37), where $\varphi(t,t_0)$ is the creep coefficient and $\varepsilon_c(t_0)$ is the instantaneous deformation due to the compressive applied stress. Moreover, EC2 sets the creep coefficient according to Eq. (38).

$$\varepsilon_{cc}(t,t_0) = \varphi(t,t_0)\cdot\varepsilon_c(t_0) \tag{37}$$

$$\varphi(t,t_0) = k_{cc,0}\cdot\varphi_0\cdot\left[\beta_c(t,t_0)\right]^{k_{cc,t}} \tag{38}$$

where φ_0 is the notional creep coefficient and $\beta_c(t,t_0)$ is a coefficient to describe the development of creep with time after loading. Similar to the shrinkage, the additional parameters, $k_{cc,0}$ and $k_{cc,t}$ were introduced in Eq. (38) so that the creep model could be scaled and adjusted to the experimental results (Santos 2002; Carlos Sousa and Neves 2009b). Therefore, the EC2 model was fitted to the strain measurements performed in the concrete prisms. Again, a more realistic model is obtained with the fitted model as it is

presented in Figure 7.10, where it is clear that the EC2 model overestimate the creep deformations. In fact, differences between observed values and code predictions were expected since the employed concretes contain superplasticizers and pozzolanic materials, whose effect in the composition cannot be accurately reproduced by code formulae (Bazant 2001). Similar to the strategy adopted for the shrinkage, the notional size was considered to scale the creep function to the structural elements of the viaduct.

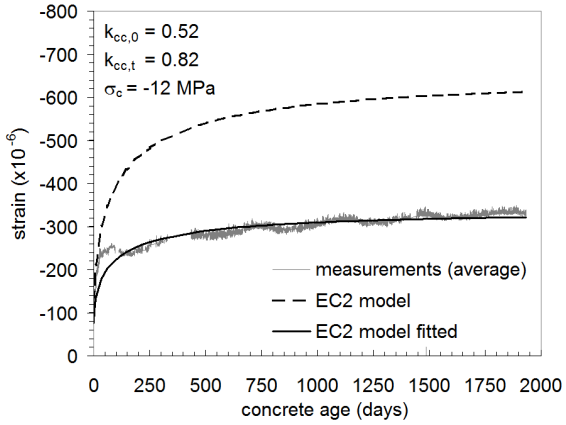

Figure 7.10 : Creep strains of the deck concrete.

7.4.4. PRESTRESS CABLES MODELLING

An exhaustive scanning was carried out to characterize the modulus of elasticity of the employed prestress steel, based on the manufacture specifications (TACE 2007). This information was considered into the FEM by taking the average value of the prestress cables used for each span. Globally, an average value of 199.7 GPa was achieved, which satisfies the EC2 limits of 195 GPa to 210 GPa (Standardization European Committee 2004). Moreover, the minimum and maximum values obtained were 193.0 GPa and 209.0 GPa, respectively, with a coefficient of variation of 1.7 %. Taking the fact that the prestressed cables have low relaxation and were conducted in flexible metal ducts: (i) the wobble coefficient K, per meter, was fixed to 0.05; (ii) the coefficient of friction, μ, was set to 0.19 and (iii) a relaxation class 2 was adopted (Carlos Sousa and Neves 2009a; FIB Commission on Practical Design 2010a).

7.4.5. SOIL MODELLING

The interaction between the piles and the soil was modelled with elastic springs based on the Winkler model. The spring stiffness is proportional to the influence area of the spring, A_{inf}, and the subgrade reaction module, k_s (Sousa 2006a). The A_{inf} is defined by the pile diameter, ϕ, multiplied by an influence length, L as expressed in Eq. (39). As regards the k_s value, it was evaluated based on field tests performed by the constructor (COBA-PC&A-CIVILSER-ARCADIS 2005b). Table 7.4 resumes the average values with interest for the FEM, which were used to compute the stiffness of the soil springs. The deepness values are reference values, which in reality they were considered variable along the viaduct lenght.

$$k_v = k_s \cdot A_{\text{inf}} \quad , \quad A_{\text{inf}} = \phi \cdot L \tag{39}$$

Table 7.4. Subgrade reaction module, ks.

Soil description	Clay deposits	Sludge	Muddy fine to medium sand	Medium sand	Clay silt
Deepness (m)	0 to 2	2 to 6	4 to 6	6 to 8	> 6
ks (MN/m3)	4 to 8	1 to 2	7 to 3	8 to 2	90 to 120

7.4.6. LOADING

The loads used in the analysis were: (i) self-weight of the reinforced concrete, with a value of 25 kN/m^3; (ii) effective forces applied on the prestressing cables, based on stretching measurements, which were estimated to be, in average, 4 % lower than the design values and corresponding to a stress level of approximately $0.71 \cdot f_{puk}$; (iii) remaining dead loads composed by the bituminous layer, border beams, service sidewalks and safety barriers with an estimated value of 28.3 kN/m; (iv) trucks full charged used in the load test with an average weight of 32.1 tons (314.6 kN) each and a standard deviation of 0.4 tons (4.2 kN).

7.5. RESULTS AND DISCUSSION

7.5.1. LOAD TEST

Any prediction obtained by a numerical model presents deviations to the real behaviour. Even tough, it is always important to have a numerical model capable of representing, as much as possible, the effective performance of the structure in order to get reliable predictions. The best strategy to achieve this objective is by validating the numerical model with measurements obtained from load tests, taking profit that the loading is perfectly known and controlled a priori. In this context, the numerical model was calibrated, and some parameters with direct influence in the viaduct behaviour were evaluated namely: (i) soil stiffness, (ii) piles with and without metallic casing, (iii) axial deformability of piles and (iv) dimensions of the pier-deck intersection zone.

Based on the calibrated model, Figure 7.11 presents the results concerning the load test (see Figure 7.4) for the curvatures (CUR) and the vertical displacements (VD) at sections P1P2 and P2P3. For the maximum values, the results for the vertical displacements show a better agreement than the ones obtained for the curvatures. This can be explained by the different parameters that are being analysed. The curvature, which is calculated based on the strain measurements, "CD-1I" and "CD-1S" (see Figure 7.5), provide local information at the viaduct cross section. Moreover, it is highly influenced by the properties of the concrete that embeds the strain gauges. In opposite, the vertical displacement reflects a global response being less susceptible to local properties. Even though, for the load configurations that led to maximum displacements for sections P1P2 and P2P3, with respect to the load cases LC1 and LC2 (see Figure 7.4), the maximum errors were 7 % and 4 %, respectively. To obtain these results, the calibrated model considers: (i) average values for subgrade reaction module, k_s (Table 7.4), (ii) piles with metallic casing, (iii) partial deformability of piles and (iv) effective dimensions of the pier-deck intersection zone. In fact, the absence of the real column-deck node dimensions would cause an error increase of almost 8 %, while the non-consideration of the metallic casing would result an error increase of 2 %. The axial deformability of the piles has an influence of 3%. Therefore, if the aforementioned errors are combined, the errors could increase from the obtained 4 % and 7 % to almost 17 % and 20 %, respectively, which is

not acceptable for reliable predictions to support the management and surveillance of the viaduct.

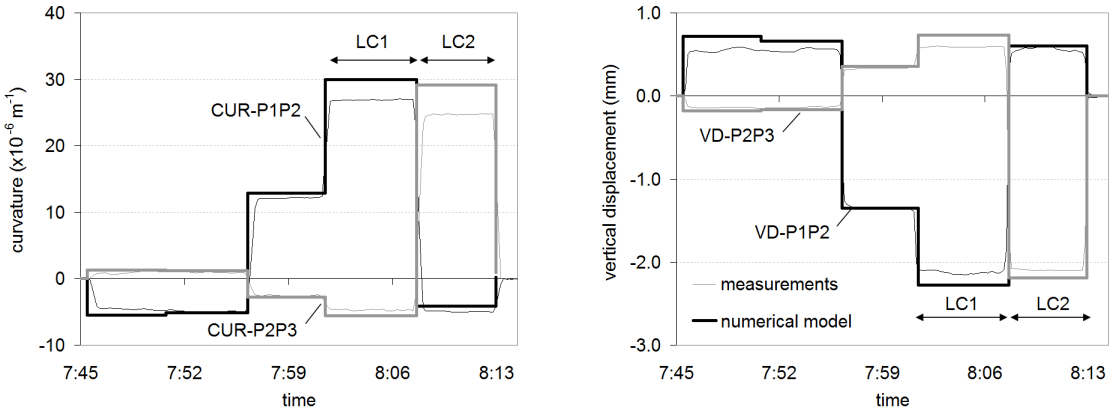

a) curvatures. **b) vertical displacements.**

Figure 7.11 : Load test results for sections P1P2 and P2P3.

7.5.2. CONSTRUCTION ASSESSMENT

As aforementioned, the girder construction can be described by the following phases: (i) positioning of the movable scaffolding – phase 0, (ii) reinforcement positioning and concrete pouring – phase 1, (iii) tensioning of the prestressing cables – phase 2, (iv) release of the movable scaffolding and moving forward – phase 3. Figure 7.12 shows the measurements obtained in section P2P3 (see Figure 7.4), where the different phases of the constructive process can be clearly identified. The most relevant change occurs at 07/08/2006 when the prestressing cables of span P2P3 were tensioned (phase 2), which caused a variation of approximately, $\varepsilon_c = -300\,\mu\varepsilon$, in the strain gauge "CD-1I" (see Figure 7.4). Short time later, a compression decrease was observed in this strain gauge, caused by the release of the movable scaffolding (phase 3). This last variation denotes that the span weight was partly supported by this structure, even after the prestressing. The measurement of the strain gauge also shows minor offsets at 11/08/2006 and 13/08/2006, corresponding to the construction phases 1 and 2 of the next span P3P4. As far as the evolution of the concrete temperature (CT) is concerned, different patterns are observed for the two thermistor of the vibrating wire sensors "CD-1I" and "CD-1S" (Figure 7.5). Although both sensors are approximately at the same distance of the concrete surface, the sensor at the

top, “CT-1S”, is more prone to the daily thermal variations. The movable scaffolding framework can explain the initial differences between both sensors. The framework bounds all faces of the girder excepting the top face, which facilitates the heat dissipation. Even though, after the end of phase 2 the daily temperature variation is greater at the top face due to the sun exposure, contrarily to the bottom face that is always on shade. The time-delay effects of concrete are also visible by smooth variations of the strain measurements along time.

Considering the shrinkage curves obtained based on the concrete prisms of Zone 1 (Figure 7.8 and Figure 7.9-a) and the fitted model for creep deformations (Figure 7.10), the results obtained from the numerical model are also plotted in Figure 7.12-a. A good agreement with the strain measurements is achieved. The zero-reference for the strain measurements is difficult to establish however, for the present study, it was considered two days after the concreting. At this stage, the concrete temperature is still decreasing, and approximately, at half path of the temperature stabilization, where it is expected a full hardening behaviour of the concrete. The most unsatisfactory agreement is observed for “CD-1I” for the period between the construction phase 2 of the span P2P3 and the construction phase 1 of the span P3P4, which can be explained by the temperature variation at the bottom of the deck girder. The temperature is still decreasing due to the heat dissipation of concrete hydration. Therefore, non-linear profiles of the temperature through the section height exist and additional mechanical deformations are originated. The results herein presented do not take into account the concrete hydration effect, which might be the possible cause for the less satisfactory agreement during this period.

In correspondence to Figure 7.12-a, Figure 7.12-b presents the stress variation in section P2P3 given by the numerical analysis. The minimum stress occurred at the bottom face with a value of $\sigma_c = -8.9$ MPa, respecting to phase 2 of the construction of the span P2P3. In fact, as aforementioned regarding the strain results, the deformability of the movable scaffolding is partly responsible for this result. After the release of the movable scaffolding the stress decreases to, $\sigma_c = -7.2$ MPa and therefore, it can be concluded that the deformability of the movable scaffolding leads to a temporary increase of stress of approximately 24 %. Recent works show that it is possible to eliminate this undesirable stress increments by using organic prestressing in the scaffolding systems (Pacheco *et al.* 2010). Even though, along the constructive process, the entire section was subjected to

compressive stresses that were always inferior to $0.45 \cdot f_{ck}(t)$ and therefore, the concrete service stress limit was not exceeded (Standardization European Committee 2004).

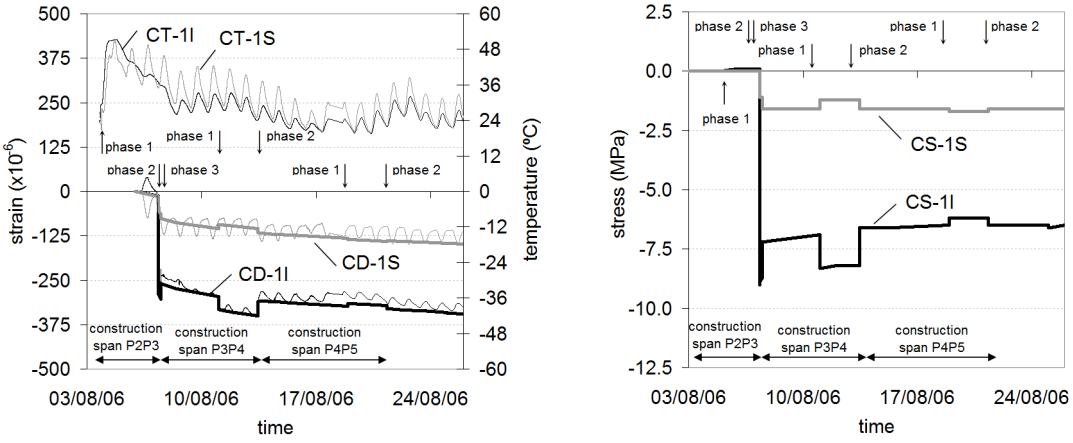

a) strains. **b) stresses (numerical results).**

Figure 7.12 : Results for the instrumented section P2P3 during the construction.

7.5.3. LONG-TERM BEHAVIOUR

As regards the long-term behaviour, Figure 7.13 presents the results concerning the observation of sections TP1, P1P2, P2 and P2P3 (see Figure 7.4), compared with the corresponding FEM results. To improve the results discussion, three different time dependent approaches are used for concrete: (i) based on the EC2 models; (ii) based on the EC2 models fitted with the measurements of the shrinkage prisms of the Zone 1, which were the basis of the results presented in Figure 7.12 for the construction phase; iii) similar to the previous approach however, the shrinkage prisms of the Zone 2 are used instead of the ones of the Zone 1.

Taking the measurements as baseline, the overestimation committed by the EC2 models is confirmed, while the results obtained with fitted models lead to a significant improvement in the results quality. This is clearly evident in Figure 7.13-a, where the trend, disregarding the variation due to the temperature effect, of the measurement on the bearing displacement at section TP1 (see Figure 7.4) presents a better agreement with data obtained using the fitted models than with the EC2 models. Similar results were obtained for the bearing displacement at TP2 section (see Figure 7.4). This result has a particular importance for the model validation, because it reflects the global behaviour of the viaduct,

in opposite to the strain results that are influenced by the local properties and conditions at corresponding cross sections, as aforementioned. As regard the strain results, although they exhibit a good agreement, some deviations must be explained. The sensors placed in the concrete near the top face of the deck girder, "CD-1S", of the mid-span sections P1P2 and P2P3 (Figure 7.13-b and Figure 7.13-d) are highly influenced by the sun exposition and the rainfall and consequently, they are subjected to particular conditions of temperature and humidity. Observing carefully the pattern evolution of the strains measurements in Figure 7.13-b and Figure 7.13-d, a significant increase of the concrete shrinkage after the construction end is observed as well as a decrease of the daily variation. In fact, the deck bituminous layer placed at the end of the construction can explain this change of pattern. The bituminous layer prevents the humidity to reach the top face of the deck girder as well as lead to an increase of the concrete temperature due to the heat absorption. Therefore, with less humidity reaching to the concrete and with a higher range of temperatures, an increase of the shrinkage deformations is expected. Another aspect that can explain the differences is the notational size of the deck girder. The higher the notational size, slower is the shrinkage evolution. As already mentioned, the notational size of the structural elements of the viaduct ranges between 360 mm to 680 mm, which is significantly higher than the shrinkage prisms that are 150 mm (140 % to 353 % higher). The shrinkage of the structural elements was in fact extrapolated based on the measurements of the concrete prisms (Figure 7.9) and therefore, errors associated with this procedure must be taken into account in the discussion of results. Similar conclusions were obtained by other authors studying different instrumented bridges in Portugal (Santos 2002; Santos 2007).

Comparing the two results obtained with the fitted models, using the shrinkage prisms of the Zone 1 and shrinkage prisms of the Zone 2 respectively, they are complementary. A better approach during the construction phase is obtained based on the shrinkage deformations of the prisms of the Zone 1 (see Figure 7.9-a), while the long-term response is better interpreted with the shrinkage deformations of the prisms of the Zone 2 (Figure 7.9-b). These results confirm the fitting curves presented in Figure 7.8.

As regards the influence of the relaxation of the prestress steel, its effect is low. For the structure lifetime, 100 years, its contribution is lower than 2.0 %.

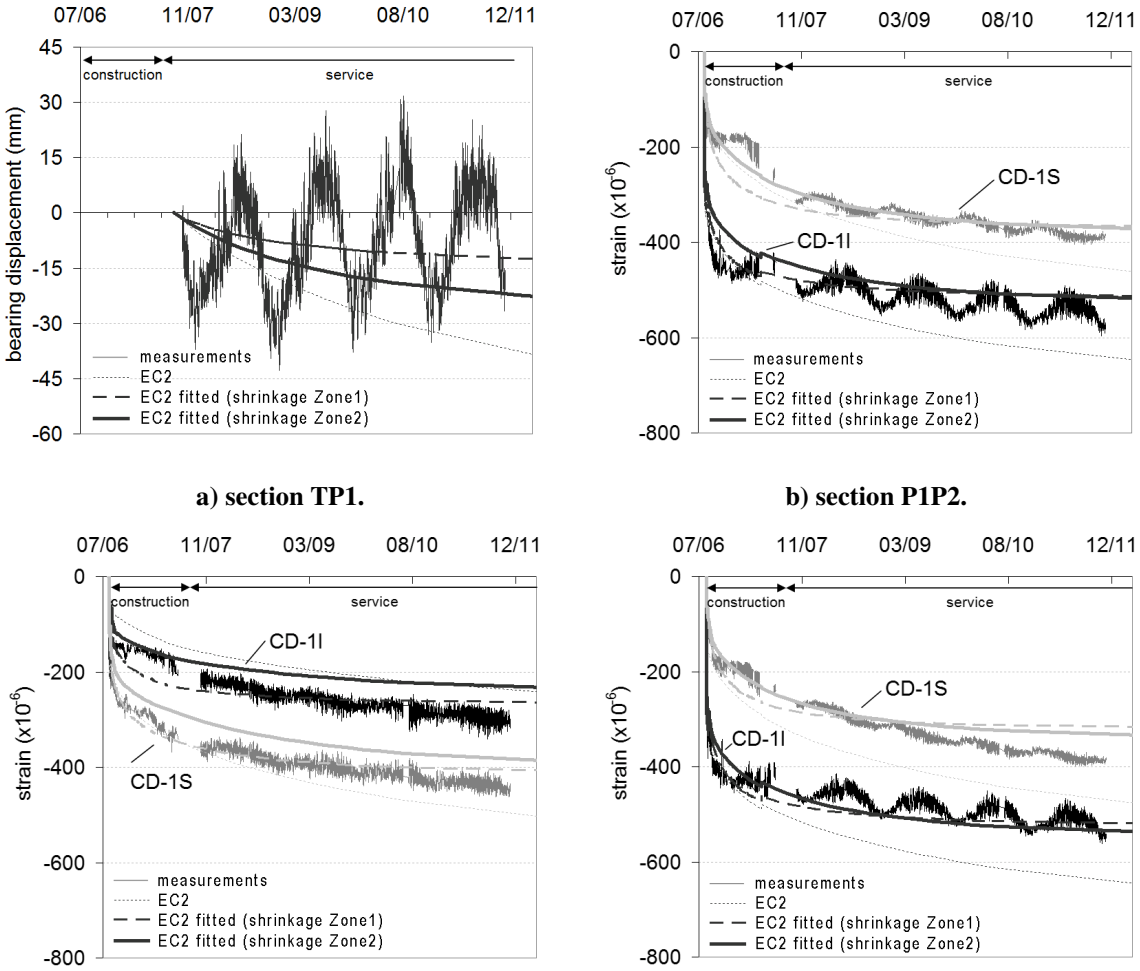

a) section TP1. **b) section P1P2.**

c) section P2. **d) section P2P3.**

Figure 7.13 : Long-term results.

7.5.4. PREDICTION FOR THE VIADUCT LIFETIME

In spite of the long-term behaviour is mostly conditioned by the time-delay properties of concrete, namely shrinkage and creep, the environment conditions has also an important contribute, namely the temperature variation, as it can be noticed by the seasonal variation of the measurements presented in Figure 7.13. Besides the EC2 models for shrinkage and creep overestimate the long-term response of the viaduct. As aforementioned, laboratory tests revealed that the thermal dilation coefficient of the employed concrete is approximately 7.9×10^{-6} ºC^{-1} (Sousa and Figueiras 2009a), , which is 21 % lower than the 10×10^{-6} ºC^{-1} specified in Eurocode 1 (EC1) (Standardization European Committee 2009). This value is consistent with results obtained by other authors (Kada *et al.* 2002; Santos

2007). As a result, the predictions based on the European standard rules are unrealistic to be considered as the expected values for the sensors' measurements and they should be calibrated focussing the viaduct lifetime.

In this context, the predictions with best performance for long-term purposes previously presented in Figure 7.13, i.e. EC2 model fitted to the shrinkage prisms of the Zone 2, were extended for the viaduct lifetime of 100 years. Additionally, the temperature effect was taken into account according with the specifications for thermal actions on bridges presented in the EC1 and the national annex for the Portuguese case (Standardization European Committee 2009). Thus, the characteristic values adopted for the minimum and maximum uniform temperature components were $T_{min} = 0\,°C$ and $T_{máx} = 40\,°C$, respectively, while for the differential temperature components the values considered were $\Delta T_{M,cool} = -5\,°C$ and $\Delta T_{M,heat} = +15\,°C$, respectively. Both effects, uniform and differential, were also considered simultaneously to explore the most adverse effect. For consistency with the previous results, two values were considered for the initial bridge temperature, T_0: (i) 15 ºC in accordance with the stipulated by EC1 in the absence of more precise information and (ii) 22 ºC, which was the average temperature when the viaduct spans were restrained to deform freely. Adding the effects due to the time-delay and the temperature – case A and case B – the results are presented in Figure 7.14. The trends obtained for the concrete deformations with the EC2 models are 55 % to 70 % superior to the ones obtained with the fitted models, which was already expected considering the results presented in Figure 7.8, Figure 7.10 and Figure 7.13. As regards the temperature effect on the concrete deformations, and considering that the most probable situation corresponds to the simultaneous action of the uniform and differential temperature components, the most adverse effect is achieved when the differential temperature component acts as the main effect. The sensors positioned near the top face exhibits the highest contractions in the summer while the highest expansions are achieved for the winter season. In opposite, the sensors positioned near the bottom face exhibit highest contractions in the summer while the highest expansions are detected for the winter season. Detailing the results presented in Figure 7.14, the concrete deformations near the bottom face at the mid-span sections P1P2 an P2P3 exhibits higher sensitivity to temperature with values ranging between $-25\,\mu\varepsilon$ to $+89\,\mu\varepsilon$ for case A and $-33\,\mu\varepsilon$ to $+107\,\mu\varepsilon$ for case B. The remaining concrete deformations exhibit variations between

$-30\,\mu\varepsilon$ and $+36\,\mu\varepsilon$ for case A and $-39\,\mu\varepsilon$ and $+32\,\mu\varepsilon$ for case B. Generally, these values are coherent with the seasonal variation of the sensors' measurements presented in Figure 7.13.

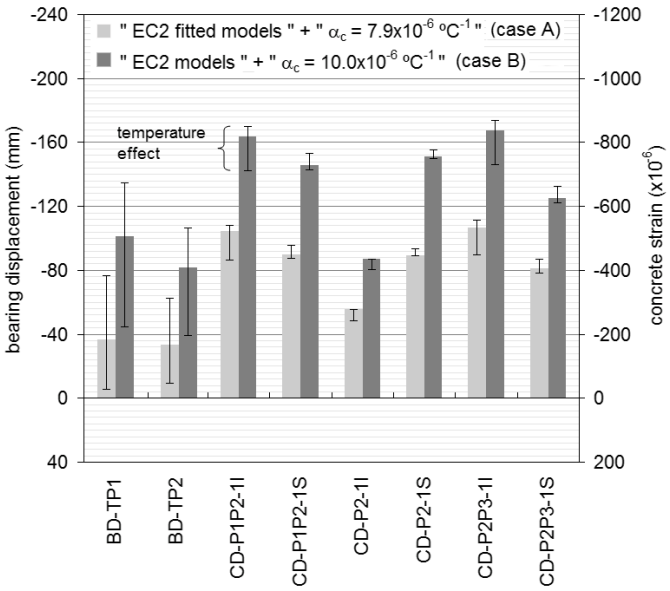

Figure 7.14 : Predictions for the sensors' measurements concerning the viaduct lifetime.

Regarding the bearing displacement (BD) at sections TP1 and TP2 (see Figure 7.4), the most adverse effect is achieved when the uniform temperature component acts as the main effect. The results presented in Figure 7.14 shows that the displacements are approximately equal for both sections. The slight difference, in trend and variations caused by temperature, are explained by the higher stiffness of the viaduct over the railway zone (see Figure 7.3), which causes a shift of the mass-centre of the viaduct to the side of section TP2, in relation to the half length of the viaduct. Consequently, higher displacements in the bearing of section TP1 are expected. In this case the temperature effect has the same influence, or more, as the time-delay effects because the unrestrained thermal deformations are included, contrarily to what happens for the concrete deformations. It should be remembered, as previously referred in the description of the monitoring system, that the measurements concerning the concrete deformations were corrected by removing the effect of the free thermal deformation of the sensor and concrete.

Based on the results herein presented, expansion and contractions movements are expected because of the reduced deformations due to creep and shrinkage in case B, in

opposite to the predictions based on the European standard rules only (case A). These results are consistent with the ones presented in Figure 7.13-a, where it is clearly visible the seasonal expansion and contraction movements due to temperature, while the results obtained with the fitted EC2 models shows that the displacements due to shrinkage and creep deformations of concrete are significantly lower. Analysing the results presented in Figure 7.14, the bearing displacement at section TP1, "BD-TP1", should present a trend value of −101 mm after 100 years, value that could range between −45 mm and −135 mm due to temperature effects. However, the study herein presented shows that the expected trend value is −37 mm (63 % less) and raging between +5 mm and −76 mm due to temperature effects (amplitude 21 % less, which is in accordance with the difference obtained for the thermal dilation coefficient of the concrete).

It is worth mentioned that the initial bridge temperature is a determinant aspect. Higher values of the initial bridge temperature will lead to higher contractions and smaller expansions due to temperature variation, which justifies the different amplitudes for the positive and negative sides of the range values obtained for both cases. Hence, the reviewed predictions, based on the fitted models of the EC2 for shrinkage and creep, are information more realistic and reliable, than the ones obtained based on the standard values prescribed on the regulation guidelines. Therefore, they should be preferred to be used in the maintenance and surveillance of the viaduct. Even though, due to the complexity of the problem, the predictions herein presented should be periodically checked. For that, the FEM should be updated as the database increases, which will promote the confidence in the obtained results.

7.6. CONCLUSIONS

The present chapter focuses the assessment of the long-term structural behaviour of viaducts constructed with movable scaffolding systems. A real structure, which was recently built in Portugal, has been monitored since the beginning of its erection. The monitoring system was carefully planned, installed and protected so that it could provide long-term reliable results. This chapter describes the viaduct, presents the monitoring system, and discusses the procedure employed to assess the structure's behaviour. This procedure is based on FEM calculations. Some relevant conclusions could be drawn:

- The presented work exposes the analysis strategy that was developed to calculate the long-term behaviour of a concrete viaduct. A FEM was employed, taking into account the effective properties of the structural materials, the actual sequence of construction and the influence of concrete time-delay effects. A good agreement between the numerical and the experimental results were observed. However, this was possible thanks to the data collected during the execution of the structure, which is not available at the design stage of each new structure. The sensors' measurements revealed to be an important element to get an optimized model, with benefits in future updating. Therefore, this type of data becomes more and more useful in the surveillance and maintenance of the structure.
- The analysis since the beginning of the construction indicates that, even after the prestressing, the span weight is partially supported by the movable scaffolding system. This is confirmed by the results obtained for the mid-span section P2P3, which show that the stress level at the bottom face increases approximately 24 %, even if temporarly. Even though, the limit of $0.45 \cdot f_{ck}$ was never exceed.
- The EC2 models overestimate the deformations due to shrinkage and creep of the employed concrete in the viaduct. The superplasticizers and pozzolanic materials used in concrete mix, whose effect cannot be accurately reproduced by code formulae might explain these deviations.
- Even with the EC2 models for shrinkage and creep fitted to experimental data, some relevant differences are observed between the sensors measurements and the FEM. Two possible explanations can be pointed out: (i) Comparing the notional size values of the deck girder with the prisms, they are substantially different and therefore, the extrapolation of the shrinkage and creep of the deck girder, based on the measurements of the concrete prisms, is more prone to errors. (ii) The sensors near the top face of the deck girder are exposed to particular conditions because of the bituminous layer that increases the concrete temperature and reduces the concrete humidity.
- Regarding the long-term response for the structure lifetime, the effect of the relaxation of the prestress steel is small, with a contribution lower than 2.0 %. The low relaxation of the applied steel and the stress level of approximately of $0.71 \cdot f_{puk}$ justify the small influence.
- As regard the long-term results, it seems to be difficult to get, simultaneously, the same results quality for the construction and service life of the viaduct. This limitation can be

explained by the use of a shrinkage model that attempts to fit to measurements that exhibit different trends during the construction and for the service life.

- The environmental effects, namely those due to the temperature, are perfectly noticeable in the sensors' measurements. The concrete deformations are more sensitivity to the differential component, namely the sensors near the bottom face of the mid-span. As regard the bearing displacements, they exhibit higher sensitivity to the uniform component. In this case, the temperature effect has the same importance as the time-delay effects because the unrestrained thermal deformations are included in the sensors' measurements, in opposite to the concrete deformations' measurements herein presented.
- It must be kept in mind that the result of the long-term analysis of a real structure is not deterministic, namely, those related to the evaluation of the concrete delayed deformation due to creep, shrinkage and temperature, which adds uncertainty to the long-term prediction.

8. MODELLING OF THE CONSTRUCTION AND LONG-TERM BEHAVIOUR OF A CONCRETE BRIDGE BUILT BY THE CANTILEVER METHOD

8.1. INTRODUCTION

The long-term assessment of large civil infrastructures such as prestressed concrete bridges is a challenging task. One of the most common and reliable strategies is to use Finite Element Models (FEM). Based on the information concerning the geometry and materials properties, the structural behaviour can be uniquely interpreted. Although the short-term behaviour, load tests for example, can be accurately interpreted with FEM analysis, the long-term prediction of these large structures is not so straightforward. The new bridge designs, the materials evolution and the advances in the constructive methods employed in the civil engineering domain are aspects with direct influence in the long-term response. Therefore, and in addition to the geometric and materials properties, all other significant aspects with influence in the bridge behaviour must be taken into account in the analysis strategies, in order to get predictions more reliable and reduce potential bias. The real time history related to the phased construction, the influence of the adopted constructive method, the characterization of the employed concrete, namely shrinkage and creep, and the environmental conditions are some of those most relevant aspects.

As regard the constructive methods, one of the most commonly used for the construction of cast in situ concrete bridges is the balanced cantilever method. This constructive process has become very popular due to the many advantages that offers and the attained structural shape of the bridge. Nowadays segmental cast-in-place concrete bridges are usually built in the 200 m to 300 m span range (Takacs 2002). The bridge girder is usually built from one or more piers, by means of movable formwork systems that advance from a short stub on top of a pier symmetrically in segments, usually ranging from

3 m to 5 m length until reach the mid-span or an abutment. To equilibrate the advance of the segmental construction, prestressing tendons are arranged in the top slab of the deck girder, with a high concentration above the pier that gradually decreases as it moves to the mid-span. This method is especially used when a fixed scaffolding is difficult or impossible to erect as, e.g., over deep valleys, wide rivers, and traffic yards or in case of expensive foundation conditions for scaffolds. Measurements obtained since early ages with appropriate sensors would be desirable to get a more comprehensive knowledge of the real behaviour of bridges constructed with this constructive method. However, databases with this type of information are still scarce.

As far as the concrete properties are concerned, several studies show that long-term predictions differ significantly from the observed response, mainly due to the evaluation of shrinkage and creep during the design phase (Robertson 2005; Goel *et al.* 2007; Santos 2007). Particularly in the segmentally cast concrete cantilever bridges, the thickness differences between the bottom and top slab of the box girder has an important influence in the long-term behaviour, which can exhibit noticeable deviations from those predicted in the design calculation (Takacs 2002; Zdenek Bazant *et al.* 2008; Malm and Sundquist 2010).

Besides the rheological effects of concrete, the variability concerning the environmental conditions, namely the humidity and temperature, are also critical for an accurate evaluation of the effective long-term response (Roberts-Wollman *et al.* 2002; Li *et al.* 2004; Catbas *et al.* 2008).

Data from long-term monitoring systems have been supporting the aforementioned studies, which demonstrate the importance of these systems to improve the knowledge concerning the effective structural behaviour. Initially, these measurements were provided to detect in advance any possible risk factor during the construction of the bridge, and thus prevent any resulting accident (Chang *et al.* 2009). With the technology evolution, the monitoring systems have become more and more powerful, offering information on structural integrity, durability and reliability, and ensuring optimal maintenance planning and safe bridge operations (Ko and Ni 2005). In fact, monitoring data have been contributing to validate the design assumptions, to calibrate the structural models, and to update the safety coefficients.

The recent construction of a major bridge in Portugal, Lezíria Bridge, comprises a 970 m eight spans bridge built with the referred constructive method, which offered the

opportunity to observe its long-term behaviour and compare with that obtained with a numerical model. The measurements were collected by a permanent monitoring system installed in the bridge since the beginning of the construction, devoted to the bridge surveillance and maintenance (Sousa *et al.* 2011b).

This chapter presents the FEM implemented to predict the long-term response of the bridge, which was calibrated with measurements obtained during the construction phase and from the load test. The effective mechanical and time-delay properties of concrete and prestressing steel were considered as well as the effective prestress forces and the real construction sequence. A full discussion concerning the real long-term behaviour is made, focussing the differences between the measurements and the results obtained with the FEM, namely the trends due to shrinkage and creep. Finally, concerning to the bridge lifetime, the predicted values for the measured parameters are reviewed, since the predictions based on the European standards are not satisfactory to be used as reference values regarding the bridge surveillance.

8.2. THE BRIDGE

Lezíria Bridge is inserted in the A10 motorway in Portugal. With a total length of 39.9 km, this motorway is an outside bound to the Lisbon Metropolitan Area. The 11 670 m total length of Lezíria Bridge are materialized by three substructures of prestressed concrete: (i) the north approach viaduct with 1 700 m of length; (ii) the main bridge substructure, crossing the River Tagus, with a total length of 970 m; (iii) and the south approach viaduct, with a total length of 9 160 m. As regards the main bridge (Figure 8.1), the 970 m length is constituted by eight spans, 95 m + 127 m + 133 m + 4 × 130 m + 95 m, which are supported on two transition piers (with the approach viaducts) and seven piers founded on pilecaps over the riverbed (COBA-PC&A-CIVILSER-ARCADIS 2005c).

The foundations have circular piles with 2.2 m diameter, constructed with a lost metallic casing that reach the Miocene layer at approximately 40 m deep. The foundations that bound the navigation channel, between piers P1 and P2, have 10 piles while the remaining foundations have 8 piles only. The pilecaps were built with precast caissons, which worked as a lost formwork. The dimensions of these pilecaps, in terms of height × width × length, are 5.0 m × 11.0 m × 16.5 m, excepting the piles caps of piers P1 and P2 that have 8.0 m ×

11.0 m × 22.0 m. All the pilecaps were dimensioned to have their top face above the river water level (Figure 8.1 and Figure 8.2-a).

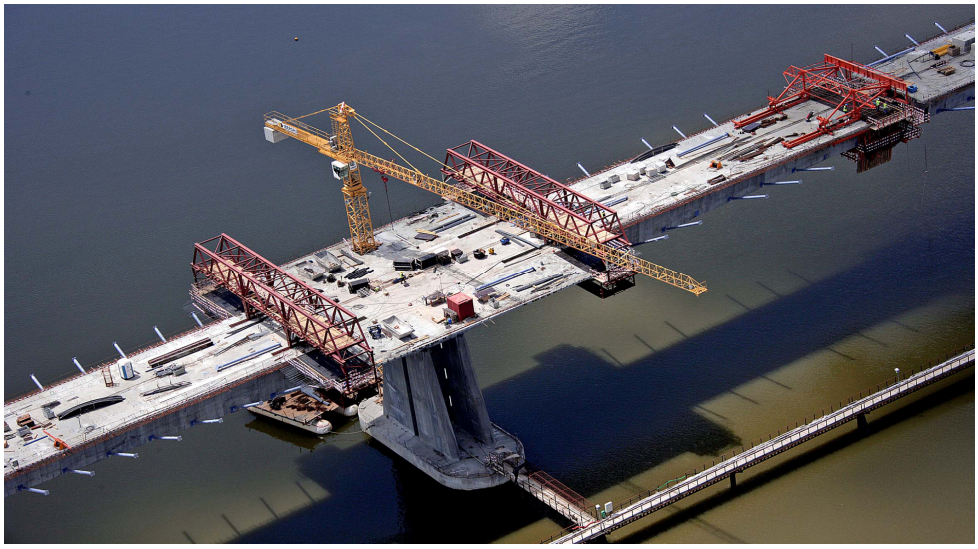

Figure 8.1 : Aerial view of Lezíria Bridge – May 2007 (© F. Piqueiro / Foto Engenho).

The seven interior piers were constructed with traditional formworks, which were supported on the pilecaps. Four walls form each pier, with constant thickness of 1.20 m, variable width ranging between 3.90 m to 7.50 m, and height varying between 13.48 m for pier P1 and 16.66 m for pier P7 (Figure 8.2-b).

The bridge deck is composed by a box girder of variable inertia with approximately 10 m wide and height raging from 4 m to 8 m. The deck has a total width of 29.95 m, where 2 × 1.15 m are sidewalk technical paths. The construction of the box girder core started with a so called *segment 0*, which later supported the positioning of the movable scaffold system for the segmental construction of the girder core – cantilever construction (Figure 8.2-c). In a straightforward description, this movable structure was recurrently mounted and dismounted. After positioning, works related with reinforcement arrangement, metallic sheaths and anchorage systems installation were performed. Then, the concrete pouring of the girder segment was performed. Finally, the prestressing cables were tensioned and the movable scaffolding was moved forward to the next segment (Figure 8.2-d). The end-spans were partially constructed with the use of a falsework, which was directly supported on provisory piles due to the low resistance of the soil. The close segments were executed with the support of one of the two movable scaffolds. In the particular case of the closes segments of spans P2P3 and P4P5, pushing forces were

applied before the concrete pouring (Figure 8.2-e). The bridge girder was finished with the concreting of the console-slabs that were built in a second stage. The construction was supported by a metallic truss with a formwork suspended in each extremity. After the formwork positioning, the construction process is similar to the adopted for the box girder core (Figure 8.2-f).

Finally, the bridge construction was finished with the concreting of the service sidewalks, the bituminous layer, positioning of expansion joints, exterior safety barriers, railings and border beams. Table 8.1 resumes the time history of the main bridge construction.

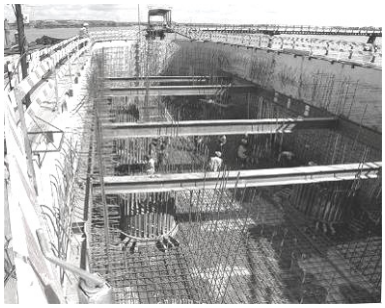

a) foundations (pilecap).

b) piers.

c) box girder – segment 0.

d) box girder.

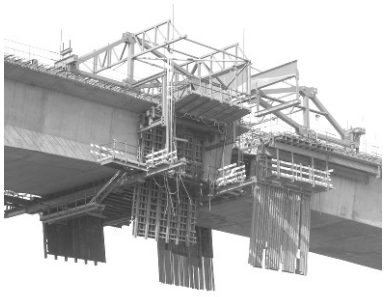

e) close segments.

f) deck consoles.

Figure 8.2 : Construction views of the main bridge.

Table 8.1 : Time history of the main bridge construction.

		2006				2007			
		1st	2nd	3th	4th	1st	2nd	3nd	4nd
Piles									
Columns									
Deck	Box girder core								
	Console-slabs								
	Continuity prestressing								
	External prestressing								

8.3. THE MONITORING SYSTEM

Lezíria Bridge is equipped with an integrated monitoring system to support the management and surveillance of the structure. In what it concerns to the main bridge, several cross sections were instrumented with suited sensors based on electrical and optical technology. Although the instrumentation cover all the length of the bridge, two zones were heavily instrumented since the construction: (i) Zone 1, referring to the first three spans between piers TPN and P3 and (ii) Zone 2, referring to the last two spans between piers P6 and TPS (Figure 8.3). Outer of these zones, the instrumentation is more sparse and only with optical sensors. Measurements concerning mainly these two zones are focussed in this chapter because they were monitored since the early age of the construction.

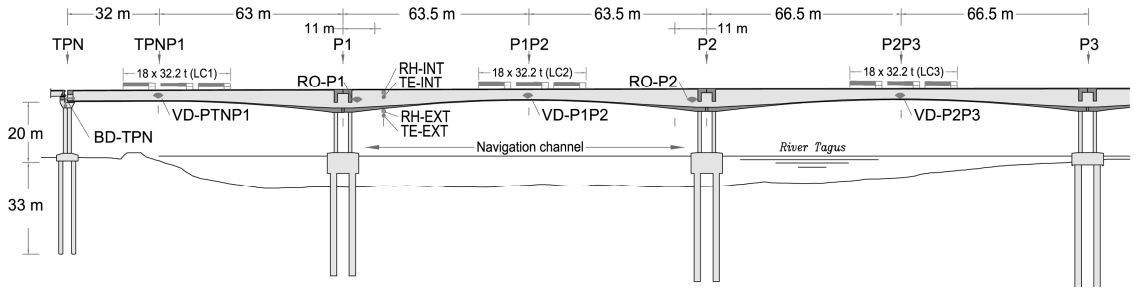

a) Zone 1.

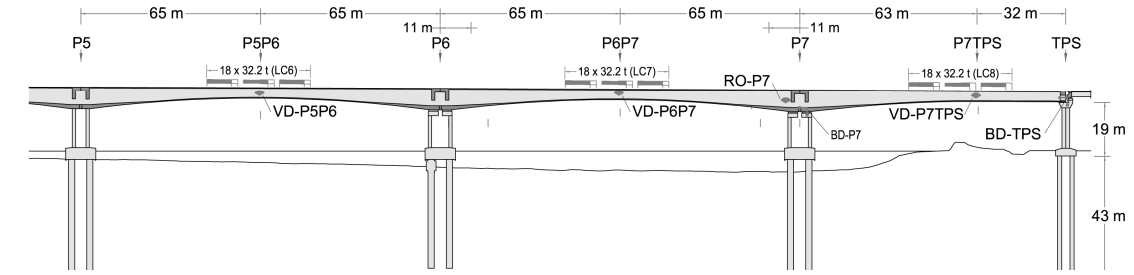

b) Zone 2.

Figure 8.3 : Elevation of the main bridge zones intensively instrumented.

Therefore, focussing the Zone 1 and Zone 2, and in accordance with Figure 8.3, the majority of the sensors installed were vibrating wire strain gauges to measure concrete deformations (CD) in specific cross sections, namely located at: (i) 11 m apart the pier axis and (ii) the mid-span. Figure 8.4 details the positioning of the strain gauges installed in these sections. Generally, six sensors were installed in each section, excepting sections P1 and P1P2 where two additional sensors were installed at the extremities of the console-slabs. The strain gauges have an internal thermistor, which was used to measure the

concrete temperature (CT), namely in the strain gauges installed in sections P1 and P1P2. The strain values captured by the vibrating wire strain gauges were corrected by removing the effect of the free thermal deformation of the wire and the concrete. For this purpose, the thermal dilation coefficient took the value 11×10^{-6} C^{-1} in the case of the wire (given by the manufacturer) and 7.9×10^{-6} C^{-1} in the case of the employed concrete (Sousa and Figueiras 2009a). Sensors measurements were generally taken since the concrete pouring, and when this was not possible, reference readings were taken before the concreting.

The bearing displacements (BD) at the supports TPN, P7 and TPS were also monitored (Figure 8.3). The vertical displacements (VD) of all mid-span sections were also measured with specific sensors developed for this bridge based on a hydrostatic leveling system (Figure 8.3) (Figueiras *et al.* 2010). Eight load cases, LC1 to LC8, are also indicated in Figure 8.3, which are used later for the results discussion. These load cases, with three alignments of six trucks placed at the girder cross section, correspond to the maximum deflection of the eight spans of the bridge, respectively.

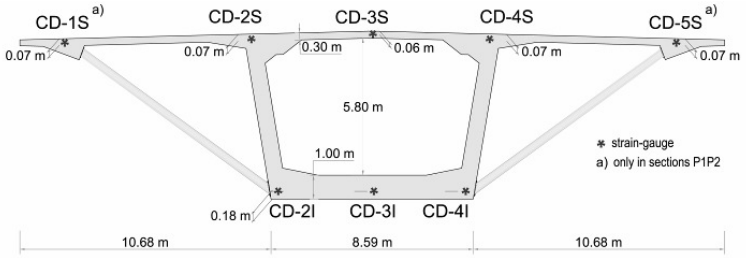

a) 11 m apart the pier axis.

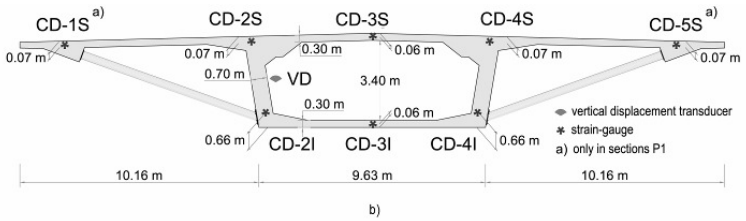

b) mid-span.

Figure 8.4 : Layout of the vibrating wire strain gauges positioning at cross section.

Regarding the long-term behaviour, strains and temperatures were also recorded in ten prisms with dimensions of 15 cm × 15 cm × 55 cm, with two long faces unsealed. Six of these ten prisms were used for shrinkage measurements while the other four prisms were used for creep measurements. The prisms were cast with the same concrete of the girder

and kept under to the same curing conditions. In order to get a more comprehensive characterization of the concrete employed in the deck girder, two shrinkage prisms were cast with concrete of Zone 2, while the remaining prisms (shrinkage and creep) were cast with concrete of Zone 1

Additionally, the environment temperature and relative humidity of the inside and outside of the box girder at section P1 were measured as well as durability parameters and accelerations. A complete description of the monitoring and data acquisition system installed in Lezíria Bridge can be found elsewhere (Sousa *et al.* 2011b). Table 8.2 summarizes the distribution of the instrumentation with relevance for this study.

Table 8.2 : Instrumentation plan for the main bridge.

Parameter	TPN	TPNP1	P1	P1P2	P2	P2P3	P6P7	P7	P7TPS	TPS
Vertical displacement	✓	✓		✓	✓	✓	✓	✓	✓	
Bearing displacement	✓								✓	✓
Rotation			✓		✓			✓		
Deformation		✓	✓	✓	✓	✓	✓	✓	✓	
Temperature			✓							
Humidity			✓							

8.4. FINITE ELEMENT ANALYSIS

8.4.1. GENERAL CONSIDERATIONS

A non-linear finite element analysis was conducted by using the general-purpose finite-element code DIANA (Witte 2005). Structural discretization was carried out using beam finite elements, in accordance with the Timoshenko theory. The elements are numerically integrated along the beam axis and at the cross sections. Longitudinally, each beam element has three nodes and is based on an isoparametric formulation (Zienkiewicz 1971). The discretized beam elements are approximately 1 m to 2 m long, depending on the structural element type (piles, piers or girder). In this model, both geometry and loading are symmetric to the girder axis. The reinforcement, both ordinary and prestressed was modelled using embedded reinforcement elements, whose deformation is calculated

from the displacement field of the concrete finite-elements in which they are embedded. In this way, prestress losses due to concrete creep and shrinkage are automatically accounted for. The piles-soil interaction was modelled with elastic springs.

A phased analysis with 105 stages was performed, where the model was changed by including new elements and/or modifying the connection to the supports at each new stage. The sequence adopted in the analysis follows the real chronology observed during the construction (see Table 8.1) (TACE 2007).

Errors are inevitable in the development of FEM devoted to large structures, namely due to data input (Catbas *et al.* 2007). To mitigate potential errors during the process, CAD tools were specifically developed to allow a full and detailed scanning of the drawing pieces with time-consuming benefits (Sousa and Figueiras 2009b). More information about these tools can be found in Appendix B.

8.4.2. STRUCTURAL MODELLING

The construction of the geometric model was based on the final drawings of the bridge project (COBA-PC&A-CIVILSER-ARCADIS 2005c). The structural elements, piles, piers and bridge girder, were reduced to their axis as presented in Figure 8.5. As aforementioned, the phased construction of the girder consisted in the construction of the box girder core and afterwards the console-slabs. In order to consider this fact, two overlapped alignments of beam elements were modelled, in correspondence with these structural elements. Moreover, the same displacement field was imposed to these two beam alignments to guarantee the compatibility between them.

The ordinary reinforcement of all structural elements was considered with layers of reinforcement near the concrete faces. An additional reinforcement layer, matching the girder axis, was modelled to take into account the effect of the web reinforcement in the concrete delay deformations. The embedded prestressed cables in the girder concrete were precisely modelled with parabolic elements, in order to have a rigorous evaluation of the prestressing forces (Figure 8.5-b). As regard the external prestressing cables, truss elements were used that were connected to the beam elements of the box girder core through dummy bars (with high inertia) to guarantee the compatibility of the displacement field. To be possible the analysis of the bridge behaviour since early ages, the movable

scaffolding system used in the cantilever construction was also modelled with beam elements, which were supported on the deck girder. Globally, the numerical model has 1804 beam elements, 633 truss elements, 5106 reinforcement elements, which include ordinary reinforcements and prestress cables, 248 spring and 16 support points.

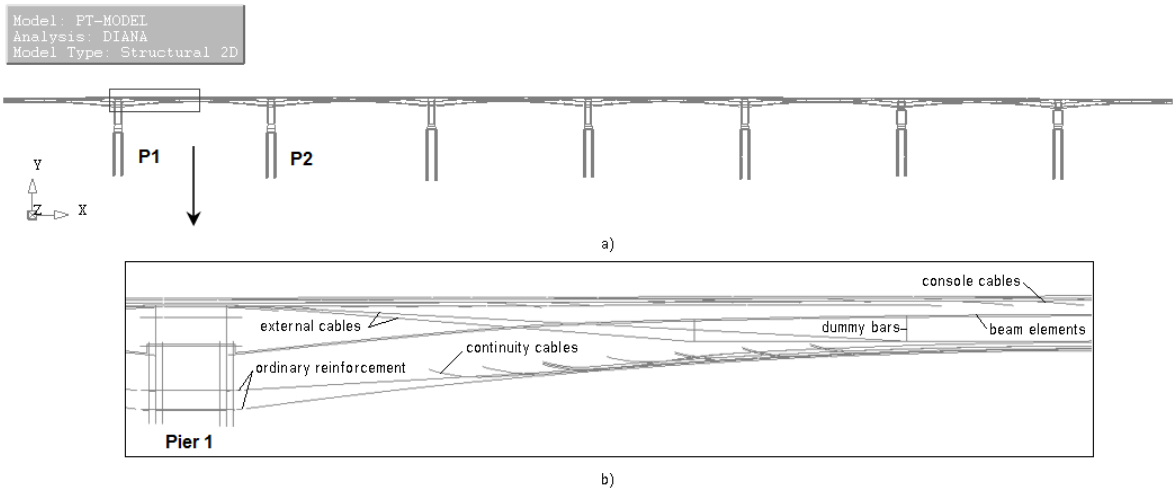

Figure 8.5 : FEM of the main bridge (DIANA output): a) general view; b) detailed view of half span P1P2.

8.4.3. CONCRETE MODELLING

In concrete structures, to obtain a correct prediction of the structural behaviour, an accurate modelling of the material properties is required, namely for the concrete. Therefore, the definition of the mechanical properties of concrete were based on the tests of 150 mm cubes, which were performed during the construction (TACE 2007), and measurements taken from the reference concrete prisms to evaluate the shrinkage and creep.

The expressions proposed by the European code Eurocode 2 (EC2), were considered to describe the time variation of the concrete properties, namely the modulus of elasticity, creep and shrinkage (Standardization European Committee 2004). Whenever possible, the value of the parameters involved in those expressions was obtained from the measurements. Moreover, concretes with different mechanical properties were considered in the FEM analysis to take into account the phased concrete pouring performed during the

bridge construction, namely grouped by piles, piers and segmental construction of the deck girder.

- **Evolution of concrete compressive strength**

The consideration of the concrete compressive strength evolution is mandatory for a long-term analysis, since it is correlated with the evolution of the concrete modulus of elasticity. The concrete compressive strength was calculated based on compressive tests performed in 15 cm cubes. An extensive study was performed to characterize the compressive strength of different structural elements, namely piles, piers and girder. Since the cylinder strength was not experimentally evaluated, it was taken as 82 % of the observed cube strength as recommended by EC2 (Standardization European Committee 2004). Table 8.3 resumes the statistical information concerning the compressive strength at 28 days.

Table 8.3 : Compressive cylinder strength of concrete at 28 days (MPa) – statistical data.

Element type	Minimum value	Maximum value	Mean value	Standard deviation	Coefficient variation
Piles (C35/45)	41.0	56.3	50.4	4.4	8.7 %
Piers (C45/55)	53.7	59.7	56.6	2.5	4.4 %
Deck (C40/50)	48.4	62.0	55.5	2.9	5.2 %

Based on these results, the compressive strength at a given age, $f_{cm}(t)$, is given in the EC2 by Eq. (40).

$$f_{cm}(t) = \beta_{cc}(t) \cdot f_{cm} \quad , \quad \beta_{cc}(t) = \exp\left[s \cdot \left(1 - \sqrt{\frac{28}{t}} \right) \right] \tag{40}$$

where t represents the concrete age in days, s is a cement-hardening coefficient that characterizes the evolution of the concrete strength, and f_{cm} is the mean value of the

concrete compressive strength, at the age of 28 days. The parameter s was determined by a curve fitting procedure, which consisted in minimizing the mean square error between the cube test results (at different ages) and the Eq. (40). Figure 8.6 illustrates the curve fitting results for the concrete in the instrumented zone, namely of pile 1, pier 1 and segment 1 of the pier P1 (Figure 8.3), whilst Table 8.4 resumes the values obtained for those parameters, grouped by different structural elements.

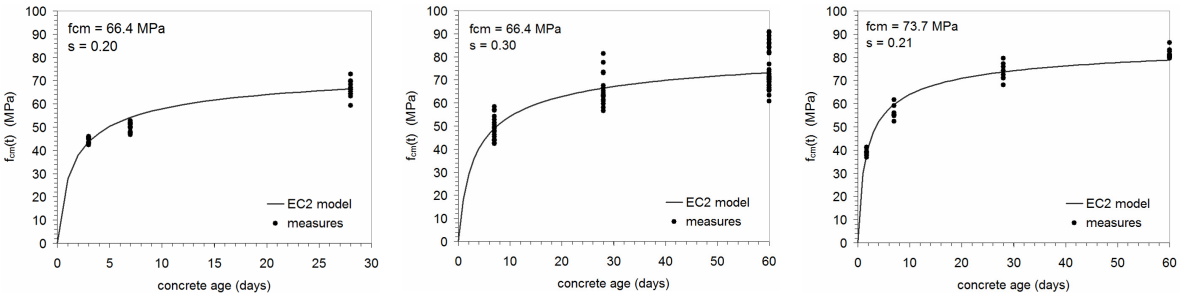

a) pile P1. **b) pier P1.** **c) segment 1 of pier P1.**

Figure 8.6 : Compressive strength evolution.

- **Modulus of elasticity**

The determination of the tangent modulus of elasticity, E_c, was based on the observed concrete compressive strength, by means of the Eq. (41).

$$E_c = 1.05 \cdot 22000 \cdot \left(f_{cm,cyl}/10\right)^{0.3} \qquad (E_c \text{ and } f_{cm,cyl} \text{ in MPa}) \tag{41}$$

where $f_{cm,cyl}$ represents the mean value of the concrete cylinder strength at the age of 28 days (Table 8.3). According with EC2, the evolution of the modulus of elasticity correlates to the time variation of the compressive strength (determined above), and is given by Eq. (42). Table 8.4 resumes the average values, depicted by structural element type.

$$E_c(t) = \beta_E(t) \cdot E_{c(28)} \quad , \quad \beta_E(t) = \exp\left[\frac{s}{2} \cdot \left(1 - \sqrt{\frac{28}{t}}\right)\right]^{0.5} \tag{42}$$

Table 8.4 : Mechanical properties of concrete - average values.

Element type	f_{cm} (MPa)	E_{cm} (GPa)	s
Piles	50.4	37.5	0.23
Piers	56.6	38.8	0.25
Deck	55.5	38.6	0.26

- **Shrinkage**

The total shrinkage strain, ε_{cs}, is set by two parts as expressed in Eq. (43): the drying shrinkage strain, ε_{cd}, and the autogenous shrinkage strain, ε_{ca}. The drying shrinkage strain develops slowly, since it is a function of the migration of water through the hardened concrete, while the autogenous shrinkage strain develops during concrete hardening phase (Standardization European Committee 2004). The mathematical models given by EC2 for the drying and autogenous shrinkage are presented in Eq. (44) and Eq. (45), respectively, and they are expressed through a multiplicative model with a nominal coefficient, $\varepsilon_{c,\infty}$ and a time factor, $\beta_s(t)$.

$$\varepsilon_{cd}(t) = \varepsilon_{cd}(t) + \varepsilon_{ca}(t) \tag{43}$$

$$\varepsilon_{cd}(t) = k_{cs,0} \cdot \varepsilon_{cd,\infty} \cdot \beta_{ds}(t, t_s)^{k_{cs,t}} \tag{44}$$

$$\varepsilon_{ca}(t) = \varepsilon_{ca,\infty} \cdot \beta_{as}(t) \tag{45}$$

where t is the time (in days) since drying begins, t_s. Additionally, $k_{cs,0}$ and $k_{cs,t}$ were introduced in Eq. (44) so that the drying shrinkage model could be scaled and adjusted to the experimental results obtained from the concrete prisms (Santos 2002). In fact, the autogenous shrinkage was not considered in the fitting problem, because the major part develops in the early days after casting (Standardization European Committee 2004). However, the autogenous shrinkage was not neglected because the measurements collected from the concrete prisms had started since the concreting. Instead, its effect was removed from the measurements by subtracting a quantity expressed by Eq. (45) to allow the fitting process to the drying shrinkage model, and afterwards it was added. Therefore, the model

presented in Eq. (43) was fitted to the strain measurements performed in the concrete prisms.

Regarding the influence of the inside and outside environments that enclose the concrete faces of the box girder, the concrete prisms were positioned inside and outside of it. The influence of each of these environments on the time-delay deformations of the concrete is difficult to establish (Santos 2007). However, and for simplicity, the contribution of each one is taken proportional to the exposed perimeter of the cross section to both environments. Therefore, the time-delay deformations of the girder concrete are calculated based on 30 % of the prisms placed inside the box girder and 70 % of the prisms placed outside. Additionally, and based on measured values, an average temperature of 18.8 ºC and 16.1 ºC, and a relative humidity of 51.8 % and 64.0 % were taken for the interior and exterior environments, respectively. The assumption of average values for temperature and relative humidity is acceptable without significant errors for long-term analysis (Barr *et al.* 1997).

In this context, Figure 8.7 presents the results achieved for the concrete shrinkage of Zone 1 and Zone 2 (see Figure 8.3). For both cases, the exterior prisms shrink more than the interior ones. Even though, the measures of the interior prism of Zone 2 seems to approximate to the exterior one as the time passes, while respecting the Zone 1 the prisms of both environments exhibited a different initial evolution during the first 250 days and after that they have been evolved with parallel patterns. The positioning of the exterior prisms over the top slab of the deck girder during the construction led to a direct exposure to the sun, which favors the evolution of shrinkage. After the construction, the exterior prisms where placed on the top of the transition piers and sheltered from the sun under the deck girder (see Figure 8.3), which altered the environment conditions and slowing down the shrinkage evolution as it can be observed in the presented results.

Regarding the theoretical models, small differences are achieved between the measured values and the predictions given by the EC2 model, namely for the trend with $k_{cs,0}$ values near the unit. Even though in a slight manner, the EC2 model overestimates the shrinkage deformations for the prisms of Zone 1 while underestimates for the ones of Zone 2. In other words, although the shrinkage deformations are almost equal for both zones, rounding 500 με after 1250 days ($k_{cs,0} \cong 0.96$), the evolution in the first ages are different with a more pronounced form for the prisms of Zone 2 ($k_{cs,t} = 0.90$ for prisms of Zone 1

and $k_{cs,t} = 0.41$ for the prisms of Zone 2). The different concrete mixing centrals that served both zones during the construction as well as the fact that pumped concrete was used are some factors with direct influence in the shrinkage evolution.

The cross-sectional shape influences the evolution of the shrinkage strains and this dependence is commonly expressed by the notional size (Standardization European Committee 2004). The notional size of the structural elements of the bridge ranges between 495 mm to 1575 mm, which is significantly higher than the shrinkage prisms that are 150 mm. The strategy employed in this work was to derive the shrinkage curves of the structural elements based on their effective notional size and the fitted curve obtained for the shrinkage prisms (Figure 8.7). Moreover, the thickness differences between the bottom slab, web and top slab is another important aspect in the long-term analysis of the structural behaviour of the bridge (Kristek *et al.* 2006; Zdenek Bazant *et al.* 2008; Malm and Sundquist 2010).

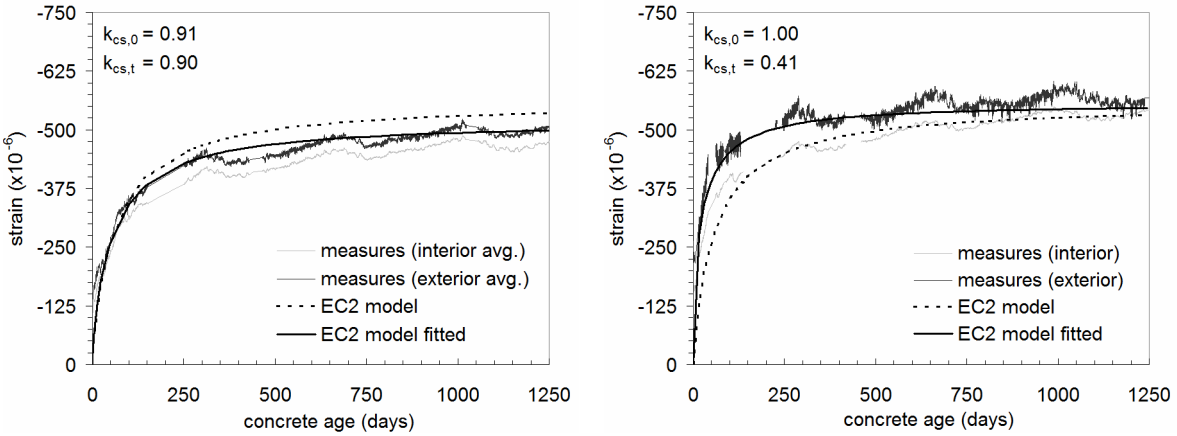

a) Zone 1. **b) Zone 2.**

Figure 8.7 : Shrinkage strains of the concrete prisms.

Detailing the Lezíria Bridge case, the bottom slab has 1.50 m thickness near the piers, while the top slab has a constant thickness of 0.30 m, which means that the evolution of concrete deformations occur more slowly in the bottom slab than the top slab. Therefore, the cross section was split in three different zones – bottom slab, webs and top slab –, and different shrinkage curves were quantified for each of these zones and also for each segment. That is, for a specific cross section, all mechanical parameters are the same excepting the notional size parameter that changes in accordance with the zone type, allowing different shrinkage evolutions in the same cross section. Figure 8.8 depicts the

shrinkage curves obtained for the different structural elements of the bridge with the box girder results unfolded into the three referred zones. Concerning the obtained results for the bottom slab, for sections near the piers the shrinkage curves are similar to the ones obtained for the webs, while for sections near the mid-span the shrinkage curves approach to the ones obtained for the top slab zone. After 1250 days, the shrinkage deformations expected for the bottom slab ranges approximately from 190 με to 370 με. In other words, after 1250 days, the shrinkage deformations of the bottom slab near the piers are expected to be approximately half of the ones near the mid-span. Globally, 333 shrinkage curves were calculated and uploaded into the input file for the FEM analysis, in order to take into account the enounced aspects.

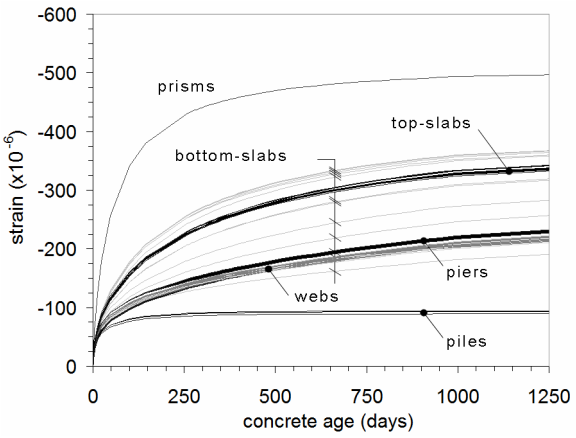

Figure 8.8 : Shrinkage curves for the structural elements of the main bridge.

- **Creep**

According with the EC2, the creep deformations of concrete, $\varepsilon_{cc}(t,t_0)$ at a generic time t for a constant applied compressive stress at the age t_0 is given by Eq. (46), where $\varphi(t,t_0)$ is the creep coefficient and $\varepsilon_c(t_0)$ is the instantaneous deformation due to the applied compressive stress. Moreover, EC2 sets the creep coefficient according to Eq. (47).

$$\varepsilon_{cc}(t,t_0) = \varphi(t,t_0)\cdot\varepsilon_c(t_0) \tag{46}$$

$$\varphi(t,t_0) = k_{cc,0}\cdot\varphi_0\cdot\left[\beta_c(t,t_0)\right]^{k_{cc,t}} \tag{47}$$

where φ_0 is the notional creep coefficient and $\beta_c(t,t_0)$ is a function to describe the development of creep with time after loading. Similar to the shrinkage, the additional parameters, $k_{cc,0}$ and $k_{cc,t}$ were introduced in Eq. (47) so that the creep model could be scaled and adjusted to the experimental results (Santos 2002; Carlos Sousa and Neves 2009b). Therefore, the EC2 model was fitted to the strain measurements performed in the concrete prisms. Moreover, the contribution of each environment, inside and outside the box girder, is taken proportional to the exposed perimeter of the cross section to both environments, i.e. the same procedure adopted for the shrinkage case.

In this context, Figure 8.9 plots the results achieved for creep. The interior prisms creep more than the exterior ones. Although the similar pattern observed to the shrinkage prisms (Figure 8.7-a), i.e. the prisms of both environments exhibited a different initial evolution during the first 250 days and after evolved with parallel patterns, in this case the interior prisms are the upper bound. By the same reasons pointed out for the case of the shrinkage prisms, it is difficult to explain this behaviour. The creep evolution is also function of the stress level applied to the concrete prisms and therefore, inaccuracies in the applied pressure can led to different creep evolutions. Nevertheless, this cannot explain the similar pattern after the end of the construction. Thus, the results led to conclude that the particular conditions of the construction phase influenced the creep evolution for the first ages with different patterns for the interior and exterior prisms.

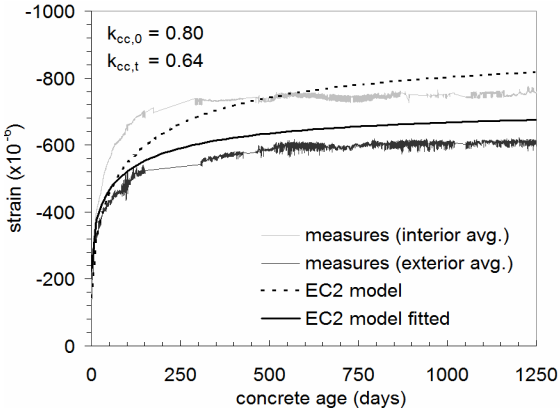

Figure 8.9 : Creep strains of the concrete prisms.

Again, a more realistic model is attained with the fitted model as it is presented in Figure 8.9, where it is clear that the EC2 model overestimate the creep deformations. In fact, differences between observed values and code predictions were expected since the

employed concretes contain superplasticizers and pozzolanic materials, whose effect in the composition cannot be accurately reproduced by code formulae (Bazant 2001). Similar to the strategy adopted for the shrinkage, the notional size was considered to scale the creep function to the structural elements of the bridge.

8.4.4. PRESTRESS CABLES MODELLING

An exhaustive scanning was carried out to characterize the modulus of elasticity of the employed prestress steel, based on the manufacture specifications (TACE 2007). This information was considered into the FEM analysis by taking the average value of the prestress cables used for each cables group. Globally, an average value of 196.6 GPa was achieved, which satisfies the limits of 195 GPa to 210 GPa EC2 (Standardization European Committee 2004). Moreover, the minimum and maximum values obtained were 188.2 GPa and 205.0 GPa, respectively, with a coefficient of variation of 2.3 %. Taking the fact that the prestressed cables have low relaxation and were conducted in flexible metal ducts: (i) the wobble coefficient K, per meter, was fixed to 0.05; (ii) the coefficient of friction, μ, was set to 0.19 and (iii) a relaxation class 2 was adopted (Carlos Sousa and Neves 2009a; FIB Commission on Practical Design 2010a).

8.4.5. SOIL MODELLING

The interaction between the piles and the soil was modelled with elastic springs based on the Winkler model. The spring stiffness is proportional to the influence area of the spring, A_{inf}, and the subgrade reaction module, k_s (Sousa 2006a). The A_{inf} is defined by the pile diameter, ϕ, multiplied by an influence length, L as expressed in Eq. (48). As regards the k_s value, it was evaluated based on field tests performed by the constructor (COBA-PC&A-CIVILSER-ARCADIS 2005b). Table 8.5 resumes the average values with interest for this work, which were used to compute the stiffness of the soil springs. The deepness values are reference values, which in reality they were taken variable along the bridge lenght.

$$k_v = k_s \cdot A_{\text{inf}} \quad , \quad A_{\text{inf}} = \phi \cdot L \tag{48}$$

Table 8.5 : Subgrade reaction modulus, ks.

Soil description	Clay deposits	Sludge	Muddy fine to medium sand	Medium sand	Clay silt
Deepness (m)	0 to 2	2 to 6	4 to 6	6 to 8	> 6
ks (MN/m3)	4 to 8	1 to 2	7 to 3	8 to 2	90 to 120

8.4.6. LOADING

The loads used in the analysis were: (i) self-weight of the reinforced concrete, with a value of 25 kN/m^3; (ii) self-weight of the movable scaffolding systems, with values ranging between 570 kN to 1127 kN, based on the equipment specifications (TACE 2007); (iii) effective forces applied in the prestressing cables based on stretching measurements, which were estimated to be, in average, 10 % lower than the design values. This deviation is mainly conditioned by the stretching results obtained for the continuity prestressing, which corresponded to 15 % less than the design values; (iv) remaining dead loads composed by the bituminous layer, border beams, service sidewalks and safety barriers with an estimated value of 93.7 kN/m; (v) trucks full charged used for the load test with an average weight of 32.2 tons (315.9 kN) each and a standard deviation of 0.5 tons (5.2 kN).

8.5. RESULTS AND DISCUSSION

8.5.1. LOAD TEST

It is a fact that any prediction obtained by a numerical model presents deviations to the real behaviour. Even tough, it is always important to have a numerical model capable of represent, as much as possible, the effective characteristics of the structure in order to get reliable predictions. The best strategy to achieve this objective is starting by validating the numerical model with measurements obtained from load tests, taking profit that the loading is perfectly known and controlled a priori.

Figure 8.10 depicts the obtained results for the load test performed on the main bridge. The vertical displacements obtained by the numerical model, concerning the mid-span sections, present good compliance with the measurements. The errors range between −4.1 % for section P7TPS and +6.6 % for section P6P7. Moreover, a similar trend is attained by the numerical model, which presents the maximum displacement for section P6P7, 28.5 mm in correspondence to the observed 26.7 mm, and the minimum for section TPNP1, 21.3 mm in correspondence to the observed 21.2 mm. Now focussing the results obtained for Zone 1 (see Figure 8.3), and as the rotation is concerned, the results presented in Figure 8.10-b exhibits higher deviations, with a maximum value of 12.1 % for section P1 and 10.2 % for section P2. These errors are approximately the double of the ones obtained for the vertical displacements. However, it must be take into account that these sections near the piers are subjected to high shear efforts, leading to a warp of the cross sections. Therefore, additional deviations are expected due to this fact. As regard the curvatures, which were calculated based on the strains measurements (see Figure 8.3), the numerical results matches the observed values for the sections P1 and P2 (Figure 8.10-c), while for the mid-span sections PTNP1, P1P2 and P2P3, the deviations are slight higher with a maximum deviation of −5.8 % for section P2P3 (Figure 8.10-d).

Globally, the results herein presented enable the validation of the numerical model and therefore, the representativeness of the effective structural behaviour of the main bridge is attained.

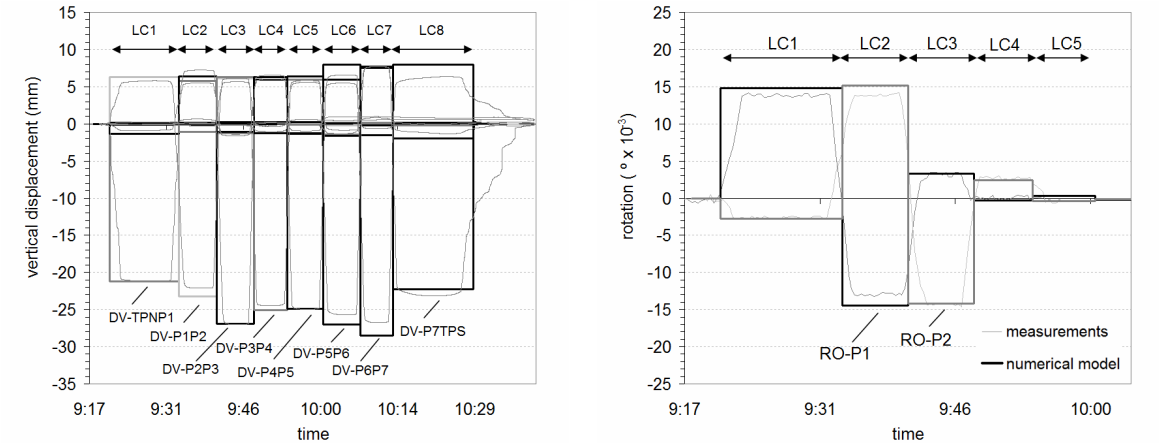

a) vertical displacements. **b) rotations.**

Figure 8.10 : Load test results for the main bridge.

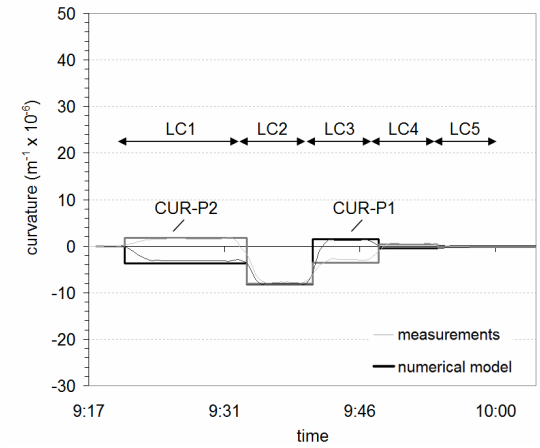

c) curvature of sections near the piers.

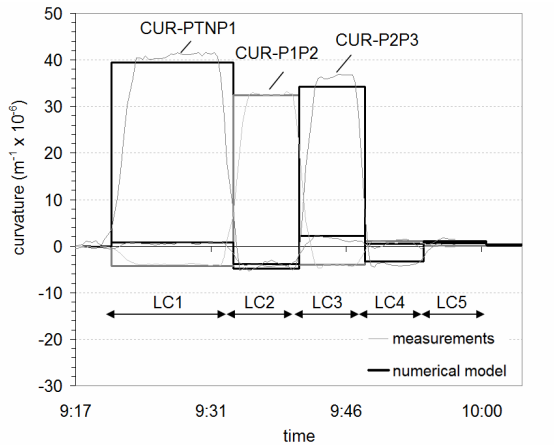

d) curvature of mid-span sections.

Figure 8.10 : Load test results for the main bridge. (cont.)

8.5.2. CONSTRUCTION ASSESSMENT

The instrumentation and observation of the main bridge behaviour during the construction was the most challenging and interesting phase. Since the early ages, the concrete deformations (CD) of the three girder sections instrumented near the piers, P1, P2 and P7 were monitored, which allowed to follow the deck girder construction based on the cantilever method. As the construction was reaching to its end, the concrete deformations of the close segments PTN3P1, P1P2, P2P3, P6P7 and P7PTS1 were also monitored since the early ages. Additionally, the bearing displacements of the supports in sections TPN and P7 and TPS and the rotations of the girder over the piers P1, P2 and P7 were also measured, namely since the construction of the close segments (see Figure 8.3).

- **Concrete pouring**

Strain and temperature measurements of the concrete since the early ages are valuable information in order to get a better understanding about the initial pattern of shrinkage and creep. During this initial period, the concrete mass is transforming to a structural material and therefore, these measurements are important to correctly establish the zero-reference for the sensors' measurements. Regarding the instrumented segment near pier P1 (see Figure 8.3 and Figure 8.4), Figure 8.11 presents the temperatures and strains evolution of the concrete at the bottom and top slabs during the first weeks after concrete pouring. The

results show a higher temperature peak in the bottom layer with a value of approximately 55 ºC, while in the top layer a peak value near the 40 ºC is registered. Focussing the temperature registers, the different patterns observed for both layers can be explained by the influence of the formwork of the movable scaffolding, which difficult the heat dissipation during the concrete hardening mainly in the bottom layer. Approximately, the concrete temperature only stabilizes five to seven days after the concrete pouring, which almost matches the construction of the following segment.

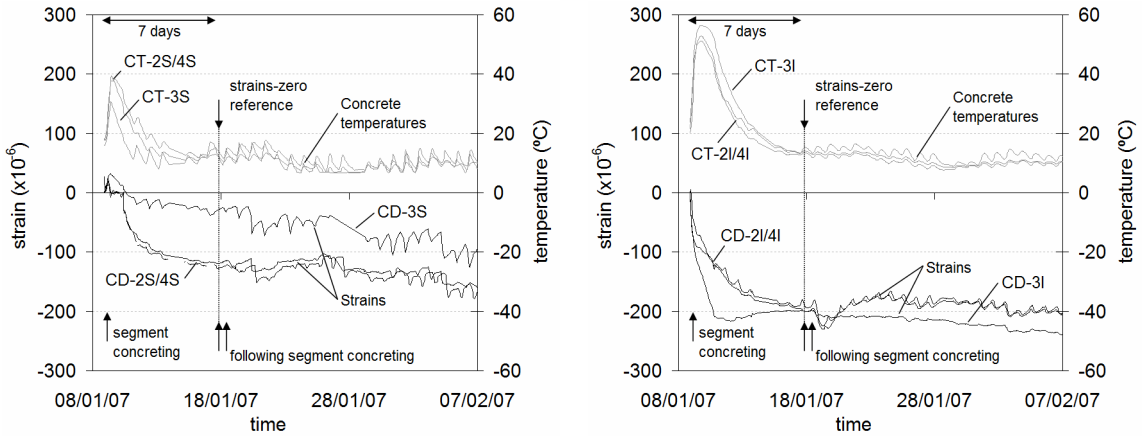

a) section P1 – top layer. **b) section P1 – bottom layer.**

Figure 8.11 : Measurements of concrete deformations and concrete temperatures during the first days after concreting.

In addition to the different patterns observed in the bottom and top layers, it worth to be highlighted the particular pattern evolution of the sensors at the position 3I and 3S. Although the sensors in each layer are approximately at the same distance of the concrete face, the sensors located in these zones have different boundary conditions when compared with the ones placed along the alignments 2 and 4 (see Figure 8.4). For example, the sensors at positions 2I and 4I have two concrete faces nearby, while the sensor at the position 3I has only one face. Therefore, a higher peak for the concrete temperature at position 3I is expected with a more broad evolution, which is in fact observed. This justification is also valid for the sensors at the top slab however, in this case, the sensor at the position 3S has two concrete faces nearby while the sensors at positions 2S and 4S have only one face. Therefore, the temperature peak is smaller and the decrease of temperature is faster when compared with the temperatures measured at 2S and 4S positions. These different temperature patterns led to different evolutions of the concrete

deformations, where an effective correlation can be observed in the results presented in Figure 8.11. Similar results were obtained in sections P2 and P7.

The main purpose of the developed model is to predict the long-term response of the structure, and in this context, the concrete hydration is not taken into account in the calculus procedures. A study concerning the effect of the concrete hydration requires a more detailed FEM analysis, which is a scope out of this work. Therefore, the zero–reference for the strain measurements was established when the temperature stabilized, which occurs approximately 7 days after the segment concreting. Curiously, the zero-reference almost matches to the pouring of the following segment as indicated in Figure 8.11.

- **Segmental construction by cantilever method**

The construction of a bridge segment by the cantilever method can be unfolded in three main phases (Figure 8.12): (i) positioning of the movable scaffolding – phase 0, (ii) reinforcement positioning and concrete pouring – phase 1, (iii) tensioning of the prestressing cables – phase 2, (iv) release of the movable scaffolding and moving forward – phase 3.

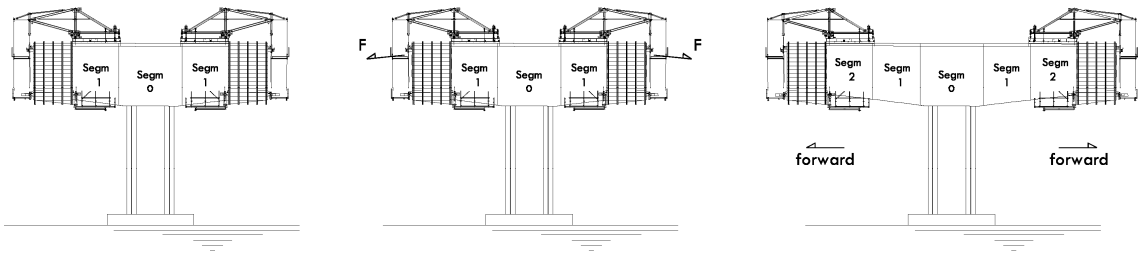

a) concrete pouring (phase 1). b) prestressing (phase 2). c) scaffolding movement (phase 3).

Figure 8.12 : Construction steps of two deck segments of the main bridge.

Figure 8.13 shows the concrete deformations (CD) measured in the sections P1 and P7, and the corresponding results obtained by the numerical model. Generally, the measured values are correctly interpreted by the FEM analysis. Focussing the results obtained for the top layer, different patterns are identified for the sections P1 and P7 during the construction of the firsts segments. The movable scaffolding systems used in both zones can explain these differences. For the cantilever construction above the pier P1, 13

segments were built with lengths ranging from 3 m to 5 m, while 9 segments with lengths between 6 m and 7 m were adopted for the cantilever construction on the pier P7. These different segments' length obligated different prestressing schemes and therefore, different patterns are expected for the evolution of the concrete deformations. The effect of these differences is not so obvious in the bottom layer, which is comprehensive due to the positioning of the console prestressing cables in the top slab.

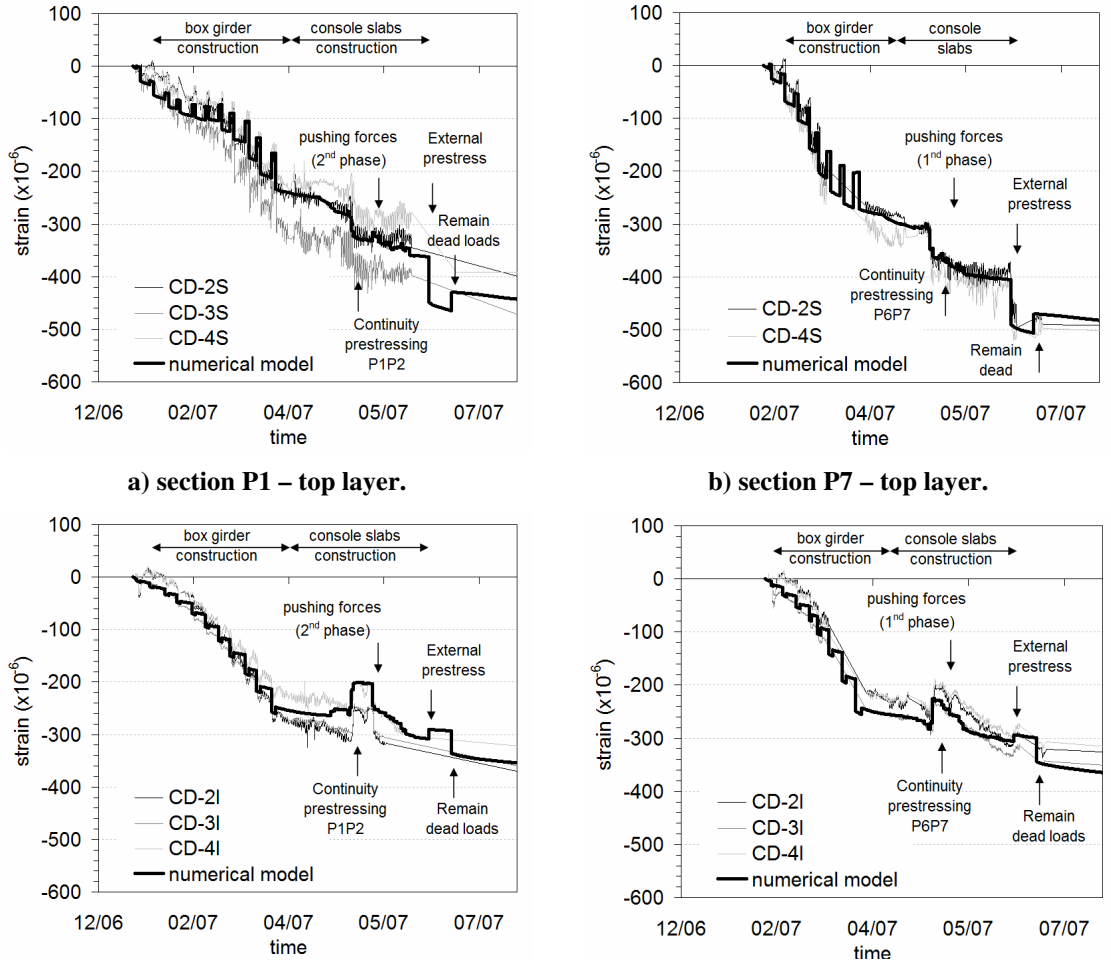

a) section P1 – top layer.

b) section P7 – top layer.

c) section P1 – bottom layer.

d) section P7 – bottom layer.

Figure 8.13 : Concrete deformations in sections P1 and P7 during the construction.

At the end of the construction, the concrete deformations range from 400 με to 500 με in the top layer, while for the bottom layer it ranges from 300 με to 400 με. This means that the sections P1 and P7 are practically uniformly compressed with low bending effect, which was only possible due to the prestressing scheme that compensates the opposite bending effect caused by the weight of the deck girder. Another relevant aspect observed

in the measured values is the mechanical deformation due to the temperature variations. This effect is more pronounced in the top layer due to the direct exposure to the sun that causes higher temperature amplitudes, which justifies the different patterns obtained for the sensors placed at the bottom and top layers.

In correspondence to the results presented in Figure 8.13, Figure 8.14 shows the evolution of the concrete stresses in the same bridge sections. Although the different segment lengths and prestressing schemes, the stress level at the end of construction is practically the same in both sections. More precisely, the concrete stress in the bottom layer is estimated to be - 8.1 MPa and - 8.3 MPa while in the top layer is -11.1 MPa and -11.9 MPa, for sections P1 and P7 respectively. Nevertheless, the stress level along the construction was always inferior to $0.45 \cdot f_{ck}$ and therefore, the concrete service stress limit was not exceeded (Standardization European Committee 2004).

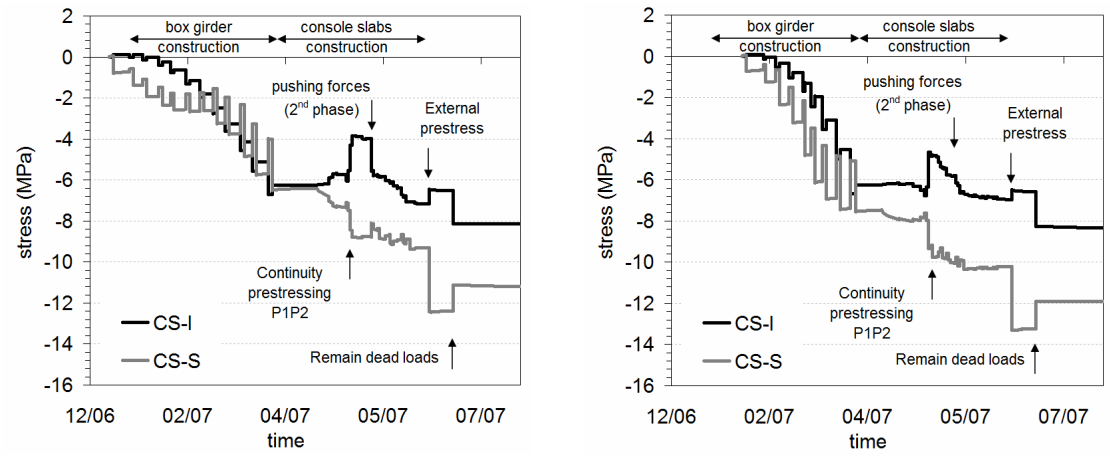

a) section P1. **b) section P7.**

Figure 8.14 : Concrete stresses in sections P1 and P7 during the construction (numerical results).

8.5.3. LONG-TERM BEHAVIOUR

- **Deck girder sections near the piers**

Regarding now the long-term behaviour, the results presented in Figure 8.13 are expanded until the most recent data and presented in Figure 8.15. For sections P7 and P6P7, the presented data is only until August 2010. To improve the results discussion, two numerical

results are plotted: (i) based on the EC2 models and (ii) based on the EC2 models fitted to the prisms measurements according with the results presented in Figure 8.7 to Figure 8.9, which was the basis of the results presented in Figure 8.13 and Figure 8.14. Taking the measurements as baseline, a slight overestimation is committed by using the EC2 models, while the results obtained with the fitted models show a better conformity. The improvement in the trends of the concrete deformations can be explained by the following reasons: (i) although the improvements in the fitting process concerning the shrinkage are relatively reduced, for the creep the decreasing in the trend achieved by the fitted model is not negligible (see Figure 8.9); (ii) the discretization of the cross section in three distinct zones lead to a slower evolution of the delay deformations mainly at the bottom slab near the piers and webs, for which the notional size parameter is clearly greater than the one for the top slab, 1250 mm and 500 mm, respectively. Even so, if the results are regarded in a long-term perspective, they appear to be, or will be soon or latter, bounded by both predictions.

Another relevant aspect is the decrease of the daily variations of the sensors' measurements in the top layer after the end of the construction, which might be justified by the bituminous layer placed at the end of the construction. In addition, the girder section near the pier P7 (see Figure 8.3) exhibits low sensitivity to the seasonal temperature variation, which is mainly visible in the measurements obtained in the top layer. This can be easily understood if the measurements for section P7 are compared to the ones of section P1 (Figure 8.15-a and Figure 8.15-b). The different connection of the girder to the piers can be the reason for the different patterns. In fact, the girder above the pier P1 is monolithically connected to the pier, which is not the case for the zone of the girder above the pier P7 that is supported through bearing supports that allow relative displacements in the longitudinal direction.

Some of the sensors embedded in the position 3S exhibit particular behaviours. The positioning of the concrete safety barriers is exactly above this alignment, which led to different conditions of the concrete surface of the deck girder. In contrary to the positions 2S and 4S, a concreting operation was performed in a second stage in order to prepare the top surface for the safety barrier positioning, which implied additional deformations in the concrete near of the top surface of the box girder due to the shrinkage of the second stage concreting. Therefore, it is expected a different behaviour for the sensor positioned in this alignment as it can be clearly perceived in Figure 8.15-a for the case of section P1. In other

cases, due to the necessity to erode the concrete surface for the positioning of the safety barriers, some sensors in this position have been affected and potentially damaged. Nevertheless, this distinguish pattern is also observed in some other sections.

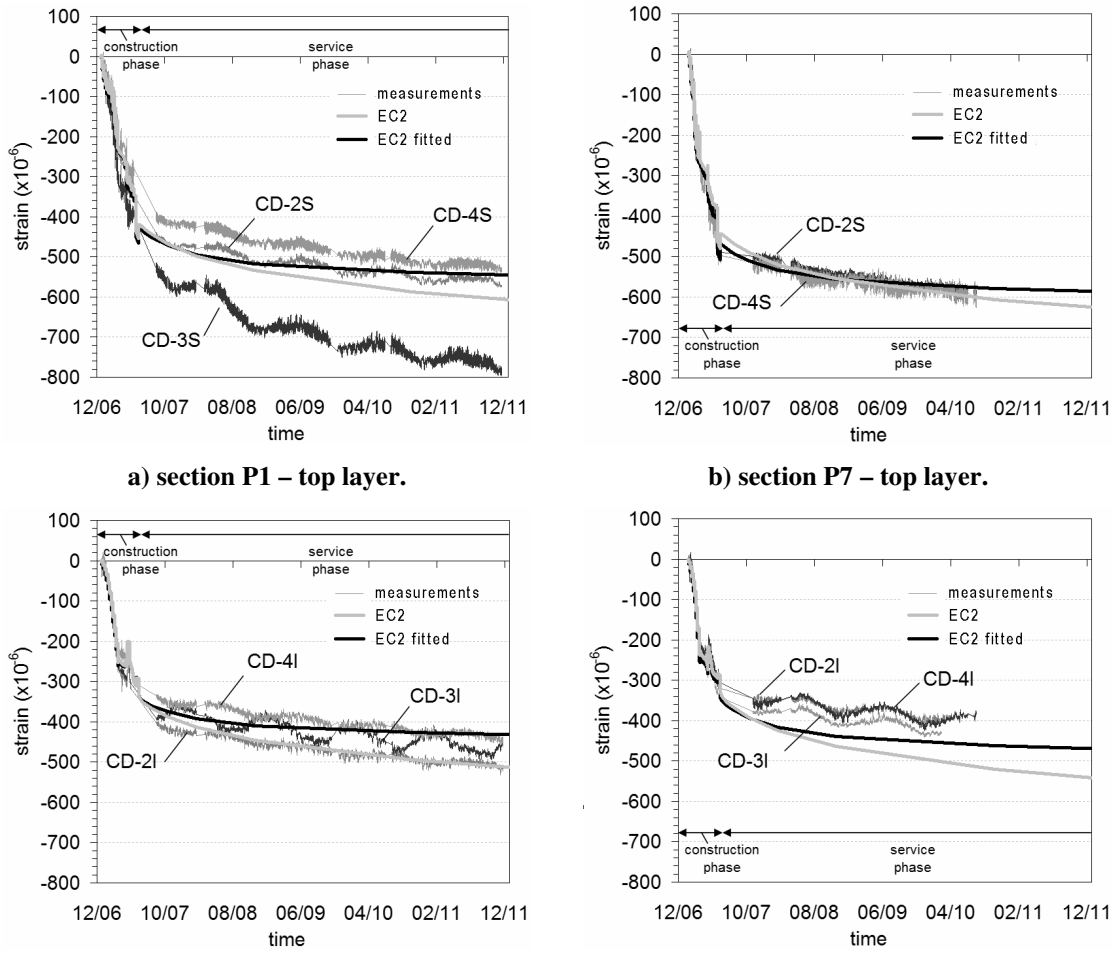

a) section P1 – top layer. **b) section P7 – top layer.**

c) section P1 – bottom layer. **d) section P7 – bottom layer.**

Figure 8.15 : Long-term results – sections near the piers.

- **Deck girder sections at the mid-span**

As regard the mid-span sections, Figure 8.16 plots the results for sections P1P2 and P6P7, in correspondence to the adjacent sections P1 and P7, respectively. Similar to the sections P1 and P7, the calculations based on the EC2 models overestimates the long-term response mainly the trend evolution. Generally, the numerical results obtained with the fitted models exhibit a better conformity, namely in the trend evolution. Even so, if the results are regarded in a long-term perspective, they appear to be, or will be soon or latter, bounded

by both predictions as stated for the obtained results of sections P1 and P7. It must be referred that the continuity prestressing of these segments are not included in the output results due to the zero-reference adopted of 7 days. Again, if an earlier zero-reference was adopted, the measurements would deviate from the numerical results with higher compressions. This effect is mainly due to the temperature variation during the concrete hardening as it was previously discussed and illustrated in Figure 8.11.

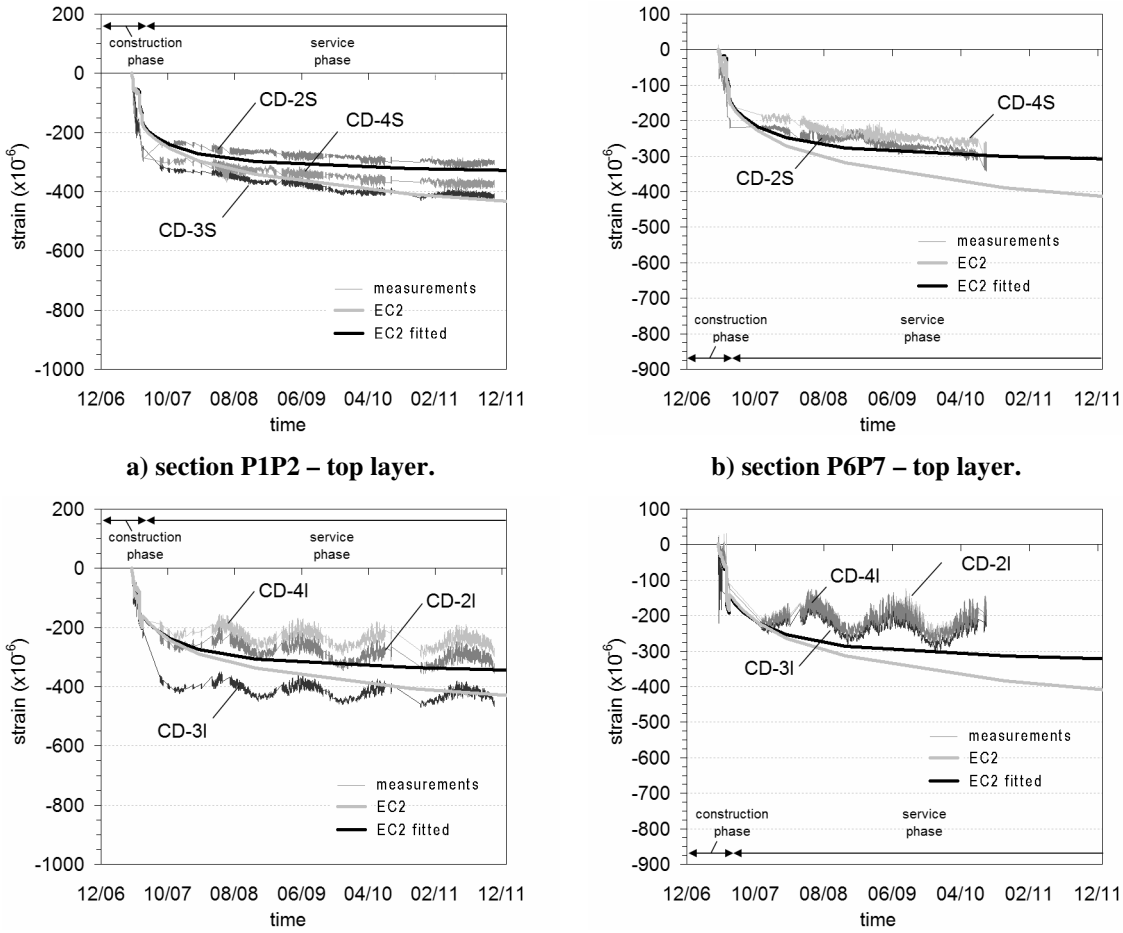

a) section P1P2 – top layer.

b) section P6P7 – top layer.

c) section P1P2 – bottom layer.

d) section P6P7 – bottom layer.

Figure 8.16 : Long-term results – mid-span sections.

- **Bearing displacements**

The knowledge of the bearing displacements evolution has a particular importance for the model validation. In contrary to the strain measurements that are namely influenced by local constraints, the bearing displacements reflect the global behaviour of the bridge.

Moreover, this information is helpful to verify the model performance for horizontal actions. Figure 8.17 depicts the bearing displacements evolution, in sections TPN and TPS (see Figure 8.3) after the end of the construction. Taking the measurements as baseline, the overestimation committed by the EC2 models is confirmed, while the results obtained with fitted models lead to a significant improvement in the results quality. For this case, the deviations committed by the EC2 models are higher than the ones obtained for the concrete deformations, which might be explained by the global representativeness of the bearing displacements that integrates the deformations along the bridge length.

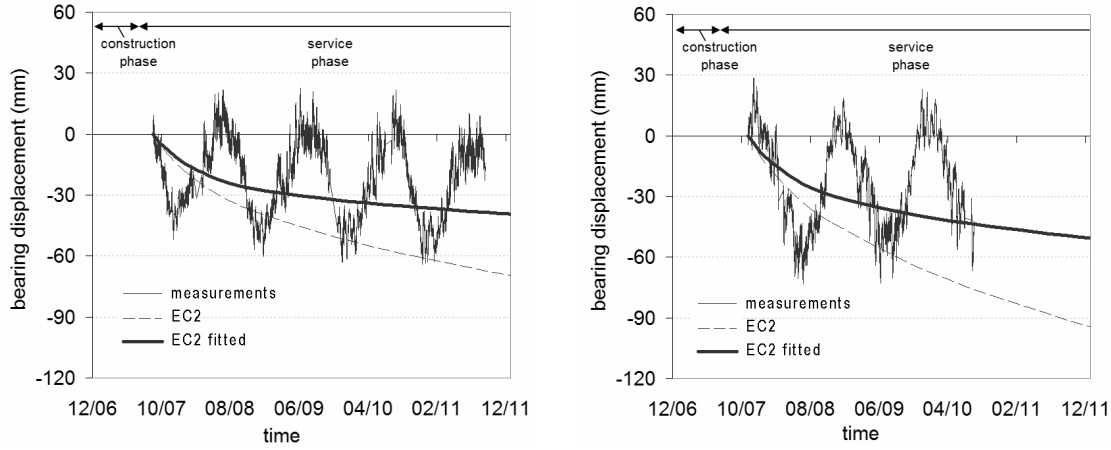

a) section TPN. **b) section TPS.**

Figure 8.17 : Long-term results – bearing displacements.

In summary, and regarding the evaluation of the long-term results herein achieved, two main aspects must be highlighted: (i) the higher the notational size is, slower the shrinkage and the creep evolution. In fact, the notational size of the girder ranges between 495 mm to 1575 mm, which is significantly higher compared to the concrete prisms that is 150 mm (230 % to 950 % higher). The shrinkage of the structural elements was in fact extrapolated based on the measurements of the concrete prisms (Figure 8.8) and therefore, errors associated with this procedure must be taken into account in the discussion of the results (Santos 2002; Santos 2007); (ii) the influence of the interior and exterior environment in the long-term deformations of concrete is another critical aspect. The strategy to consider the contribution of each environment proportional to the exposed perimeter of the cross section to both environments leads to acceptable results. However, the correct quantification is not straightforward and is still difficult to establish (Santos 2007).

8.5.4. PREDICTION FOR THE BRIDGE LIFETIME

Based on the results previously presented, the predictions based on the EC2 (Standardization European Committee 2004) exhibits some deviations, when compared with the measured values, namely in the trends. Therefore, to be considered as the expected values for the sensors' measurements, they should be calibrated focussing the bridge lifetime. In this context, the predictions previously presented were extended for the bridge lifetime of 100 years. In accordance with the monitoring plan presented in Figure 8.3 and Table 8.2, the results are summarized in Figure 8.18. Two results are plotted: (i) based on the EC2 models and (ii) based on the EC2 models fitted to the prisms measurements.

Starting with the results obtained for the vertical displacements (Figure 8.18-a), the gathered values with the EC2 models are superior to the ones obtained with the fitted models, which was already expected considering the results presented until now. Excepting the extreme sections, TPNP1 and P7TPS, the calibrated results correspond to 22 % – 47 % of the ones obtained with the EC2 models. The highest value is attained for section P2P3, 44 mm / 17 mm, which correspond to the span with the highest length (133 m long). In opposite, the section with the lowest displacement is P5P6, 7 mm / 3 mm, which can be explained by the existence of bearing displacements between the piers and the deck girder at sections P6 and P7 (see Figure 8.3). Moreover, those bearings allow the longitudinal expansion/contraction of the deck girder and therefore, bending restrains are lower, if compared to other spans with monolithic connection to the piers and consequently smaller vertical displacements are expected.

Concerning now the results achieved for the bearing displacements (Figure 8.18-b), the higher values are registered for the sections P7 and TPS. This can be explained, again, by the bearing displacements at sections P6 and P7 that causes the shift of the mass centre toward the left in relation to the mid length of the bridge. The predictions based on the fitted models correspond approximately to 39 % of the values obtained with the EC2 models, which are in conformity with the results presented in Figure 8.17.

As regard the results for rotations (Figure 8.18-b), the highest rotation is attained for the section P1, 41×10^{-3} º / 8×10^{-3} º, which is comprehensive because this section belongs to the extreme span TPNP1 (see Figure 8.3). Perhaps in a first observation, the same behaviour could be expected for the section P7 however, due to the bearing displacements at the sections P6 and P7 that allow the movement of the deck girder along the longitudinal

direction, the rotation magnitude of the section P7 is expected to be lower than the P1 and P2 sections. Moreover, the results achieved with the fitted models indicate that the direction of rotation might change.

Finally, concerning the concrete deformations (Figure 8.18-c and Figure 8.18-d), the predicted values with the fitted models correspond to 46 % – 74 % of the ones obtained with the EC2 models. Generally, higher deformations are expected for the sections near the piers, conclusions that can be confirmed by the results presented in Figure 8.15 and Figure 8.16. It should be highlighted that concerning the mid-span sections, the section P2P3 exhibits the highest deformations, which is comprehensive because this section belongs to the longest span of the bridge.

Hence, the revised predictions with the fitted models are information more realistic and reliable, than the ones obtained based on the guidelines only. Nevertheless, both predictions should be used as boundary values to the measurements, as previously referred. Therefore, the measurements can be compared with these predictions through the bridge lifetime and establish alarm levels if they are exceeded inferiorly (predictions based on the fitted models) or superiorly (prediction based on the EC2 models), and use it for the maintenance and surveillance of the bridge. Even though, due to the complexity of the problem, the predictions herein presented should be periodically checked. For that, the FEM should be updated as the database increases, which will promote the confidence in the obtained results.

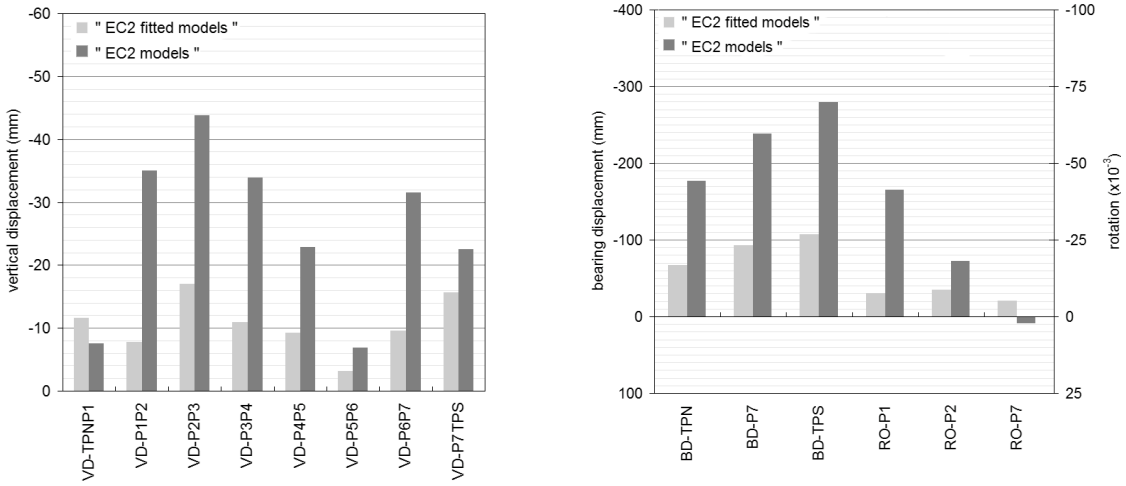

a) vertical displacements. **b) bearing displacements and rotations.**

Figure 8.18 : Predictions for the sensors' measurements concerning the main bridge lifetime.

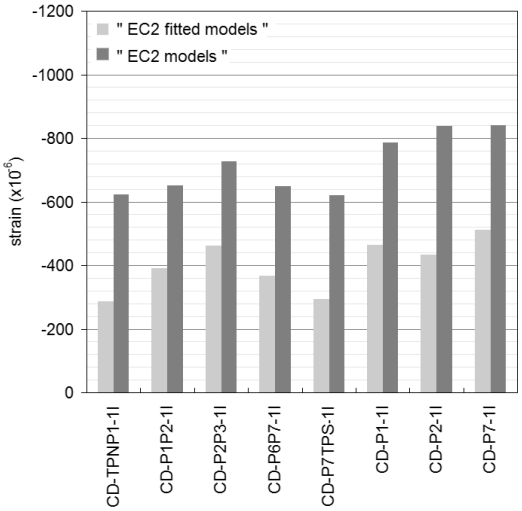

c) concrete deformations (bottom layer).

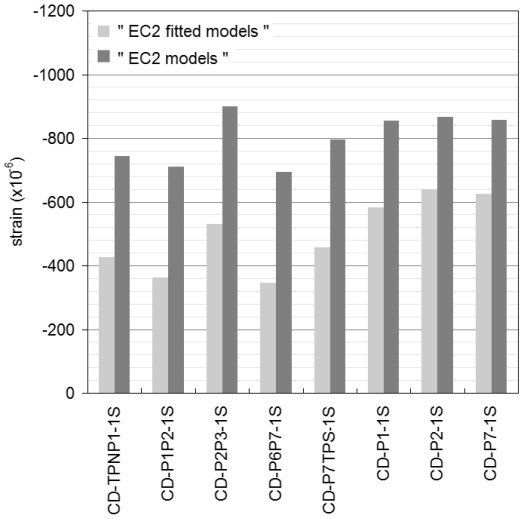

d) concrete deformations (top layer).

Figure 8.18 : Predictions for the sensors' measurements concerning the main bridge lifetime. (cont.).

8.6. CONCLUSIONS

The present chapter focuses the assessment of the long-term structural behaviour of bridges constructed by the cantilever method. A real structure, which was recently built in Portugal, has been monitored since the beginning of its erection. The monitoring system was carefully planned, installed and protected so that it could provide long-term reliable results. This chapter describes the structure, presents the monitoring system, and discusses the procedure employed to assess the structure's behaviour. This procedure is based on FEM calculations. Some relevant conclusions could be drawn:

- This chapter exposes the analysis strategy that was developed to calculate the long-term behaviour of a box girder bridge built by the segmental cantilever method. A FEM was employed, taking into account the effective properties of the structural materials, the actual sequence of construction and the influence of concrete time-delay effects. A good agreement between the numerical and the experimental results were observed. However, this was only possible thanks to the data collected during the execution of the structure, which is not available at the design stage of each new structure. The sensors' measurements revealed to be an important element to get an optimized model, with benefits for future updates. Therefore, this type of data becomes more and more useful in the surveillance and maintenance of this type of structures.

- The prisms placed outside the deck girder shrink more than the ones placed inside the deck girder, which is comprehensive considering the sun exposure during the construction and the small difference of the relative humidity between both environments – inside and outside of the box girder. However, an opposite behaviour was achieved for the creep prisms, which is difficult to explain based on the same arguments enounced for shrinkage. In spite of that, the results led to conclude that the particular conditions of the construction phase influenced the creep evolution for the first ages with different patterns for the interior and exterior prisms. Concerning the EC2 models for shrinkage and creep, although these models interpret acceptably the shrinkage of the employed concrete in the bridge, the EC2 model for creep overestimates the measured values, namely in the trend. The superplasticizers and pozzolanic materials used in concrete mix, whose effect cannot be accurately reproduced by code formulae can explain these deviations.
- The numerical model was initially validated with the data collected from the load test performed at the end of the construction. The numerical results achieved for the different parameters exhibits a good conformity, which for the vertical displacements of all mid-span sections the errors are inferior to 6.6 %. The developed FEM simulates rightly the bridge behaviour for static loads and therefore, the necessary confidence is attained for subsequent analysis. In addition, the numerical results obtained for the concrete deformations during the construction stage show high accuracy with the measured values.
- The definition of the zero-reference for the concrete deformations is an important aspect, which influences the accuracy of the long-term predictions. For this type of measurements, the results herein presented shows that the zero-reference should be established 7 days after concreting. Until that time, the concrete exhibits considerable compressive strains mainly due to the temperature variation related with the concrete hydration. This effect was not taken into account in the FEM analysis, which for long-term predictions is not normally considered.
- The long-term behaviour of the bridge is acceptably attained by the FEM when confronted with the measurements until now gathered. Although the numerical results obtained with the fitted models exhibit a better conformity with the measured values, the predictions obtained by both cases (based on the EC2 models and based on the EC2 models fitted to the prism measurements) seems to define a boundary zone for which

the sensors' measurements are expected to evolve. Some sensors, namely positioned in the alignment 3S, exhibit particular behaviour, higher compressions evolution, that is not correctly interpreted by the numerical model due to local conditions that are not modelled in this work. The second stage concreting, for the safety barrier positioning, appears to be the most probable cause.

- Even with the EC2 models for shrinkage and creep fitted to experimental data, obtained in concrete prisms, some differences are observed between the sensors' measurements and the FEM results. Three possible explanations can be pointed out, which might change the results patterns: (i) The notional size of the deck girder is considerable superior to the shrinkage prisms and therefore, the extrapolation of the deck girder shrinkage based on the measurements of the concrete prisms is subjected to errors. (ii) The influence of the interior and exterior environment in the long-term deformations of concrete is another critical aspect. The simplified strategy to consider the contribution of each environment proportional to the exposed perimeter cross section to both environments leads to acceptable results. (iii) The thickness differences between the bottom slab, web and top slab causes different evolutions of shrinkage and creep, which influences the long-term response of the bridge. The simplified procedure of taking three different layers for each zone and consider different shrinkage and creep curves lead to acceptable results.
- Concerning the structure lifetime, 100 years, the global discussion and explanation of the different achieved results increases the confidence in the FEM herein presented and therefore, to gain confidence for the effective use of this measurements for the maintenance and surveillance of the bridge.
- It must be kept in mind that the result of the long-term analysis of a real structure is not deterministic, namely, those related to the evaluation of the concrete delayed deformation due to creep, shrinkage and temperature, which makes uncertainty the long-term prediction.

9. CLOSURE

9.1. GENERAL CONCLUSIONS

Since the first log fell across water, people have been fascinated with bridges and their power to bring together what had been separated. Bridges span history and are more than they appear to be. They are crossing over rivers, landscape objects, engineering work, heritage of mankind. During the last decades, the number of bridges has grown exponential and, through ageing, the malfunctions that naturally appear in their service phase become a critical problem. Therefore, it is a moral, social and economic responsibility to watch, preserve and supervise these unique infrastructures. SHM have progressively become a reliable tool, capable of acting as an integrated part of the management system in complementing the inspections procedures. However, the application of monitoring data for bridge management is not yet a straightforward exercise. The main reasons appear to be:

- The quantity and variety of the collected data that makes it difficult to establish standard procedures for knowledge extraction;
- The uncertainties concerning the effective behaviour of the structure, material properties, environmental conditions and loading, render the task even more difficult;
- The final target, being it operational, tactical or management-related, which dictates the level of complexity of the data processing.

In this context, the author believes that data-based engineering techniques that are being developed worldwide must be continuously improved and integrated into a common framework, by taking advantage of the continuous technological evolution, in order to

achieve procedures with higher levels of efficiency to help in the bridge management. Conceptually, the advanced data-based engineering techniques mobilized in the present approach rely on the use of FEM, duly calibrated and continuously updated with information derived from the collected data by the SHM. In a complementary, but not less usefully, other data-based engineering techniques are used to find patterns in statistical data, suggesting potential damage at a structural section or component. With these potentialities, it is no doubt that this will be the next step in the effective use of monitoring data for bridge management.

In view of the above observations, the central theme of this thesis is to conceive and fully develop a framework enabling the fostering and reinforcement of the effective application of monitoring data for bridge management. The work is strongly supported by a large-scale bridge recently built in Portugal – Lezíria Bridge – equipped with an integrated monitoring system devoted to long-term management. The author has established the following priorities to undertake the research, which constitute the principal objectives of the thesis as previously stated in Chapter 1:

- To enounce, describe and detail all the main phases of the implementation of an integrated monitoring system in a large-scale bridge regarding its life-cycle management;
- To develop and integrate the required data-based engineering techniques in a software system able to illustrate the implementation of the suggested approach;
- To build a detailed and rigorous FEM enabling the evaluation and discussion of the quality of the monitoring data extracted;
- To analyse and discuss the monitoring data in order to generate confidence for its effective use in the bridge management, based on the developed and implemented engineering techniques.

For the achievement of these objectives, and to attain the final goal, the developed work imposed multifarious tasks and incursions into areas that were beyond the initial scope. Therefore, besides the new results herein presented focussing the analysis of the health of concrete bridges, this thesis may also be viewed as a sequential compilation of contributions from a number of different disciplines, such as laboratory and field

techniques, electronic and computer science, drawing programming, data mining and statistics, besides the main area that is the structural engineering.

Concerning the objectives put forward in Chapter 1, they are all judged to have been satisfactory achieved. In summary, the accomplishment of the purposed objectives and the sequence as they are presented set a framework devoted to SHM, going from the guidelines for the implementation of a SHM project, through the development and implementation of specific engineering techniques, to FEM-driven data validation analysis; all, taking the main focus into consideration – data-driven bridge management.

9.2. MAIN CONTRIBUTIONS

Following the sequence of the four main objectives previously presented, a more detailed description of the practical results achieved by the research carried out may now be recorded:

- **Setting up of integrated monitoring systems**

The first of the aforementioned contributions, result from the fact that the design and the implementation of integrated monitoring systems for large-scale bridges is a complex subject. Chapter 2 provides a detailed description of the fundamental procedures concerning the design and installation of a concrete bridge monitoring system spanning from construction to life-cycle surveillance. The complexity of the project and its scale were thoroughly illustrated adopting a hands-on approach and reflecting an implementation viewpoint.

Several hierarchical stages had to be crossed to turn this system into a physical and manageable reality, with emphasis in three fundamental phases: (1) the first phase consists of a conceptual design based on a set of structured documents (Table 2.1). It is fundamental to have a full preview of the overall system that integrates different sub-systems (static, dynamic and optical sub-systems) and components, as to anticipate potential difficulties or problems at the implementation stage; (2) the second phase comprises the installation works that were performed during the bridge construction

(Figure 2.6 to Figure 2.9). Capabilities such as dynamism, flexibility, adaptability and integration to follow the rhythm imposed by the construction works (often 24h/day) were demanded to the author and its team in the field. Several tests were performed to get the system ready and operational as well as the waterproofing and sealing of all connection boxes and sensors in order to maximize the system robustness and durability (Figure 2.10); (3) the third phase takes care of data acquisition and treatment. The reading procedures were established according to the project requirements, and the collected measurements were stored in a remote database linked to the field system, in order to deliver the desire information to the management authority. Since the opening to traffic, the monitoring system has been working in full mode, despite some minor failures that have been registered, advising for a closer and periodical checking of the system.

- **Monitoring data processing**

Regarding the second objective, one should note that, in general, the amount of information obtained by these systems becomes extremely large and therefore, the reading of this type of information becomes a hard task without specific processing tools. In fact, the programmable platforms currently available offer a set of tools already prepared to build a fully functional graphical interface in order to satisfying all specified requirements. The MENSUSMONITOR software introduced in Chapter 3 – a hybrid implementation resorting to LABVIEW, MATLAB and C++ platforms –, allowed for a significant reduction of the time expended in data input, analysis and knowledge extraction (Figure 3.12 to Figure 3.17). It assembles functionalities from the acquisition apparatus and produces results then exported using various formats. Without the support of this new software, the diversity of results presented in this thesis would not have been effectively successful in due time. Comparing with other commercial solutions devoted to the analysis and treatment of monitoring data, in spite of the limited number of available tools, MENSUSMONITOR offers the following advantages: (1) a set of numerical instruments – engineering techniques – specifically designed and prepared to provide an adequate response for the essential steps of monitoring data processing and analysis; (2) these numerical tools are a result of the authors' practical experience and therefore, enable robust, efficient and optimized solutions to be attained; (3) it is a evolutionary software, with a conceptual design prepared to integrate new or updated modules; (4)

MENSUSMONITOR is an executable software, which can be installed in any computer without particular requirements.

Summarizing, the set of numerical tools supported by the functional capabilities of MENSUSMONITOR, is a new contribution for the management of bridges based on monitoring data. It is a user-friendly tool turning monitoring data more adaptable for management purposes.

From the set of numerical tools – engineering techniques – currently available in the MENSUSMONITOR package, three of them were fully detailed and discussed in chapters 4 to 6. They have demonstrated potential for the bridge management based on the collected monitoring data, by also taking advantage of a unique framework as MENSUSMONITOR:

- Prediction models – the matter of Chapter 4 – is a new methodology that establish the normal correlation patterns between non-structural parameters, such as temperature and shrinkage strains, and the observed structural response, such as strains, rotations and movements of expansion joints (Figure 4.9). If the new structure exhibits a healthy behaviour in the first years after construction, it is possible to determine the normal correlation pattern, which can be used to assess the adequacy of the structural behaviour in the future. In fact, good correlation results were obtained for the relative displacements at the expansion joints, with maximum relative errors lower than 4 % for a probability of occurrence of 95 % (Figure 4.16). Moreover, an example of anomaly detection is successfully noticed and illustrated (Figure 4.15). The quick calculation results with minimum time and computational efforts encourages its implementation in automatic monitoring systems, to be confronted with the alarm levels previously established;

- Bridge deflections calculation supported on strain and rotation measurements and polynomial functions is the theme of Chapter 5 (Figure 5.4). The best results are attained for spans instrumented in three cross sections – two near the piers and the other one at the mid-span –. For cross sections with higher displacements, generally at mid-span sections, the obtained errors are less than 5% (Figure 5.11 and Figure 5.15). Although the methodology is not new, several novel analyses were performed, namely a parametric study with several configurations of inclinometers regarding the improvement and optimization of

the instrumentation plans for this purpose. The optimal solution conducted to a maximum relative error lower than 3% and a perfect agreement between the bridge deflection computed with the polynomial functions and the one obtained by the numerical models (Figure 5.21 and Figure 5.23). Drawings with the relative positioning of the inclinometers are provided with the intention to be used for further instrumentation plans (Figure 5.24);

- In Chapter 6, a model to detect traffic events and evaluate the structural effects based on strain measurements is proposed (Figure 6.8). Taking advantage of the high frequency capabilities of the current acquisition apparatus, a model is purposed to correlate the strain measurements to the respective loads caused by traffic events. Only heavy vehicles are detectable due to the precision of the measuring system. Loads were statistically characterized with the Weibull density function and characteristic loads were extrapolated for the structure life-cycle (Table 6.2 and Table 6.3). The results shows the importance of a pre-processing of the sensors' readings (namely removing the environmental effects) and a field calibration through a load test, taking into account the load length used in the test and the viscous-elastic behaviour of concrete. In spite of the satisfactory results obtained, as well as promising, periodical and larger observation periods are recommended to refine the obtained values of the parameters of the Weibull density function thus attaining higher confidence in the estimated characteristic loads.

- **Implementation of FEM based on monitoring data**

To address the third objective, a detailed and rigorous phased FEM analysis was performed, in order to corroborate the effective usefulness of the monitoring data and the information extracted by the developed engineering techniques previously enounced. Although the three substructures were analysed, the present thesis focused in work done in the north viaduct and the main bridge (Chapters 7 and 8, respectively). Nevertheless, a brief reference concerning the FEM of the south viaduct is made in Chapter 4. Structural discretization was carried out using 2D beam finite elements, in accordance with the Timoshenko theory. The CAD tools specifically developed to allow a full and detailed scanning of the drawing pieces (see Appendix B) were crucial to mitigate errors during the

process with time-consuming benefits. The full scanning of the prestressing cables with their real path was one of the most challenging tasks (Figure 7.6 and Figure 8.5), although considered necessary to correctly predict the evolution of the prestressing forces and to take into account the knowledge about the effective cables stretching.

It was observed that the effective prestressing forces were 10% to 15% lower than the values specified in the design project. The effective properties of the structural materials and soil, the actual sequence of construction and the influence of concrete time-delay effects were other important aspects taken into account. A structured methodology, organization and systematization were fundamental to bring up the numerical models. Moreover, the raw data concerning the FEM was organized into databases in order to enable future updates such as moving to a 3D model and/or changing the type of elements used.

- **Monitoring data evaluation and discussion regarding the bridge management**

Finally, concerning the last of the four objectives, a good conformity was observed between the numerical and the experimental result. However, this was only possible thanks to the data collected during the execution of the structure. This information is not available at the design stage of each new structure and consequently, it is not possible to get appropriate measurements in a design stage. Moreover, the numerical models developed by most bridge designers are devoted to express the bridge geometry and to enable structural analysis and ensure structural safety – not the purpose of the numerical models herein presented that focus on the effective behaviour of the structures. In this context, if relevant information is available concerning the effective properties and conditions of the monitored structure, it should be considered for FEM analyses, in order to eliminate justified deviations and therefore, getting predictions more reliable focussing the bridge management.

As a first assessment of the FEM developed for both north viaduct and main bridge, and concerning the load test performed at the end of the construction, the numerical results obtained for the vertical displacements exhibit errors inferior to 7 % (Figure 7.11 and Figure 8.10). In addition, the numerical results achieved for the construction stage have provided a correct interpretation of the behaviour of the structures (Figure 7.12 and Figure

8.13). One may therefore, positively conclude that the developed FEM adequately represent the effective behaviour of the structures under analysis.

Focussing the structure life-cycle, the predicted values with the numerical models for 100 years can be effectively used to define the health pattern evolution for the sensors' measurements and therefore, establish more accurate alarm levels than the ones determined at the design stage. The good conformity achieved between measurements and numerical values enables this alternative (Figure 7.13 and Figure 8.15 to Figure 8.17). In fact, the threshold values presented in Table 2.2 are significantly higher than the predictions for the sensors' measurements presented in Figure 7.14 and Figure 8.18 for the north viaduct and main bridge, respectively. Additionally, reference values were also defined for concrete deformations and rotations, for which threshold values were not initially established (n/d in Table 2.2). For example, concerning the surveillance level, the threshold established for the vertical displacements of the main bridge is 50 mm (Table 2.2) while the numerical results herein presented predicts a maximum value of 17 mm (Figure 8.18). In other words, this difference corresponds to a safety coefficient of 2.9, which increases for 5.9 for the alert level. However, it should be remembered that the threshold values were established considering the frequent and characteristic combination of actions, which, in part, explain these high safety coefficients. Nevertheless, the high threshold values of Table 2.2 might disable the earlier detection of abnormal behaviours due to minor changes in the sensors' trends. Even under the effect of extreme live loads, focussing the structure lifetime, the safety coefficient obtained for the vertical displacements of the main bridge is 1.23 (see Table 6.3), which indicates that the structure is perfectly safe even if subjected to extreme loads. Additionally, reference values were also defined for concrete deformations and rotations, for which threshold values were not initially established (n/d in Table 2.2). Therefore, regarding the management of the bridge, these results reinforce the using of the predictions presented in this thesis instead of the values of Table 2.2, which complemented with engineering techniques such as the one presented in Chapter 4 might detect, since early ages, any abnormal trend in the sensors' measurements.

The monitoring data collected from concrete prisms were crucial for the quality of the results by fitting the shrinkage and creep models of EC2. Some deviations were nevertheless, observed between the measurements and the values set by the EC2 models. The highest deviation is observed for the north viaduct, where the EC2 model

overestimates in almost 50% the shrinkage and creep of the applied concrete after 2000 days (Figure 7.8 and Figure 7.10). These results reveal how important such measurements may be, since the predictions given by regulations and design codes might be less suitable to be used as reference for the sensors' measurements. In the case of the main bridge, and regarding the long-term results, besides the importance of having the EC2 models fitted to monitoring data, the definition of different zones of the cross section – bottom slab, webs and top slab – with different properties, revealed to be crucial to the improvement in the quality of the results (Figure 8.8). These aspects were, and are, fundamental for the accuracy of the prediction for long-term behaviour of concrete bridges, and they should not be disregarded for this type of analyses.

The definition of the zero-reference for the concrete deformations is another important aspect, which influences the accuracy of the long-term predictions. For this type of measurements, the results herein presented show that the zero-reference should be established 2-3 days after concreting for the case of structures like the north viaduct and 6-7 days for the case of box girder decks like the main bridge of Lezíria Bridge. Prior to that, the concrete exhibits high thermal strains due to the concrete hydration. However, this effect was not taken into account in the FEM analysis, which for long-term predictions is not normally considered. In spite of that, the knowledge of the concrete evolution during these first ages might be important for the sections subjected to the highest internal forces to accurately evaluate the stress level installed in the concrete.

It was also concluded that the interaction between the concrete structure and the movable scaffolding systems that supported the bridge construction might be a critical aspect. Particularly for the north viaduct, after the prestressing, it is concluded that the span weight is partially supported by the movable scaffolding system. This effect lead to an increase of the stress level at the bottom face of approximately 24 % at the mid-span section, with the $0.45 \cdot f_{ck}$ limit never being exceeded (Figure 7.12). In fact, the correct modelling for the construction stage, namely the construction sequence, time history, prestressing forces besides the correct modelling of the concrete properties (as previously referred), were crucial for the accuracy of the long-term results.

Nevertheless, some differences between the values predicted by the numerical model and the sensors' measurements are observed, which deserve to be explained. The following aspects can be pointed out as reasons for the deviations: (1) comparing the notional size

values of the deck girder with the prisms, they are substantially different and therefore, the extrapolation of the concrete shrinkage and creep of the deck girder based on the measurements of the concrete prisms, is more prone to errors; (2) the sensors near the top face of the deck girder are exposed to particular conditions because of the application of the bituminous layer that increases the concrete temperature and reduces the concrete humidity; (3) for the main bridge, the thickness differences between the bottom slab, web and top slab cause different evolutions of shrinkage and creep and therefore, determine the long-term response of the bridge. The simplified procedure of taking three different layers for each zone and considering different shrinkage and creep curves lead to a significant improvement in the results; (4) due to local conditions, for the correct interpretation of which, more detailed and refined models should be developed. All of these aspects deserve additional and more detailed investigation in further studies.

In one sentence, the good agreement between field measurements and the FEM results validates the monitoring procedures and encourages the effective use of this information in surveillance and assessment tasks.

9.3. FUTURE WORK

Bridges will continue ageing and therefore, the use of integrated monitoring systems is expected to increase during the next years. Even more so, with the advances in progress in technology those are rendering monitoring apparatus and sensors cheaper and more powerful.

In this context, the present work may be extended in many ways in order to improve the efficiency of the monitoring data for bridge management. Moreover, the present thesis also widens perspectives to problems requiring further exploration. For the near future, the author suggests the following streams of works:

- Due to the high complexity of this type of systems, a compilation of standard manuals should be addressed to detail and help in the establishment of the main phases for a SHM project design. The variety of parameters, sensors and equipment that are commonly used, the multi-technical aspects concerning systems integration involving multi-disciplinary teams, the characteristics of the

monitored structure and the full functioning for long-term management are aspects that have to be controlled beforehand. The existence of those manuals might avoid sensors' damage, inadequate selection of equipment and failures in sensors' readings during the structure lifetime. In fact, these aspects dictate the full success or failure of a monitoring system devoted to life-cycle structural surveillance;

- Engineering techniques devoted to process monitoring data, leading to generation of information and, from there, to the formation of knowledge, must be continuously developed and updated to build a comprehensive library of tools. The lack of a standard procedure for data handling implies that developers may freely express their creativity. However, more integrated platforms such as MENSUSMONITOR should be preferred, for they offer higher order advantages, such as flexibility and predictability, and provide a single application approach to a comprehensive coverage of the relevant functions. In fact, this type of integrated platforms has a promissory future for the organization of monitoring data, as schematically presented in Figure 1.11. Nevertheless, real time tools, local and remote communications and database processing are some of the current limitations that, in the author's opinion, deserve particular attention.

- As stated in Chapter 1, sensors do not know how to *lie*. Excluding malfunctions with known causes, the monitoring is currently an enigma for the analysts, namely for those who develop FEM to interpret the effective structural behaviour of bridges. Foreseeing long-term predictions, new models with higher degree of detail and refinement should be integrated with global models as the ones herein presented for Lezíria Bridge. Those refined models should focus on aspects such as: (1) the evolution of the concrete deformations during the early ages, where concrete properties change very quickly; (2) concrete deformations near the anchorage zones of the prestressing cables where local stresses distorts the section shape; (3) deck zones near of bearing supports where friction movements influences the bridge behaviour; (4) the soil-foundations interaction if the foundations are instrumented, should also be considered a relevant target. All of these aspects contribute to the improvement of the final goal – to generate

forecasts as close as possible to the real behaviour, in order to more efficiently lead to the identification of possible anomalies. More than ever, this can and must be done by taking profit of the continuous improvement of the processing capabilities of the computers and FEM software packages that are continuously being updated with higher capabilities.

Finally, the author's experience, namely that acquired along his PhD work, gave him a profound awareness about the wide requirements that are needed to stand up an integrated monitoring system as the one that was installed in one of the World's longest bridges – Lezíria Bridge.

There remains little doubt that these systems have a promising future. However, it is important that engineers from different fields, namely from civil, electronic, mechanic and informatics engineering, work more and more in partnership, in order to attain robust and solid solutions concerning bridge management based on monitoring data.

Our bridges, our patrimony, our history deserve undoubtedly such commitment.

REFERENCES

Aktan, A. E., Catbas, F. N., et al. (2003). *Development of a Model Health Monitoring Guide for Major Bridges*. Philadelphia, Drexel Intellgient Infrastructure and Transportation Safety Institute.

ambiente2008. (2009). *Construção da Ponte 25 de Abril em Lisboa*. Retrieved January 21, 2012, from http://www.skyscrapercity.com/showthread.php?t=870308. (in Portuguese)

Andersen, J. E. and Fustinoni, M. (2006). *Structural Health Monitoring Systems*. (First Edition). Kongens Lyngby, Denmark: COWI A/S and Futurtec OY.

Andersen, J. E., Toivola, P., et al. (2005), Maximizing Return Of Investment to a Structural Monitoring System by optimal configuration and good User Interface, *IABSE Symposium*, Lisbon, Portugal.

Azeredo, M. (1998). *As pontes do Porto*. Retrieved January 12, 2012, from http://paginas.fe.up.pt/~azr/pontes/arra_fig.htm. (in Portuguese)

Azeredo, M. and Azeredo, M. A. (2002). *Bridges of Oporto: a love story*. Porto: FEUP Edições.

Balageas, D., Fritzen, C.-P., et al. (2006). *Structural Health Monitoring*. (1st ed). London, United Kingdom: ISTE Ltd.

Barcina, J. M. G. and Mato, F. M. (1997). IV Puente sobre el río Guadiana, en Badajoz: Instrumentación y control del atirantamiento. *Hormigón y Acero*, 206, 63-78. (in Spanish)

Barr, B. I. G., Vitek, J. L., et al. (1997). Seasonal shrinkage variation in bridge segments. *Materials and Structures*, 30(196), 106-111.

Bazant, Z. P. (2001). Prediction of concrete creep and shrinkage: past, present and future. *Nuclear Engineering and Design*, 203(1), 27-38.

Bergmeister, K., Aktan, A. E., et al. (2002). *Monitoring and Safety Evaluation of Existing Concrete Structures: State-of-the-Art Report (final draft)*, fib Task Group 5.1.

Bergmeister, K. and Santa, U. (2001). Global monitoring concepts for bridges. *Structural Concrete*, 2(1), 29 –39.

Bernard-Gely, A., Calgaro, J. A., et al. (1994). *Conception des ponts*. Paris: Presses de L'école Nationale des Ponts et Chaussées. (in French)

Beyon, J. Y. (2001). *LABVIEW programming data acquisition and analysis*. Upper Saddle River, NJ: Prentice Hall PTR.

Bishop, C. M. (2006). *Pattern recognition and machine learning*. New York: Springer.

Björck, A. (1996). *Numerical methods for least squares problems*. Philadelphia : Society for Industrial and Applied Mathematics.

Boller, C., Chang, F. K., et al. (2009). *Encyclopedia of Structural Health Monitoring*. John Wiley & Sons.

BRITE/EURAM (1997). *SMART STRUCTURES – Integrated Monitoring Systems for Durability Assessment of Concrete Structures. Project Nº BRPR-CT98-0751.*

Burdet, O. and Zanella, J.-L. (2000), Automatic Monitoring of Bridges using Electronic Inclinometers, *IABSE, , Lucerne Congress Structural Engineering for Meeting Urban Transportation Challenges*, IABSE, , Lucerne Congress Structural Engineering for Meeting Urban Transportation Challenges.

Caetano, E. and Cunha, A. (1996). Identificação de Parâmetros Modais em Estruturas de Engenharia Civil: Desenvolvimento de "Software" e Aplicações. *Revista Portuguesa de Engenharia de Estruturas (RPEE)*, 40, 17-26. (in Portuguese)

Calado, L., Proença, J. M., et al. (2007). Monitorização Contínua de Obras de Engenharia Civil – O caso das escoras metálicas da Estação do Terreiro do Paço. Ingenium**:** 77-79. (in Portuguese)

Carlos Sousa and Neves, A. (2009a). *DIANA user-supplied subroutine for computation of prestress losses due to steel relaxation*, Porto: LABEST, Faculty of Engineering, University of Porto.

Carlos Sousa and Neves, A. (2009b). *DIANA user-supplied subroutine for concrete creep modelling.*, Porto: LABEST, Faculty of Engineering, University of Porto.

Catbas, F., Susoy, M., et al. (2008). Structural health monitoring and reliability estimation: Long span truss bridge application with environmental monitoring data. *Engineering Structures*, 30(9), 2347-2359.

Catbas, F. N., Ciloglu, S. K., et al. (2007). Limitations in structural identification of large constructed structures. *Journal of Structural Engineering-Asce*, 133(8), 1051-1066.

Cavadas, F., Oliveira, P., et al. (2009). *Análise da resposta estrutural de uma viga de betão armado e pré-esforçado, simplesmente apoiada, face a duas cargas pontuais (internal report)*. Porto: LABEST, Faculty of Engineering, University of Porto. (in Portuguese)

Cezzar, R. (1995). *A Guide to programming languages Overview and Comparison*. Boston: Artech House.

Chang, S.-P., Yee, J., et al. (2009). Necessity of the bridge health monitoring system to mitigate natural and man-made disasters. *Structure and Infrastructure Engineering: Maintenance, Management, Life-Cycle Design and Performance*, 5(3), 173 - 197.

Chung, W., Kim, S., et al. (2008). Deflection estimation of a full scale prestressed concrete girder using long-gauge fiber optic sensors. *Construction and Building Materials*, 22(3), 394-401.

COBA-PC&A-CIVILSER-ARCADIS (2005a). *Construção da Travessia do Tejo no Carregado Sublanço A1/Benavente, da A10 Auto-Estrada Bucelas/Carregado/IC3; Volume I – "Viaduto Norte". Empreitada de Concepção, Projecto e Construção da Travessia do Tejo no Carregado, Volume I – Viaduto Norte*. Portugal. (in Portuguese)

COBA-PC&A-CIVILSER-ARCADIS (2005b). *Construção da Travessia do Tejo no Carregado Sublanço A1/Benavente, da A10 Auto-Estrada Bucelas/Carregado/IC3; Volume IV – Estudo Geológico e Geotécnico. Empreitada de Concepção, Projecto e Construção da Travessia do Tejo no Carregado, Volume IV – Estudo Geológico e Geotécnico*. Portugal. (in Portuguese)

COBA-PC&A-CIVILSER-ARCADIS (2005c). *Construção da Travessia do Tejo no Carregado Sublanço A1/Benavente, da A10 Auto-Estrada Bucelas/Carregado/IC3; Volume IV – Estudo Geológico e Geotécnico. Empreitada de Concepção, Projecto e Construção da Travessia do Tejo no Carregado, Volume II – Ponte sobre o Rio Tejo*. Portugal. (in Portuguese)

COBA-PC&A-CIVILSER-ARCADIS (2006). *Construção da Travessia do Tejo no Carregado Sublanço A1/Benavente, da A10 Auto-Estrada Bucelas/Carregado/IC3; Volume XV – "Plano de Monitorização Estrutural e de Durabilidade". Empreitada de Concepção, Projecto e Construção da Travessia do Tejo no Carregado, Volume XV – Plano de Monitorização Estrutural e de Durabilidade*. Portugal. (in Portuguese)

Costa , B. J. A., Faria, R., et al. (2008). *Instrumentation and observation of the Pinhão Bridge behaviour during the load tests.* Porto: LABEST, Faculty of Engineering, University of Porto. (in Portuguese)

Costa, B. J. A., Félix, C., et al. (2009), Design and installation of an electric based monitoring system applied to a centenary metallic bridge. *ASCP'09 - 1º Congresso de Segurança e Conservação de Pontes*, Lisbon. (in Portuguese)

Cremona, C. (2001). Optimal extrapolation of traffic load effects. *Structural Safety*, 23(1), 31-46.

De Brito, J., Santos, S., et al. (2002). 'Inspectionability' of bridges. *Structural Concrete*, 3(1), 29-34.

Diario de Noticias (1877), *Inauguração da ponte sobre o Douro*. November 5, 1877: nº 4:214, 13º. Lisbon. (in Portuguese).

Diario de Noticias (1998), *A maior ponte da Europa abre amanhã*. March 28, 1998: nº 47121, ano 134º. Lisbon. (in Portuguese).

Diário de Notícias (1886), *Inauguração da ponte Luiz I no Porto*. November 1, 1886: nº 7:469, 22º anno. Lisbon. (in Portuguese).

Dimande, A. O. (2010). *Análise Experimental de Pontes durante a Construção e em Serviço, PhD thesis.* Porto: LABEST, Faculty of Engineering, University of Porto. (in Portuguese)

Dupré, J. (1997). *Bridges - A history of the world's most famous and important spans*. Hong Kong: Könemann Verlagsgesellschaft mbH.

Eiffel, G. (1879). *Notice Sur Le Pont Du Douro, A Porto : Pont Maria-Pia*. (in French)

Farrar, C. R. and Worden, K. (2007). An introduction to structural health monitoring. *Philosophical Transactions of the Royal Society A: Mathematical, Physical and Engineering Sciences*, 365(1851), 303-315.

Fernandez Troyano, L. (2004). *Tierra sobre el agua visión histórica universal de los puentes*. Madrid: Colegio de Ingenieros de Caminos Canales y Puertos. (in Spanish)

Fernando, G. F., Hameed, A., et al. (2003). Structural integrity monitoring of concrete structures via optical fiber sensors: sensor protection systems. *Structural Health Monitoring*, 2(2), 123-135.

FIB Commission on Practical Design (2010a). *fib Bulletin 55: Model Code 2010, First complete draft – Volume 1*. London: International Federation for Structural Concrete (fib).

FIB Commission on Practical Design (2010b). *fib Bulletin 56: Model Code 2010, First complete draft – Volume 2*. London: International Federation for Structural Concrete (fib).

Figueiras, J., Félix, C., et al. (2010). *Transducer for mesuring vertical displacements*. Universidade do Porto and Instituto Politécnico do Porto. WO/2010/053392.

Figueiras, J., Félix, C., et al. (2007a). *Construção da Travessia do Tejo no Carregado Sublanço A1/Benavente, da A10 Auto-Estrada Bucelas/Carregado/IC3: Projecto Executivo Monitorização Estrutural e de Durabilidade 0 – Apresentação*. Porto: LABEST, Faculty of Engineering, University of Porto. (in Portuguese)

Figueiras, J., Félix, C., et al. (2007b). *Construção da Travessia do Tejo no Carregado Sublanço A1/Benavente, da A10 Auto-Estrada Bucelas/Carregado/IC3: Projecto Executivo Monitorização Estrutural e de Durabilidade A – Memória Descritiva*. Porto: LABEST, Faculty of Engineering, University of Porto. (in Portuguese)

Figueiras, J., Félix, C., et al. (2007c). *Construção da Travessia do Tejo no Carregado Sublanço A1/Benavente, da A10 Auto-Estrada Bucelas/Carregado/IC3: Projecto Executivo Monitorização Estrutural e de Durabilidade B – Peças Desenhadas*. Porto: LABEST, Faculty of Engineering, University of Porto. (in Portuguese)

Figueiras, J., Félix, C., et al. (2007d). *Construção da Travessia do Tejo no Carregado Sublanço A1/Benavente, da A10 Auto-Estrada Bucelas/Carregado/IC3: Projecto Executivo Monitorização Estrutural e de Durabilidade C – Caderno de Especificações e Procedimentos*. Porto: LABEST, Faculty of Engineering, University of Porto. (in Portuguese)

Figueiras, J., Félix, C., et al. (2007e). *Construção da Travessia do Tejo no Carregado Sublanço A1/Benavente, da A10 Auto-Estrada Bucelas/Carregado/IC3: Projecto Executivo Monitorização Estrutural e de Durabilidade G – Manual de utilização*. Porto: LABEST, Faculty of Engineering, University of Porto. (in Portuguese)

Figueiredo, E. J. F. (2010). *Damage identification in civil engineering infrastructure under operational and environmental conditions, PhD thesis.* Porto: Faculty of Engineering, University of Porto.

Fraser, M. S. (2006). *Development and implementation of an integrated framework for structural health monitoring, PhD thesis.* California: University of California.

Gage Technique International, L. (2011). *Vibrating wire embedment strain gauges*. Retrieved February 18, 2011, from http://www.gage-technique.com/vw-embedment-strain-gauge.htm.

GEOSIG. (2009). *ARTeMIS Extractor.* Retrieved March 01, 2012, from *http://www.geosig.com/product-print.html?productid=10352*.

Getachew, A. and Obrien, E. (2007). Simplified site-specific traffic load models for bridge assessment. *Structure & Infrastructure Engineering: Maintenance, Management, Life-Cycle Design & Performance*, 3(4), 303-311.

Goel, R., Kumar, R., et al. (2007). Comparative Study of Various Creep and Shrinkage Prediction Models for Concrete. *Journal of Materials in Civil Engineering*, 19(3), 249-260.

GRID (2003). *A13 – Auto-estrada Almeirim-Marateca, Sublanços Salvaterra de Magos – A10 – Santo Estevão, Ponte sobre o rio Sorraia, Projecto de Execução, Memória Descritiva e Justificativa*. Lisbon, GRID - Consultas, Estudos e Projectos de Engenharia, Lda. (in Portuguese)

Hou, X., Yang, X., et al. (2005). Using Inclinometers to Measure Bridge Deflection. *Journal of Bridge Engineering*, 10(5), 564-569.

Howells, R. W., Lark, R. J., et al. (2005). A study of the influence of environmental effects on the behaviour of a pre-stressed concrete viaduct. *Structural Concrete*, 6(3), 91-100.

Hunt, B. R., Lipsman, R. L., et al. (2001). *A Guide to MATLAB for Beginners and Experienced Users*. Cambridge, United Kingdom: Cambridge University Press.

Huston, D. (2011). *Structural Sensing, Health Monitoring, and Performance Evaluation*. Taylor and Francis Group, LLC.

Inaudi, D. (1999). Long-gage fibre Optic sensors for structural monitoring. *Optical Measurement Techniques and Applications. Artech House, 1997*, 255-275.

infopédia. (2001). *Ponte Hintze Ribeiro após a tragédia de 4 de março de 2001*. Retrieved January 21, 2012, from http://www.infopedia.pt/$ponte-hintze-ribeiro,2.

Johnson, R. K. (2011). *The elements of MATLAB® style*. New York: Cambridge University Press.

Jornal de Notícias (2001), *Arrábida continua em fila de espera*. March 7, 2001. Porto. (in Portuguese)

Jornal de Notícias (2001a), *Câmara ajuda a pagar obras no Pinhão*. March 6, 2001. Porto. (in Portuguese)

Jornal dee Notícias (2001b), *Causas dividem especialistas*. March 7, 2001. Porto. (in Portuguese)

Jornal de Notícias (2001c), *Nove meses para voltar a ligar Montemor e Soure*. March 6, 2001. Porto. (in Portuguese)

Jornal de Notícias (2001d), *Ordem inicia inventário*. March 6, 2001. Porto. (in Portuguese).

Jornal de Notícias (2001e), *Ponte Luiz I precisa de obras*. March 7, 2001. Porto. (in Portuguese)

Jornal de Notícias (2001f), *Quatro mil veículos intranquilizam Constância*. March 6, 2001. Porto. (in Portuguese)

Jornal de Notícias (2011), *Ponte de Constância reabre com acesso vedado a pesados*. April 4, 2011. Porto. (in Portuguese)

Jowell, R. (2001). *Entre-Os-Rios Bridge Tragedy*. Retrieved February 20, 2011, from http://www.europeansocialsurvey.org/index.php?view=details&id=6231%3Aentre-os-rios-bridge-tragedy&option=com_eventlist&Itemid=326.

Kada, H., Lachemi, M., et al. (2002). Determination of the coefficient of thermal expansion of high performance concrete from initial setting. *Materials and Structures*, 35(1), 35-41.

Karoumi, R., Wiberg, J., et al. (2005). Monitoring traffic loads and dynamic effects using an instrumented railway bridge. *Engineering Structures*, 27(12), 1813-1819.

Ko, J. and Ni, Y. (2005). Technology developments in structural health monitoring of large-scale bridges. *Engineering Structures*, 27(12), 1715-1725.

Kristek, V., Bazant, Z., et al. (2006). Box girder bridge deflections - Why is the initial trend deceptive? *ACI Concrete International*, 28(1), 55-63.

Li, D., Maes, M. A., et al. (2004). Thermal design criteria for deep prestressed concrete girders based on data from Confederation Bridge. *Canadian Journal of Civil Engineering*, 31(5), 813-825.

Liljencrantz, A. and Karoumi, R. (2009). Twim: A MATLAB toolbox for real-time evaluation and monitoring of traffic loads on railway bridges. *Structure and Infrastructure Engineering: Maintenance, Management, Life-Cycle Design and Performance*, 5(5), 407 - 417.

Liljencrantz, A., Karoumi, R., et al. (2007). Implementing bridge weigh-in-motion for railway traffic. *Computers & Structures*, 85(1-2), 80-88.

Maaskant, R., Alavie, T., et al. (1997). Fiber-optic Bragg grating sensors for bridge monitoring. *Cement and Concrete Composites*, 19(1), 21-33.

Malm, R. and Sundquist, H. (2010). Time-dependent analyses of segmentally constructed balanced cantilever bridges. *Engineering Structures*, 32(4), 1038-1045.

Martinez, W. L., Martinez, A. R., et al. (2010). *Exploratory data analysis with MATLAB*. Boca Raton: CRC Press.

Massonnet, C. (1968). *Résistance des matériaux*. Paris: Dunod. (in French)

Math, W. (1992). *MATLAB high-performance numeric computation and visualization software reference guide*. Natick, MA: The Math Works.

MathWorks. (2007). *MATLAB : The Language of Technical Computing*. Retrieved January 29, 2012, from http://www.mathworks.com/products/MATLAB/index.html.

Melchers, R. E. (1999). *Structural reliability analysis and prediction*. Chichester: John Wiley & Sons.

Minchin, J. R. E., Zayed, T., et al. (2006). Best Practices of Bridge System Management - A Synthesis. *Journal of Management in Engineering*, 22(4), 186-195.

Montgomery, D. C. and Runger, G. C. (2003). *Applied Statistics and Probability for Engineers*. (3rd ed.). John Wiley.

Monumentos Desaparecidos. (2009). *A Ponte Hintze Ribeiro*. Retrieved January 12, 2012, from http://monumentosdesaparecidos.blogspot.com/2009/10/ponte-hintze-ribeiro.html. (in Portuguese)

Moses, F. (1979). WEIGH-IN-MOTION SYSTEM USING INSTRUMENTED BRIDGES. *Transportation Engineering Journal of Asce*, 105(3), 233-249.

Mufti, A. (2001). *Guidelines for Structural Health Monitoring*. (Design Manual No. 2). Winnipeg, Manitoba, Canada: ISIS Canada Corporation.

Ni, Y. Q., Hua, X. G., et al. (2007). Assessment of Bridge Expansion Joints Using Long-Term Displacement and Temperature Measurement. *Journal of Performance of Constructed Facilities*, 21(2), 143-151.

O Commercio do Porto (1877), *Inauguração da ponte sobre o Douro*. November 5, 1877. Porto. (in Portuguese)

O Commercio do Porto (1886), *Inauguração da Ponte Luiz I*. November 1, 1886: nº 270; XXXIII anno. Porto. (in Portuguese)

O Seculo (1963), *Inaugurada a Ponte da Arrábida*. June 23, 1963: nº 29166, ano 83. Lisbon. (in Portuguese)

O Seculo (1966), *Abraço sobre o Tejo - A Ponte Salazar*. August 7, 1966: nº 30286, ano 86. Lisbon. (in Portuguese).

Oliveira, C. B. d. (2006). A Nova Travessia do Tejo do Carregado à Lezíria pela A10. *INGENIUM*. Portugal, II Série - Setembro/Outubro 2006**:** 36-41. (in Portuguese)

Pacheco, P., André, A., et al. (2010). Automation robustness of scaffolding systems strengthened with organic prestressing. *Automation in Construction*, 19(1), 1-10.

Perdigão, V., Barros, P., Matos, J., Sousa, H., Figueiras, J., Dias, I., Pereira, D. (2006), Development and implementation of a long-term structural health monitoring, *IABMAS'06 - Third International Conference on Bridge Maintenance, Safety and Management*, Porto, Portugal.

Pines, D. and Aktan, A. E. (2002). Status of structural health monitoring of long-span bridges in the United States. *Progress in Structural Engineering and Materials*, 4(4), 372-380.

Portugal - Ministério das Obras Públicas (1956). Plano de melhoramentos de 1956, para a cidade do Porto: Decreto-Lei n.º 40616/56 de 28 de Maio. Habitação social/Renovação urbana / Porto. Lisboa : MOP, 1956. (in Portuguese)

Roberts-Wollman, C. L., Breen, J. E., et al. (2002). Measurements of Thermal Gradients and their Effects on Segmental Concrete Bridge. *Journal of Bridge Engineering*, 7(3), 166-174.

Robertson, I. (2005). Prediction of vertical deflections for a long-span prestressed concrete bridge structure. *Engineering Structures*, 27(12), 1820-1827.

Rodrigues, C., Félix, C., et al. (2007a). *Fiber Optic Strain Transducer : Conception, analysis and calibration (Internal Report)*. Porto: LABEST, Faculty of Engineering, University of Porto. (in Portuguese)

Rodrigues, C., Sousa, H., et al. (2007b). *Travessia do Tejo no Carregado, no sublanço A1 / Benavente, da A10 – Auto-Estrada Bucelas/Carregado/IC3 - Ensaios de Recepção*. Porto: LABEST, Faculty of Engineering, University of Porto. (in Portuguese)

Rodrigues, P., Pereira, P., et al. (2005). *Programação em C++ conceitos básicos e algoritmos*. (7ª ed). Lisboa: FCA - Editora de Informática. (in Portuguese)

ROGERS, C. A. (1993). *Intelligent Material Systems and Structures*, Report from the Center for Intelligent Material Systems and Structures, Program Div. of Technomic Publishing Co, Inc, Lancaster, PA.

Rucker, W., Hille, F., et al. (2006). *F08b: Guideline for Structural Health Monitoring*. Berlin, Germany, SAMCO - Structural Assessment Monitoring and Control; Federal Institute of Materials Research and Testing (BAM), Division VII.2 Buildings and Structures.

Rudaz, S., Kunding, C., et al. (2006). *AC-23-DH Downhole Accelerometer – Installation Instructions Version 1*. Retrieved September 16, 2008, from http://www.geosig.com/downloads/manuals/AC-23-DH_Installation_Instructions.pdf.

Santos, L. M. P. d. O. (2002). *Observação e análise do comportamento diferido de pontes de betão, PhD thesis.* Lisboa: LNEC. (in Portuguese).

Santos, T. O. (2007). *Retracção do betão em pontes observação e análise, PhD thesis.* Lisboa: LNEC. (in Portuguese).

Saraiva, J. H., Cruz, A. A. F. d., et al. (1983). *História de Portugal: 1640-Actualidade*. Selecções Reader's Digest, Publicações Alfa, SARL. (in Portuguese)

Savitzky, A. G. M. J. E. (1964). Smoothing and Differentiation of Data by Simplified Least Squares Procedures. *Analytical Chemistry*, 36(8), 1627-1639.

SMARTE (2004). *SMARTE - Management systems devoted to highway bridges by using remote monitoring sensors based on electrical and optical fibers*. Porto: LABEST, Faculty of Engineering, University of Porto. (in Portuguese)

SMARTEC.(2009). *Data Acquisition, Management, Publishing and Analysis*. Retrieved March 02, 2012, from http://smartec.ch/products.htm.

Sol (2007), *415 pontes em estado grave*. 2007. Retrieved March 02, 2012, from http://canais.sol.pt/PaginaInicial/Sociedade/Interior.aspx?content_id=65472. (in Portuguese)

Sousa, C. (2006a). *Ensaios e análise de resposta de estacas em solo residual do granito sob acções horizontais, Master thesis.* Porto: Faculty of Engineering, University of Porto. (in Portuguese)

Sousa, C., Sousa, H., et al. (2009a). *Finite-element analysis of the long-term behaviour of the precast access viaduct of the Leziria Bridge*, Porto: LABEST, Faculty of Engineering, University of Porto.

Sousa, C., Sousa, H., et al. (2012). Numerical evaluation of the long-term behaviour of precast continuous bridge decks. *Journal of Bridge Engineering,* 17(1), 89-96.

Sousa, H. (2002). *Comportamento de uma viga de betão armado e pré-esforçado em modelo reduzido*. Estágio do PRODEP III. Porto: LABEST, Faculty of Engineering, University of Porto. (in Portuguese)

Sousa, H., Dimande, A., et al. (2008), MENSUSMONITOR – Tool for the treatment and interpretation of experimental results in Civil Engineering, *CCC 2008 – Challenges for Civil Construction*, FEUP - Faculty of Engineering, University Porto, Porto, FEUP.

Sousa, H., Dimande, A., et al. (2009b). MENSUSMONITOR - Software for the treatment and interpretation of experimental results. *RPEE – Revista Portuguesa de Engenharia de Estruturas*, Serie 2(6). (in Portuguese)

Sousa, H., Felix, C., et al. (2011b). Design and implementation of a monitoring system applied to a long-span prestressed concrete bridge. *Structural Concrete*, 12(2), 82-93.

Sousa, H. and Figueiras, J. (2009a). *Experimental evaluation of thermal compensation for vibrating wire strain gauges placed in concrete prisms. Internal report.*, Porto: LABEST, Faculty of Engineering, University of Porto.

Sousa, H. and Figueiras, J. (2009b). *LABVIEW and C++ tools to automate drawings scanning in AutoCAD environment for FEM analysis. Internal report.* Porto: LABEST, Faculty of Engineering, University of Porto.

Sousa, H. and Figueiras, J. (2010). *Finite-element analysis of the long-term behaviour of the main bridge of the Leziria Bridge. Internal report.* Porto: LABEST, Faculty of Engineering, University of Porto.

Sousa, H., Henriques, A., Figueiras, J. (2006b), Tratamento de resultados experimentais em estruturas com base em filtros de alisamento de Savitzky-Golay, *4 Jornadas Portuguesas de Engenharia de Estruturas*, LNEC – Laboratório Nacional de Engenharia Civil, Lisboa, Portugal. (in Portuguese)

Sousa, H., Matos, J. A., et al. (2005). *Ensaio de carga da ponte sobre o rio Sorraia - Relatório Técnico.* Porto: LABEST, Faculty of Engineering, University of Porto. (in Portuguese)

Sousa, H., Matos, J., Figueiras, J. (2006c), Development of an Embedded Sensor Holder for Concrete Structures Monitoring, *The Second Congress fib*, Naples, Italy.

Standardization European Committee (2002). *EN 1990: Eurocode: Basis of Structural Design.* Brussels: CEN.

Standardization European Committee (2004). *Eurocode 2 EN 1991-1-1 Design of concrete structures Part 1-1 General rules and rules for buildings*. Brussels: CEN.

Standardization European Committee (2009). *Eurocode 1 - Actions on structures. Part 1-5: General actions; Thermal actions (portuguese version)*. Brussels: CEN.

Stroustrup, B. (1997). *The C++ programming language*. (3rd ed). Reading, MA, Addison Wesley.

TACE (2007). *Construção da Travessia do Tejo no Carregado Sublanço A1/Benavente, da A10 Auto-Estrada Buce-las/Carregado/IC3: Plano de Qualidade*. Portugal. (in Portuguese)

Takacs, P. F. (2002). *Deformations in concrete cantilever bridges: Observations and theoretical modelling, PhD thesis.* Norway: Norges teknisk-naturvitenskapelige universitet.

Top 10 Places. (2012). *Vasco da Gama Bridge (Portugal).* Retrieved January 21, 2012, from http://top10places.com/Place/Vasco_Da_Gama_Bridge_in_Portugal/1136.htm

Tormenta, J. P. and Fiéis, P. (2005). *A primeira invasão Francesa: As batalhas da Roliça e do Vimeiro*. (1). Caldas da Rainha: Livraria Nova Galáxia. (in Portuguese)

Van der Auweraer, H. and Peeters, B. (2003). International Research Projects on Structural Health Monitoring: An Overview. *Structural Health Monitoring*, 2(4), 341-358.

Vurpillot, S., Krueger, G., et al. (1998). Vertical deflection of a pre-stressed concrete bridge obtained using deformation sensors and inclinometer measurements. *ACI Structural Journal*, 95(5), 518-526.

Witte, F. C. (2005). *DIANA user's manual, Release 9*. Delft, The Netherlands, TNO DIANA, BV.

Wong, K.-Y. (2007). Design of a structural health monitoring system for long-span bridges. *Structure & Infrastructure Engineering: Maintenance, Management, Life-Cycle Design & Performance*, 3(2), 169-185.

Zdenek Bazant, Guang-Hua Li, et al. (2008), Explanation of Excessive Long-Time Deflections of Collapsed Record-Span Box Girder Bridge in Palau. Preliminary Structural Engineering Report No. 08-09/A222e, *8th International Conference on Creep and Shrinkage of Concrete*, Japan.

Zienkiewicz, O. C. (1971). *The finite element method in engineering science*. McGraw-Hill.

APPENDIX A : MONITORING SYSTEM IMPLEMENTATION AT LEZÍRIA BRIDGE

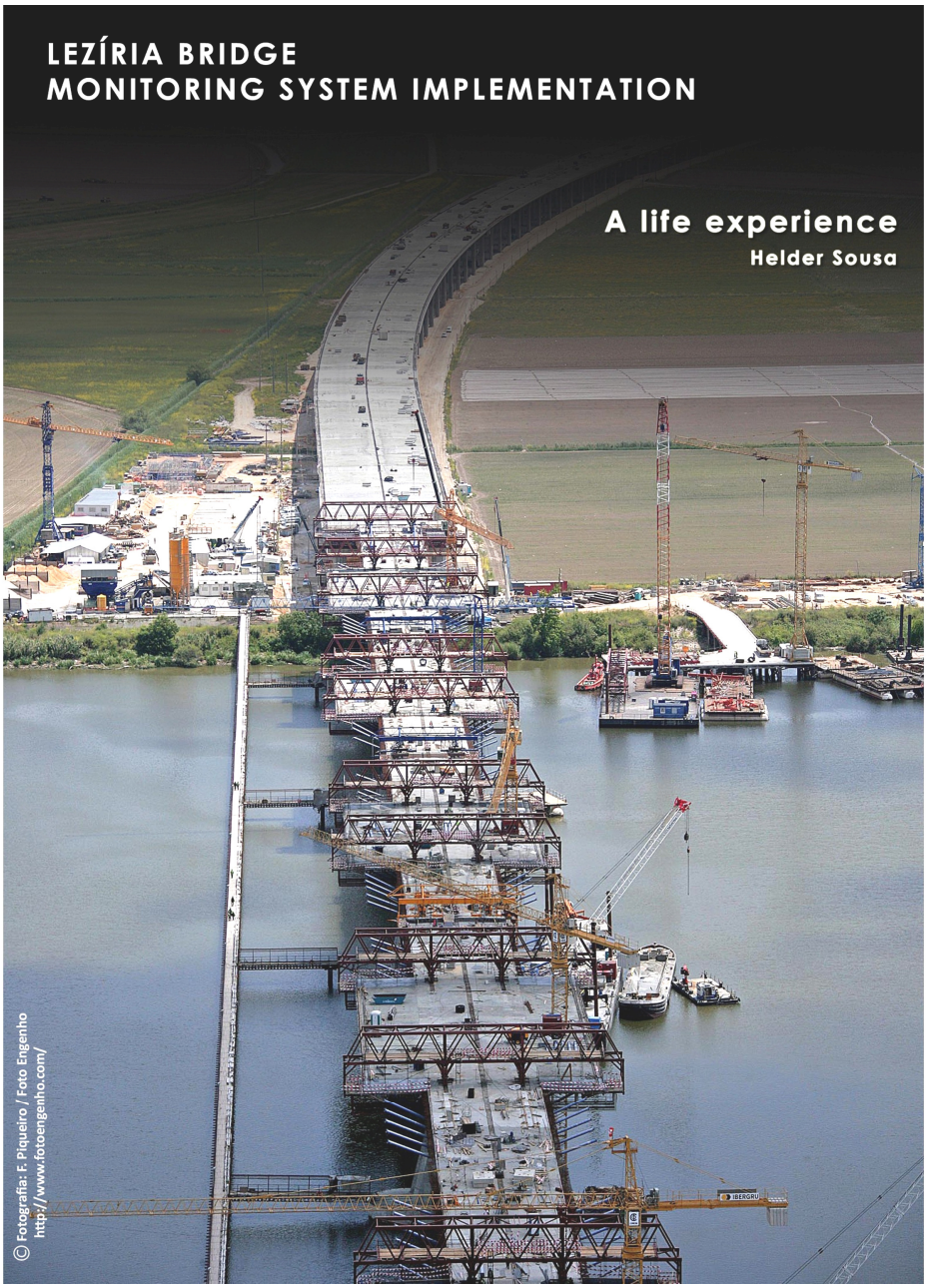

To my father, Nelson

A great men.
A great father,
and a great fa of S.L. Benfica!

We knew that the challenge would be high when NewMENSUS and LABEST-FEUP decided to accept the responsibility of design, install and put on the Structural and Durability Monitoring System of the New Bridge over River Tagus – The Lezíria Bridge –, one of the biggest bridges in the world. A new high-tech technology was proposed to be installed, for which the investigation unit LABEST has been gathering know-how during the last years. However, the structure size, the assortment and the quantity of parameters to be monitored and the rigid schedules of the construction made this challenge even greater.
High challenges are overcome when reliable partners are found. It was necessary to have someone with scientific knowledge, concerning this new technology devoted to the structural monitoring, go-ahead, capable of leading with different task teams in the field, motivated to learn in a demanding atmosphere and most of all capable to take decisions without fear. The installation of the Monitoring System of the Lezíria Bridge was surely a wealthy life experience for Helder Sousa, who has demonstrated to be at the level of this high challenge.

Joaquim Figueiras
Full Professor and PhD Supervisor

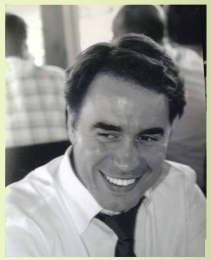

Generally, the human being has a more accurate perception of "something" when he experiences directly that 'something'. Fortunately, my career has been filled with valuable experiences not only at a professional level but also, and principal, to a social and human level. The monitoring of real structures has this benefit, the contact with so many people with so distinct life experiences.

In the scope of my PhD, it was proposed to me the highest challenge that I ever had until the moment – To be the main responsible of the installation of the monitoring system of Lezíria Bridge over River Tagus. Without any hesitation I accepted, and with the same determination that I said "yes", I toke this high challenge until its end with a very own vision and great passion.

From May 2006 to February of 2008, I virtually lived "on the next door" to the Lezíria Bridge. During that period, I devoted gladly to a cause that I am being involved since I left the university – The Structural Health Monitoring. Today, when I cross the Lezíria Bridge, I do it smoothly and without rush. Ten minutes full of memories and experiences that made my life today more complete. Memories of strength, determination, effort, will and courage, as well as companionship and friendship.

In the following pages, I illustrate short extracts of this intensive work. Essentially, I would like to show a life experience, a proper way of thinking, a main propose based on effort and commitment.

With the consciousness of my best,

Helder

Lezíria Bridge, May 2007

First stage
Bridge construction monitoring

The first stage of the installation of the monitoring system was the observation of the bridge behaviour during the construction. Essentially, this task was based on the measurement of concrete deformations with suitable sensors – vibrating wire strain gauges – installed along the bridge construction. It was always my commitment to get measurements as soon as possible. With this effort, measurements were obtained even before the beginning of the concrete pouring, and therefore, the deformations and temperatures evolution of concrete since early ages were registered with success.
From May 2006 to June of 2007, we were always limited by the rhythm of the constructions works, and because of that, me and my team lived periods of hard and intensive work. Sometimes, with imprecise time schedules as well as with parallel tasks related with the sensors installation in distinguish zones of the bridge.

Second stage
Monitoring system installation completion

Third stage
Checks and final works

time

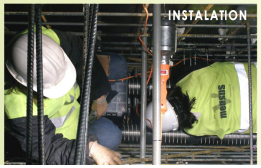

First stage - Bridge construction monitoring

From all the sensors that would be installed, strain gauges, durability and temperature sensors were installed during the construction. All these sensors were embedded in the concrete before the pouring, which required special precautions in the sensors' installation, in order to avoid accidents during the concrete pouring and the consequent loss of sensors. The sensors were placed in safe positions (zones where the reinforcement cage offered an acceptable protection), and the sensors' cables were conducted always near to the reinforcement in a way that avoided free cables to be trod during the concrete pouring.


EMBEDDED SENSORS INSTALLATION (VIBRATING WIRE STRAIN GAUGE)


PROVISORY CABLES PATHS


SHRINKAGE AND CREEP PRISMS


PROVISORY ACQUISTION NODES

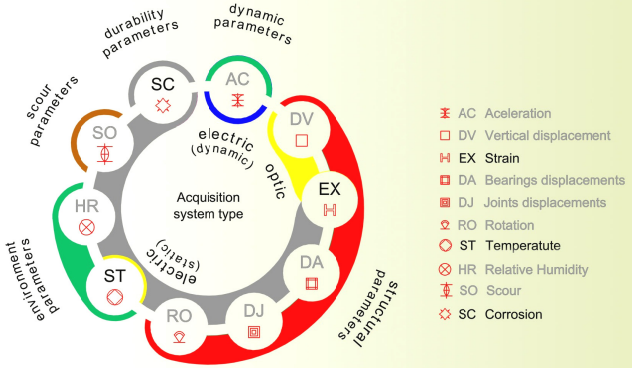

- AC Aceleration
- DV Vertical displacement
- EX Strain
- DA Bearings displacements
- DJ Joints displacements
- RO Rotation
- ST Temperatute
- HR Relative Humidity
- SO Scour
- SC Corrosion

In order to get the sensors records in a continuous mode during the bridge construction, cables paths, connections and acquisition nodes were installed in provisory conditions. In fact, a complete monitoring system was necessary to install, even temporarily and restricted by the construction facilities.

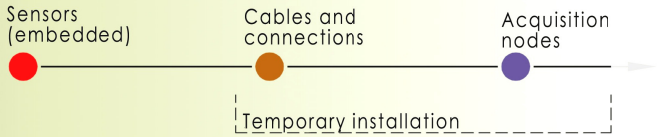

The embedded sensors were fixed to the reinforcement cage using, in some cases, a specific setup that was developed to guarantee a proper sensor's supporting and offer the required robustness to survive to the aggressiveness of the concrete pouring. I must confess that the team physical condition was crucial for the installation of some of these sensors. Sometimes it was necessary to enter in the interior of the reinforcement cages and work in confined and uncomfortable spaces to get the sensors properly installed.


EMBEDDED SENSORS INSTALLATION INSIDE OF A REINFORCEMENT CAGE

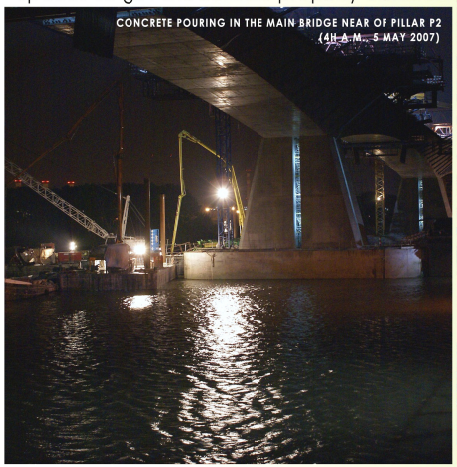
CONCRETE POURING IN THE MAIN BRIDGE NEAR OF PILLAR P2 (4H A.M., 5 MAY 2007)


TEMPORARY ACQUISITION NODES INSTALLATION BEFORE THE CONCRETE POURING

The available time to install the embedded sensors was always limited, because the installation works could only start after the reinforcement cages positioning and at the same time finished before the concrete pouring. In general, a typical installation, which consisted in the positioning of a set of embedded sensors with the connections to the cables that allowed the signal acquiring into provisory acquisition nodes, was approximately made during 1 day.


CONCRETE POURING


CONCRETING OPERATIONS


PRESTRESSING OPERATIONS


SHRINKAGE AND CREEP EVOLUTION


PRECAST BEAMS POSITIONING


PRECAST SLABS POSITIONING

The effort dispended in the embedded sensors installation was reward with the gathered results. With the sensors acquiring since the early ages, with sampling rates that reached to one sample per second, it was possible to observe the structural behaviour during the construction. Construction operations such as concrete pouring, prestressing operations, and load tests at the end of the construction are highlighted. The measurements obtained during the bridge construction show a high potential for knowledge extraction and were one of the start points of my PhD.


LOAD TESTS AT THE END OF CONSTRUCTION

First stage - Bridge construction monitoring

As an example, it is presented below the measurements from one section of the main bridge over River Tagus. This section is located near of pier P1, and the measurements started since the concrete pouring of that section, i.e. from January 2007 until the end of the construction on July 2007. From the presented chart, it is possible to observe the structural effects of the concrete pouring and the prestressing operations.

These results are part of periodic reports delivered to the bridge constructor. In those reports, the final positioning of the sensors after installation, the chronologic tables with the significant construction events, and the main statistical information such as minimum and maximum values are also detailed. These reports were fundamental for the early data organization and for the following works that meanwhile were developed.

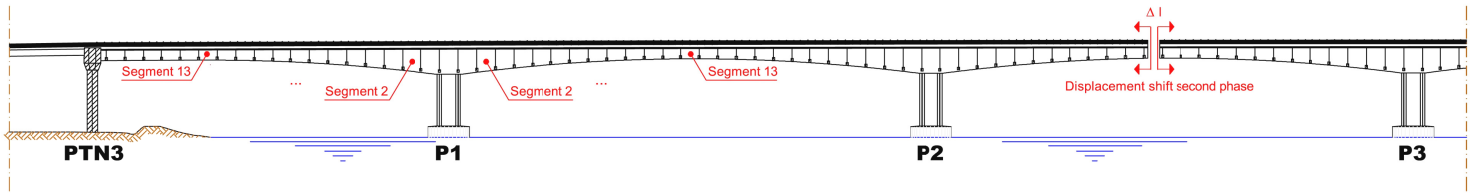

A-PT	Segment bridge 2 concreting
B-PT	Segment bridge 2 prestressing
C-PT	Movable scaffoldirg move to the segment bridge 3 construction
D-PT	Segment bridge 3 concreting
E-PT	Segment bridge 3 prestressing
F-PT	Movable scaffoldirg move to the segment bridge 4 construction
...	...
AB-PT	Close segment bridge PTN3P1 concreting
AC-PT	PTN3P1 span continuity prestressing
AD-PT	Close segment bridge P1P2 concreting
AE-PT	P1P2 span continuity prestressing
AF-PT	Displacement shifts second phase

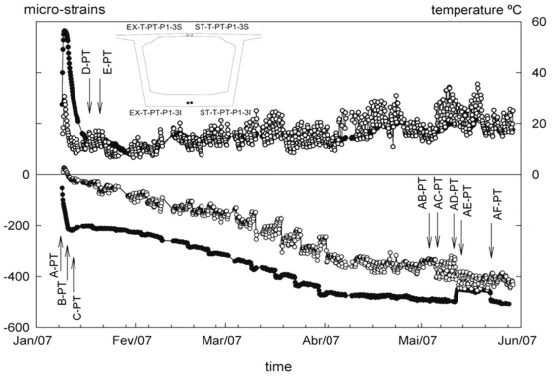

Sensor	Sampling (31/07/06 at 07/07/07)	$y_{initial}$ (31/07/06)	$y_{min.}$ (occur)	$y_{max.}$ (occur)	y_{final} (07/07/07)
EX-T-PT-P1-3I	3422	-1με (08/01/07 22:00)	-565με (05/07/07 3:00)	0με (8/01/07 21:00)	-565με (05/07/07 3:00)
EX-T-PT-P1-3S-1	3307	-1με (09/01/07 3:00)	-501με (05/07/07 3:00)	+28με (9/01/07 :5:00)	-501με (05/07/07 3:00)
ST-T-PT-P1-3I	3425	21.7ºC (08/01/07 22:00)	+8.4ºC (29/01/07 11:00)	+56.4ºC (9/01/07 :7:00)	+21.9ºC (05/07/07 0:00)
ST-T-PT-P1-3S-1	3323	16.5ºC (09/01/07 3:00)	+6.7ºC (24/01/07 12:00)	+35.5ºC (18/05/07 16:00)	+24.7ºC (05/07/07 0:00)

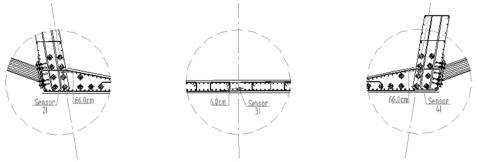

First stage
Bridge construction monitoring

Secong stage

Monitoring system installation completion

Third stage
Checks and final works

time

With the concreting operations finished, the installation of the embedded sensors was also concluded and a second stage of the works began. During this period, the remaining sensors were installed, namely the external sensors, cables paths and acquisition nodes in definitive positions.

Personally, this stage was the most critical because it matched the conclusion of the bridge construction. During this period, the works' intensity increases exponentially, and the interaction between different working teams of the constructor becomes critical. Physical and intellectual capabilities are deeply tested, sometimes to the limit. Generally, the work schedule was set from 7 h a.m to 22 h p.m, including Saturdays and Sundays, which in some cases, extended along the night period. The months of May, June and July of 2007 will be unforgettable, not only for me and my team, but also for all workers who lived there.


MAIN BRIDGE OVER TAGUS RIVER (AUGUST DE 2007)

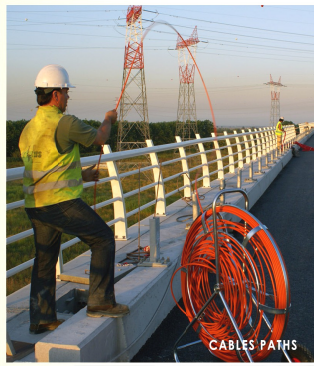
CABLES PATHS


EXTERNAL SENSORS

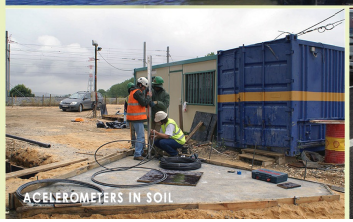
ACELEROMETERS IN SOIL


ACQUISITION NODES

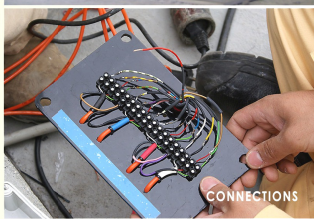
CONNECTIONS

Second stage - Monitoring system installation completion

The completion of the monitoring system installation consisted in four main tasks, namely, (1) the installation of all external sensors, (2) the cables conduction through definitive paths, (3) the installation of the acquisition nodes and (4) the execution of all connections in proper boxes.

Accelerometers, optical sensors for the measurement of vertical displacements, displacement transducers to measure bearings displacements, sonar, temperature and relative humidity were installed.

The reduced time available to do these tasks obligated to reinforce the specialized team in order to answer the needs. Nevertheless, full effort and commitment of the team was always required, with the works distribution performed, between us, in order to optimize the constructor facilities, namely the accesses to inaccessible points of the bridge deck.

EXTERNAL SENSORS INSTALLATION

CABLES CONDUCTION THROUGH FINAL PATHS

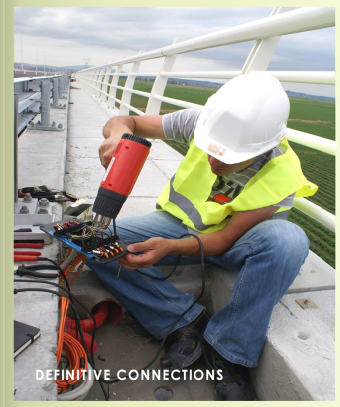

DEFINITIVE CONNECTIONS

DEFINITIVE ACQUISITION NODES INSTALLATION

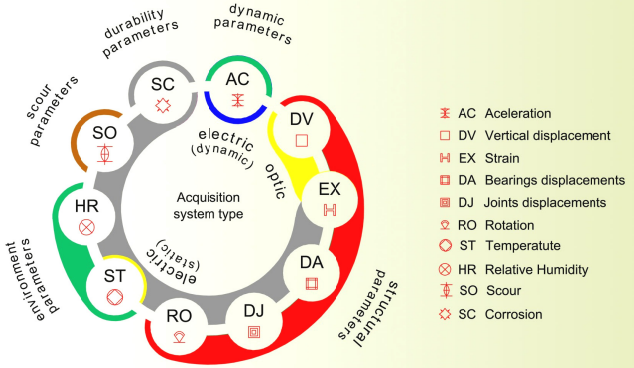

AC Aceleration
DV Vertical displacement
EX Strain
DA Bearings displacements
DJ Joints displacements
RO Rotation
ST Temperatute
HR Relative Humidity
SO Scour
SC Corrosion

Following the work carried out during the bridge construction, the physical installction of the monitoring system was completed with the installation of all external sensors, reposition of cables through definitive paths, definitive positioning of the acquisition nodes and all necessary connections properly protected. Basically, and in addition to the external sensors, it was necessary to remake up the temporary system meanwhile installed during the construction, in order to achieve a robust installation for long-term.

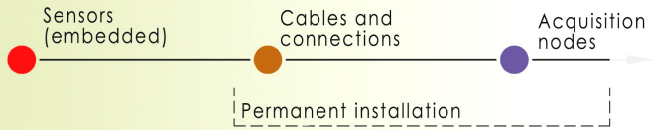

Second stage - Monitoring system installation completion

The installation of the external sensors was different from the embedded sensors, because they are permanently exposed and therefore, the mechanical protection and the durability performance are critical aspects in the setup.
Basically, the adopted setup consists in a support made of stainless steel, specifically designed to fix the external sensor to the structure, which in turn is encapsulated in a protection box with proper strength to protect the sensor against accidental impacts.


PROTECTION BOXES FOR EXTERNAL SENSORS


STAINLESS STEEL SUPPORT


FINAL SETUP FOR EXTERNAL SENSORS


EXTERNAL SENSOR INSTALLED


INSTALLATION SETUP OF A DISPLACEMENT TRANSDUCER


JOINT BALLS TO PREVENT THE SENSOR DISTORTION


MECHANICAL PROTECTION OF THE DISPLACEMENT TRASNDUCERS

A different setup was adopted for the displacement transducers installed near the bearings. They were fixed in two points of the structure (one at the pier top and the other one in the lateral face of the deck) and protected with a stainless steel form specifically designed for that purpose, because it was not possible the sensors' encapsulation into a box. The durability aspect was taken into account by using a protection spray that was applied along the sensor body and oil paste applied in the sensor's extremities in order to prevent distortions in the sensors' movements.

Second stage - Monitoring system installation completion

The connections are undoubtedly one of the weakness points of any electrical/electronic installation. To achieve a good long-term performance of the monitoring system, all connections were carried out meticulously. Firstly, all the connections were made inside of waterproofed boxes. Inside of these boxes, the connections are strictly ordered and perfectly identified. The connections were tin welded and bounded with thermo-retractable casing to guarantee a perfect and durable connection between wires.
This procedure was time consuming, but the sensitivity of the sensor signal to noise sources justifies entirely this option. Besides that, the final product attains a higher level of quality and durability. The acquisition nodes were fixed to the structure by using stainless steel supports for the viaducts, while stainless steel plugs were applied inside the main bridge. As soon as all necessary equipments were installed inside of each acquisition node, like acquisition equipments, electric protections, communication modules, and the connection of all cables to the respective equipments, the physical installation was concluded.


CABLES INSTALLATION THROUGH DEFINITIVE PATHS


CONNECTION BOXES INSTALLATION

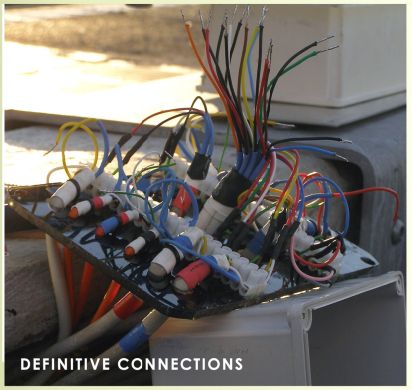
DEFINITIVE CONNECTIONS


CONNECTION BOXES FINISHED


ACQUISITION NODES BOXES


STAINLESS STEEL SUPPORTS

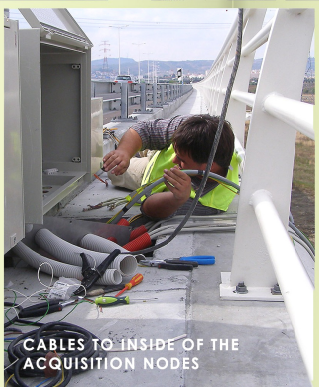
CABLES TO INSIDE OF THE ACQUISITION NODES


EQUIPMENTS INSTALLATION INSIDE OF THE ACQUISITION NODES


FINAL ACQUISITION NODE

First stage
Bridge construction monitoring

Second stage
Monitoring system installation completion

Third stage
Checks and final works

time

With all components of the monitoring system installed, checks and meticulous works were afterwards performed. This was the last stage of the works, where all system was tested to guarantee a good functioning. An image manual was implemented as well as all external sensors, connection boxes and acquisition nodes were waterproofed and sealed. It was a work stage that I particularly appreciated to do, because I was finally seeing the final product taking its shape like I mentally designed when I started this journey one year before.
It was my judgment that due to the structure scale and the socio-economic importance, as well as the desired long-term functioning of the monitoring system, an image manual should be implemented to offer an integrated view of all components and in accordance with project. In the perspective of my PhD I consider that this task expressed the consistency and standardization of all work developed since the beginning.

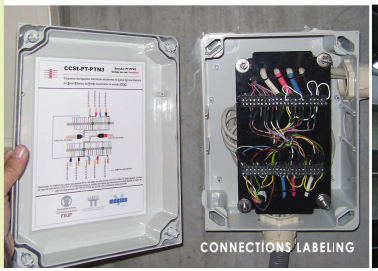

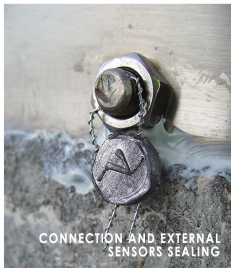

The image manual offers an easy and fast identification of all equipment installed in the bridge. A set of identification plates and plastic sheets (with the project names of the sensors), cables and acquisition nodes are the basis of the referred image manual. In addition, in each protection box of an external sensor, or near to them, a plastic sheet exists, with a summary procedure in order to guide and help in the resolution of an eventual sensor malfunctioning. Excepting serious damage, the procedures referred in those plastic sheets are sufficient to repair a sensor malfunctioning.

All cables placed in the north and south viaducts are identified with small plastic sheets for easy identification and eventual replacement. The cables inside the main bridge are rightfully ordained along a metallic trail and therefore, it is easy to identify a specific cable if needed.

All connection boxes have a connection scheme inside of them. This was one of the most methodical tasks during the image manual implementation. Those schemes were thought to offer a clear reading and perception of the existing connections in each box.

The acquisition nodes are all identified, with identification plates in accordance with the project references as it was done for the external sensors. Inside of each acquisition node, a plastic sheet exists with the identification of all sections that have sensors interrogated by that acquisition node. With this image manual, possible maintenance tasks on the system can be made with lower efforts, namely in the access and identification of specific components of the system, and consequently the maintenance costs concerning the monitoring system might be reduced.

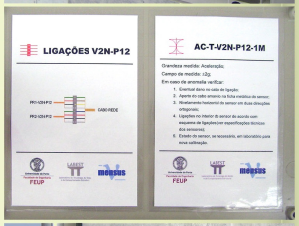

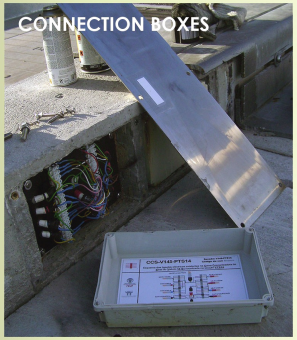

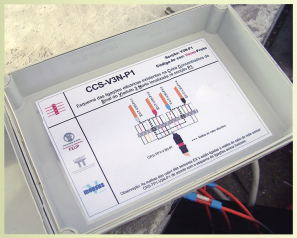

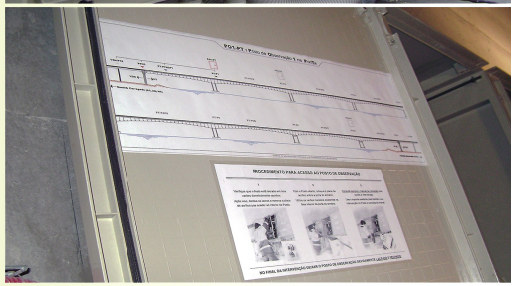

Finally, two more tasks were performed to finish the installation – waterproofing and sealing. The long-term performance of the system, the environment exposure of some system components, and the possibility of unauthorized access are the main reason to perform these two tasks.
For that, all the connection boxes were waterproofed with silicone. Particularly emphasis was given to the sensors protection and connection boxes installed near the piers base over the river. After the waterproofing, the installation works finished with the sealing of the monitoring system. All the external sensors, connection boxes and acquisition nodes were sealed (as it is done in the electrical switchboard in our houses).

The responsibility of installing a monitoring system with this complexity, even more in a bridge with this scale, must be faced with high conscious. The system sealing allows, in a certain way, the identification of unauthorized access to the monitoring system, which otherwise would be difficult to be detected.


WATERPROOFING


SEALING

WATERPROOFING DETAIL

SEALING WAX DETAIL

To arrive at the end of this journey with success is because I had the privilege to make many friends. These friends crossed with me, in this journey along 21 months, by helping me to win the challenge that was proposed to me, which I had accepted with high responsibility. I worked with people from different regions and countries, as well as from basic skills to advanced studies. To all of them, and not only for those that are bellow presented, I am deeply grateful, because they make this experience more than professional – a life experience.
For ever remembered, thanks to all!!


MR. FRANCISCO (MAIN BRIDGE -WELDER) JUNE 2006


MR. BONDIA (MAIN BRIDGE) JUNE 2006


ENG. BRUNO and WORK TEAM (NORTH VIADUCT) MAY 2007


WORK TEAM (NORTH VIADUCT) JUNE 2006

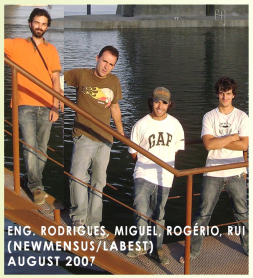
ENG. RODRIGUES, MIGUEL, ROGÉRIO, RUI (NEWMENSUS/LABEST) AUGUST 2007


WORK TEAM (NORTH VIADUCT - REFER ZONE) DECEMBER 2006

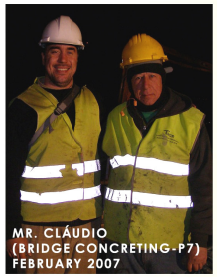
MR. CLÁUDIO (BRIDGE CONCRETING-P7) FEBRUARY 2007


MR. VASCO, (BRIDGE - ELECTRICIAN) MAY 2007


AMÂNDIO, MR. MONTEIRO, CLÁUDIO (LABORATORY TEAM) DECEMBER 2008


MR. CABRERA (NORTH VIADUCT) JUNE 2007

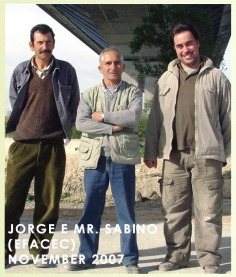
JORGE E MR. SABINO (EIFFAGE) NOVEMBER 2007


ENG. RUI NARCISO (CENTRAL JOBSITE) JULY 2007


M.C. (BRIDGE CLOSE-P6P7) MAY 2007


PROF. PIQUEIRO and the AIRPLAIN PILOT (COVER PHOTO) MAY 2007


ENG. GUIMARÃES (MAIN BRIDGE) JUNE 2007

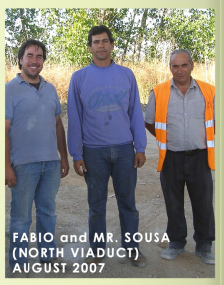
FABIO and MR. SOUSA (NORTH VIADUCT) AUGUST 2007


WORK TEAM OF THE DECK CONSTRUCTION (NORTH VIADUCT) JULY 2006


WORK TEAM OF THE BRIDGE FINISHING (MAIN BRIDGE) NOVEMBER 2007

APPENDIX B : SUPPORTING TOOLS FOR STRUCTURAL MODELLING

INTRODUCTION

Errors are inevitable in the construction of numerical models concerning large-scale structures, namely due to input data. Therefore, a set of tools were developed in order to mitigate and support the development of Finite Element Models (FEM) for concrete bridges, in a systematic and standardized mode. The focus of this appendix is to present and detail the developed tools that supported the FEM presented in this thesis.

Generally, the input data that supports the construction of FEM is related with a set of geometric and mechanical properties of the structure under analysis namely: shapes and thicknesses, materials, boundary conditions, loads and time history. The management and consulting of this wide information can be difficult for the case of large-scale structures. In fact, considering the large-scale of Lezíria Bridge, the developed supporting tools have demonstrated to be crucial in the information scanning, assembly and building of the input files for the FEM analysis, and also with time-consuming benefits.

In more detail, these supporting tools are a set of interface tools developed with C++/ObjectARX and LABVIEW programming languages. The interface tools can be unfolded in two parts (Figure B.1):

- A first one so called as "*AutoCAD tools"*, which comprises a set of drawing commands available in the AUTOCAD environment (developed in C++/ObjectARX);
- A second one so called "*Data Manager"*, which through a user-friendly interface a set of manipulating commands supports, helps and accelerates the information update, assembly and set up of the input files for the FEM analysis.

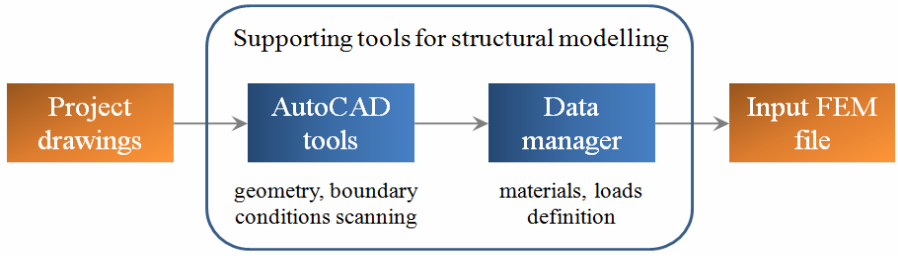

Figure B.1 : Sequence of the interface tools.

PART 1 : "*AUTOCAD TOOLS*"

As aforementioned, the information scanning of large-scale structures can be a difficult task. To make a complete and rigorous scanning of structural elements namely: concrete and/or steel components, prestressing cables and ordinary reinforcement it is necessary to have standard and controlled procedures in order to mitigate potential errors during the scanning operations.

The developed "*AutoCAD tools*" herein presented take advantage of the AutoCAD drawing accuracy, by scanning and/or manipulating the drawing entities to export the coordinates of those entities for the FEM construction. These tools, previously compiled in C++ environment into a file with extension *arx*, can be afterwards installed in the AutoCAD library folder, and easily used in the command line during a working session. Table B.1 resumes the developed tools, with a brief description of each one.

For a better understanding, the sequence that they are presented is logical regarding the geometry scanning for the FEM construction, by starting from local aspects to the global scale.

Table B.1 : "*AutoCAD tools*" library.

Command name	**Brief description**
"hfms_section_offset"	Slab offset for a box girder section type
"hfms_I_equiv_section"	I-cross-section creation and equivalent to a box girder section
"hfms_section_properties"	Cross section properties (area, perimeter, etc.)
"hfms_section_position"	Centroid position for a cross section
"hfms_bar_sections"	Beam element construction cross section definition
"hfms_geometric_model"	Geometric model construction

- ***"hfms_section_offset"***

This command draws a slab offset of a specific section. This operation can be particularly useful for box girder decks, for which a variation of the thickness and positioning of the bottom slab normally exist and normally hundreds of sections have to be generated for the FEM construction. Using this command, a new slab is automatically drawn in a specific position in function of the user's input. For that, it must be selected a box girder section, and in addition, reference points of the bottom and top faces of the bottom slab. These reference points can be selected through an elevation drawing as illustrated in Figure B.2. As it can be perceived, two pairs of reference points are selected in correspondence to the reference slab (drawn in the reference cross section) and the target slab that is intended to be created over the reference section drawing. Table B.2 resumes the AutoCAD entities involved in the input/output operation.

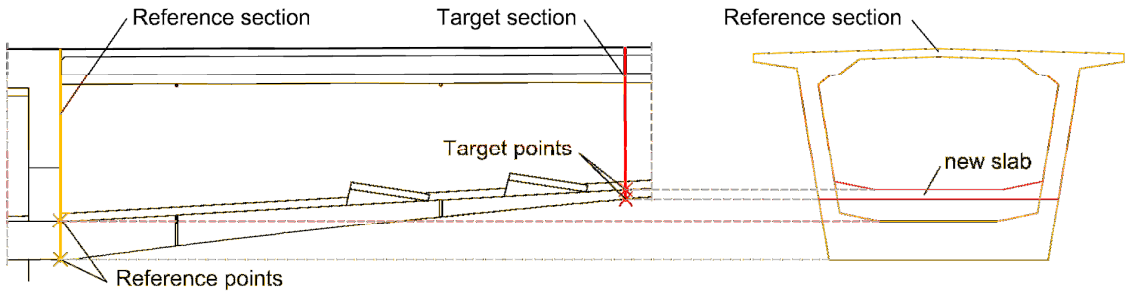

Figure B.2 : Bottom slab offset of a box girder section.

Table B.2 : Input/Output AutoCAD entities (*"hfms_section_offset"*).

Input	Output
• Reference section (line entities) • Pairs of reference and target points of the reference and target slab (point entities)	• New slab (line entities)

- ***"hfms_I_equiv_section"***

This command draws an *I-cross-section*, based on the geometry of a box girder section. This command is powerful for 2D FEM, because generally is not possible to use the real box girder section for this type of models. For the FEM of Lezíria Bridge, 179 equivalent

I-cross-sections were calculated, which clearly is a demanding task without automatic tools as the one herein presented. Therefore, a practical procedure is to use an equivalent cross section, an I-shape section that has the same mechanical properties with respect to the horizontal axis (X-axis). Obviously, if both sections are equivalent, they have the same centroid. Additionally, the sub-zones that performs the I-section is also drawn, which is an important information for the input file of the FEM. Figure B.3 plots a box girder section (reference section) and the equivalent *I-cross-section* that has the same centroid, area and moment of inertia relative to the X-axis. Table B.3 resumes the AutoCAD entities involved in the input/output operation.

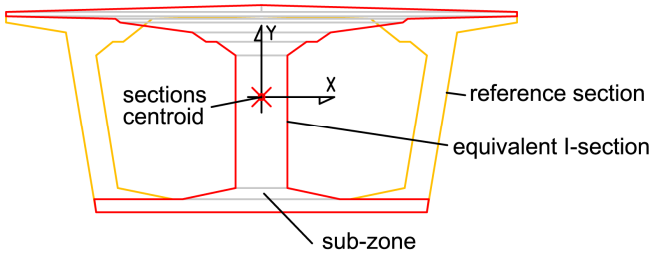

Figure B.3 : I-cross-section generation based on a box girder section.

Table B.3 : Input/Output AutoCAD entities (*"hfms_I_equiv_section"*).

Input	Output
• Reference section (line entities)	• New slab (polyline entities) • Sub-zones (polyline entities

- ***"hfms_section_properties"***

This command calculates the main geometric and mechanical properties of a cross section, namely: area, perimeter, centroid position, momentum of inertia as well as maximum height and maximum width. Moreover, the centroid position is automatically drawn, as it is presented in Figure B.3, and the calculated properties can be stored into an output file. The drawing of the section centroid is particularly useful for the definition of the elements axis, even more when made in automatic mode in the presence of hundreds of sections to be operated. Table B.4 resumes the AutoCAD entities involved in the input/output operation.

Table B.4 : Input/Output AutoCAD entities (*"hfms_section_properties"*).

Input	Output
• I-section (region entity)	• Centroid drawing (circle + two line entities) • Geometric and mechanical properties (values displayed in the command line)

- ***"hfms_section_position"***

The centroid position of a cross section can be drawn with this command, namely in two locations (Figure B.4): (i) over the selected cross section, drawing a local reference-axis system X-Y (as it is also presented in Figure B.3) and, (ii) over a line entity, which marks the location of the respective cross section in an elevation drawing of the structure. This command is particularly useful to draw quickly, and with the maximum accuracy, the longitudinal axis of box girder decks. Table B.5 resumes the AutoCAD entities involved in input/output operation.

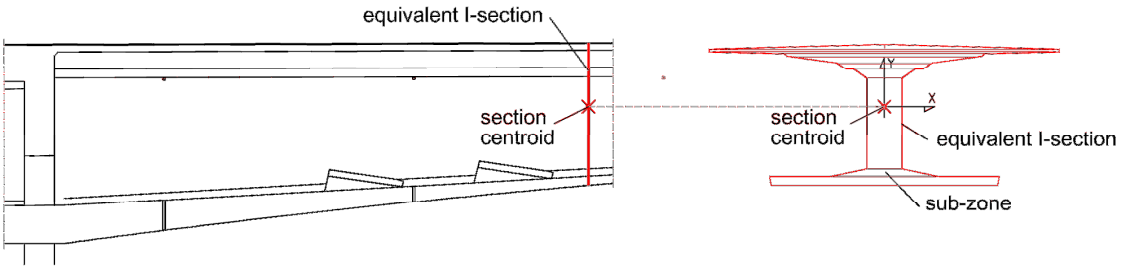

Figure B.4 : Drawing of the cross section centroid in an elevation drawing of the structure.

Table B.5 : Input/Output AutoCAD entities (*"hfms_section_position"*).

Input	Output
• *I-Cross-section* (region entity) • Section location (line entity)	• Centroid drawing over the *I-cross-section* and section location (circle + two lines entities)

- ***"hfms_bar_sections"***

Regarding the FEM analysis, the definition of beam elements with variable cross section is a time-consuming task, namely if the cross section is not a standard type (such as

rectangular, circular, etc.). In fact, this is the case of box girder decks. Hence, this command supports the definition and drawing of beam elements of three nodes. Selecting the three *I-cross-sections* and the respective localization in the elevation drawing (basically, by repeating the procedure illustrated in Figure B.4 for a single cross section), the beam element is drawn and the coordinates are exported into an output file for future use. The number of zones for each *I-cross-section* and the respective coordinates composes the information that is exported for that output file, which has a proper data format in order to be, afterwards, directly assembled to the input data file that is used for the FEM analysis. Figure B.5 and Figure B.6 illustrates, respectively, the beam element drawing and the information that is stored in the output data file. Table B.6 resumes the AutoCAD entities involved in the input/output operation.

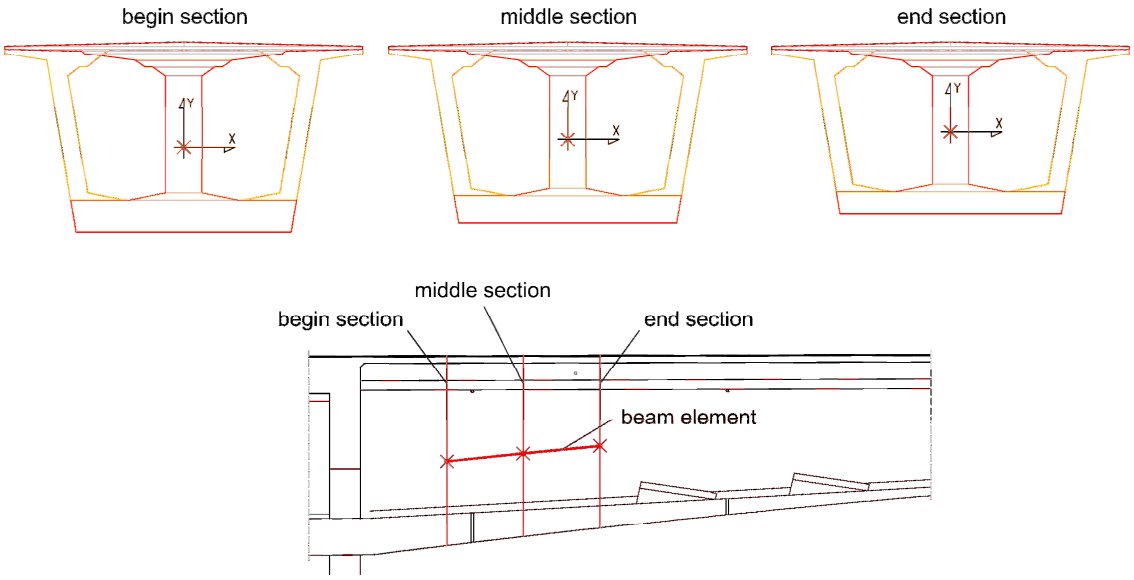

Figure B.5 : Beam element drawing.

P1DA3.txt - Bloco de notas

Ficheiro Editar Formatar Ver Ajuda

```
NZONES 11
ZONE2D -3.87 -3.84 -3.81 4.34 4.37 4.40 -3.00 -3.06 -3.12 4.49 4.50 4.52
       -3.00 -3.06 -3.12 2.16 2.16 2.16 -2.70 -2.76 -2.82 0.71 0.71 0.71
       -2.70 -2.76 -2.82 0.71 0.71 0.71 1.63 1.46 1.31 0.71 0.71 0.71
       1.63 1.46 1.31 0.71 0.71 0.71 1.99 1.83 1.67 1.23 1.23 1.23
       1.99 1.83 1.67 1.23 1.23 1.23 2.00 1.84 1.68 1.53 1.53 1.53
       2.00 1.84 1.68 1.53 1.53 1.53 2.25 2.09 1.94 1.90 1.90 1.90
       2.25 2.09 1.94 1.90 1.90 1.90 2.51 2.35 2.20 3.88 3.88 3.88
       2.51 2.35 2.20 3.88 3.88 3.88 2.61 2.45 2.30 4.01 4.01 4.01
       2.61 2.45 2.30 4.01 4.01 4.01 2.69 2.53 2.37 7.01 7.01 7.01
       2.69 2.53 2.37 7.01 7.01 7.01 2.81 2.65 2.50 7.01 7.01 7.01
       2.81 2.65 2.50 7.01 7.01 7.01 2.99 2.83 2.67 0.01 0.01 0.01
```

Figure B.6 : Output file with the information of the three cross sections that defines the beam element.

Table B.6 : Input/Output AutoCAD entities (*"hfms_bar_sections"*).

Input	Output
• Three *I-Cross-sections* (region entities) • Sections location (lines entity)	• Beam element (line entity) • Centroid drawing over the *I-cross-section* and section location (circle + two cross lines entities) • Output file with the geometric coordinates

- ***"hfms_geometric_model"***

Based on the line entities that define the structural elements axis, this command performs the geometry scanning of all points' coordinates. After selecting the elements, a numbering system is drawn over the elements and an output file is created with this information, namely numbering and coordinates. Four different element types are distinguished: (i) piles, (ii) beams, (iii) reinforcements and (iv) supports. Particularly for the reinforcement elements, three sub-types are defined: (i) ordinary reinforcements; (ii) console cables, and (iii) external cables. This disposal allows a more flexible geometry scanning, where it is possible to create different output files with different elements type. Moreover, the scanning process can be interrupted and resumed in a following work session by saving the scanning information of the current session into a backup file. This possibility is very useful for the case of large-scale structures, such as Lezíria Bridge. At the end, the geometric model is completely scanned and saved into a set of data files. It should be highlighted that at this stage, only the geometric information needed for the FEM analysis is updated. Other properties, namely mechanical and loads, must be afterwards defined. Figure B.7 illustrates the geometric model of a span of a box girder bridge, including piles and piers, which is afterwards stored into an output file as illustrated in Figure B.8. Table B.7 resumes the AutoCAD entities involved in the operation.

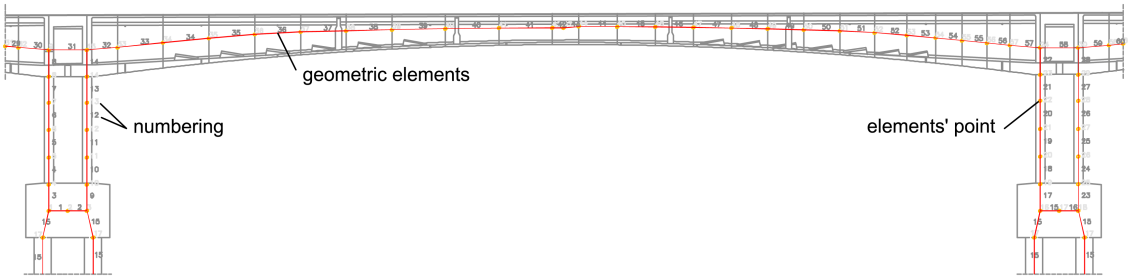

Figure B.7 : Geometric model based on the project drawings.

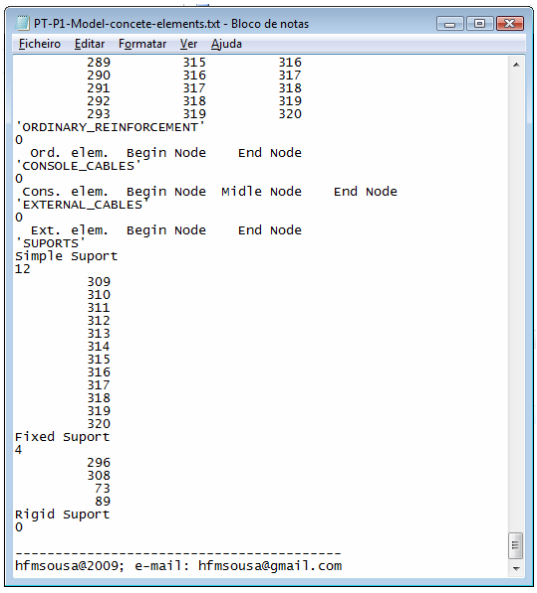

Figure B.8 : Data file with all information of the geometric model.

Table B.7 : Input/Output AutoCAD entities (“*hfms_geometric_model*”).

Input	Output
• Structural elements (line entity)	• Geometric model (lines, splines, circles entities and label texts) • Output file with the numbering and coordinates of the structural elements

PART 2: “*DATA MANAGER*”

As aforementioned, after the completion of the scanning of the structure geometry, attributes such as materials and loads must be defined as well as the attachment of these properties to the geometric model. To support this task, a user-friendly interface was built, with a set of manipulating commands to support, help and accelerate the information

update, assembly and set up of the input file for the FEM analysis – "*Data Manager*". Figure B.9 illustrates the front panel of this tool, where three main sets can be identified:

- AutoCAD/backup files management,
- Tab folders for data organization and easier handling,
- Materials, cross sections and loads databases.

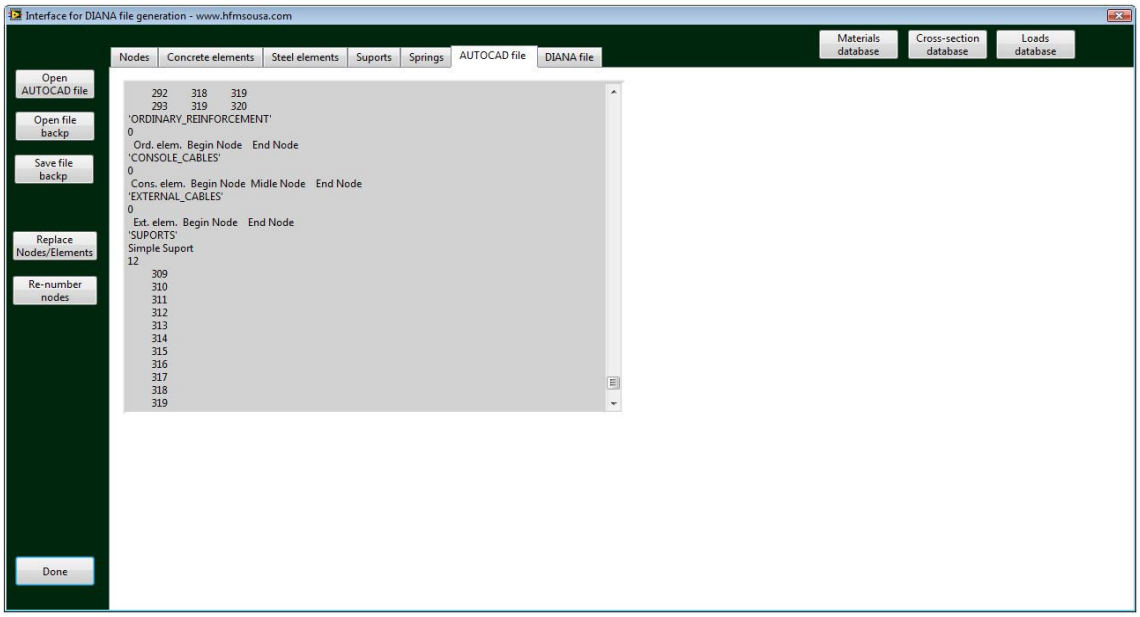

Figure B.9 : Data file with all information of the geometric model.

- **AutoCAD/backup files**

The input/backup files buttons are the main entering point for the model data. Files that were previously created with the "*AutoCAD tools*" as well as backup files that can be created during a working session when using the "*Data Manager*", can be accessed through this buttons.

- **Tab folders for data organization and easier handling**

The uploaded data is automatically unfolded in different groups and organized into different tab folders, namely: (i) nodes; (ii) concrete elements; (iii) steel elements; (iv)

supports (v) springs. Additionally, two more tabs are implemented: (vi) AutoCAD file, which displays the content of the files created with the "*AutoCAD tools*" and accessed with the AutoCAD button (Figure B.9), and (vii) DIANA file, which displays the final data to be exported into data files to be used in the FEM analysis by using the DIANA software. For all tabs, the data is only editable by activating proper commands and not editing directly in the tables where the data is prompted, which highly prevents potential editing errors during the data updating, editing and assembling.

Nodes tab

This tab folder contains the coordinates 'x' and 'y' of all points of the geometric model, previously defined in an AutoCAD session by using the "*AutoCAD tools*" (Figure B.10). As aforementioned, the data displayed in the table is not directly editable. In order to improve the efficiency in the data handling, the coordinate points can be edited through the operations available in this tab, namely: (i) default values, (ii) point reference edition, (iii) suffix addition, (iv) comment addition, (v) edition of nodes' coordinates and (vi) offset of points' coordinates.

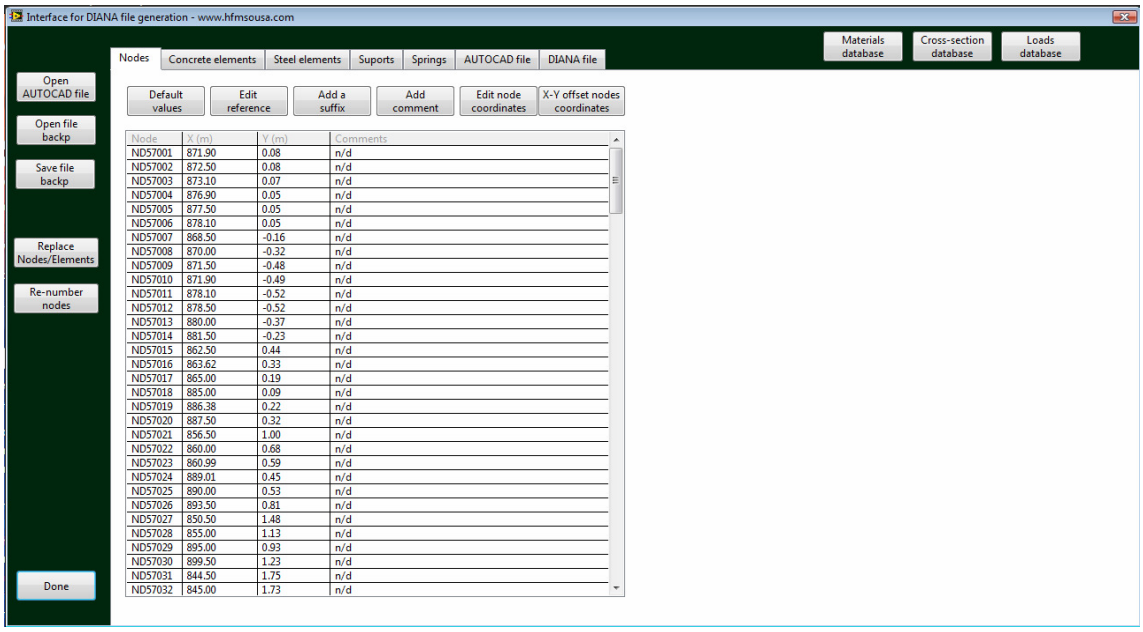

Figure B.10 : Nodes tab.

Concrete elements tab

In this tab, all beam elements of three nodes are displayed (Figure B.11). In accordance with the designations plotted in the "*Nodes tab*", for each beam element is displayed the three points that geometrically defines that beam element. It should be highlighted that beam elements are used for all structural elements namely, piles, piers and girder, which justifies the tab name as "*Concrete elements tab*". For this case, the data can be edited through the commands buttons available in this tab, namely: (i) default values, (ii) point reference edition, (iii) suffix addition, (iv) comment addition, (v) mesh division, (vi) add to a concrete set and (vii) material, physical and/or load property attachment. For this last functionality, the respective databases are available at the right side of the front panel, as illustrated in Figure B.11, which enables a comprehensive database consulting and at the same time the properties attachment to the beam elements displayed in the table on the left side.

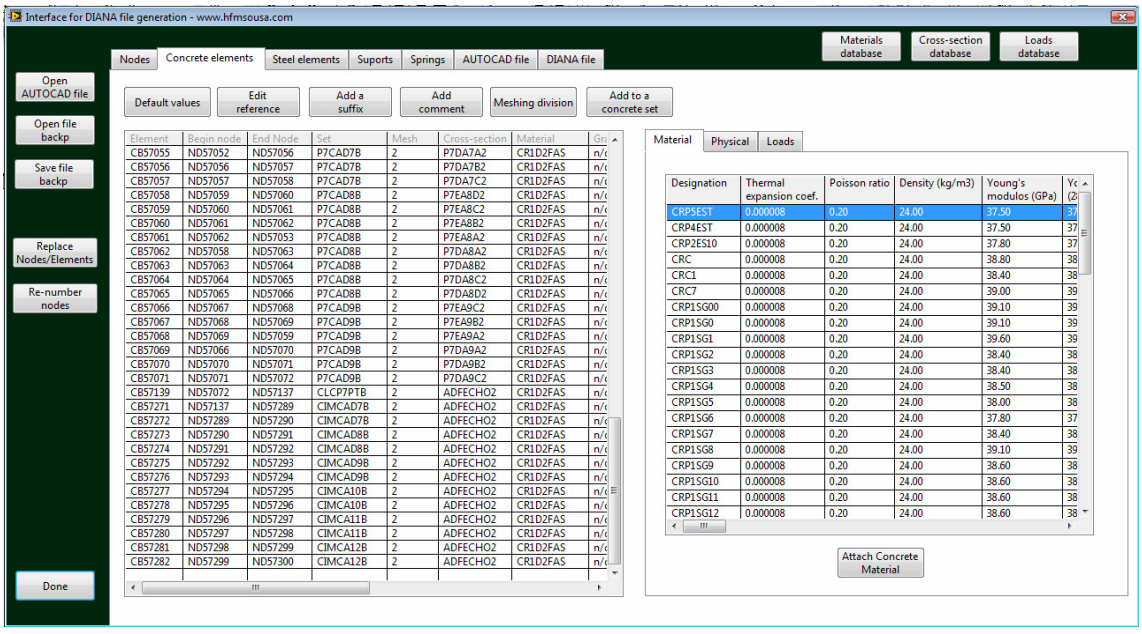

Figure B.11 : Concrete elements tab.

Steel elements tab

With a very similar operational behaviour to the "*Concrete elements tab*", all the steel elements are displayed in this tab. The main difference to the previous tab is that the steel

elements are grouped into three different types in three sub-tabs, namely: (i) ordinary reinforcements, (ii) console prestressing cables and (iii) external prestressing cables (Figure B.12). For this case, the data can be edited through the commands buttons available in this tab, namely: (i) default values, (ii) point reference edition, (iii) suffix addition, (iv) comment addition, (v) add to a reinforcement set, (vi) attach to a concrete set and (vii) material, physical and/or load property attachment. For this last functionality, the respective databases are available on the right side of the front panel, as illustrated in Figure B.12. This enables a comprehensive database consulting and at the same time the properties attachment to the beam elements displayed in the table on the left side. However, observing carefully, the database presented for this case concerns only the steel materials, while for the previous tab, "*Concrete elements tab*", the database concerns the concrete materials. Thus, the material/physical and loads database is automatically prompted regarding the element types that are presented in a specific tab.

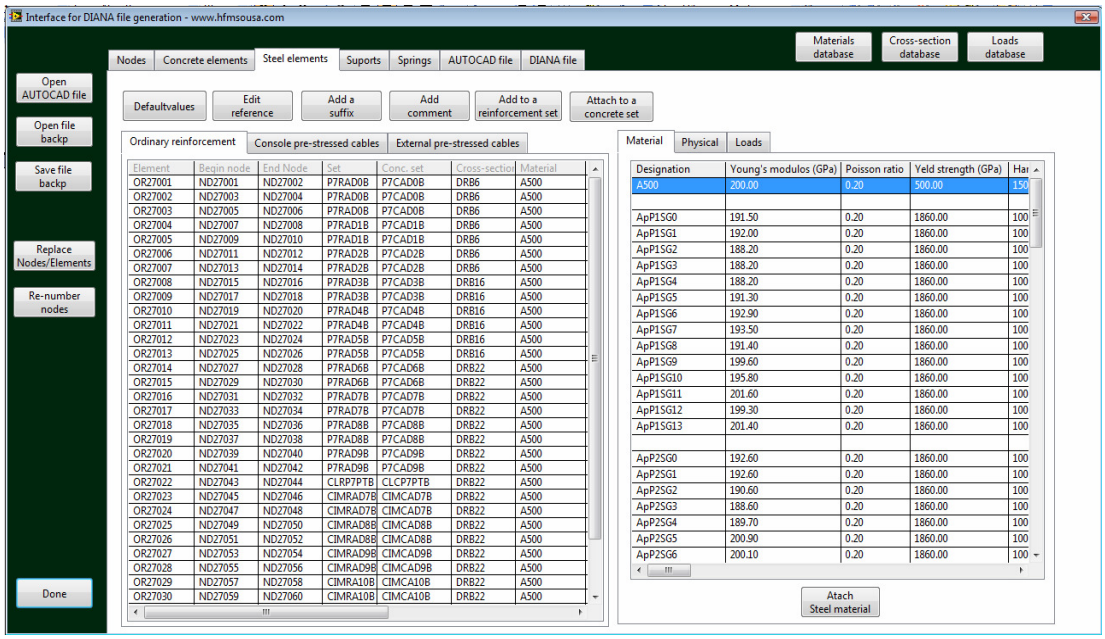

Figure B.12 : Steel elements tab.

Supports tab

This tab focuses the definition of the structure supports (Figure B.13). Three support types are considered, depending on the restrained degree of freedom in the x, y and z directions

For this case, the data can be edited through the commands buttons available in this tab, namely: (i) default values, (ii) support parameters edition, (iii) support set definition, (iv) comment addition.

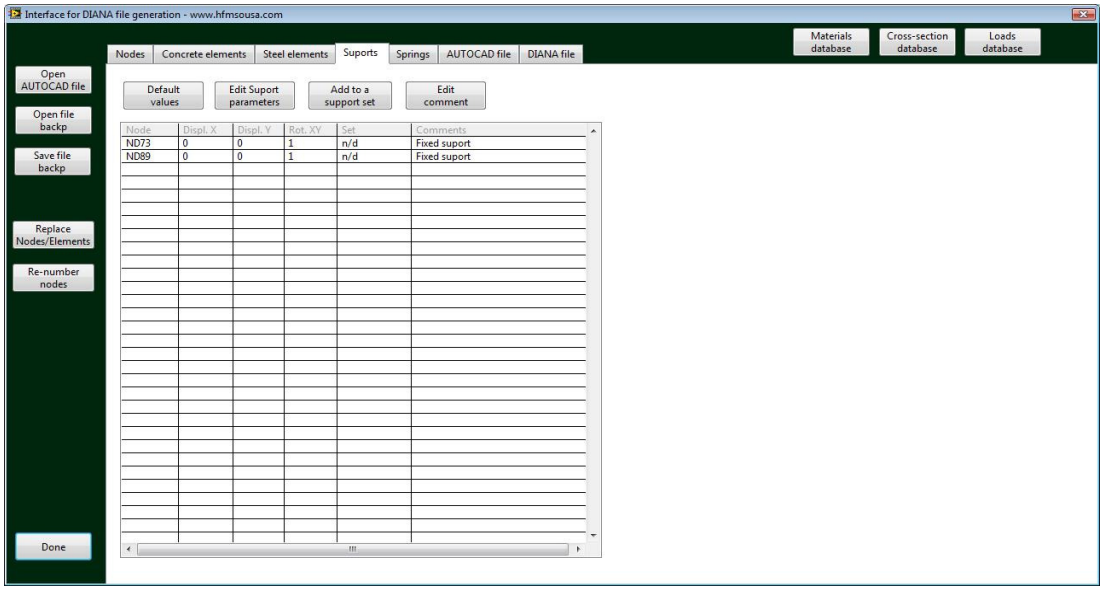

Figure B.13 : Supports tab.

Springs tab

To complement the support tab, a "*Spring tab*" is also considered, which manages the definition of elastic supports (Figure B.14). Two spring types are considered namely, punctual and linear. For this case, the data can be edited through the commands buttons available in this tab, namely: (i) spring set definition, (ii) comment adding and (iii) material and/or physical property attachment. As aforementioned, for the concrete and steel tabs, the respective database is available at the right side of the front panel, as illustrated in Figure B.14, which enables a comprehensive database consulting and at the same time the properties attachment to the beam elements displayed in the table on the left side. Only the material and physical properties with respect to the spring elements is herein displayed.

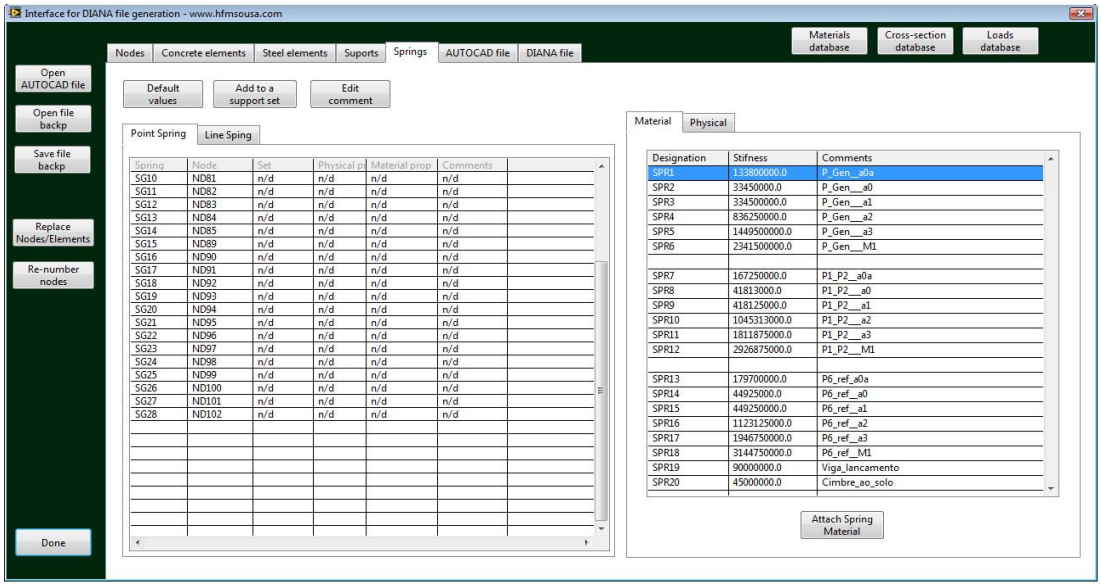

Figure B.14 : Springs tab.

AutoCAD file tab

In addition, a specific tab is devoted to display the data contained in the AutoCAD files generated by the "*AutoCAD tools*" and accessed by the AutoCAD file button (Figure B.15). The intention is to allow a direct data consulting, in order to clarify any potential doubt that might appear in the data displayed in the previous tabs.

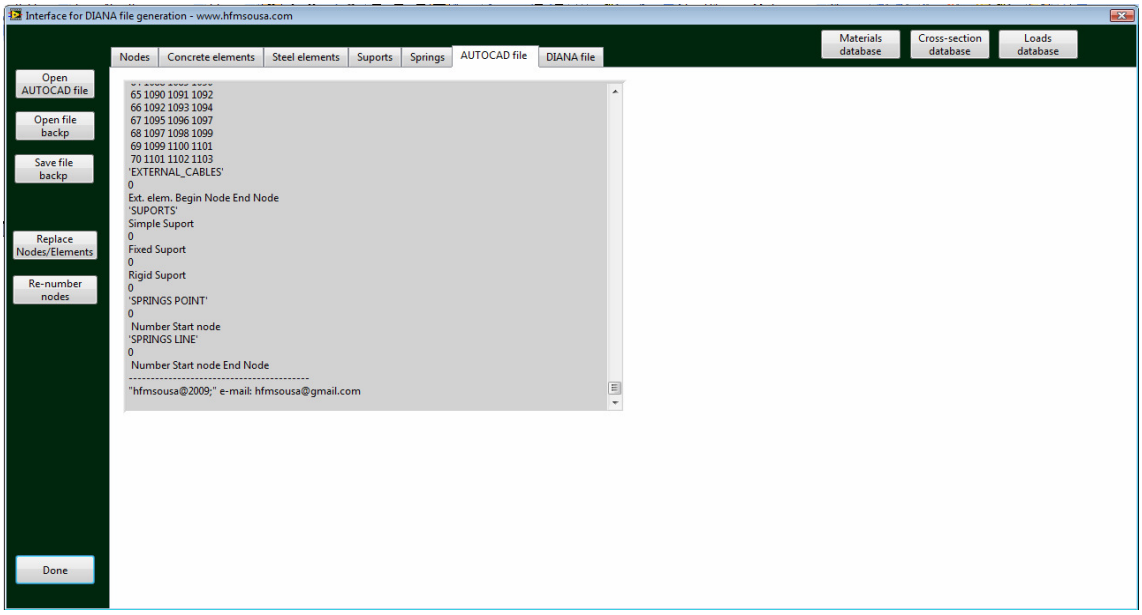

Figure B.15 : AutoCAD tab.

DIANA file tab

Finally, this tab allows the information selection and the creation of input files to be used for the FEM analysis. In this tab, a set of check boxes, respecting to different information type, are available in order to ease the files generation. This allows the data files structuring, depending the information type that is intended to be created. For example, a specific file can be created for the materials definition, other for loads definition, etc. This can be very useful for large-scale structures, even more important if it is intended to update the numerical model in future developments. Without this structuring, it can be very difficult to perform future FEM updates, aggravated by potential errors. The data format of the created files must be in accordance with the software that is used for the FEM analysis. Specifically for this case, the adopted format is in conformity with the DIANA software, which is the software used in the present work for FEM analysis. Nevertheless, the "*Data Manager*" is prepared to be updated with other data formats.

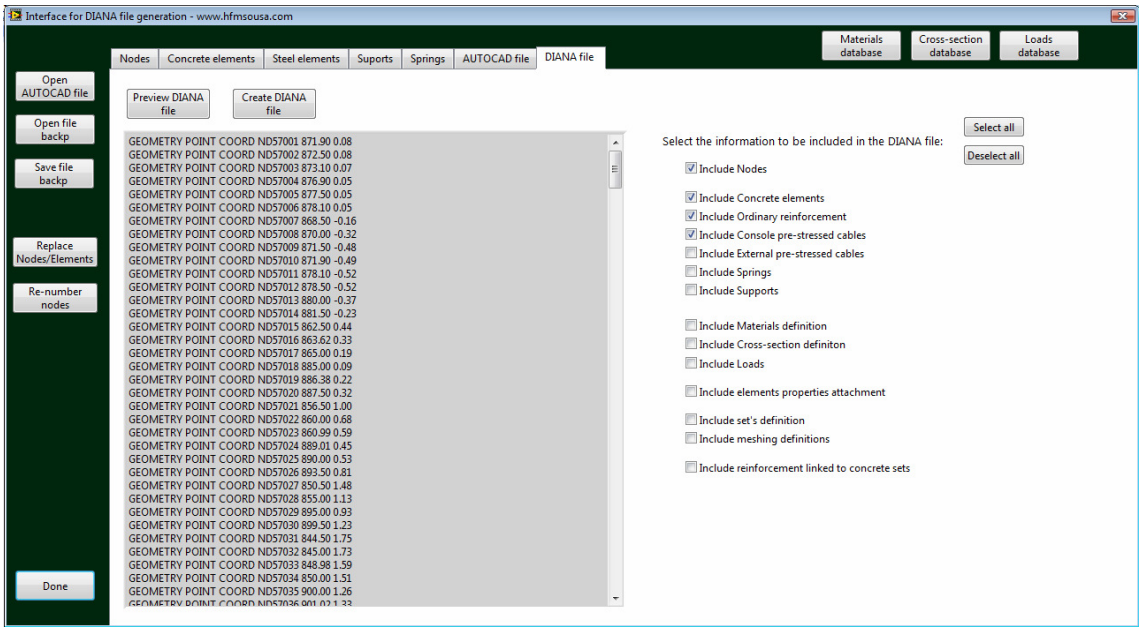

Figure B.16 : DIANA file tab.

- **Databases concerning the materials, cross sections and loads definition**

For large-scale structures, the information handling such as materials, cross sections and loads becomes a critical aspect. To illustrate how complex might be the data handling for a

large-scale structure, for the Lezíria Bridge case 573 materials, 479 cross sections and 192 loads were taken into account. Therefore, in order to get more efficient and flexible procedures to the definition and edition of these properties, three different databases exist, namely: (i) materials database; (ii) cross sections database, and (iii) loads database.

Materials database

The materials database was implemented in order to manage the different structural materials that commonly compose a concrete bridge, namely: concrete and steel (Figure B.17). In this database, it is possible to create, edit and/or remove materials, as well as save or import a database file containing the materials definition. The procedures are flexible and the possibility of save/import files with all information reveals to be very useful in the data handling.

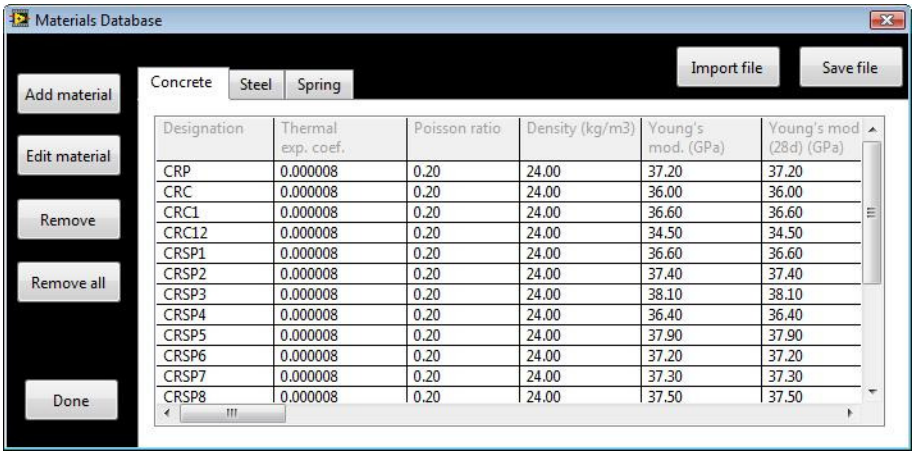

Figure B.17 : Materials database.

The definition of a concrete material and a steel material is different as it is illustrated in Figure B.18. User-friendly interfaces were implemented in order to support the definition of a new/existent material, by interactively define their parameters through the menus illustrated in Figure B.18.

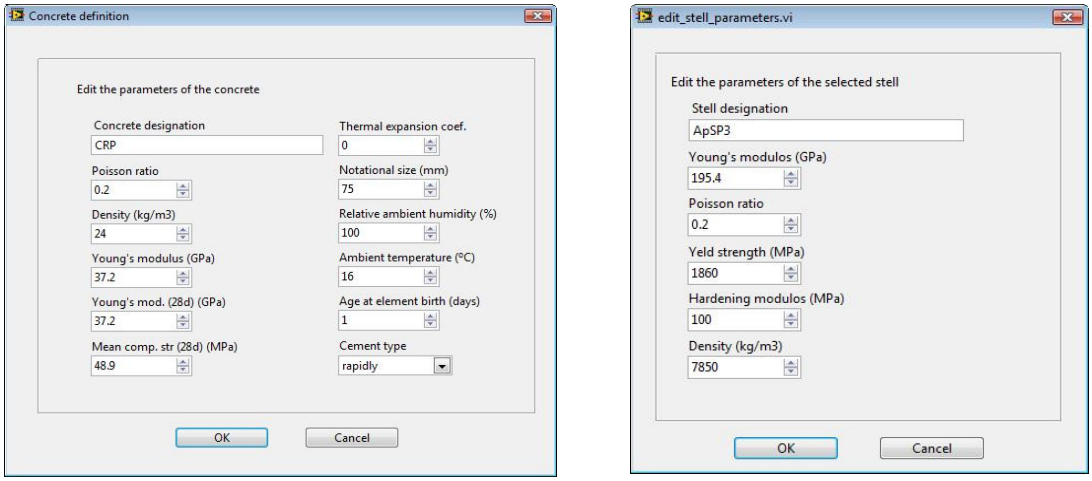

a) concrete. **b) steel.**

Figure B.18 : Material definition.

Cross sections database

With a very similar operational behaviour to the materials database, the cross sections database allows the creation/edition/remove of different cross section types, as well as the saving or importation of a database file containing cross section definitions (Figure B.19). Particularly for the *I-cross-sections*, which are generated with the "*AutoCAD tools*" previously presented, the database allows the importation of the information contained in data files. Nevertheless, other shapes are available, namely rectangular, circular cross sections.

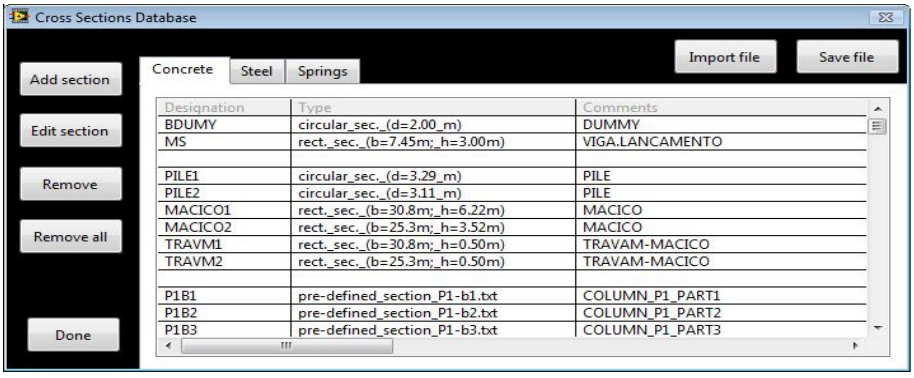

Figure B.19: Cross sections database.

Again, similar to the materials database, user-friendly interfaces were implemented in order to support the definition of a new/existent cross section, by interactively define their parameters through the menus illustrated in Figure B.20. In more detail, Figure B.20-a shows a backup file of a cross section database, while Figure B.20-b shows the interface that allows the definition of a steel section namely, the bar diameters, layers and distance to a reference surface.

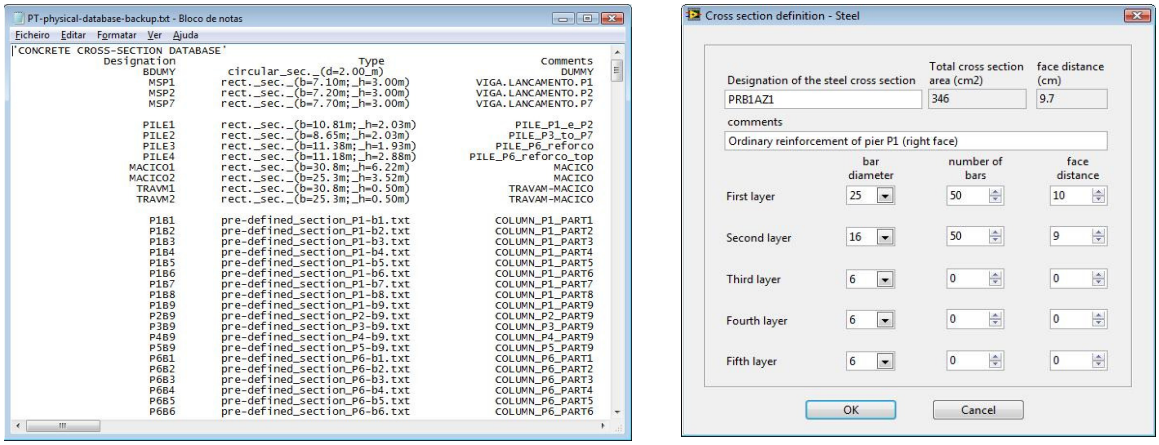

a) backup file. **b) steel section.**

Figure B.20 : Cross section definition.

Loads database

Finally, the loads database manages the different loads that can be used for the FEM analysis. Herein, it is possible to create/edit/remove loads, as well as save or import a database file containing the loads definition (Figure B.21). Regarding the long-term analysis of concrete bridge, the loads are unfolded into five main types, namely: (i) gravity loads, (ii) forces, (iii) pressures, (iv) displacements and (v) temperature variations.

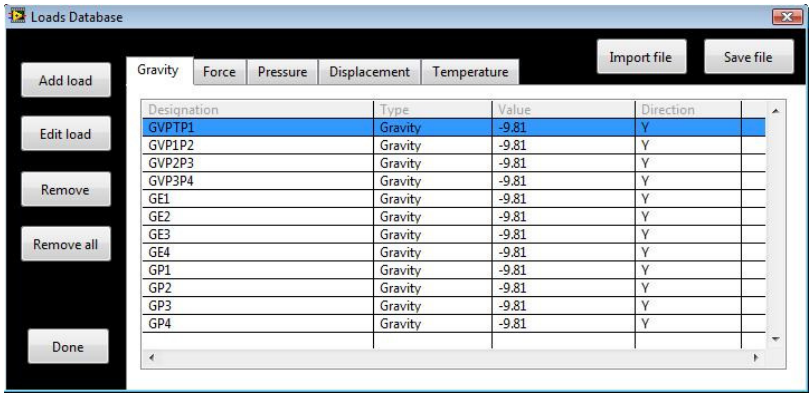

Figure B.21 : Loads database.

For each load type, it is possible to edit their parameters values such as: (i) load name; (ii) load type; (iii) value, and (iv) direction. Figure B.22 shows the user-friendly interface that is used for the load parameters definition.

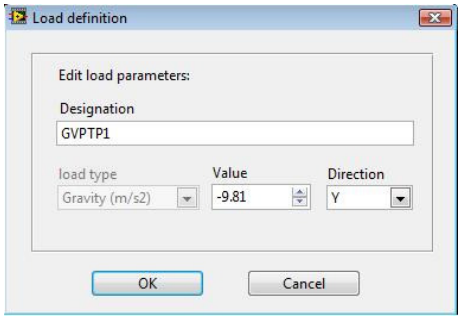

Figure B.22 : Load definition.